2010-08-09

Sacroiliac Joint Biomechanics and Effects of Fusion

Dinah Baria
University of Miami, d.baria@umiami.edu

UNIVERSITY OF MIAMI

SACROILIAC JOINT BIOMECHANICS AND EFFECTS OF FUSION

By

Dinah Baria

A DISSERTATION

Submitted to the Faculty
of the University of Miami
in partial fulfillment of the requirements for
the degree of Doctor of Philosophy

Coral Gables, Florida

August 2010

UNIVERSITY OF MIAMI

A dissertation submitted in partial fulfillment of
the requirements for the degree of
Doctor of Philosophy

SACROILIAC JOINT BIOMECHANICS: EFFECTS OF FUSION

Dinah Baria

Approved:

Loren Latta, Ph.D. Professor of Biomedical Engineering	Terri A. Scandura, Ph.D. Dean of the Graduate School
Weiyong Gu, Ph.D. Professor of Biomedical Engineering	Chun Yuh Huang, Ph.D. Professor of Biomedical Engineering
Peter P. Tarjan, Ph.D. Professor of Biomedical Engineering	Seth K. Williams, M.D. Assistant Professor of Orthopedics

BARIA, DINAH (Ph.D., Biomedical Engineering)
Sacroiliac Joint Biomechanics (August 2010)
And Effects of Fusion

Abstract of a dissertation at the University of Miami.

Dissertation supervised by Professor Loren Latta.
No. of pages in text. (166)

Lumbar spine fusion (LSF) is a common surgical procedure used in the treatment of lower back pain. Numerous studies have been conducted investigating the effects of LSF. Biomechanical studies have found that mechanical changes at adjacent joints create cumulative stress and pain, while clinical studies suggest that many patients develop symptomatic adjacent segmental disease (ASD) following LSF, which may necessitate additional surgery. Recently, ASD pain following LSF has been attributed to accelerated sacroiliac (SI) joint degeneration. Normal SI joints are mobile segments adjacent to the lumbosacral spine articulation and it has been hypothesized that altered biomechanics at the SI joints due to LSF could accelerate degeneration of the joints. The purpose of this study was to obtain a better understanding of the biomechanics at the SI joints and to determine whether LSF causes biomechanical changes at the SI joints. Six cadaver pelves were tested in flexion/extension, torsion, double leg compression and single leg compression, under four conditions: 1) intact, 2) after a 360º instrumented fusion at L4-5, 3) after a 360º instrumented lumbosacral fusion at L4-S1 and 4) after a unilateral SI joint fusion. Anterior and posterior SI joint movements were recorded during the study, along with load/displacement data. This study proved that motion does exist at the SI joints, although it is quite variable between specimens and between right and left SI joints within an individual specimen. It was also determined that changes in biomechanics do

occur at the SI joints following fusion (L4-5, L4-S1 and unilateral SI joint fusion). Anteriorly, an overall increase in motion was detected at the SI joints during axial compression as fusions were performed. The posterior SI joints also demonstrated increased motion, however, this increase was detected in all of the parameters tested (flexion/extension, torsion and axial compression). However, due to the small number and variability of specimens tested, significance could not be established. The results of this study may help surgeons make more informed decisions, by being made aware of SI joint degeneration as a possible side effect of fusion surgeries, and taking that into consideration when determining a treatment plan.

ACKNOWLEDGEMENTS

I would like to thank all the people that were involved, helped out and stood by me during this study. A special thanks to all the members of my committee Dr. Latta, Dr. Gu, Dr. Huang, Dr. Tarjan and Dr. Williams; Ted Milne and David Kaimrajh from the Max Biedermann Institute for Biomechanics in Miami Beach, FL; Dr. Ron Lindsey for realizing the importance of the SI joint and the need for research in this area and Dr. Rob Norton, an orthopedic resident at the University of Miami who had the thankless job of dissecting all the test specimens. Additionally, thank you to Biedermann Motech GmbH for their financial support of this study.

TABLE OF CONTENTS

LIST OF FIGURES

LIST OF TABLES

CHAPTER 1 - INTRODUCTION

Lower back pain is the fifth most common reason for physician visits in the United States and affects approximately one quarter of the adult population at some point during their life time.[12] Lumbar and lumbosacral spinal fusions are common surgical procedure used in the treatment of lower back pain. Numerous studies, clinical and biomechanical, have been conducted investigating the effects of spinal fusion on various parts of the spine; including the fused segment and adjacent segments.[3, 28,44, 70] Biomechanical studies show lumbosacral spinal fusions cause mechanical changes due to transference of forces to adjacent joints, which may create cumulative stress and pain that can reduce the functional capacity of the whole spine.[18, 25] Clinical studies show a range from 5.2% – 49% of patients undergoing lumbar fusion report an incidence of adjacent segmental disease.[28]

In the late 1980's, many physicians "rediscovered" the sacroiliac (SI) joint as a possible source of back pain. It has been found that a painful SI joint is a common cause of lower back pain, and the term SI joint dysfunction is used to describe the condition. Nonetheless, the SI joint is often overlooked as a cause of lower back pain due to the lack of proper understanding of this joint and its biomechanics. Many physicians are also reluctant to believe a joint that has such little movement, if any at all, could cause pain. However, studies have shown that the SI joint has been the cause of chronic lower back pain in 13% – 30% of patients.[7] One hypothesis for the cause of SI joint dysfunction is altered biomechanics of the SI joint as a result of lumbar/lumbosacral fusion and/or unilateral SI joint fusion.[43] In fact, Frymoyer et al. proposed the possibility of

accelerated degeneration of the SI joint due to lumbar fusion, though, their hypothesis was not confirmed by the study.[27]

Thus far, biomechanical and clinical studies have only examined the proximal segments adjacent to the lumbar/lumbosacral fusions. There has been no attention paid to the SI joint and how it is affected by lumbosacral fusion. The SI joint is a mobile segment that is adjacent to the lumbosacral segment (L5-S1), so it would only make sense to examine this joint as well. Ha et al. were the first to conduct a clinical study to determine the effect of lumbosacral fusion on SI joint degeneration. They found the incidence of degeneration at the SI joint was 75% higher in the group of patients with fusion than the control group of patients without lumbar fusion.[28] As of now, there have been no biomechanical studies of this sort, examining the effects of lumbar and lumbosacral fusions on the SI joint.

CHAPTER 2 - BACKGROUND

Anatomy of the SI Joint

Structure

The SI joint connects the spine to the pelvis and has multiple functions. It aids in absorbing vertical forces from the spine and transmitting them to the pelvis and lower extremities; it also allows forces to be transmitted from the extremities to the spine.[6,17, 48] The SI joint is a relatively immobile joint that connects the sacrum (the spinal segment that is attached to the base of the lumbar spine at the L5 vertebra) and the ilium of the pelvis. Each of the two SI joints are about 1-2 mm wide and join the spine to the pelvis and thus, the entire lower half of the skeleton. Figure 1 shows a diagram of the SI joint and its location relative to the whole skeleton.

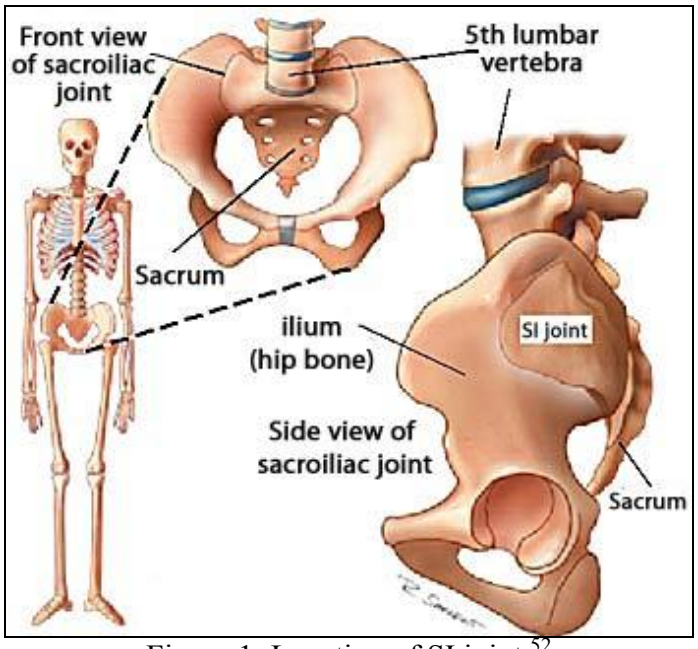

Figure 1: Location of SI joint.[52]

The SI joint is a strong, weight bearing synovial joint with articular cartilage on both sides of the joint surface. The SI joint is a very unique joint due to the fact that unlike any other joint in the body it is covered by two different kinds of cartilage; hyaline which has a clear, shiny "glass-like" appearance and fibrocartilage which is spongy in nature. The sacrum has a rough irregular surface with many large ridges and depression causing it to form an interlocking mechanism with the ilium, fitting together like pieces of a puzzle.[5, 62, 63] The SI joint is roughly six times more resistant to lateral forces than the lumbar spine, has 1/20 the resistance to forces in axial compression and 1/2 the resistance to rotational forces compared to the lumbar spine.[18]

Ligaments

The SI joint is held together by several ligaments including the anterior, interosseous and posterior SI ligaments. The anterior SI ligament, which can be seen in Figure 2, is not very strong and sometimes described as just a thickening of the anterior joint capsule. It consists of numerous thin bands that connect the anterior, lateral surface of the sacrum to the articular surface of the ilium.

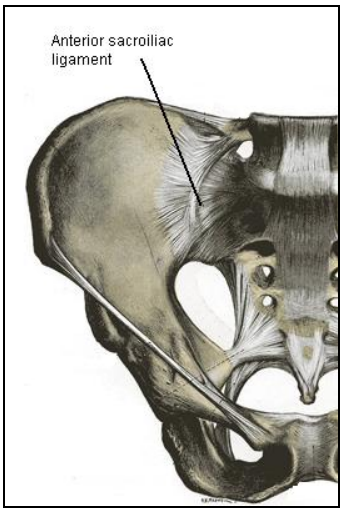

Figure 2: The anterior SI ligament.[18]

The posterior SI ligament is stronger than the anterior ligament and connects the sacrum to the posterior, superior iliac spine. This ligament is categorized into two sets; the short (superior) posterior SI ligament, which is nearly horizontal and the long (inferior) posterior SI ligament, which is vertical. An illustration of these ligaments and several others can be seen in Figure 3. The interosseous SI ligament is extremely strong and consists of a series of short, strong fibers connecting the sacrum and ilium deep within the joint. This ligament structure is actually stronger than bone, and the pelvis would fracture before the ligament would tear.[23]

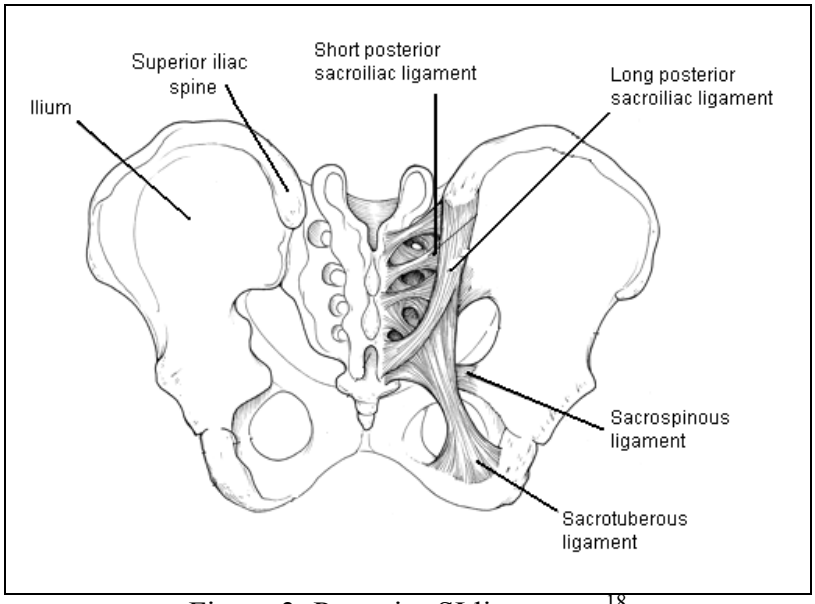

Figure 3: Posterior SI ligaments.[18]

Movement and Motion

The SI joint is a fairly stable joint and unlike most other joints, there are no muscles acting directly across it. Clinical SI joint motion is found using ultrasound or x-ray technology. Under normal conditions the motion of the SI joint is quite small, although there is much debate about how much it moves, or whether it moves at all. In

some cases it is thought that the SI joint may be completely ankylosed (stiffened or bound by adhesions) in as much as 76% of the population over the age of fifty.[67] Weigel, in 1955, conducted a study with cineradiographs and found a 5 mm ventral shift of the sacrum in relation to the ilium.[68] Frigerio et al. reported movements of 2.6 cm of the iliac crest in relationship to the sacrum in a 1974 study.[24] While Walheim and associates reported between 2 – 3 mm translations and up to 3 degrees rotational movement of the SI joint, with a single leg in vivo study.[65]

Motion of the SI joint is actually quite a controversial topic due to the complexity of the joint and the lack of proper understanding of its biomechanics. In 1911, the distinguished German anatomist Fick, described the motion at the SI joint as being "slight and merely of a rocking type."[67] While Bogduk described the motion as the ilium gliding backward and downwards during flexion of the hip, and the ilium glides forward and away from the sacrum during extension.[70] Kapanji describes the motion of the SI joint as having nutation and counter-nutation movements. Nutation comes from the Latin root meaning "to nod", and according to Kapanji, this was a good way to describe the complex movement of the sacrum, similar to nodding of the head.[32] There have been a few different theories and studies done on the movement and motion of the SI joint, yet no consensus has been reached. White and Panjabi summed it up well saying, "Relatively little is known about the kinematics of this important set of articulations, which constitute a fertile region for future research."[67]

Lower Back Pain

Back pain is a common ailment that affects both men and women equally, and is usually most prevalent in people between the ages of 30 and 50, due in part to the aging process and a sedentary life style. As people age, bone quality, muscle elasticity and intervertebral disc quality tend to decrease. During the normal aging process there is a loss of viable cells and modification of matrix proteins, which can lead to disc degeneration.[8] Though age is the most common cause of back pain, other causes include obesity/weight gain, poor physical condition, stress and bad posture. The lumbar/sacrum area of the lower back is predominantly the most common region where pain is felt. This is most likely due to the fact that the lumbar region of the spine supports the weight of the entire upper body, approximately 60% of total body weight. Figure 4 below illustrates the different regions of the spine and where they are located.

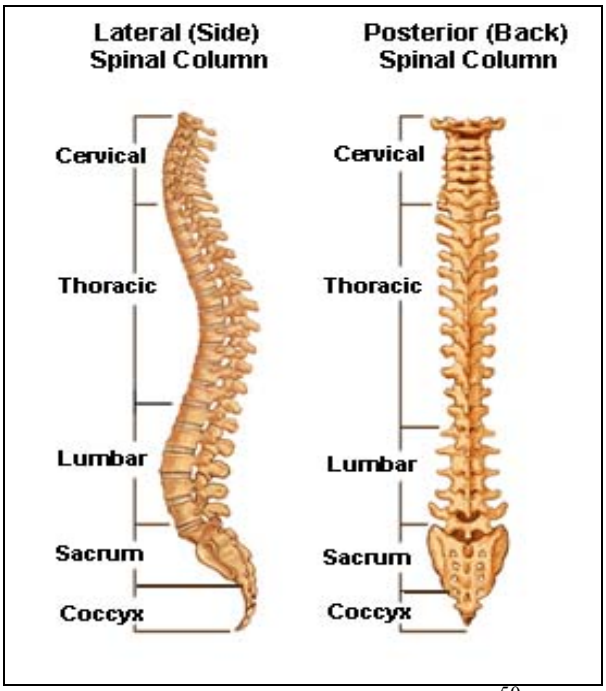

Figure 4: Segments of the spine.[50]

Back pain can be grouped into two categories, chronic and acute. Pain is considered chronic if it persists for more than three months and is often progressive. The exact cause of chronic back pain can be difficult to determine and may include disc disease and degeneration, spinal degeneration and/or arthritis. Degeneration of the discs and spine may lead to spinal stenosis, a condition where the space in the center of the vertebral body narrows and squeezes the spinal cord and nerve roots, causing pain in the back and extremities. Acute back pain usually lasts from a few days to a few weeks and is mostly mechanical in nature. It typically occurs due to trauma caused by injuries at home, work, sports or an accident. Examples of events that could cause acute back pain include lifting something too heavy, overstretching while exercising or being in an automobile accident. These events could possibly lead to a sprain, strain or spasms of the ligaments or muscles in the back, which in turn cause pain. If the spine becomes overly strained or compressed, a disc may bulge or herniate. In a herniated disc the outer layer of the disc, the annulus, cracks and the gel like substance of the nucleus breaks through, causing the disc to protrude and put pressure on the spinal cord and nerve roots, therein causing back and extremity pain. Figure 5 shows examples of disc problems, including bulging and herniated disc.

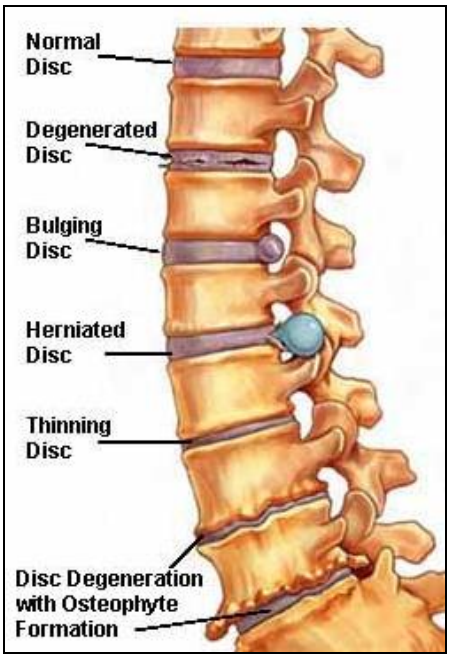

Figure 5: Intervertebral disc problems.[50]

Treatments

Though surgery is always the last option as a treatment method, sometimes it is unavoidable. Common surgical treatments for people who suffer from back pain include discectomy, laminectomy and/or spinal fusion. A discectomy is done by removing the pathologic disc that is between two vertebral bodies and is traditionally done in the case of a herniated, diseased or degenerated disc. Through removal of the disc, pressure is relieved from the nerve roots and/or spinal cord, thus alleviating the pain. A laminectomy, like a discectomy, is used to relieve pressure on the spinal cord and nerve roots by removing the curved posterior part of the vertebral body to make additional room at the effected area. Figure 6 shows a diagram of a vertebral body and its parts. Laminectomies are usually preformed due to spinal stenosis, bone spurs or any other reason causing the spinal canal to be compromised and apply pressure on the spinal cord.

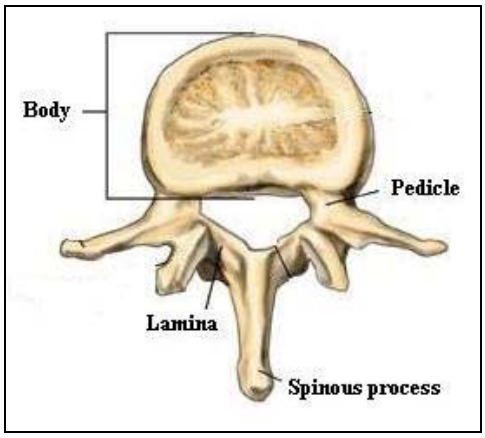

Figure 6: Parts of a vertebral body.

For both a discectomy and laminectomy, sometimes bone graft, interbody cages or pedicle screws may be used to strengthen the area.

Spinal fusion, also known as spinal arthrodesis, is a surgical technique where two or more adjacent vertebra are fused together to inhibit motion. This is done in a variety of ways, including the possible use of bone grafts, interbody cages and pedicle screws with rods. Spinal fusion is often done in addition to other procedures, such as discectomy, laminectomy or corpectomy, where a part of the vertebral body is removed. Grafts can be synthetic or autographs, coming from the patient's own body, usually from the pelvis. Grafts and interbody cages, hollow threaded titanium or carbon fiber cylinders, are placed in the open space between two or more vertebral bodies from where the disc(s) have been removed. The cages act to stabilize the fusion, while the graft material grows through the holes of the cages and fuses the vertebral bodies. Pedicle screws and rods are sometimes used in spinal fusions with the cage and grafts, or by themselves as a separate treatment option. The screws are placed in the pedicles of the vertebral body, above and below the area to be fused or treated. A solid or dynamic rod is used to connect the screws vertically, preventing or limiting movement in that area.

Adjacent Segment Disease

As with all medical procedures there are always some risks and side effects involved, lower back surgery is no exception. Risks due to surgery include blood loss, infection, nerve damage, and in the case of fusion surgeries, hardware and/or fusion failure. Even a successful fusion can pose a risk of developing adjacent segment degeneration and further complications. Clinical studies have suggested a noticeable increase in the rate and incidence of adjacent segment disease at levels immediately adjacent to fused segments.[2, 10, 22, 36, 55] Several biomechanical studies using animal and human cadaveric models also agree with the above statement of adjacent segment disease after spinal fusion surgery.[4, 13, 21, 29, 35, 70] Adjacent segment disease (ASD) is defined as degeneration that develops at mobile segments above and below a fused spinal segment. ASD was noted in cases nearly five decades ago and reported as a relatively unusual complication of lumbar or lumbosacral fusions.[1] Since these initial reports, it has been found that ASD occurs more often than originally thought and is now considered a potential long-term complication of spinal arthrodesis. The reason ASD is recognized as such a great problem is its potential to necessitate further surgical intervention and adversely affect the functional outcomes of the initial surgery.[10, 46, 55, 68] Interestingly, it was found that ASD is more common after lumbar or lumbosacral spinal fusions than after cervical fusions, and is fairly rare after thoracic procedures.[22] There is a great concern that ASD will become more widespread, due partially to the increased rate of spinal surgery in the United States over the past two decades and the fact that spinal fusions are now being preformed on patients at younger ages.[16] This growing concern

and the essential need for better understanding of this complication is the reason behind many clinical and biomechanical studies.[44]

The rationale behind fusion surgery is based on the assumption that symptoms can be relieved by eliminating motion in the degenerated/painful segment.[70] However, this may very well be the same reason for the development of ASD. The exact mechanism of why ASD develops is uncertain, though changes in biomechanical behaviors at fused and adjacent levels appear to play a key role.[44] These changes are presumably due to increased mechanical stresses on the adjacent segments after the fusion.[22, 29, 35, 70] Also, there is increased stiffness in the fused segment which leads to a compensatory increase in motion at the adjacent mobile segments. White and Panjabi have stated that there is a close correlation between the risk for developing adjacent segment disease and the magnitude of motion at a given level.[67] There is also increased intradiscal pressure, facet loading and hypermobility, which in animal studies have caused disc degeneration at adjacent levels.[44]

Certain factors have been found to increase the potential risk of ASD, one being the addition of instrumentation in fusion surgery, which can cause earlier development of ASD. In other words, the interval of occurrence of ASD after fusion with instrumentation appears to be shorter. Aota et al. found that the average time for a diagnosis of radiographic instability was 25 months after instrumented fixation[2] and Etebar and Cahill observed an average interval of 26.8 months before symptomatic ASD.[22] In contrast, two studies involving fusions without instrumentation found intervals of 8.5 and 13.1 years before the development of ASD.[36, 55] Other studies have also corroborated a trend toward earlier development of ASD with instrumentation.[11, 34]

This is most probably due to the immediate rigidity produced by instrumentation, which causes more stress, leading to accelerated degeneration at adjacent levels.[22, 31] The number of segments fused can also increase the risk of developing ASD, since the longer lever arm, produced with multilevel fusions, causes more stress at the remaining free segments.[9, 13, 40] In the study by Etebar and Cahill, mentioned above, it was noted that 78% of their patients that had ASD involved fusions of two or more segments.[22] Two other clinical studies, one by Wimmer et al. and the other by Rahm & Hall, also observed a trend toward increasing ASD development with multilevel fusions.[49, 69]

Although many studies, including the ones mentioned above suggest a correlation between spinal fusion surgery and the development of ASD, some researchers have a differing view and are skeptical of this claim. Several researchers have argued that ASD is actually just a normal degenerative process, rather than a consequence of the biomechanical stresses caused by fusion surgeries. They state that most spinal fusions are performed for severe degenerative disease and it is not likely that the degeneration is isolated only to the treated segment(s). Therefore, the adjacent segments were already in the process of degenerating before the surgery and not caused by it.[30, 45, 56]

SI Joint Pain

Pain due to the SI joint can be a tricky situation and is often misdiagnosed as lower back pain. SI joint problems can create numerous symptoms including: back pain (particularly in the lower back), thigh pain, buttock pain, pelvic pain and gluteal or lower limb pain. Numbness, tingling, popping and clicking in the above areas are also

associated with SI joint dysfunction. These symptoms, if not examined properly by a person familiar with the lumbar and sacral region of the spine, can be misinterpreted as common lower back issues. Symptoms associated with SI joint dysfunction are usually found below the beltline and are commonly unilateral.[48] Under normal circumstances unilateral pain is 25% more prevalent over bilateral, due to everyday tasks such as walking, running, climbing stairs, etc. Unilateral SI joint pain has also been found to be quite common in athletes that participate in sports requiring frequent kicking, throwing or any other motion that involves asymmetrical loading.[51] Due to several factors, SI joint pain is also fairly common in women who are and have been pregnant. A major factor may be the release of relaxin, a hormone which allows the SI joints to relax and promotes the pelvis to expand and become more flexible in order to facilitate the birthing process.[17, 51] Other factors that may increase the chance of pregnant women developing SI joint pain include altered posture, weight gain, increased lordosis in the lumbar spine and the actual trauma caused during birth.

Diagnosis

Diagnosing the exact point where pain is coming from is a very important step in determining the right course of treatment. As mentioned above, many times SI joint pain gets misdiagnosed as lower back/lumbar pain. Appropriate diagnosis of SI joint pain usually begins with a proper patient history, which includes a family history and description/history of the pain. This would be followed by a clinical exam, possibly including x-rays or an MRI of the lower back/pelvis area. An X-ray or MRI can show abnormalities of the joints or ligaments in the area of the pain and it can help determine

the exact location. The clinical exam may include certain orthopedic tests to determine if the SI joint is the actual location causing the pain. If pain is found during these tests described below, it would be a good indicator that the SI joint is the cause of the problem. These tests include; the Distraction Test, where the SI joint is stressed by attempting to slightly pull it apart, the Compression Test, where the two sides of the SI joint are forced together, Patrick's Test, where the leg is brought up and bent at the knee, then pressure is applied to the knee to test for hip mobility. These procedures are performed on both sides in order to test both SI joints. The last test is the Gaenslen's Test, where the patient lies on an examining table with both legs brought up to the chest. The patient then shifts to the side of the table so that one buttock and leg drops over the edge, and the supported leg is flexed. If this position causes pain, due to the stress at the joint hanging over the edge, it is known there is a problem with that SI joint. Again, this test is preformed on both sides to test left and right SI joints.

Treatment

If it is found that the SI joint is the cause of pain, treatment will usually start with a conservative option. Manipulation or stabilization of the SI joint during physical therapy could be the first step in treatment. Manipulation would be used in cases where the SI joint seems to be “locked” or too stiff, and would attempt to increase mobility and function. This type of therapy would comprise of exercises and movements intended to loosen up the SI joint ligaments, allowing for normal movement and function. Conversely, in other cases, especially in those where arthritic changes are noticed, the opposite is done in the form of stabilization. Stabilization treatment is used to reduce the

mobility at the SI joint to eliminate or control pain. This may include exercises that strengthen the muscles in the pelvic area in order to stabilize and reduce movement of the loose joint.

Unfortunately, conservative treatments don't always work and in some cases, even apply. In this situation surgery has to be considered as a treatment option and for the SI joint this usually consists of fusing the joint. SI joint arthrodesis was often used as a treatment for arthritic joints for many years, however, is not that common anymore. Though it is still sparingly done when it is absolutely sure the SI joint is the source of pain and the surgeon feels it is necessary in order to alleviate it. A SI joint arthrodesis is performed by making a posterior incision over the SI joint (in the lower back) and inserting metal screws across the joint to hold the bones together. Sometimes, in addition to the screws, bone graft is also used. The bone graft is usually removed from the pelvic bone right beside the SI joint and placed around the joint to help fuse it. Typically it takes 12 to 18 weeks for the fusion to become strong enough to resume normal activities.

Adjacent Segment Disease and the SI Joint

As discussed earlier, adjacent segment disease is quite prevalent after lumbar fusion surgeries. Therefore, logic would dictate that a fusion of the lower lumbar or lumbosacral region would probably affect the SI joint in the same way, since it is the next adjacent joint to the lumbosacral segment (L5-S1). The same could be said about a unilateral SI joint fusion and its affect on the ipselateral SI joint. It is hypothesized that the increase in rigidity of the lower lumbar spine associated with fusion at one or more levels will cause an increase in loading on the SI joint. This could therefore cause

abnormal movements and strains on the ligaments and the joint itself, perhaps leading to back spasms, pain and arthritic changes that could necessitate additional surgery. It has been said that not only can spinal surgery cause SI joint pain, but is one potential cause of failed back surgery syndrome (FBSS), and tends to be more common after lumbosacral fusions.[26, 60, 64] Many researchers think that spinal surgery can increase impact loading on the SI joint leading to mechanical overload and sacroiliitis.[25, 26, 35, 37, 70] There have been a few clinical studies done that corroborate this thought, Maigne and Planchon conducted a study from 1996 to 2002, where they saw sixty-one patients who were having pain after lumbar fusion. Among these patients, forty-five had unilateral persistent pain (or with unilateral prevalence) for more than 6 months with a sacroiliac origin.[39] Onsel et al. used SPECT to follow up on 753 patients complaining of lower back pain and found that patients who had increased uptake of the SI joint, 35% (15 of 43) had prior lumbar laminectomy and/or spinal fusion. They concluded that the sites of increased SI joint uptake were most likely due to mechanical sacroiliitis created by altered postoperative spinal mechanics.[43] In 2005 Katz et al. used fluoroscopically guided SI joint injections to identify the cause of lower back pain in patients following lumbosacral arthrodesis. They followed 34 patients and found SI joint dysfunction to be the cause of pain in 32% of the patients. They stated, that at that time, it was the first report of a large number of patients who had SI joint pain after lumbar fusion to the sacrum.[33]

Many studies have been conducted attempting to study the effects of spinal fusion on various parts of the spine, within and beyond the fused segments.[70] However, up to date, only one clinical study has investigated lumbar and lumbosacral fusions and how they effect the SI joints. Ha et al. conducted a study in which they examined thirty-two

patients who underwent decompression and instrumented posterolateral lumbar and lumbosacral fusion, and compared them to a control group of thirty-four patients with no history of spine or SI joint surgery or disease. They found a significantly higher rate of incidence of SI joint degeneration in the fusion group by 75% over the control group. Additionally, they divided the fusion group into two sub-groups; group 1 underwent lumbar surgery (not including S1) and group 2 underwent lumbosacral surgery (including S1). Interestingly, they found the incidence of SI joint degeneration to be higher with group 2 patients over group 1. However, they concluded that regardless of whether the fusion involves S1 or not, the forces that develop as a result of fusion increase the mechanical stress that is transmitted to the SI joints and accelerate degeneration; even though SI joint degeneration developed more frequently when fusion included the sacrum (S1). They also recommended that surgeons be aware and consider SI joint degeneration before and after instrumented lumbar/lumbosacral fusion.[28]

There have been many biomechanical studies done on lumbar/lumbosacral fusion and its effects on developing ASD, however, most of these studies focused on the proximal segments adjacent to the fusion site.[2, 20, 22, 34, 49] As of now, there have been no biomechanical studies done to examine the effects of lumbar/lumbosacral fusion on the SI joint. A study of this type would provide valuable data that could aid in the further understanding of the SI joint and how the altered mechanics of a lumbar/lumbosacral fusion could cause changes and degeneration.

CHAPTER 3 - PURPOSE

It is thought that there is a connection between certain spinal procedures, such as fusions, and an incidence of SI joint problems. This could possibly be due to altered biomechanics of the SI joint as a result of lumbar/lumbosacral fusion.[43] Researchers have proposed, but not yet proven, the possibility of accelerated degeneration of the SI joint due to these fusions. It seems this may just be another form of ASD, which is widely recognized in other areas of the spine, yet, has not been looked at in terms of the SI joint.

The purpose of this study is twofold, the first is to obtain a better understanding of the SI joint and its biomechanics. The second is to observe the effects, if any, lumbar and lumbosacral fusions have on the joint and determine if the fusions cause biomechanical changes at the SI joints. During the course of this study an appropriate biomechanical testing configuration will be developed, that will allow for the measurement of the physiologic movements at the SI joints. Data shall be collected for a normal intact pelvis, after a single level 360º instrumented fusion at L4-L5, after a two level 360º instrumented lumbosacral fusion at L4-S1 and after a unilateral SI joint fusion.

The hypothesis of this study is measureable motion will be detected at the SI joints, and lumbar/lumbosacral fusions will alter the biomechanics at the SI joints. The increased rigidity associated with fusion will cause an increase in loading on the SI joints; consequently, this will produce atypical movements and increase strain on the ligaments and the joint itself. These atypical movements and altered biomechanics may, in turn, lead to ASD of the SI joint, which could possibly require additional surgery to correct.

CHAPTER 4 - MATERIALS AND METHODS

This study was performed at the Max Biedermann Institute for Biomechanics at The Pearlman Biomedical Research Facility at Mount Sinai Medical Center in Miami Beach, FL. The experimental portion of this study was conducted during the span of seven months from September 2009 through March 2010.

Materials

Six fresh frozen cadaver pelves consisting of an intact lumbosacral spine (L4-S1) were used in this study. All specimens had the pubic symphysis and SI joints, iliolumbar, sacrotuberous, sacrospinous and posterior SI ligaments preserved. With the aid of an orthopedic surgeon, the specimens were denuded; making sure no ligament or joint capsule was damaged in the process. The average age of the specimens was 56.5 years +/- 7.74 years, see Table 1 for information about the specimens. All the pelves were individually wrapped in plastic bags and stored in a freezer until they were ready to be tested. In addition to the fresh frozen pelves, six pairs of fourth generation composite bone femurs from Sawbones® (Pacific Research Laboratories, San Diego, CA) were used in this study.

The equipment used in this study included the MTS® (Eden Prairie, MN) model 858 MiniBionix II machine to apply all the loads and torques to the specimens, accurate to 1 N in axial loading and 0.1 N·m in torsion. The Selspot 3-D motion analysis system,

along with light emitting diode (LED) brackets, was used to track posterior motion between the sacrum and both ilia, accurate to 20 μm. Anterior motion at the SI joints was tracked using MicroStrain® (Williston, VT) differential variable reluctance transducers (DVRTs), accurate to 1.5 μm.

Specimen	Sex	Age
2	Male	58
3	Male	70
4	Female	57
5	Male	48
6	Male	56
7	Male	50
Average Age		56.5
Standard Deviation		7.74

Table 1: Specimen information.
(Note: Specimen 1 was used as a pilot test and the data was not analyzed in this study.)

Methods

The Methods section is broken down into four subcategories; development of the experimental model, specimen preparation, biomechanical testing and analysis of the data. For every specimen tested, a specific checklist was followed and all the tests were carried out identically. A sample copy of the checklist used may be found in Appendix A.

Development of the Experimental Model

The development of an appropriate experimental model was a long and arduous process. Many different materials and configurations were investigated, discussed, and tested before finalizing the experimental configuration. Initially, two major decisions had to be made; the first was what material should be used for the test specimens, Sawbones® or human cadavers. The second was whether to use a single or double leg stance testing model. Figures 7 and 8 show diagrams of a single and double leg stance model, respectively.

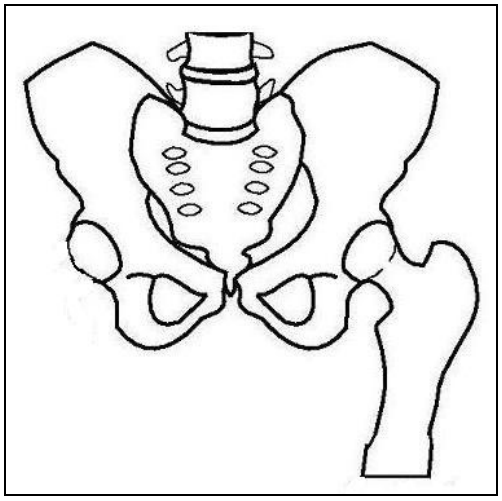

Figure 7: Example of single leg stance.

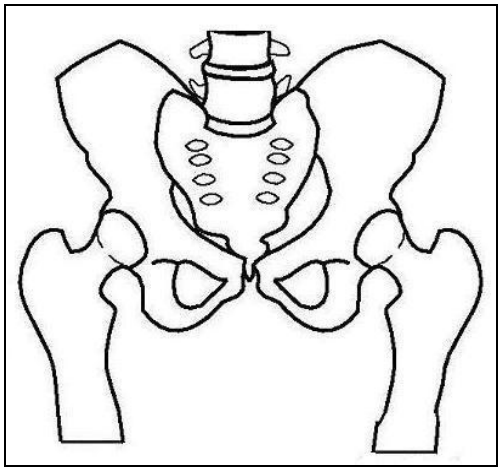

Figure 8: Example of double leg stance.

Sawbones® pelves would provide consistency among all test specimens and perhaps less variation would arise during testing due to the standardized specimens. The downfalls, however, include the lack of physiological hard and soft tissue and joint capsules. A human pelvis has complex parts and movements that would be lost with Sawbones® pelves and wouldn't accurately depict human biomechanics. According to numerous biomechanical studies of the SI joints and/or the pelvis, it was found that the majority of them chose to use cadaver specimens; only one study was found where Sawbones® specimens were used.[19, 41, 47, 53, 57-59, 71]

Multiple biomechanical studies were evaluated in the research of single and double leg stance testing models. A double leg stance simulates a patient standing with both feet planted on the floor, which is considered a typical situation for patients after early stabilization surgery and is therefore, the rationale behind choosing this model.[59] Many of the studies involving a double leg stance model used specimens with the proximal femurs intact, consequently resolving the concerns about how to attach the femurs to the pelvis and whether to use cadaver or Sawbones® femurs.[15, 58, 59] Nonetheless, this is not the only way to carry out a double leg stance test model. One study was found where bipolar cephalic hip prostheses articulated with the acetabulum, and the distal ends of the prostheses were potted in Cerrobend®, a low fusing alloy, in order to achieve the proper stance.[61] Conversely, other researchers believe the single leg stance model is optimal, claiming the double leg stance model fails to account for the large vertical shear and bending moments that occur during common activities such as walking, running and climbing stairs.[38, 54] Due to the asymmetry of a single leg stance, the position lends itself well to simulating gait in a static model and is historically most

often used in laboratory biomechanical studies.[41] A major issue that arises with the single leg stance model however, is the lack of stability (the pelvis only rests on one femur) and how to simulate the abductor forces which act as a counter balance to keep the pelvis in place. Many studies used a rope and pulley system to simulate the abductor forces,[38, 41, 47, 54] while one used a computerized linear actuator system.[42] A range of femur types were used in different single leg stance studies including prosthetic hip joints, Sawbones® femurs and cadaver femurs that were still attached to the pelvis.

There were three phases in the process of developing of a suitable experimental model. Phase 1 investigated the pelves without intact femurs, and a single leg stance. A Sawbones® femur was chosen, with the distal end being held in a vise, while the femoral head sat freely in the acetabulum. Turnbuckles were used to simulate muscle and ligament forces that act as the abductor mechanism attaching at the proximal femur and ilium, as discussed in multiple single leg stance studies.[38, 41, 54] Pins, used to anchor one end of the turnbuckle, were drilled into the ilium, while the other end of the turnbuckle was screwed into the proximal femur near the greater trochanter. This experimental model was unfortunately found to be quite unstable and could not withstand much force. The femoral head easily rotated in the acetabulum and caused the whole pelvis to fall over. In an attempt to establish greater stability an array of pin locations, in the ilium, were tried, however none were found to be satisfactory. This model was tested on both Sawbones® and cadaver pelves with the same problems arising for both. Additionally, osteoporotic cadaver pelves and certain thin areas in the Sawbones® pelves made proper pin purchase in the illum quite hard. The next step was to try a double leg stance to see whether it would provide additional stability. The same approach explained above was

used, however this time two femurs supported the pelvis. The distal ends of each femur were held in separate vises and the femoral heads sat freely in each acetabulum. Once more, turnbuckles were used to simulate the abductor mechanism and stabilize the model. The double leg stance was slightly more stable than the single leg stance; though the same problems with pin placement and purchase came up again. Additionally, slight movements could cause the whole pelvis to fall over and the set-up could not withstand ideal forces needed to simulate physiological conditions; therefore, this model was deemed unacceptable.

After additional literature reviews, an attempt was made to eliminate the unstable portion of the set-up by forgoing the hip joints, as seen in a few other biomechanical studies.[19, 53, 57] In this second developmental phase the pelvis was held by the ramus of each ischium by wrapping polymethylmethacrylate (PMMA) around the ramus and extending it out creating an area that can be gripped by a vise. Angle vises (one for each ramus), which allowed for lateral rotation, were used. Furthermore, one of the two vises was also mounted on a sliding plate, allowing for lateral translation. The concept behind using the angle vises and sliding plate was to allow the pelvis to move naturally, as it would under physiologic conditions, and not create supplementary shear forces. This test model was found to be quite stable and addressed many of the problems that came up in phase one. This test model was a major step in the right direction in determine an appropriate way to conduct the study, however, it also had some shortcomings. Questions arose on the accuracy of the physiologic loading; under normal circumstances, a person has their upper body weight distributed through the pelvis and down the femurs through the hip joints. In the Phase 2 model however, the force was being introduced

onto the ischium which is not a natural occurrence. Another question that came to mind was whether holding the pelvis by the ramus would allow for normal movements, or would it introduce shear forces and cause unnatural movement. Due to these queries, additional ideas were explored in order to determine whether an optimal model could be devised.

Phase 3 started with the decision to use femurs, as it was the best way to keep the test model as close to normal physiologic conditions. It was determined the femurs would be rigidly connected to the acetabulum by screwing them in place and making sure no motion occurred at the hip joints. This would allow the model to load properly through the acetabulum into the femurs, and also maintain stability. Eliminating motion at the hip joints stabilizes the test model in a simple maneuver, as one would expect to occur naturally when the muscles stabilize the hip joints during weight baring activities, and would not adversely affecting the outcome of the study. Initially, Sawbones® femurs were chosen to be used, however, after determining that cadaver pelves could be ordered with proximal femurs intact, this option was selected. It was also decided that a double leg stance would be used for flexion/extension, lateral bend and torsion testing, while a single leg stance would be used to test axial compression. The greater stability provided a double leg stance was the reason it was selected for tests that cause complex motions. Furthermore, the action of flexion/extension, lateral bending and torsion would normally happen while a person has both feet on the ground, hence, making the double leg stance an accurate choice for real life scenarios. As explained above, the single leg stance model is the most common choice for axial compression testing, simulating the

maximum and unsymmetrical forces a pelvis undergoes during common everyday activities such as walking, running or climbing stairs. [38, 41, 54]

Lag screws were used to secure the intact cadaver femurs to the pelvis and the distal ends were potted in PMMA to be gripped by angle vises, which allowed for lateral rotation (A in Figure 9 & 10). Additionally, one angle vise was mounted on a sliding plate, as described above, allowing for lateral translation (B in Figure 9 & 10) and the other vise was mounted on a stationary block in order to adjust for the height of the sliding plate. Theoretically, the angle vises and sliding plate would prevent unnatural shear forces on the pelvis and allow for free motion, without affecting the stability of the construct. See Figure 9 for a schematic diagram of the double leg test model and Figure 10 for the single leg model, which was created by removing a femur from the angle vise and letting it hang freely.

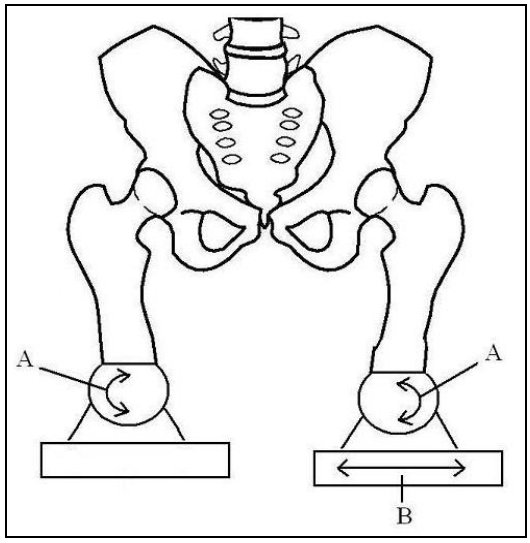

Figure 9: Schematic diagram of the double leg test model.

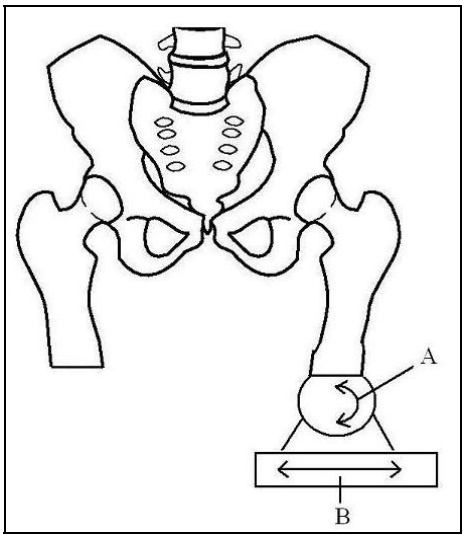

Figure 10: Schematic diagram of the single leg test model.

Two pilot tests were conducted to assess the experimental model and determine the proper loads and conditions needed to establish ideal physiologic conditions. Overall, the pilot tests were successful and helped to identify optimal testing conditions, however, some inadequacies were also found and had to be addressed. The first issue encountered dealt with using cadaver femurs. Initially, the lag screws rigidly held the femurs in place, yet, as testing progressed, motion was detected at the hip joint. Given the high forces and repetitive nature of the tests, it was found that the lag screws loosened in the cancellous bone of the femoral head. PMMA was applied around and injected into the femoral head in an attempt to prevent the loosening, however, it was unsuccessful. Due to this problem, it was decided Sawbones® femurs would be tried in the second pilot test to determine whether they would solve the loosening problem. During the second pilot test it was observed that the lag screws had much better purchase in the Sawbones® femurs and they were held in place, without motion at the hip joint, throughout the whole study. Therefore, the decision was reached to use Sawbones® femurs over cadaver femurs in the final test model. The second issue that came up during the pilot tests was the use of

the angle vises. They did not move with a smooth motion, and caused the test model to be too tall to fit properly within the MTS® frame. Replacing the angle vises with shorter stationary vises was decided as the best solution for this problem; yet the sliding plate was still be used. This decision was justified by the fact that hardly any movement was observed in lateral rotation, which was the reason behind using the angle vises in the first place. The test model was tried again with the stationary vises and sliding plate and it was observed that the sliding plate provided enough freedom of motion so no unnatural movements or shear occurred. A picture of the final test model can be seen in Figure 11.

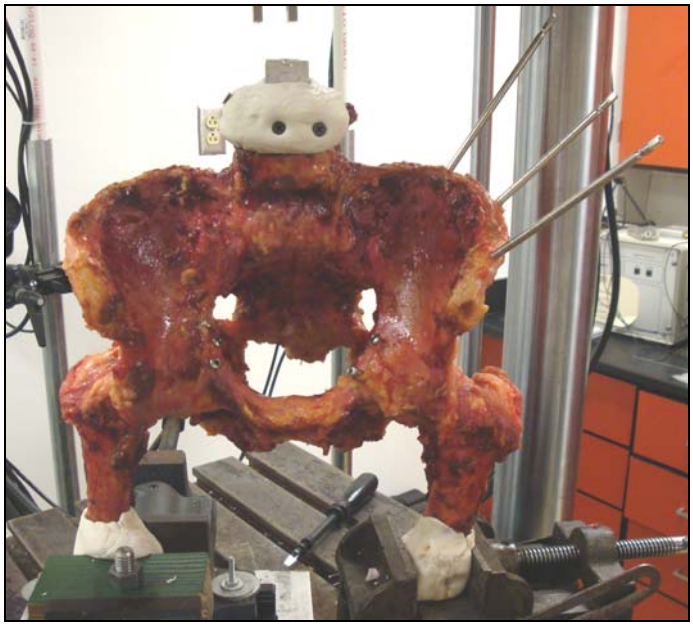

Figure 11: Final test model, double leg stance.

The final issue observed during the pilot tests dealt with the lateral bend test. Due to the width of a pelvis (compared to a spine) the current fixtures used to test lateral bend did not allow the MTS® machine to achieve optimal forces and range of motion. It has also been observed in the past, with previous spinal studies, that lateral bend tests take a major toll on the specimens, causing them to deteriorate more rapidly than usual.

Additionally, the data from the pilot tests showed that no motion could be detected at the SI joint during lateral bend, while motion was seen with all the other parameters (flexion/extension, torque and axial compression). Because of all these issues and observations, it was determined that the parameter of lateral bend would not be tested. Since one testing parameter was eliminated, it was decided axial compression with a double leg stance would be added in its place. This would allow for observations of what occurs at the SI joint during different phases of gait.

Specimen Preparation

Test specimens were removed from the freezer and thawed to room temperature the night before testing occurred. It was made sure the lumbar spine was intact and separated through the L3-L4 disc space. The specimens were then denuded, taking care to preserve the iliolumbar, sacrotuberous, sacrospinous, anterior and posterior SI ligaments, the pubic joint and the SI joints. Before testing, anteroposterior and lateral radiographs of the spines were taken to rule out any anatomic abnormality and make sure the pelves were suitable for testing. If a specimen had abnormalities, such as skeletal or bone disease, or signs of soft tissue disease, it was not used and another one was chosen in its place.

The Sawbones® femurs were cut at the distal diaphyseal, potted in PMMA and each was gripped in a vise while the PMMA was still soft to assure a good grip area/fit between the vise and PMMA. While the PMMA cured, specially made brackets for the DVRTs (two for each SI joint) were attached to the pelvis. This was done with exceptional care, using the fluoroscope to make sure each bracket was correctly placed on

either side of the SI joint, for both SI joints. Figure 12 shows a picture of two DVRTs attached to the bracket set-up on one SI joint.

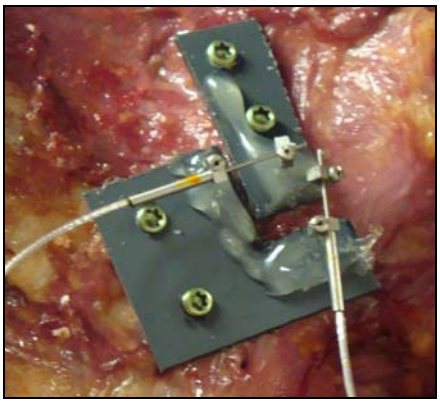

Figure 12: DVRTs attached to brackets.

In the next step the pelvis was attached to the proximal femurs using lag screws that went through the acetabulum into the femoral head; three to four screws were used on either side. During this process, it was made sure the pelvis was aligned to the center of rotation of the hip joint in the sagittal plane. In addition to ensuring the correct position, it was also important to make sure there was no motion at the hip joint, and the fixture was stable. Subsequently, the loading fixture block was mounted to the superior surface of L4, with PMMA, making certain it was centered and horizontally level on the vertebra, so the vertical compression load would be in line with the gravity load line of the lumbar spine. Three blunt-tipped half pins were then drilled into one iliac crest and used to anchor the turnbuckles that would simulate the abductor mechanism in the single leg stance model. One side of the turnbuckle was slipped onto the half pin, while the other side was attached to the proximal femur near the greater trochanter using screws and washers. Figure 13 shows the turnbuckle set-up that was used to simulate the abductor mechanism.

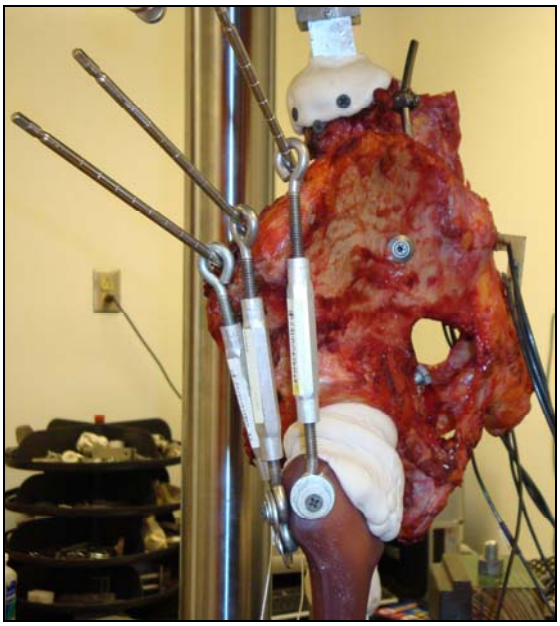

Figure 13: Turnbuckle set-up used to simulating abductor mechanism.

LED brackets, which work in conjunction with the Selsopt system to detect motion, had three LEDs mounted onto each bracket. Rubber cement was used around the LEDs to make certain they would stay in place and not fall out during testing. A total of three LED brackets were used in this study; one bracket was screwed into the posterior side of the sacrum, while the other two were screwed into the posterior side of each ilium. Each bracket was labeled with a number and the corresponding bracket number and its location on the test specimen were recorded. The sacrum and each ilium were considered rigid bodies and strain within them was deemed negligible. Therefore, it was not important to place the brackets in the same exact location, on the sacrum and each ilia, for different specimens since the measurements recorded were between two rigid bodies and only the relative movement between them was reported. Two Selspot cameras used to detect the LED motion and were calibrated before testing each specimen to make sure their parameters were properly optimized. The photograph in Figure 14 is a posterior view of a specimen with all LED brackets attached.

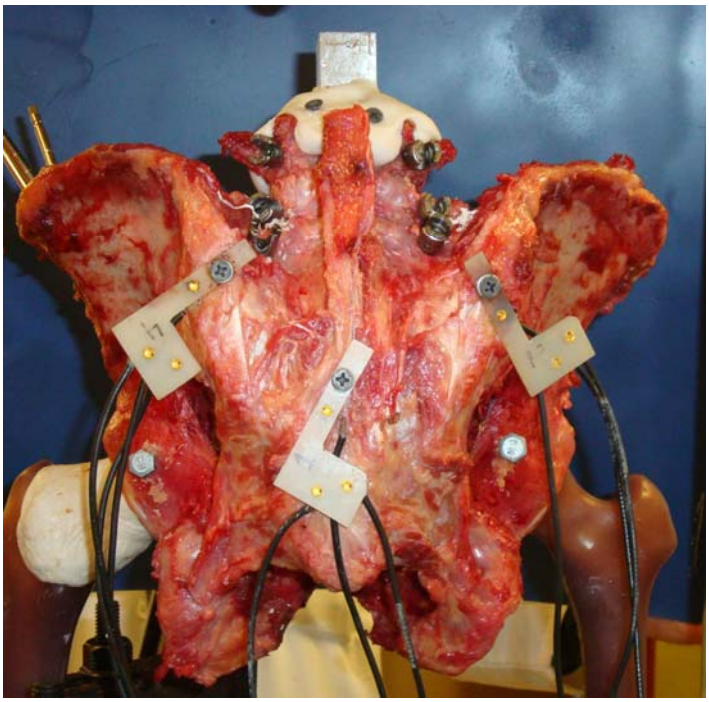

Figure 14: Test specimen with LED brackets.

The final step in preparing the specimen for testing was to attach the DVRTs. This was done last because of the delicate nature of the DVRTs, especially once they are attached to their brackets. A total of four DVRTs were used on each specimen, one horizontal and one vertical on each SI joint. Refer to Figure 12, above, for a picture of the DVRT set-up on one SI joint. The DVRTs were plugged into a multichannel MicroStrain® control panel that was color coded by channel. The channel and corresponding DVRT orientation and location, on the pelvis, were recorded for each specimen tested.

Testing of the Specimen

Once the specimen was prepared for testing it was secured onto the load cell table of the MTS® machine. Three motions; flexion/extension, torsion and axial compression (single and double leg stance) were simulated in each test specimen. All procedures were

done using the MTS® machine, flexion/extension and torsion tests were conducted in load control, while the axial compression tests were done under stroke control. An 8.5 N·m preload was added to the test specimen in order to induce proper coupled flexion/extension motion. The preload moment was applied in flexion by placing a 60 N (≈ 6 kg) weight on a lever arm, which was attached to L4, at a distance of 14.2 cm from the center of the vertebra. An x-y roller plate that allowed for free motion and eliminated shear was attached to the cross head of the MTS® machine with a clevis joint screwed into it. The clevis secured onto the extension end of the lever at a distance of 10 cm from the center of the L4 vertebra. The force applied by the MTS® machine cycled from 16.8 N to approximately 168 N during a single flexion/extension cycle; which resulted in an 8.5 N·m moment both in flexion and extension. A schematic diagram and photograph of the flexion/extension test set-up can be seen in Figures 15 and 16, respectively.

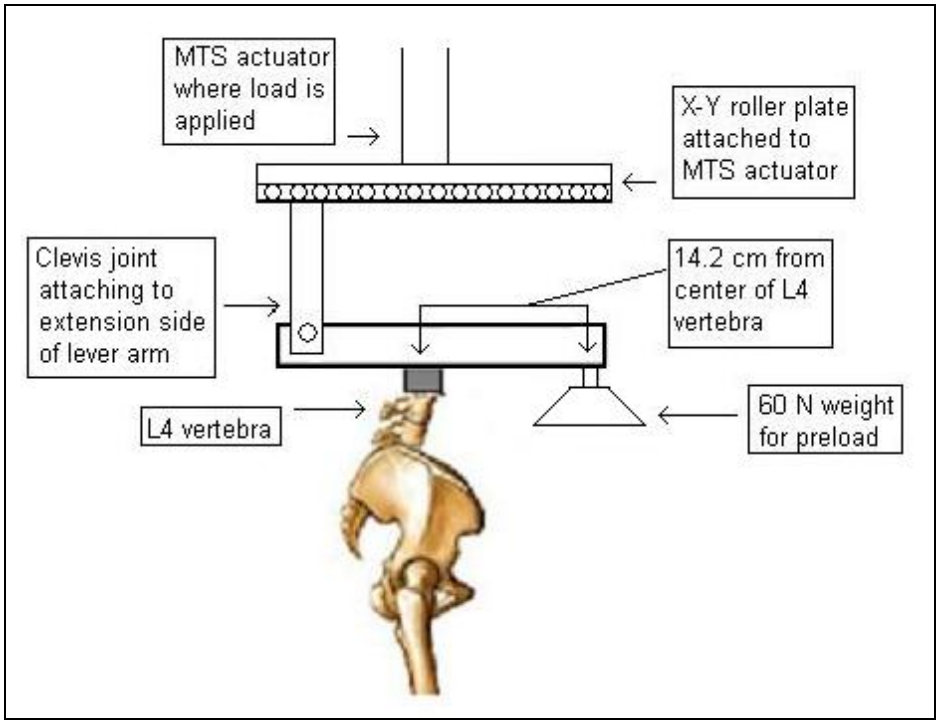

Figure 15: Schematic diagram of flexion/extension test set-up.

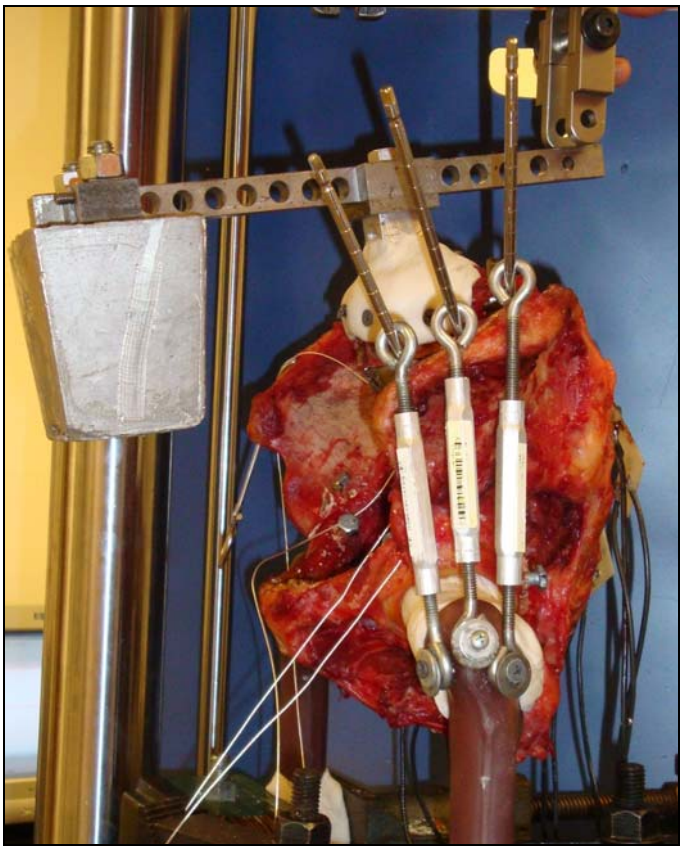

Figure 16: Photograph of flexion/extension test set-up.

For the torsion tests, the MTS® machine applied +/- 7.5 N·m moment to the specimen at 0.25 Hz. This means the specimen rotated 7.5 N·m in one direction from center/neutral, returned back to center and then rotated 7.5 N·m in the other direction. The axial compression tests were conducted with both a single leg and double leg stance in order to simulate various scenarios such as gait, with the single leg stance, and standing with the double leg stance. Compression forces used during double leg stance testing, cycled from 150 N to 1500 N (for male specimens) and 100 N to 1000 N (for female specimens); while in single leg stance, compression forces cycled from 60 N to 600 N (for male specimens) and 25 N to 400 N (for female specimens); both tests were cycled at 0.25 Hz. The loads used in this study were deemed appropriate to simulate physiologic conditions and were comparable to loads seen in other biomechanical pelvic

studies.[45, 56, 57, 69] The MTS® machine recorded load/displacement data during all the tests, which was later used to calculate the construct stiffness and neutral zones of each specimen.

In order to establish baseline data, all the specimens were initially tested intact. The measurements recorded were:

1) Load/displacement data from the MTS® machine.

2) Posterior motion between the sacrum and both ilia from the Selspot system.

3) Anterior motion at the SI joints from the DVRT system.

Following intact baseline testing, the specimens underwent a single level 360º instrumented fusion at L4-L5 with ALIF (anterior lumbar interbody fusion) cages and posterior fixation with pedicle screws and rods; the ALIF cages can be seen in Figure 17.

Figure 17: ALIF cages and screws.

After the L4-5 fusion was performed, the specimen underwent the same testing as the intact specimen and the same measurements (load/displacement data, posterior motion between the sacrum and both ilia and anterior motion at the SI joints) were recorded. The photographs in Figure 18 show the anterior (A) and posterior (B) sides of the test specimen after it underwent a 360º instrumented fusion at L4-5.

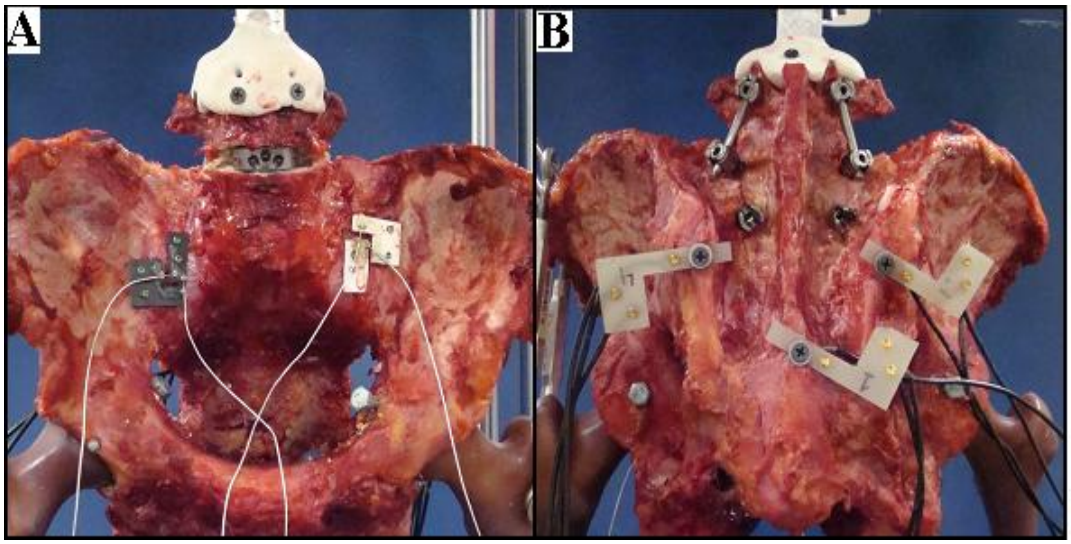

Figure 18: Anterior (A) and posterior (B) view after L4-5 fusion.

Following L4-5 fusion testing, the specimens underwent a two level 360º instrumented lumbosacral fusion at L4-S1, again with ALIF cages and posterior fixation. Once more, the specimens were tested in all directions (flexion/extension, torsion, single and double leg axial compression) and the same measurements were recorded. The photograph in Figure 19 shows an anterior view of a specimen after a 360º instrumented lumbosacral fusion at L4-S1.

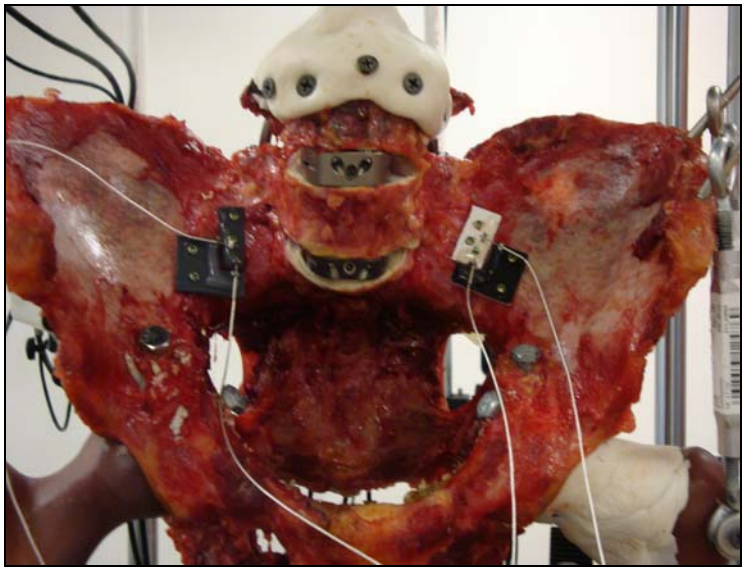

Figure 19: Anterior view of specimen after L4-S1 fusion.

The final testing step in this study was a unilateral SI joint fusion which was performed on the left SI joint, which was on the contralateral side of the femur that hung freely during single leg stance compression. The fusion was initially done using two seven mm cannulated cancellous bone screws; however, it was decided to switch to a single nine mm TSM screw, which can be seen in Figure 20, and was inserted from the lateral side, as would happen in a percutaneous screw fixation surgery for SI joint fusion.

Figure 20: TSM screw used for SI joint fusion.

Finally, following the unilateral fusion, the specimens were tested again in all directions and the same measurements, as stated above, were recorded. Figure 21 shows a fluoroscopic image of a SI joint fusion with the single TSM screw.

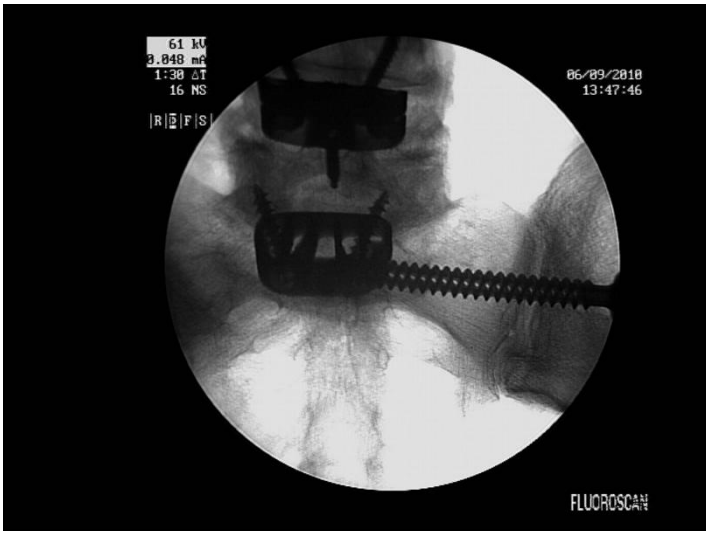

Figure 21: Fluoroscopic image of the single screw SI joint fusion.

After every testing step was completed on each specimen, all the hardware used for the fusions, the three blunt-tipped half pins, both the femurs and the test block on L4 were removed. The specimen would then be wrapped in a plastic bag and either placed back in the freezer for use in future experiments, or was discarded. If the specimen was to be discarded it was disposed of in a manner that was acceptable, and met all laboratory rules and regulations for human waste products.

Analysis of Data

The raw data measured in this study included:

1) Load/displacement data using the MTS® machine.
2) Posterior motion between the sacrum and both ilia using the Selspot system.
3) Anterior motion at the SI joints using DVRTs.

The raw data collected by the MTS® machine was used to create load displacement curves by opening the data in Microsoft Excel and taking the running average (40 point running average). The running average acts as a low pass filter and eliminates noise, creating a smooth curve. For each type of test; flexion/extension, torsion, single and double leg axial compression, the running average was used to plot a single cycle segment (each test went through anywhere between 10 – 20 cycles) creating the load/displacement curve. The displacement, in mm, is found on the X-axis and the load, in N, (or N·m in the case of torsion) is found on the Y-axis. Load displacement curves for all the specimens tested under every condition can be found in Appendix B.

The load/displacement curves for flexion/extension testing can be broken down into three parts, the top part of the curve shows the flexion segment, the bottom part

represents the extension segment and the middle portion is the neutral zone. The neutral zone is defined as "the displacement between the neutral position and the initiation point of spinal resistance to physiological motion."[65] The same concept holds true for the torsion curves, the top part of the curve is torque in one direction from neutral, the bottom part is torque in the opposite direction, and the middle represents the neutral zone. Due to these similarities, the shapes of the torsion and flexion/extension curves are comparable. Figure 22 is a sample load/displacement curve for a flexion/extension test with the flexion, extension and neutral zone segments labeled. These load/displacement curves were used to find the stiffness of the entire pelvic construct for all the different tests and conditions. This was done by identifying the straight line portions of the top and bottom of the curve and determining the equations for those lines.

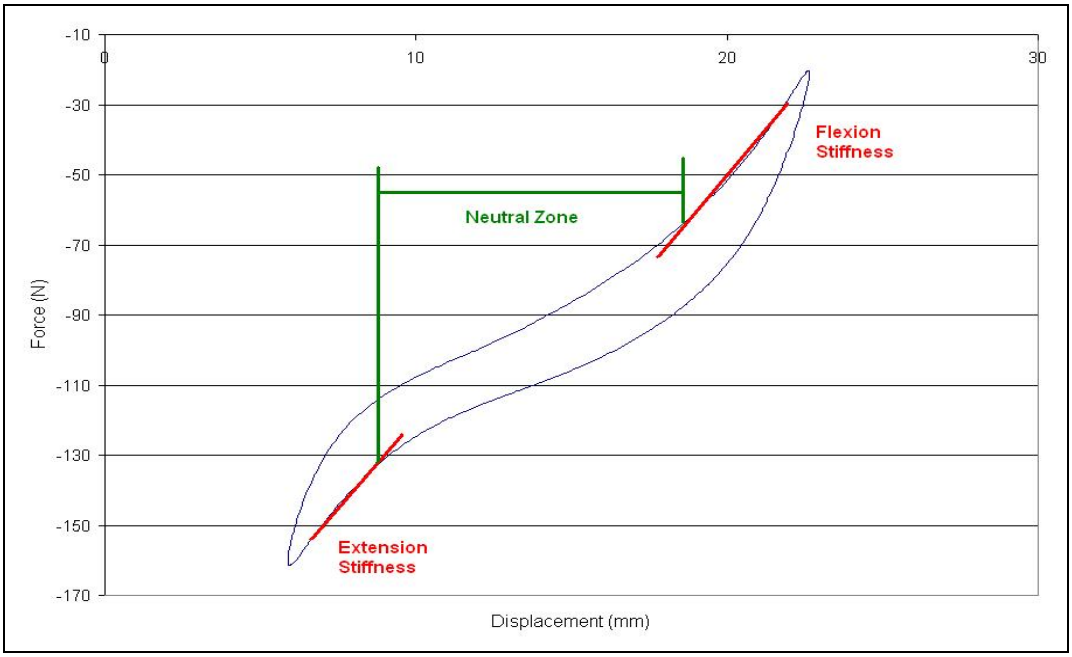

Figure 22: Sample load/displacement curve for flexion/extension tests.

The equation for each straight line portion was found using the "Trendline" function in Microsoft Excel, and the resulting slope of the line represents the stiffness value. For

flexion/extension tests, the straight line portion was identified for both the flexion and extension regions, allowing for separate flexion and extension stiffness values. For torsion, the straight line portion was identified for both top and bottom parts of the curve and the slopes were averaged to find an overall stiffness. The neutral zone values for both flexion/extension and torsion curves were found by extending out the straight line portion of the middle part of the curve. The distance between the points where the extended straight line bisected the curve, on either side, was the neutral zone. This was done to the top and bottom segments of the middle part of the curve and both neutral zone displacements were averaged for the overall neutral zone value.

Single and double leg stance axial compression tests had different shaped load/displacement curves than the flexion/extension and torsion curves, and were therefore analyzed slightly differently. The load/displacement curves in axial compression testing did not have a neutral zone, which was seen quite clearly by their oval shape in Figure 23.

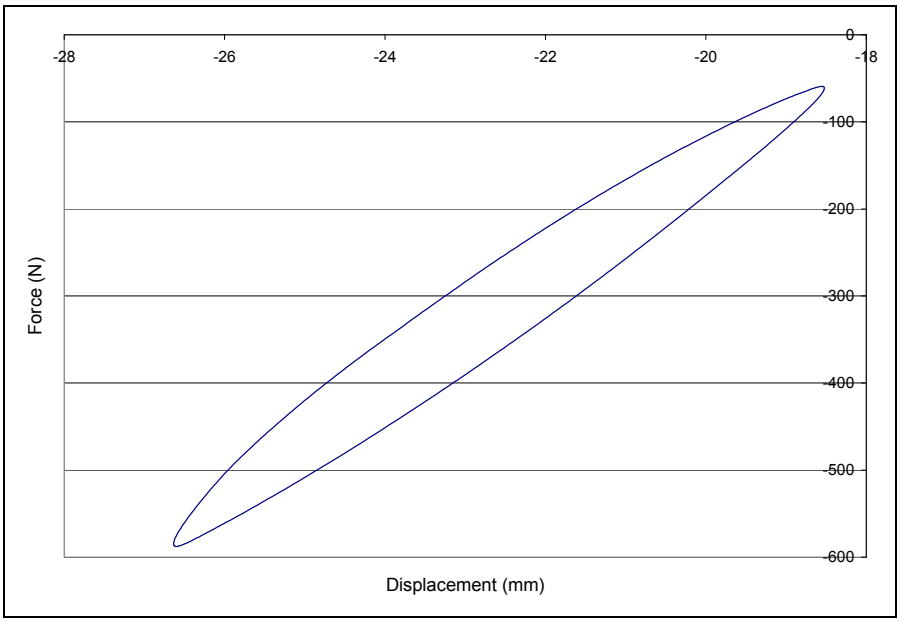

Figure 23: Sample load/displacement curve for axial compression tests.

The majority of the time, stiffness was calculated by applying an overall "trendline" to the whole curve, however, certain curves had a bend to them, causing the overall trendline to produce inaccurate results. In this case straight line segments on either side of the curve were identified and the slopes of these line segments were averaged to obtain the overall stiffness. An example of this can be seen in Figure 78 on page 117 in Appendix B, along with all the other straight line segments used to calculate stiffness.

The raw data collected by the Selspot system corresponded to the posterior motion seen by the LEDs and camera setup, and was used to calculate relative motion between the sacrum and each ilium. This motion was analyzed and output into useable maximum and minimum displacement values by the Selspot system. The data was divided into two parameters by the Selspot software, translation (in mm) and rotation (in degrees). Data for translational motion was collected in the medial-lateral (X-direction), anterior-posterior (Y-direction) and vertical (Z-direction) directions, while rotational motion was collected in the lateral, rotational and sagittal directions. Using the maximum and minimum displacement values obtained by the Selspot system, the motion range for each bracket (that had three LEDs on them) was calculated by subtracting the minimum displacement from the maximum displacement. To assure all the motion data was approximately in the same ballpark, outlier tests were preformed on all the calculated range values through box-and-whiskers plots using SYSTAT software. Motion between the sacrum and each ilium was acquired by subtracting the range value at the sacrum from the range value at each ilium. The absolute value of this range was used in order to eliminate negative motion value and taken as the relative motion of the SI joint.

The raw data collected by the DVRT system through the DataQ program was analyzed to determine anterior motion at each SI joint. The raw data was displayed in the DataQ program as sinusoidal shaped graphs, with the measurements in volts. Refer to Figure 24 for a sample of the raw data graphs in DataQ.

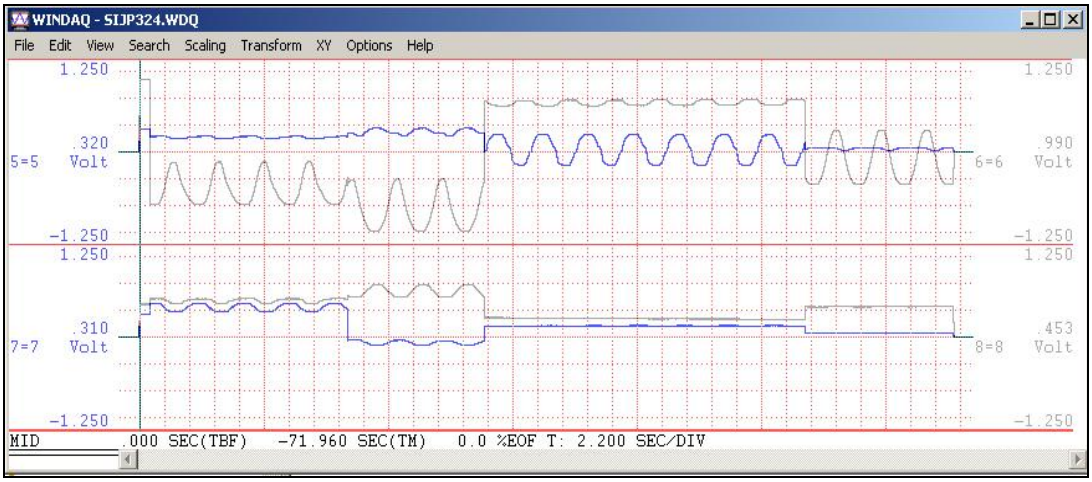

Figure 24: Raw DVRT data in DataQ.

The maximum and minimum voltage values were found by taking an average of the peaks (maximum) and valleys (minimum) during a test (three to four cycles were recorded during each test). These maximum and minimum voltage values were then converted to millimeters using calibration equations that were calculated and are individual to each transducer. The calibration equations were calculated for each of the four transducers (red, yellow, black and blue) with each of the four DVRT connectors. Four graphs were made for each transducer, one for every DVRT connector, and the average slope was used as the calibration factor to convert voltage to millimeters. Refer to Appendix C for the graphs and conversion equations for each transducer. The newly converted maximum and minimum displacement values were then used to calculate the range of motion in the SI joint by subtracting the minimum displacement values from the

maximum displacement values. Again, outlier tests using box-and-whiskers plots were preformed on all the calculated range values through the SYSTAT software.

Raw data collected by the Selspot system and the DVRTs for compression tests for specimen 4 (the only female specimen) were normalized to the rest of the specimens by multiplying the data by 1.5. This was done since the compression loads, for both single and double leg stance, on the female specimen were one and a half times lower than the compression loads on the male specimens.

CHAPTER 5 - RESULTS AND DISCUSSION

The purpose of this study was to obtain a better understanding of the biomechanics of the SI joint, and how it is affected by adjacent (lumbar/lumbosacral) fusion. It was found that motion certainly does occur at the SI joint, however, it can be somewhat variable among individuals and even in a single pelvis between the right and left side. As fusions were performed (L4-5, L4-S1 and a unilateral SI joint fusion) altered biomechanics at the SI joints were noticed; changes in the amount of motion and in the overall stiffness of the entire pelvic construct were observed. The results section is broken down into two major parts; intact SI joint biomechanics and effects of fusion on the SI joint. In the first section, the biomechanics of intact SI joints and their movements and orientations are discussed. In the latter section, the altered biomechanics observed after fusions are discussed and analyzed. Changes due to fusion were evaluated for statistical significance with a 95% confidence level using the Student's t-Tests, where statistical significance is defined as p-values of less than 0.05.

Intact SI Joint Biomechanics

In this section only the intact specimens and their motions and movements are discussed. This section is broken up into three parts: anterior SI joint motion, posterior SI joint motion and orientation of motion. All results and graphs reported in this section do not include data that was deemed to be outliers, unless specifically stated.

Anterior SI Joint Motion

As discussed earlier, anterior SI joint motion was measured using the DVRT system, with two DVRT transducers attached to each bracket set-up on each SI joint. Refer to Figure 12, in the *Specimen Preparation* section in the Methods subchapter (p.31), for a picture of the bracket and DVRT set-up on one SI joint. The data recorded, in volts, by the DVRTs were first converted to millimeters and then used to find the motion that occurred at each SI joint in the vertical and horizontal directions. As previously mentioned, a great deal of variability was seen between the specimens and also between the left and right SI joints within a specimen. This is not a new phenomenon, examining other studies of the SI joint it has been stated that there is wide variability in the adult SI joint, and disparities may even exist within a single individual.[14] One hypothesis for the variability between sides in a single specimen could be the dominant leg theory. Everyone has a dominant leg, for example this would be the leg an athlete prefers to kick a ball with or a dancer prefers to turn on. That dominant leg and SI joint get more use, especially in the case of sports or activities with repetitive movements, which could possibly promote stretching and loosening of the SI joint liagments, therefore causing more motion at one joint than the other. Interestingly, it is noticed that the SI joint that has greater motion in the vertical direction, is the same joint that has less motion in the horizontal direction. This can be graphically seen in Figures 25 – 27, as an average of all the intact specimens tested in; flexion/extension, torsion and double leg compression, respectively.

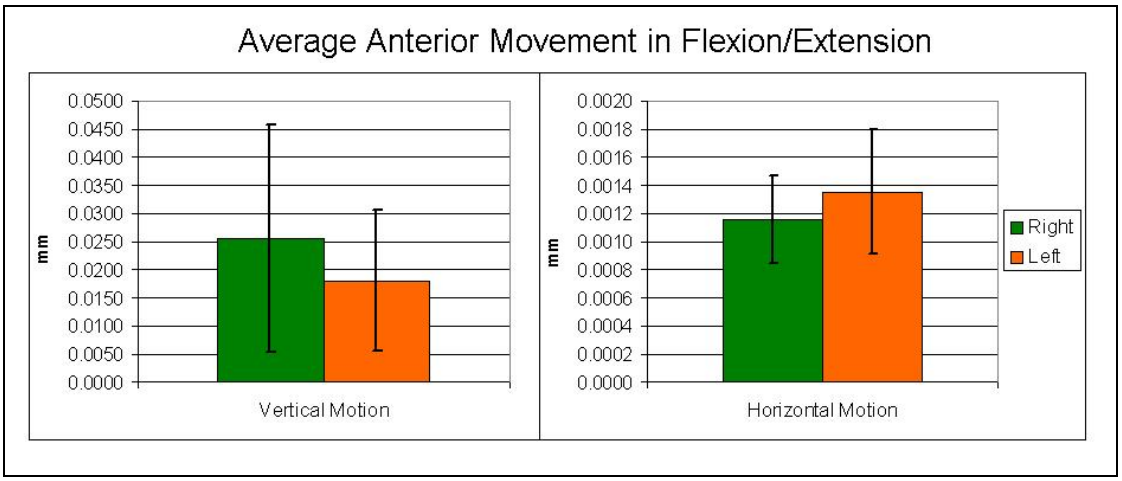

Figure 25: Average intact anterior movement in flexion/extension.

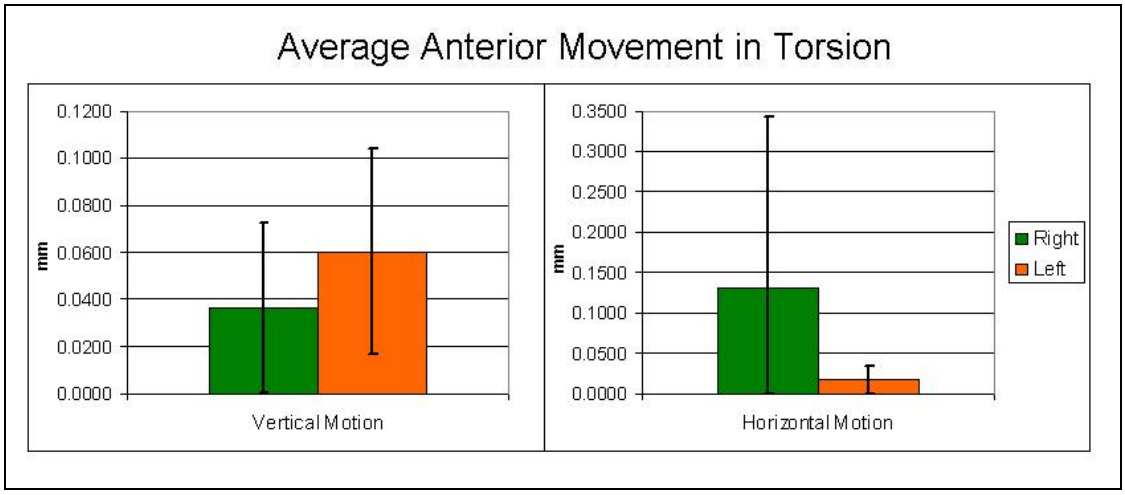

Figure 26: Average intact anterior movement in torsion.

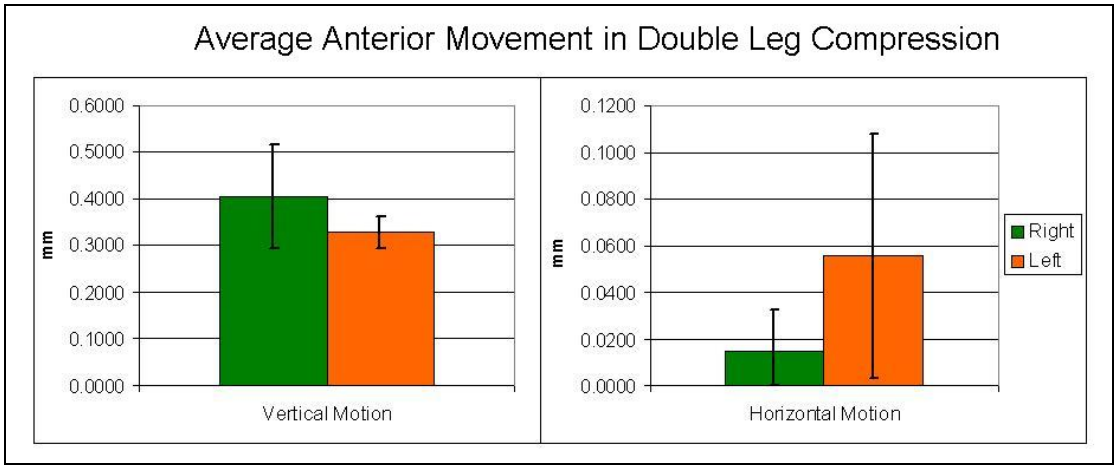

Figure 27: Average intact anterior movement in double leg compression.

The only exception was seen in the single leg compression test, where the left SI joint had the larger amount of movement in both the horizontal and vertical directions. This makes sense however, since the left leg was the one that was held stationary during this test parameter, and the forces applied to the construct translated down the left SI joint through the femur. Figure 28 shows a graph of the average anterior motion of all the intact specimens during single leg compression testing.

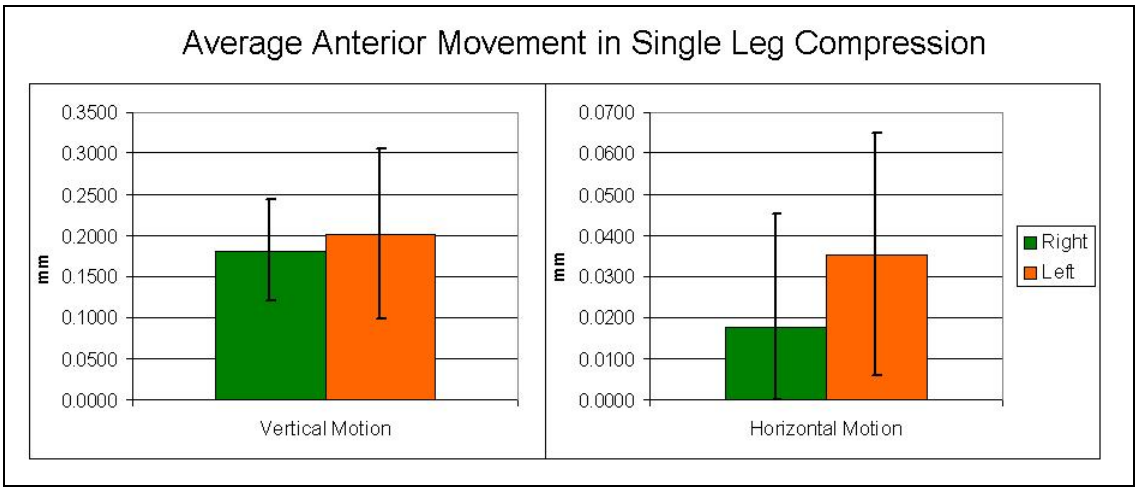

Figure 28: Average intact anterior movement in single leg compression.

The percent difference between the movements at the left SI joint and the right SI joint, for all the intact specimens tested in every parameter can be seen in Table 2. The differences in movement between left and right SI joints vary quite a bit, depending on test parameter and DVRT orientation, however, none of these changes were statistically significant; which could be due, in part, to the small sample size.

Percent Difference Between Left and Right SI Joint		
	Vertical	Horizontal
Flexion/Extension	159.2%	25.46%
Torsion	576.3%	182.4%
Double Leg Compression	28.43%	2580%
Single Leg Compression	54.81%	2475%

Table 2: Percent difference between left and right SI joint anterior movements.

No two human bodies are exactly the same and that couldn't be more apparent than with the SI joint. The motion that occurs at the SI joints differs quite a bit between specimens and also depends on the type of parameter being tested and direction of motion. It is important to note that Figures 29 – 36, and the numerical analysis of them, uses all the raw data, including outliers. This was done in order to show the wide range of motions that were found between specimens. Figures 29 and 30 show graphs for the anterior movements of all the intact specimens tested in flexion/extension in the vertical and horizontal directions, respectively.

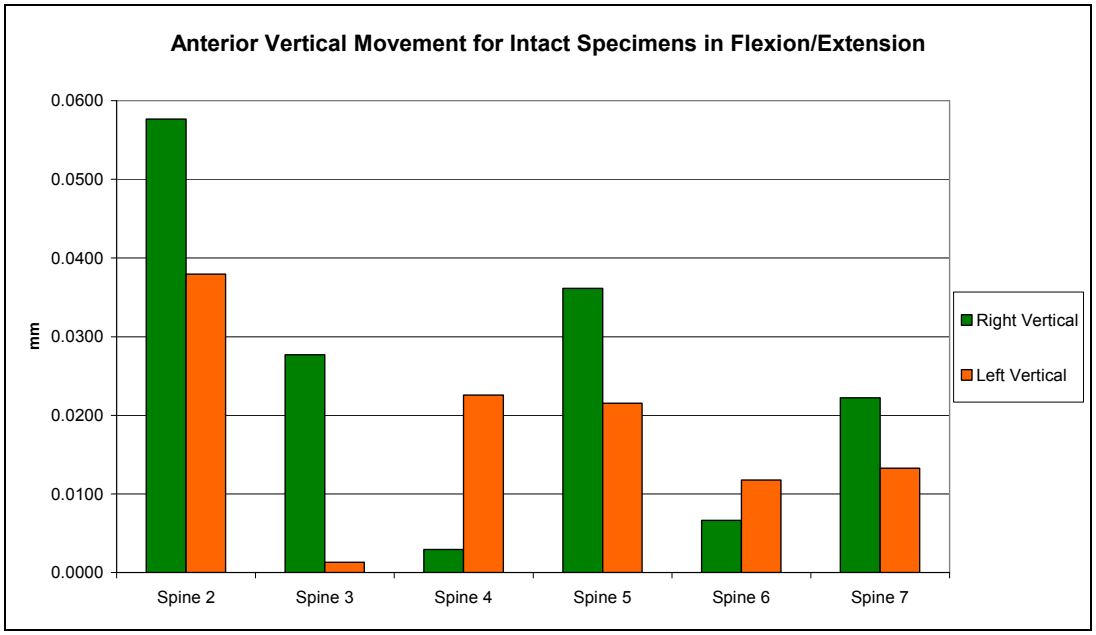

Figure 29: Intact anterior vertical movements in flexion/extension.

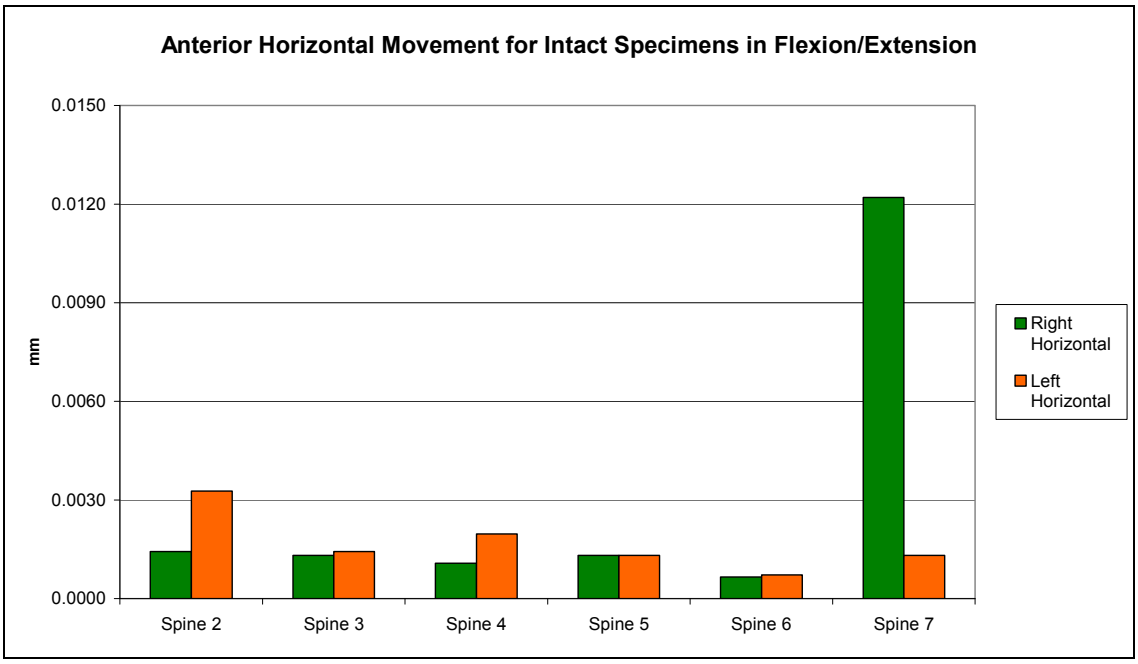

Figure 30: Intact anterior horizontal movements in flexion/extension.

A difference of 0.0547 mm was found between the highest and lowest amount of movement in the vertical direction for the right SI joints and a 0.0366 mm difference for the left SI joints. In the horizontal direction the right SI joints had a difference of 0.0115 mm between greatest and least amount of movement and 0.0026 mm for the left SI joints. Figures 31 and 32 show graphs for the anterior movements of all the intact specimens tested in torsion in the vertical and horizontal directions, respectively. A difference of 0.0949 mm was found between the highest and lowest amount of movement in the vertical direction for the right SI joints and a 0.1095 mm difference for the left SI joints. In the horizontal direction the right SI joints had a difference of 0.5143 mm between greatest and least amount of movement and 0.1373 mm for the left SI joints.

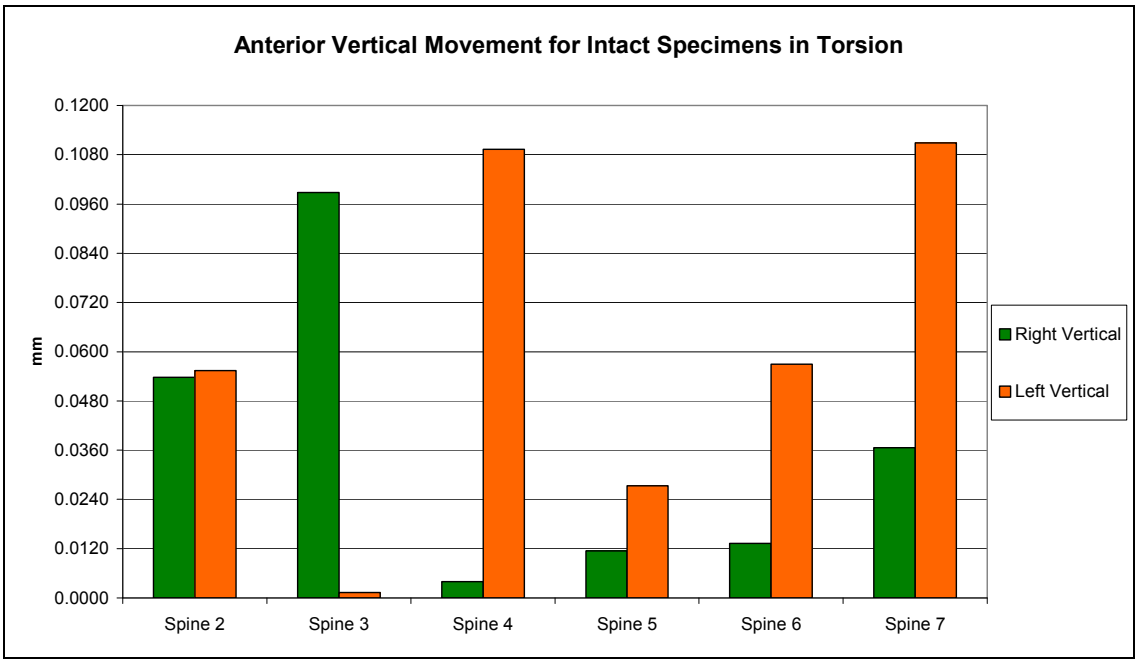

Figure 31: Intact anterior vertical movements in torsion.

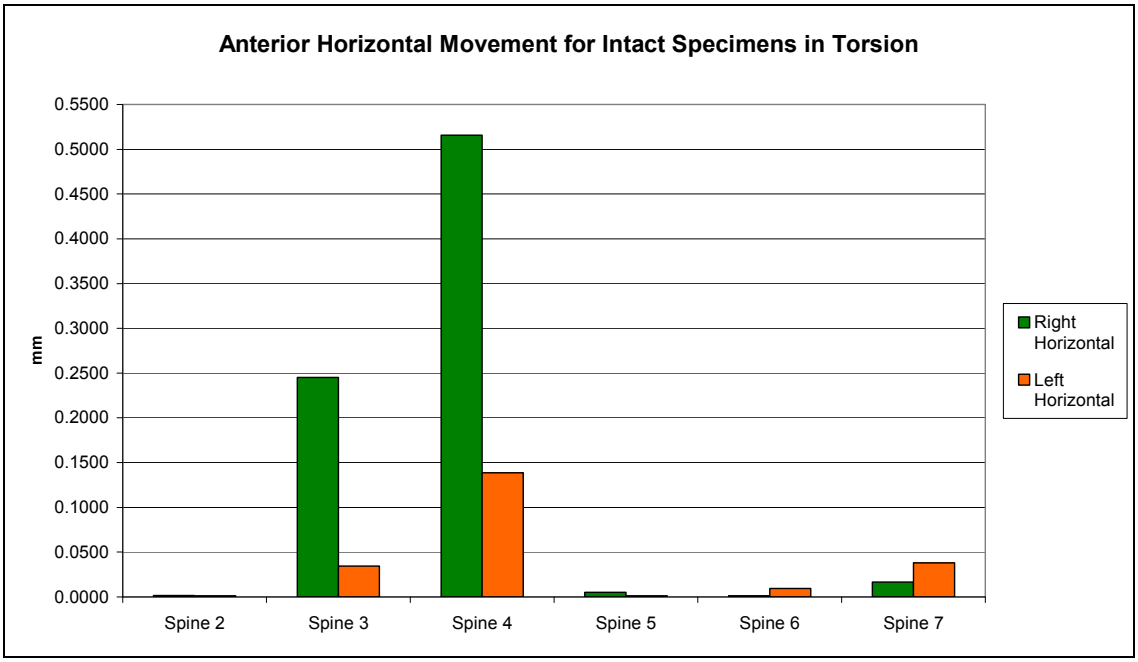

Figure 32: Intact anterior horizontal movements in torsion.

Figures 33 and 34 show graphs for the anterior movement of all the intact specimens tested in double leg compression in the vertical and horizontal directions, respectively.

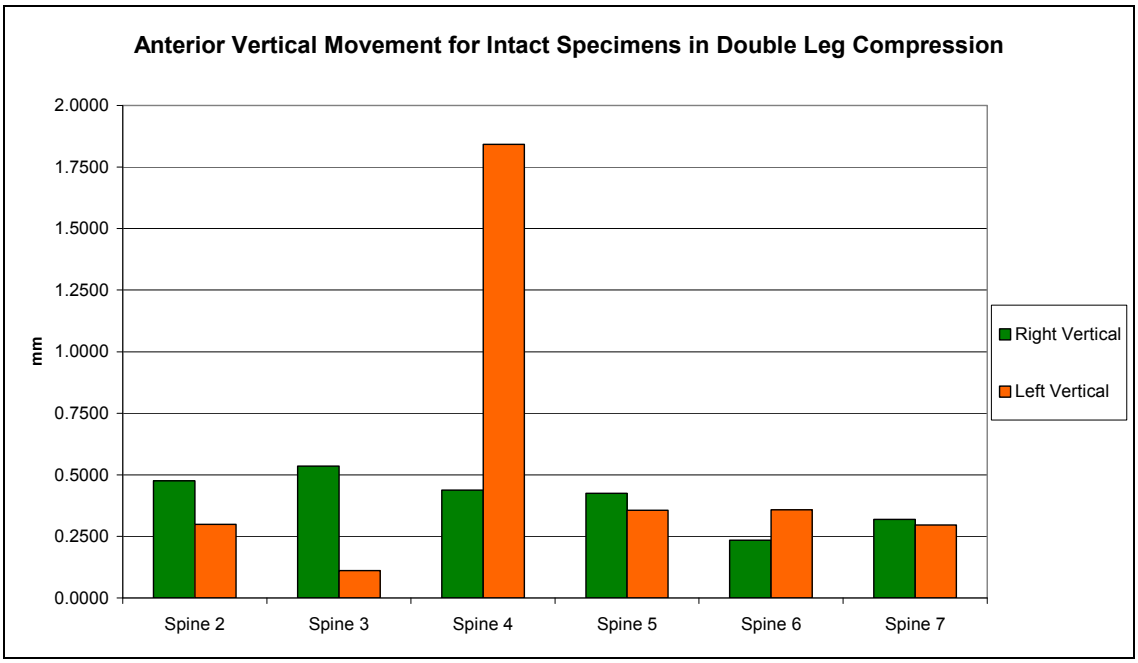

Figure 33: Intact anterior vertical movements in double leg compression.

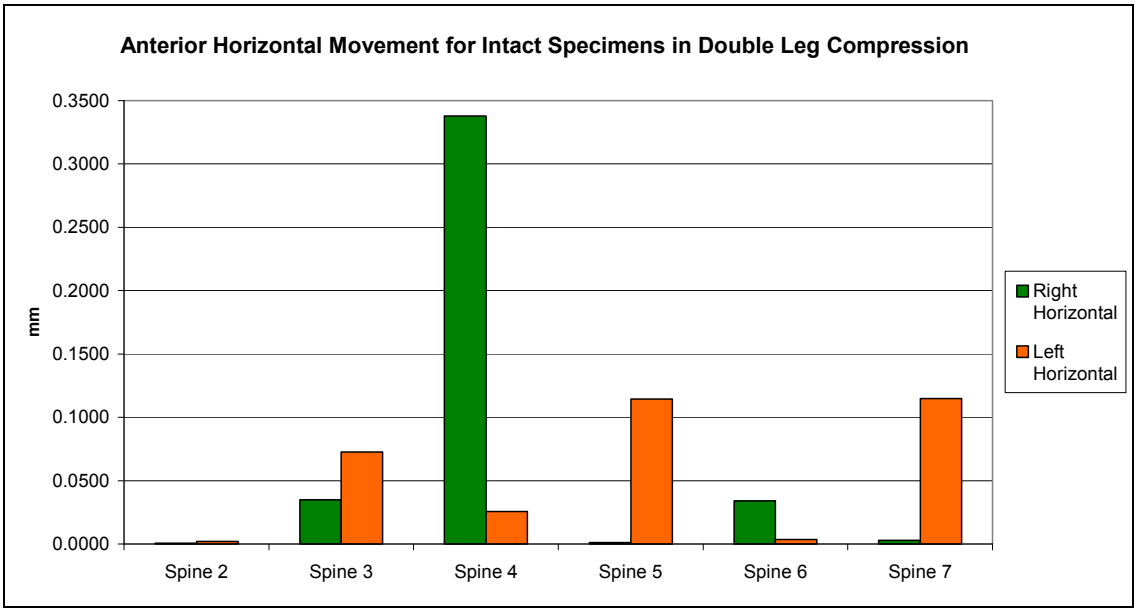

Figure 34: Intact anterior horizontal movements in double leg compression.

Comparing the highest and lowest amount of movement in the vertical direction for the right SI joints a difference of 0.3012 mm was found and there was a 1.7319 mm difference for the left SI joints. In the horizontal direction the right SI joints had a

difference of 0.3373 mm between greatest and least amount of movement and 0.1127 mm for the left SI joints. Figures 35 and 36 are graphs of the anterior movement of all the intact specimens tested in single leg compression in the vertical and horizontal directions, respectively.

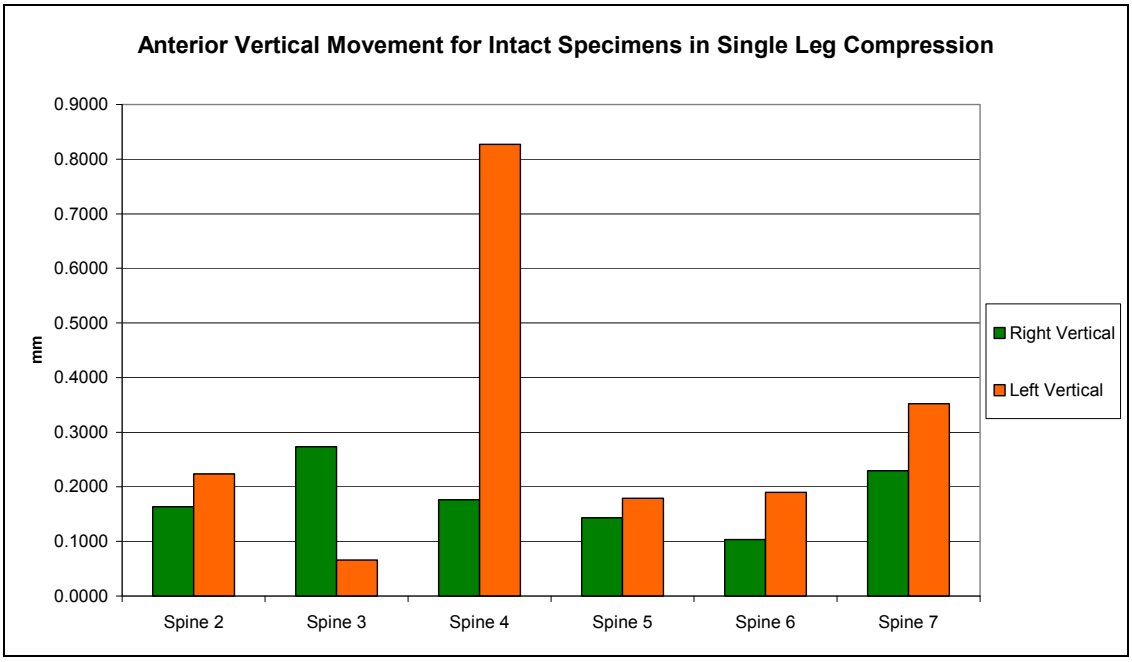

Figure 35: Intact anterior vertical movements in single leg compression.

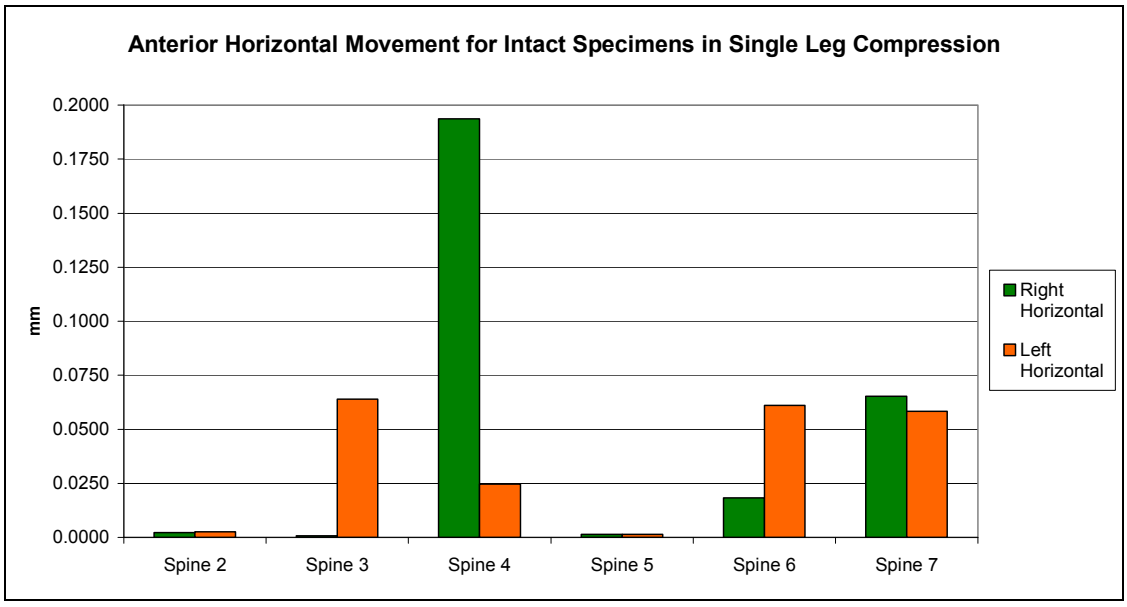

Figure 36: Intact anterior horizontal movements in single leg compression.

The difference that there was found between the highest and lowest amount of movement in the vertical direction for the right SI joints was 0.1699 mm, while a difference of 0.7607 mm was found for the left SI joints. In the horizontal direction the right SI joints had a difference of 0.1931 mm between greatest and least amount of movement and 0.0626 mm for the left SI joints.

As a result of using all the raw data, including the outlier points, some of the differences found between test specimens were fairly large. It is thought that the outlier points could have been caused by data that was incorrectly recorded or translated by the DVRT system, or in some cases it could just be the nature of the test specimen having elastic SI joint ligaments. Nonetheless, the graphs above still give a good perspective as to how movements differ between pelves. Table 3 shows a summary of the range of movements for all specimens and parameters tested, while Table 4 gives a summery of the range of movements after excluding outliers (ranges from which outliers were removed are highlighted in red).

Range of Movements in Intact Specimens with outliers (mm)				
	Right Vertical	Left Vertical	Right Horizontal	Left Horizontal
Flexion/Extension	0.0547	0.0366	0.0115	0.0026
Torsion	0.0949	0.1095	0.5143	0.1373
Double Leg Compression	0.3012	1.7319	0.3373	0.1127
Single Leg Compression	0.1699	0.7607	0.1931	0.0626

Table 3: Range of anterior movements for intact specimens with outliers.

Range of Movements in Intact Specimens without outliers (mm)				
	Right Vertical	Left Vertical	Right Horizontal	Left Horizontal
Flexion/Extension	0.0547	0.0366	0.0008	0.0012
Torsion	0.0949	0.1095	0.5143	0.0367
Double Leg Compression	0.3012	0.0620	0.0340	0.1127
Single Leg Compression	0.1699	0.2863	0.0646	0.0626

Table 4: Range of anterior movements for intact specimens without outliers.

Posterior SI Joint Motion

The raw data used to calculate the posterior SI joint motion was collected through the Selspot system. As mentioned earlier, the motion at each SI joint was found by subtracting the relative motion at the sacrum from the relative motion at either ilium. Therefore, the difference between the right ilium and sacrum represented the motion that occurred at the right SI joint, while the difference between the left ilium and sacrum signified the motion that took place at the left SI joint. The Selspot system recorded motion in six directions; three translational directions: medial-lateral (x-direction), anterior-posterior (y-direction) and vertical (z-direction), and three rotational directions: lateral, rotational and sagittal. The rotational movements that occurred at the SI joint were very small, if any; and it has been found in the past, that the Selspot system is not very accurate when it comes to small angle calculations. Therefore, it was decided that only the motions recorded in translation would be used and analyzed in this study. Similar to the anterior motion, the motion seen on the posterior side also had a great deal of variability, both between specimens and between left and right SI joints. During the flexion/extension test a large difference in motion between the left and right SI joint was seen in the anterior-posterior (y) direction. The medial-lateral (x) and vertical (z) directions however, showed relatively the same amount of motion at both SI joints. This can graphically been seen in Figure 37.

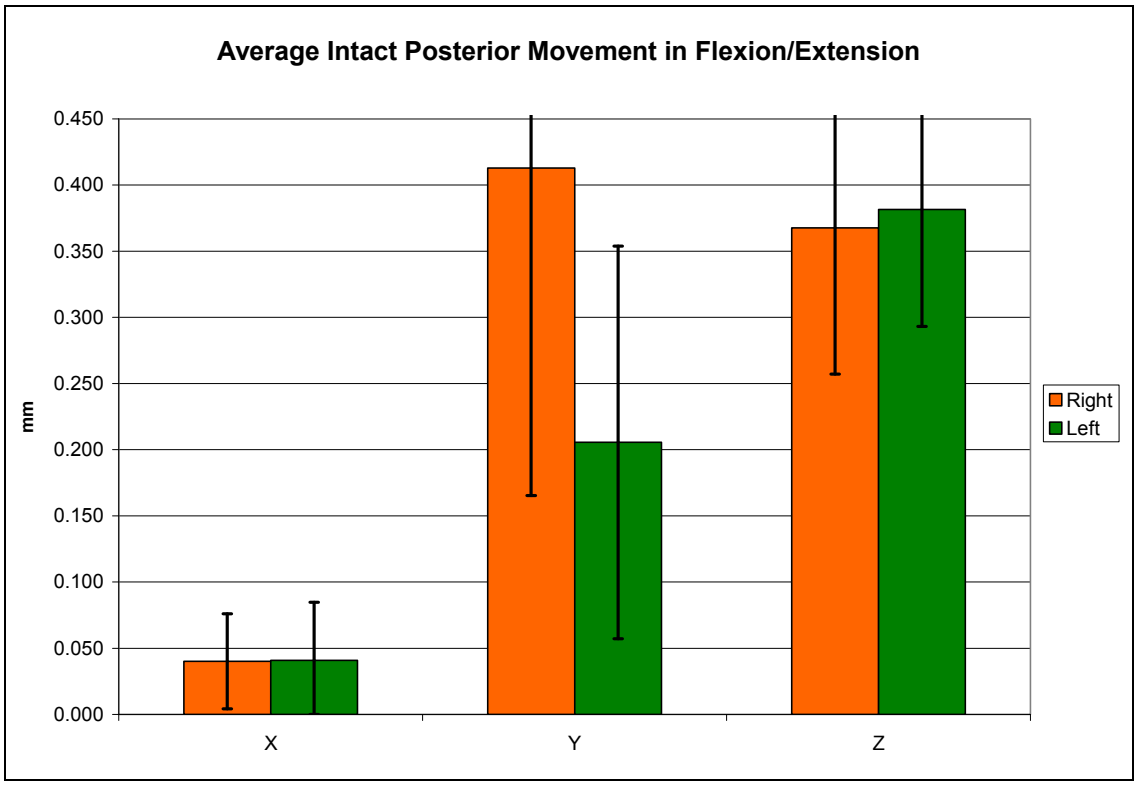

Figure 37: Average intact posterior movement in flexion/extension.

Notably, in both torsion and double leg compression tests the right SI joint had greater movement than the left in all directions; while for the single leg compression test the left SI joint had greater movements than the right. These trends seem to be intuitive for torsion and double leg compression due to the dominant leg theory and for single leg compression due to the left side being held in place while the right hung freely, as explained in the above section. Figures 38-40 show graphs that compare the right versus left SI joint movements for intact specimens in torsion, double leg and single leg compression, respectively.

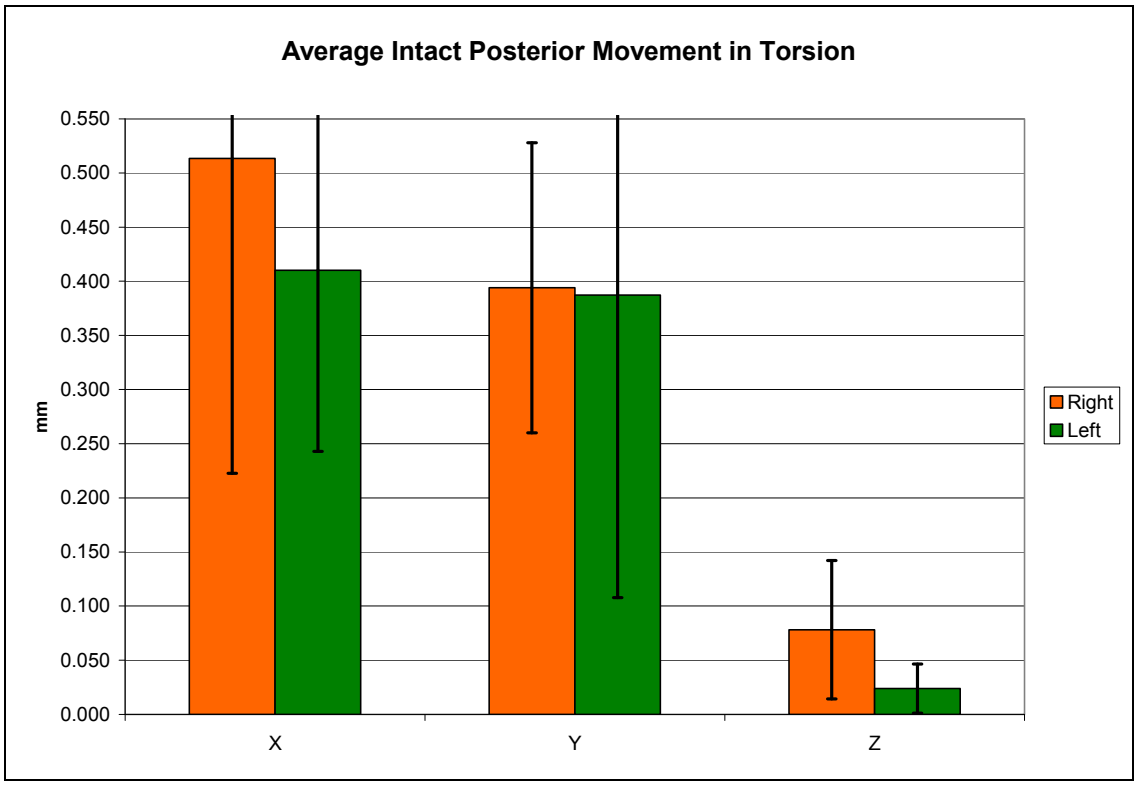

Figure 38: Average intact posterior movement in torsion.

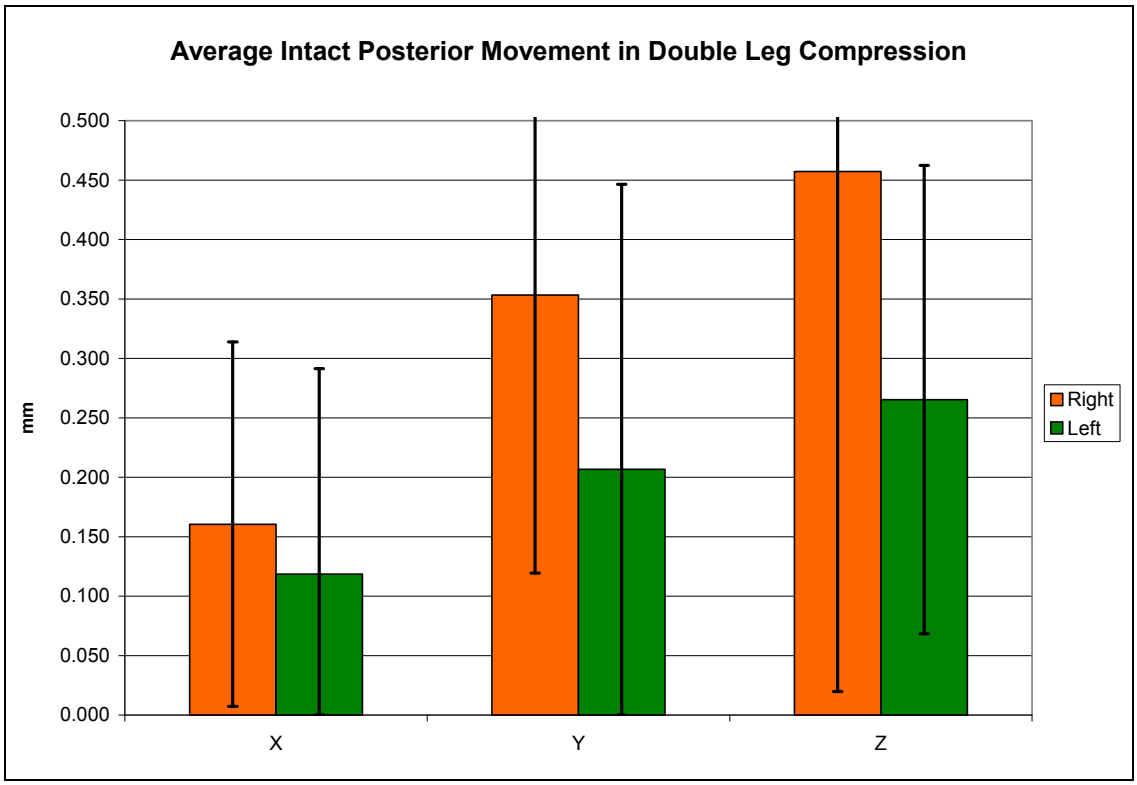

Figure 39: Average intact posterior movement in double leg compression.

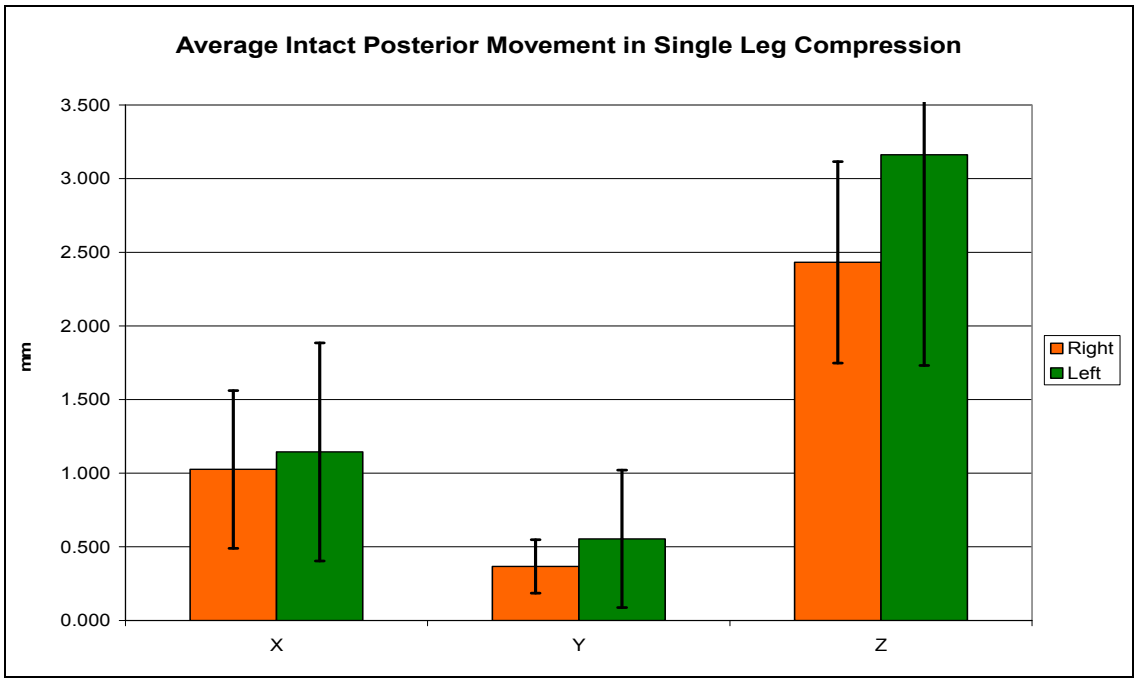

Figure 40: Average intact posterior movement in single leg compression.

In Table 5 shows the percent difference between the movements at the left SI joint and right SI joint, for intact specimens in all the testing parameters. Interestingly, a few of these differences were found to be statistically significant. The percentage difference between movements in the left and right SI joints in the anterior-posterior (y) direction were significant in flexion/extension ($p = 0.020$) and in double leg compression ($p = 0.010$), while the vertical (z) direction saw a significant difference in torsion ($p = 0.028$). There was no significance, in any direction, between the left and right SI joint movements in single leg compression. (Significance is highlighted in red).

Percent Difference Between Left and Right SI Joint			
	X	Y	Z
Flexion/Extension	1380%	50.7%	37.0%
Torsion	46.6%	45.8%	61.7%
Double Leg Compression	67.5%	53.9%	109%
Single Leg Compression	24.2%	85.1%	53.5%

Table 5: Percent difference between left and right SI joint posterior movements.

Once more, the variability between specimens can clearly be seen with the posterior movement data and an overview can be seen in Figures 41-44. As it was in the anterior section, the following graphs use all the raw data, including outliers, to visually show the extensive differences in motion found between specimens.

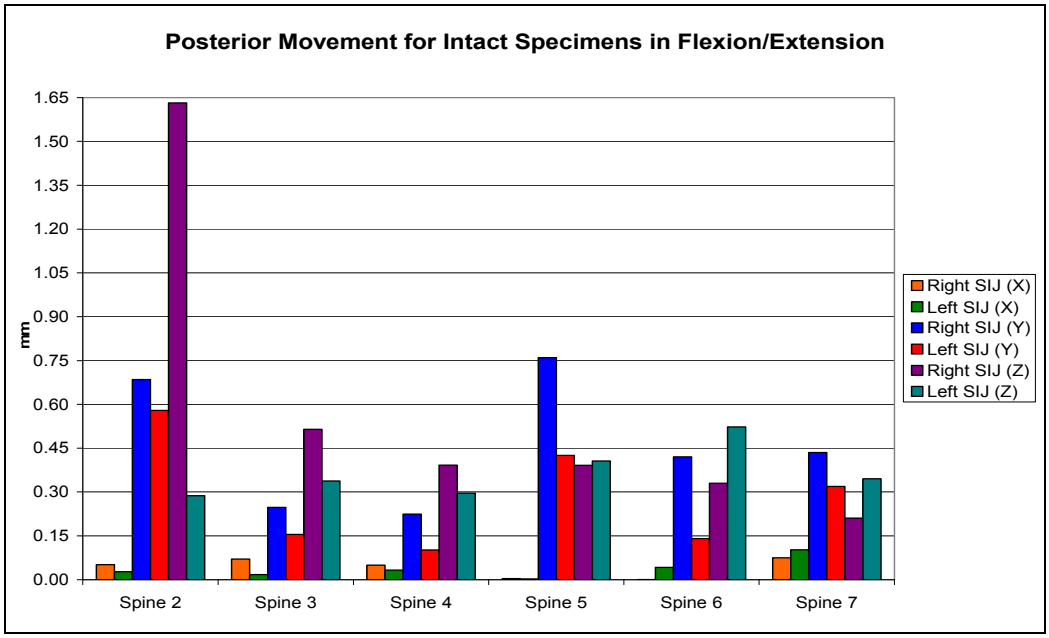

Figure 41: Posterior movements for intact specimens in flexion/extension.

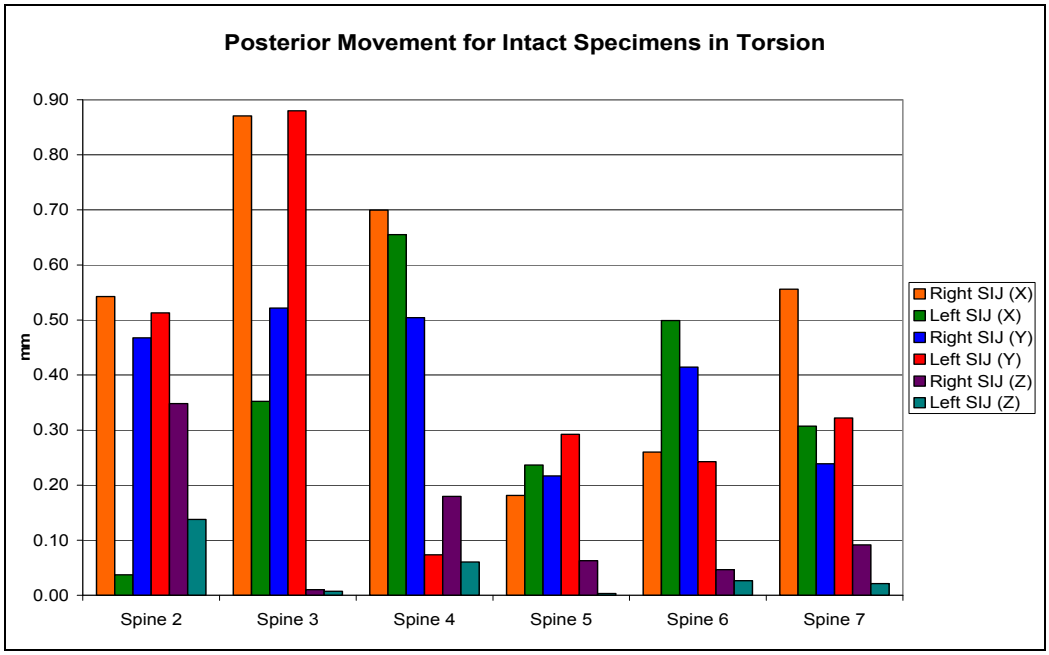

Figure 42: Posterior movements for intact specimens in torsion.

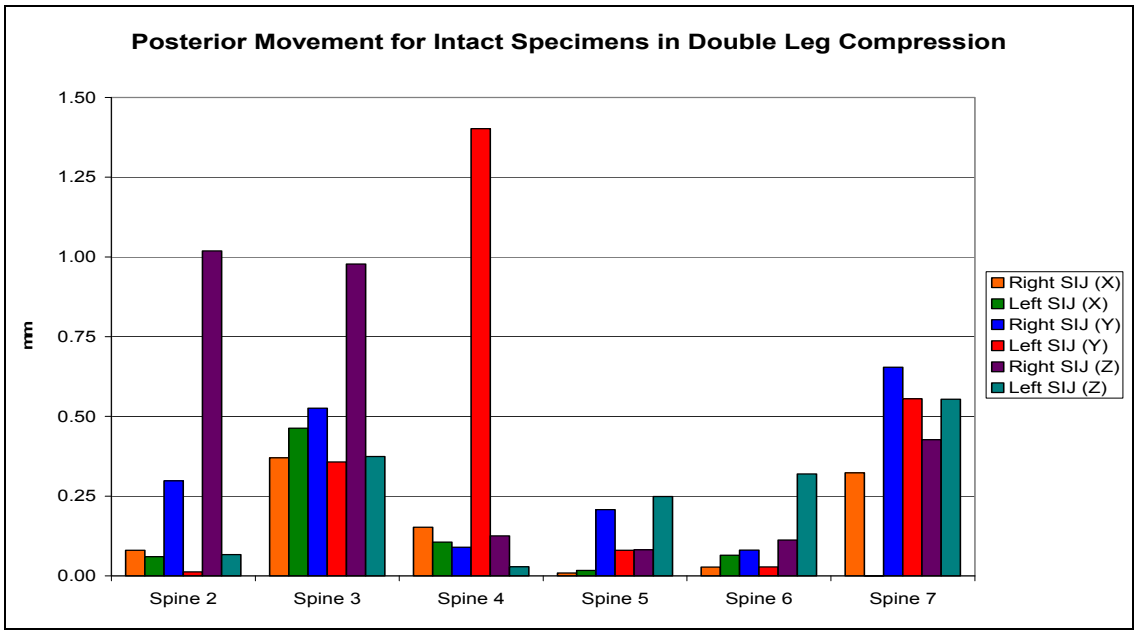

Figure 43: Posterior movements for intact specimens in double leg compression.

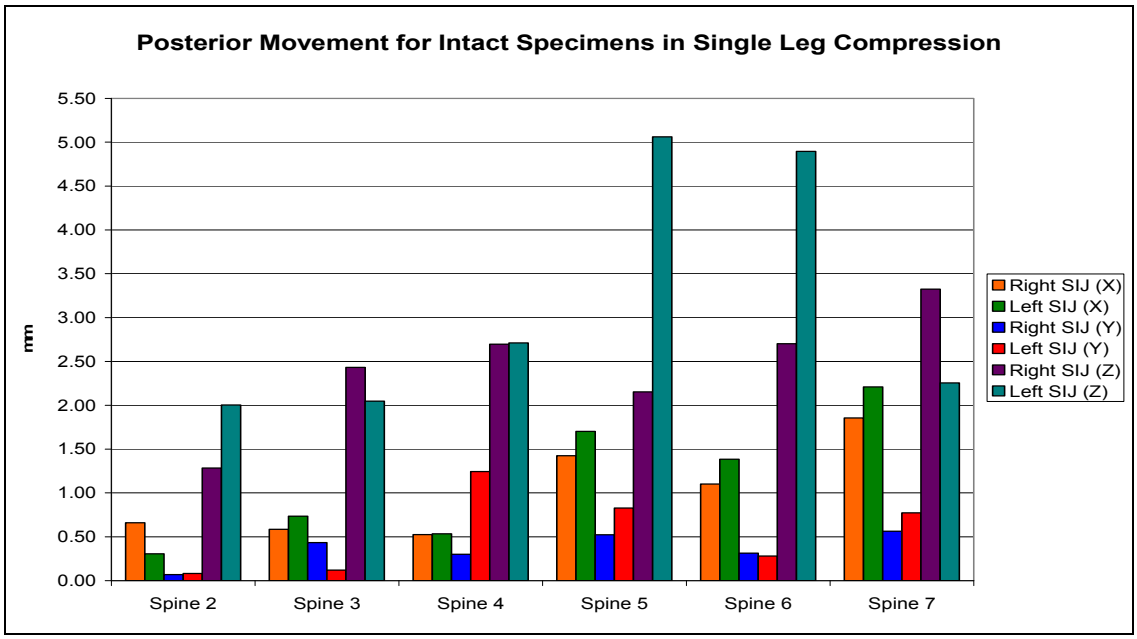

Figure 44: Posterior movements for intact specimens in single leg compression.

It was observed that movements detected during single leg compression were quite a bit larger than movements in all the other parameters and seemed suspect. After further investigation it was found that the data recorded was actually the motion of the whole pelvic construct tilting during single leg compression, and not the motion at the SI

joints. As the compression force was applied to the pelvic model in single leg compression the whole pelvic construct leaned to the right, since the right femur was hanging freely and had nothing to support it under the force of compression. Due to the occurrence of this type of motion the movement that was recorded by the Selspot was actually the movement of the whole pelvic construct. Table 6 and 7 show summaries of the range, between the greatest and least amount, of movements for all intact specimens and different parameters tested with and without outliers, respectively. In Table 7, the ranges from which outliers were removed are highlighted in red.

Range of Movements in Intact Specimens with outliers (mm)						
	Right X	Left X	Right Y	Left Y	Right Z	Left Z
Flexion/Extension	0.07	0.10	0.54	0.48	1.42	0.24
Torsion	0.69	0.62	0.30	0.81	0.34	0.13
Double Leg Compression	0.36	0.46	0.57	1.39	0.94	0.53
Single Leg Compression	1.33	1.90	0.49	1.17	2.04	3.06

Table 6: Range of posterior movements in intact specimens with outliers.

Range of Movements in Intact Specimens without outliers (mm)						
	Right X	Left X	Right Y	Left Y	Right Z	Left Z
Flexion/Extension	0.07	0.10	0.54	0.32	0.30	0.23
Torsion	0.69	0.42	0.30	0.81	0.17	0.06
Double Leg Compression	0.36	0.46	0.57	1.54	0.94	0.53
Single Leg Compression	1.33	1.90	0.49	1.17	2.04	3.06

Table 7: Range of posterior movements in intact specimens without outliers.

Orientation of Motion

In flexion/extension testing it was found that the SI joint moved with a rotational type motion in the sagittal plane, as described by Fick and Kapanji in the *Movement and Motion* section of the Anatomy of the SI Joint subchapter (p.6). This was determined by comparing anterior DVRT and posterior Selspot data during a flexion/extension cycle. It was observed that during extension the LED bracket on the sacrum tracked downward in a negative Z-direction while the vertical DVRTs on the anterior part of the pelvis indicated an upward motion in the positive Z-direction. This leads to the belief that the motion occurring at the SI joints, between the sacrum and each ilium, is a rotational movement in the sagittal plane. Movements in flexion/extension were found to be on a fairly small scale and were, for the most part, the lowest values measured among all the parameters tested. The orientation of movement, rotation in the sagittal plane, stayed consistent throughout all fusion steps.

Double and single leg compression tests produced strictly translational motion (there was no evidence of rotation) and was predominantly a vertical shear in the z-direction, however some linear shear in the anterior-posterior plane (y-direction) was also seen. This seems intuitive since there are no moments applied during axial compression, therefore, not creating angular or rotational type of movements; which again, was determined by comparing anterior DVRT and posterior Selspot data. It was observed that during compression the LED bracket on the sacrum tracked vertically downward in the negative Z-direction and the vertical DVRTs on the anterior part of the pelvis also indicated a downward motion in the negative Z-direction. It was noted that the sacrum moved down a greater distance compared to both ilia. Additionally, looking

at the Selspot data it was determined that translational motion also occurred in the anterior-posterior plane (y-direction). During compression the sacrum and both ilia traveled anteriorly, with both ilia moving a greater distance with reference to the sacrum. The orientation of the motion for both double and single leg compression stayed the same throughout all fusion steps. Torsion tests also produced strictly translational motions and moved predominantly in the medial-lateral plane (x-direction), though some movement in the anterior-posterior plane (y-direction) was also detected. Overall, it was also found that during all fusion tests and every parameter tested (flexion/extension, torsion, double and single leg compression) the posterior movements were larger than the anterior movements.

Effects of Fusion on the SI Joint

In this section the results of all the fusion steps, L4-5, L4-S1 and the unilateral SI fusion will be discussed and compared to the intact specimens and each other. The results in this section do not include outliers and as mentioned earlier, changes will be evaluated for statistical significance using the Student's t-Test. Results in this section are broken down into three categories; overall construct stiffness measured by the MTS® machine, anterior SI joint motion measured by the DVRT system, and posterior SI joint motion measured by the Selspot system.

Overall Construct Stiffness

The overall stiffness for the entire pelvic construct was calculated using the load/displacement curves obtained from the MTS® machine. Stiffness was calculated for every test parameter (flexion/extension, torsion, double and single leg compression) and during each testing step (intact, L4-5 fusion, L4-S1 fusion and unilateral SI joint fusion). It was hypothesized that as levels undergo fusion and motion is eliminated, the entire pelvic construct will get stiffer. This theory was proven true by the MTS® data collected through this study and it was found that the stiffness of the entire construct increased as each additional fusion was performed for all parameters tested. Table 8 shows the average stiffness of all the specimens tested and how they increase with fusion.

Construct Stiffness (N=6)								
	Intact		L4-L5 Fused		L4-S1 Fused		SIJ Fused	
	Mean	S.D.	Mean	S.D.	Mean	S.D.	Mean	S.D.
Flexion (N/mm)	13.4	2.7	14.2	3.8	18.7	7.7	19.4	5.7
Extension (N/mm)	5.8	2.4	10.5	4.6	24.3	12.0	25.0	8.2
Torsion (N·m/mm)	2.03	0.54	2.52	0.71	3.49	0.69	4.01	1.00
Double Leg Compression (N/mm)	337.2	106.0	365.6	81.5	379.7	72.5	383.3	75.9
Single Leg Compression (N/mm)	68.3	4.2	69.4	7.4	77.8	20.0	79.2	18.4

Table 8: Average construct stiffness for all parameters tested.

The average stiffness in flexion increased by 5.7% ($p = 0.294$) when a L4-5 fusion was performed compared to an intact specimen. The stiffness increased again by 31.6% ($p = 0.061$) with the L4-S1 lumbosacral fusion compared to the L4-5 fusion. Finally, the unilateral SI joint fusion also saw an increase in stiffness by 4.1% ($p = 0.342$) compared

to a lumbosacral fusion. Refer to Figure 45 to see a graphical representation of the average construct stiffness in flexion.

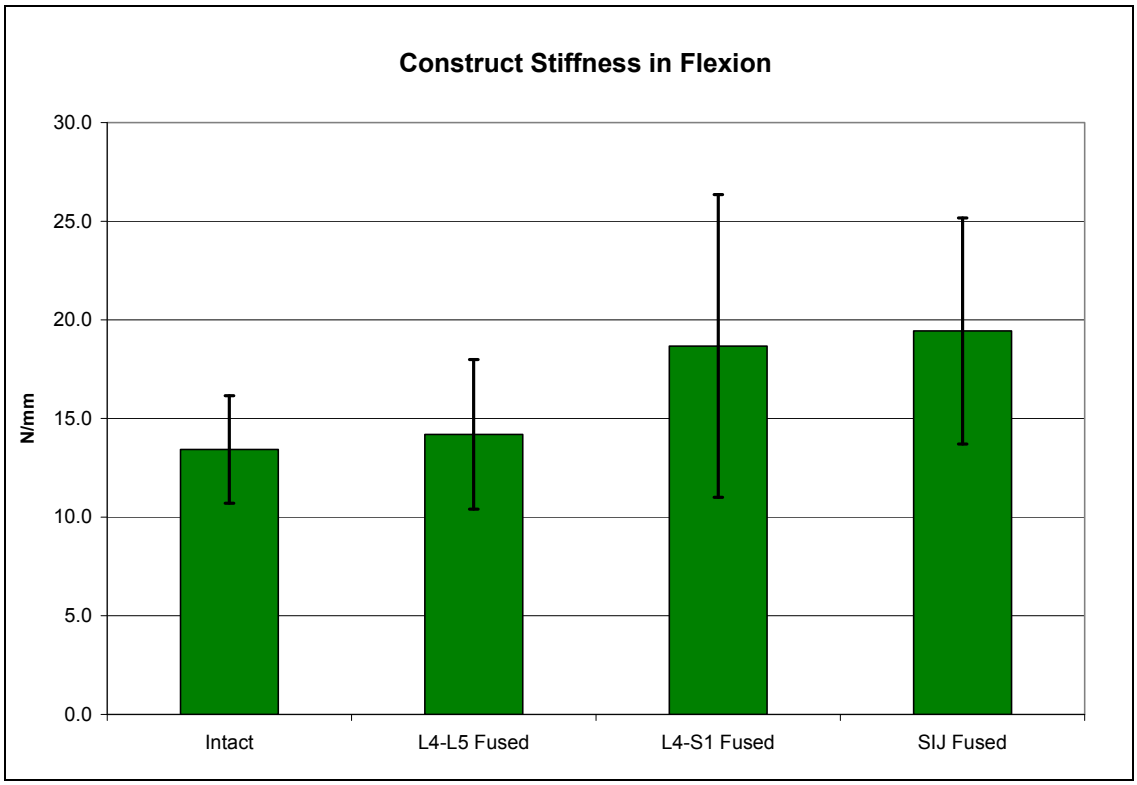

Figure 45: Average construct stiffness in flexion.

For extension, an increase in overall construct stiffness of 80.4% ($p = 0.005$) was seen with a L4-5 fusion compared to an intact specimen. Comparing the L4-S1 lumbosacral fusion to the L4-5 fusion, an increase of 131.8% ($p = 0.016$) in stiffness was observed. A much lower percentage of increase in stiffness was seen with a unilateral SI joint fusion compared to the L4-S1 fusion at 2.8% ($p = 0.378$). A graphical representation of the average construct stiffness in extension can be seen in Figure 46. An interesting observation was made, noticing the overall construct stiffness in flexion was greater than in extension for intact and L4-5 fused specimens. However, following a

L4-S1 lumbosacral fusion and a unilateral SI joint fusion, the extension stiffness was found to be greater than flexion.

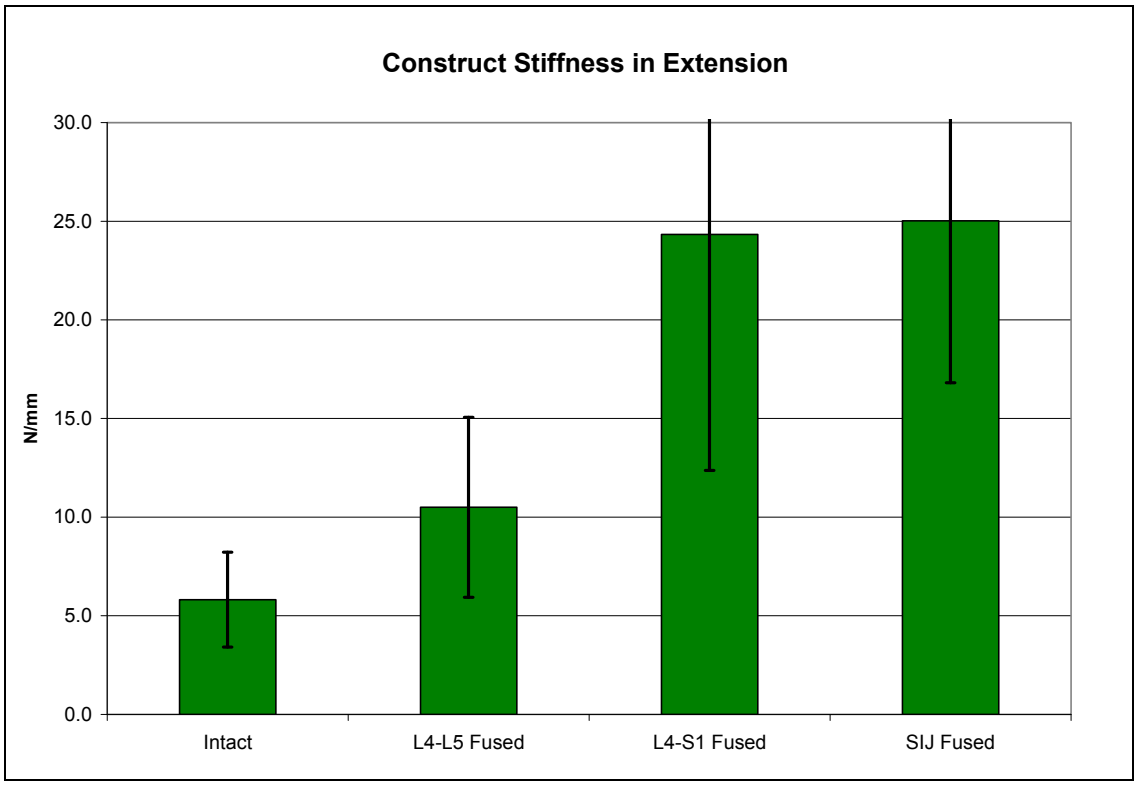

Figure 46: Average construct stiffness in extension.

In the torsion tests the same trend as above was observed, a 23.86% ($p = 0.001$) increase in overall construct stiffness with a L4-5 fusion compared to an intact specimen. Comparing a L4-S1 lumbosacral fusion to a L4-5 fusion an increase of 38.86% ($p = 0.018$) was observed and an increase of 14.88% ($p = 0.075$) was found comparing a unilateral SI joint fusion to the L4-S1 lumbosacral fusion. The construct stiffness for flexion, extension and torsion all increased the most going from a L4-5 fusion to the L4-S1 lumbosacral fusion. The next largest increase was seen going from an intact specimen to a L4-5 fusion, while the increase in stiffness from a L4-S1 lumbosacral

fusion to a unilateral fusion was the lowest. Graphical representation of the average construct stiffness in torsion can be seen in Figure 47.

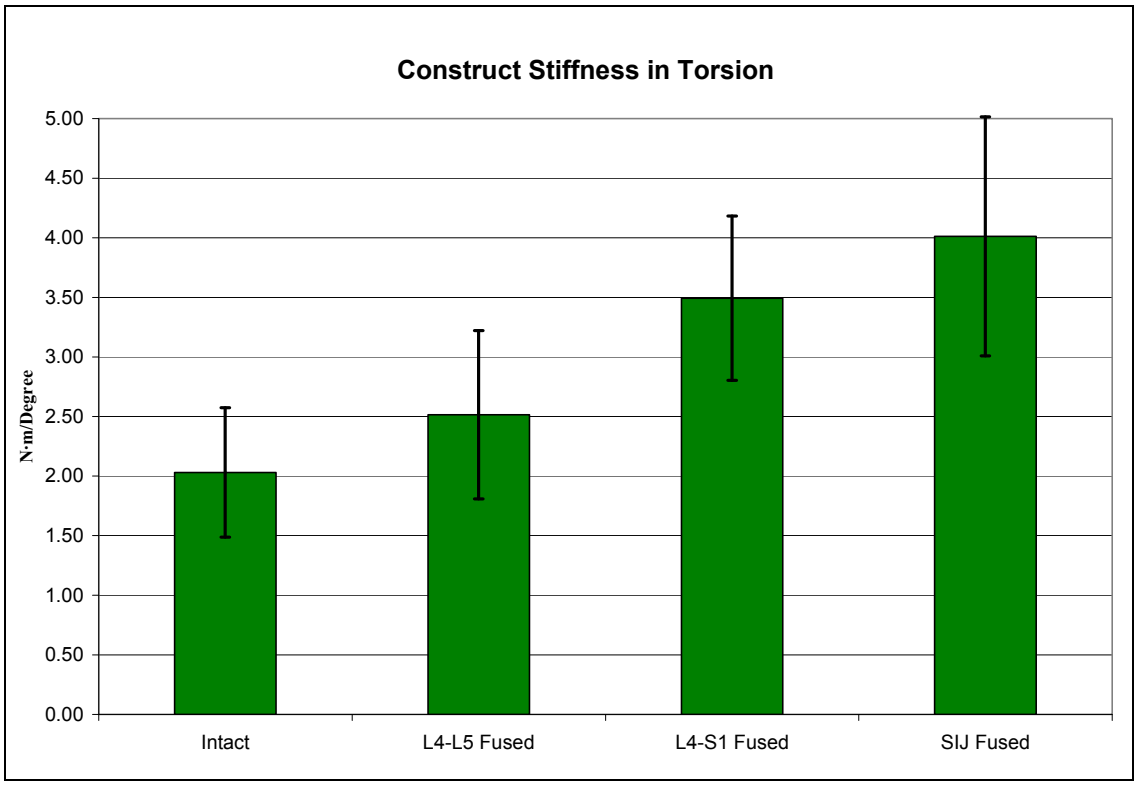

Figure 47: Average construct stiffness in torsion.

In the compression tests, double leg compression saw an increase in stiffness of 8.4% ($p = 0.031$) from an intact specimen to a L4-5 fusion, while single leg compression saw a 1.7% ($p = 0.363$) increase in stiffness. When L4-5 fused specimens were compared to L4-S1 lumbosacral fused specimens, single leg compression increased by 12.1% ($p = 0.094$) while double leg compression only increased by 3.9% ($p = 0.019$). Comparing the stiffness of a unilateral SI joint fusion with a L4-S1 fusion, the single leg stance again increased more at 1.8% ($p = 0.291$) than the double leg stance which increased 0.9% ($p = 0.407$). Figures 48 and 49 show graphical interpretations of the overall construct stiffness in double leg and single leg compression, respectively.

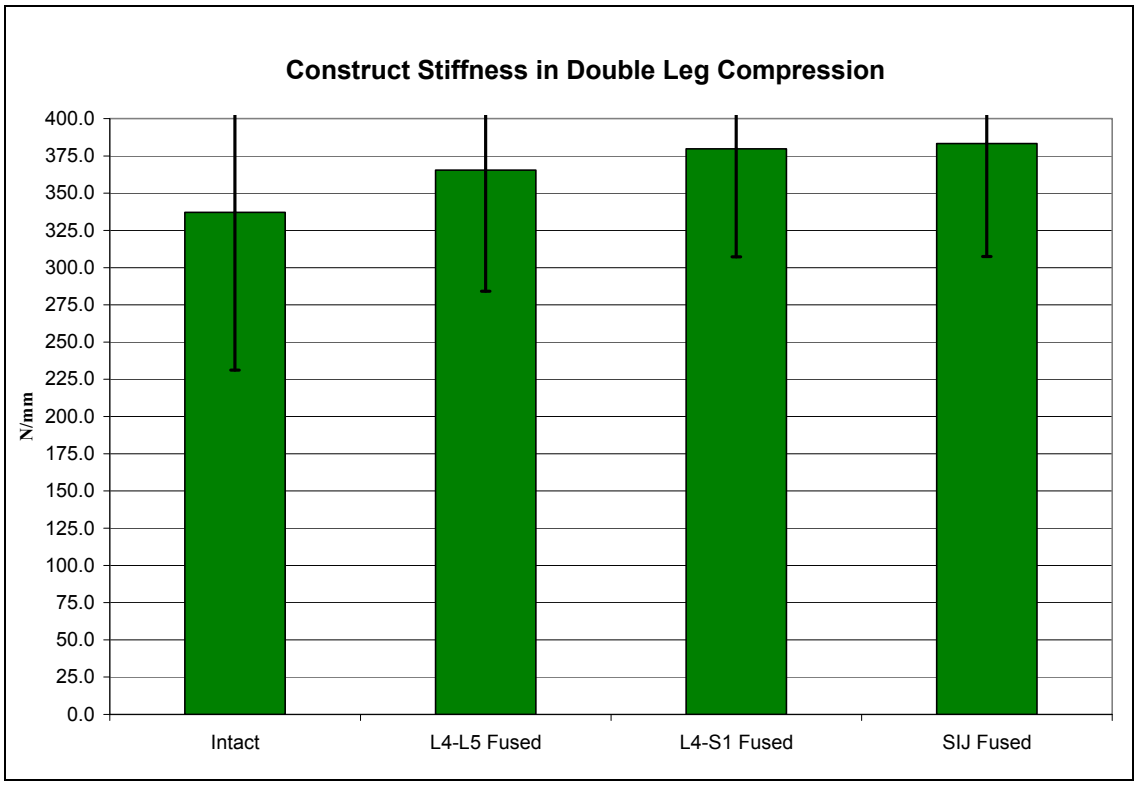

Figure 48: Average construct stiffness in double leg compression.

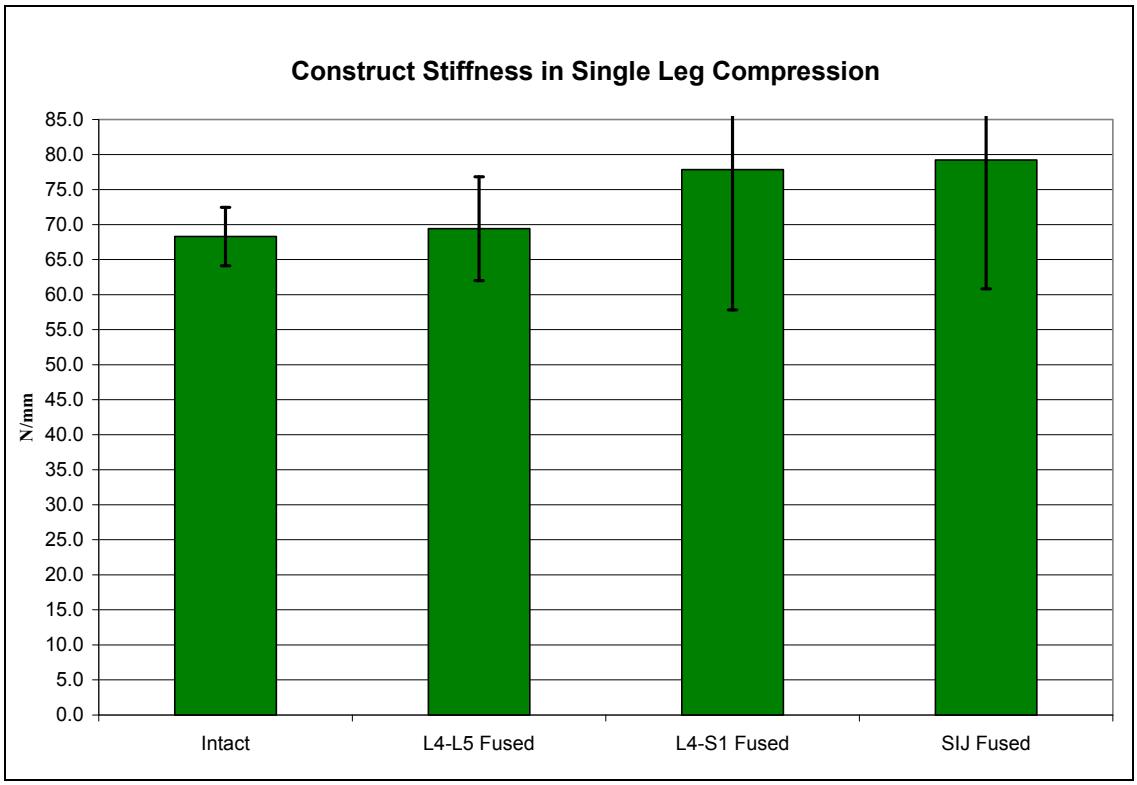

Figure 49: Average construct stiffness in single leg compression.

A summary of all the percent changes between fusions for all parameters tested can be seen in Table 9.

Percent Change in Construct Stiffness				
	Intact vs. L4-5 Fusion	L4-5 Fusion vs. L4-S1 Fusion	Intact vs. L4-S1 Fusion	L4-S1 Fusion vs. SIJ Fusion
Flexion	5.7%	31.6%	39.1%	4.1%
Extension	80.4%	131.8%	318.2%	2.8%
Torsion	23.86%	38.86%	72.00%	14.88%
Double Leg Compression	8.4%	3.9%	12.6%	0.9%
Single Leg Compression	1.7%	12.1%	14.0%	1.8%

Table 9: Summary of percent change in overall construct stiffness.

The majority of the changes, discussed above, for overall construct stiffness have been found to be significant. Through the Student's t-Test it was determined that most of the increases in construct stiffness were significant for extension, torsion and double leg compression. The stiffness changes in flexion and single leg compression, though they followed the same trend, were not significant; however, some were close to being significant and if a few more specimens were tested significance might have been reached. None of the parameters tested showed a significant change comparing a L4-S1 lumbosacral fusion to a unilateral SI joint fusion. Table 10 shows a summary of the p-values comparing different fusion tests in all parameters tested. (Significance is highlighted in red).

Student's t-Test p-values for Construct Stiffness				
	Intact vs. L4-5 Fusion	L4-5 Fusion vs. L4-S1 Fusion	Intact vs. L4-S1 Fusion	L4-S1 Fusion vs. SIJ Fusion
Flexion	0.294	0.061	0.067	0.342
Extension	0.005	0.016	0.007	0.378
Torsion	0.001	0.018	0.002	0.075
Double Leg Compression	0.031	0.019	0.020	0.407
Single Leg Compression	0.363	0.094	0.146	0.291

Table 10: Summary of p-values for overall construct stiffness.

Along with the increase in overall construct stiffness, as additional levels were fused, it was also found that the neutral zones (flexion/extension and torsion) decreased. This was to be expected since motion is eliminated by fusions, and in turn, tightens up the entire pelvic construct, which is seen by a decrease in neutral zones. Table 11 shows neutral zone measurements for all flexion/extension and torsion tests.

Neutral Zones (N=6)								
	Intact		L4-L5 Fused		L4-S1 Fused		SIJ Fused	
	Mean	S.D.	Mean	S.D.	Mean	S.D.	Mean	S.D.
Flexion/Extension (mm)	6.1	2.6	3.5	1.5	1.5	1.0	1.2	0.4
Torsion (mm)	1.90	0.71	1.39	0.27	0.93	0.25	0.82	0.11

Table 11: Flexion/extension and torsion neutral zones.

The neutral zone in flexion/extension decreased by 42.4% ($p = 0.017$) after a L4-5 fusion compared to an intact specimen. It decreased again comparing the L4-5 fusion to the L4-S1 lumbosacral fusion by 56.8% ($p = 0.005$). The neutral zone decreased once more comparing a L4-S1 fusion to a unilateral SI joint fusion by 22.2% ($p = 0.124$). For torsion testing the neutral zone decreased 26.75% ($p = 0.022$) following a L4-5 fusion compared to an intact specimen. Another decrease of 33.23% ($p = 0.005$) was seen when

comparing a L4-S1 fused specimen to a L4-5 fused specimen. A final decrease of 11.66% ($p = 0.120$) was seen comparing L4-S1 lumbosacral fusion to unilateral SI joint fusion. The changes in neutral zones for both flexion/extension and torsion tests were statistically significant when comparing intact to L4-5 fused specimens and L4-5 fusions to L4-S1 fusions. However, the changes found between a L4-S1 lumbosacral fusion and a unilateral SI joint fusion were not statistically significant. Figure 50 shows a graphically representation of the neutral zones, while Tables 12 and 13 show the percent change and p-values, respectively. (Significance is highlighted in red).

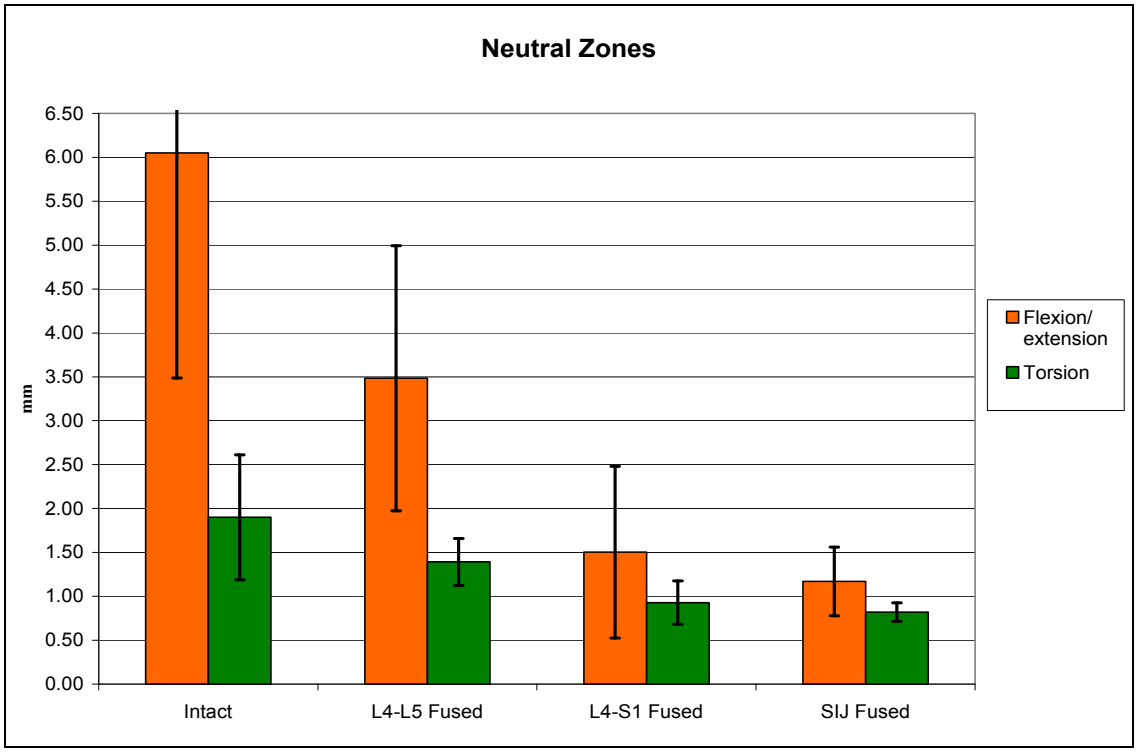

Figure 50: Average neutral zones.

Percent Change in Neutral Zones				
	Intact vs. L4-5 Fusion	L4-5 Fusion vs. L4-S1 Fusion	Intact vs. L4-S1 Fusion	L4-S1 Fusion vs. SIJ Fusion
Flexion/Extension	-42.4%	-56.8%	-75.1%	-22.2%
Torsion	-26.75%	-33.23%	-51.10%	-11.66%

Table 12: Summary of percent change in neutral zones.

Student's t-Test p-values for Neutral Zones				
	Intact vs. L4-5 Fusion	L4-5 Fusion vs. L4-S1 Fusion	Intact vs. L4-S1 Fusion	L4-S1 Fusion vs. SIJ Fusion
Flexion/Extension	0.017	0.005	0.003	0.124
Torsion	0.022	0.005	0.010	0.120

Table 13: Summary of p-values for neutral zones.

Anterior SI Joint Motion

An interesting observation was made during this study that the motion detected on the anterior side of the SI joint was always less than the motion on the posterior side. It is known that the posterior SI joint ligaments are stronger than the anterior ligaments; however, we now see that they may also be more flexible/elastic. Out of all the parameters tested, the flexion/extension tests produced the smallest amount of motion at the SI joints, both horizontally and vertically. Figure 51 shows a graph of the vertical motion in flexion/extension for all the steps tested, while Figure 52 shows the anterior horizontal motion in flexion/extension for all the steps tested.

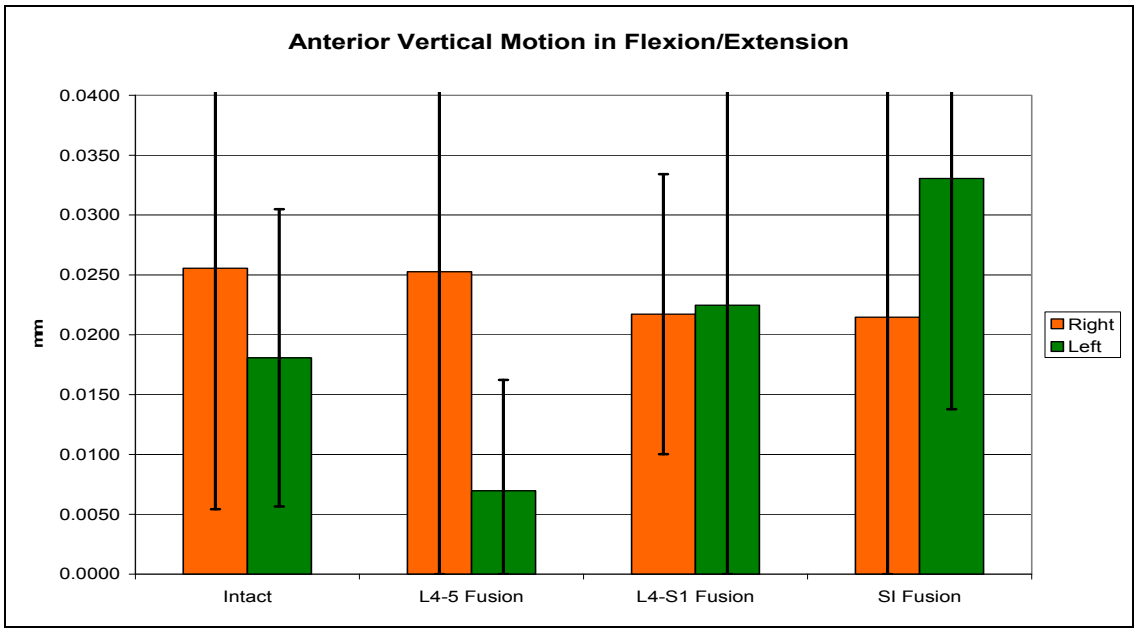

Figure 51: Anterior vertical motion in flexion/extension.

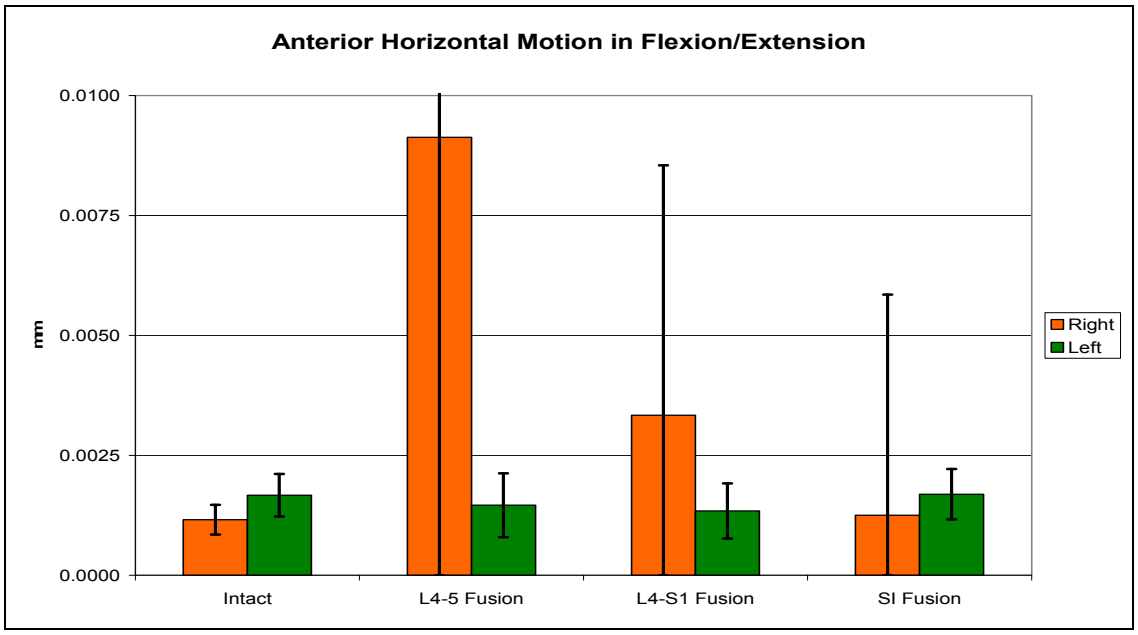

Figure 52: Anterior horizontal motion in flexion/extension.

A trend was detected in the vertical motion on the right SI joint where motion decreased by 1.131% ($p = 0.494$) when L4-5 was fused compared to an intact specimen. There was also a decrease in motion comparing a L4-5 fusion to a lumbosacral L4-S1 fusion by 14.05% ($p = 0.143$) and a 15.02% ($p = 0.079$) decrease in motion between an intact and lumbosacral fusion. A 15.99% ($p = 0.265$) decrease in motion was also seen when comparing intact specimens to specimens that had a unilateral SI joint fusion. No other major trends were found during flexion/extension testing and none of the changes in motion were considered statistically significant. A reason for the lack of significance could be due to the small sample size. A summary of the percent change in motion during the flexion/extension tests can be seen in Table 14, while the p-values from the Student's t-Test for these changes can be seen in Table 15.

Percent Change in Anterior Motion for Flexion/Extension				
	Intact vs. L4-5 Fusion	Intact vs. L4-S1 Fusion	L4-5 Fusion vs. L4-S1 Fusion	Intact vs. SIJ Fusion
Right Vertical	-1.131%	-15.02%	-14.04%	-15.99%
Left Vertical	-61.45%	24.32%	222.5%	82.89%
Right Horizontal	688.9%	188.1%	-63.47%	8.266%
Left Horizontal	-12.45%	-19.62%	-8.190%	1.269%

Table 14: Percent change in anterior motion for flexion/extension tests.

p-values for Changes in Anterior Motion for Flexion/Extension				
	Intact vs. L4-5 Fusion	Intact vs. L4-S1 Fusion	L4-5 Fusion vs. L4-S1 Fusion	Intact vs. SIJ Fusion
Right Vertical	0.494	0.079	0.143	0.265
Left Vertical	0.067	0.308	0.147	0.296
Right Horizontal	0.088	0.233	0.176	0.388
Left Horizontal	0.377	0.492	0.348	0.101

Table 15: P-values for changes in anterior motion during flexion/extension tests.

The torsion tests showed slightly larger movements than flexion/extension in both the horizontal and vertical directions. Torsion was the only parameter tested that had larger motions in the horizontal direction than the vertical. This intuitively seems to make sense since there are no real compression forces being applied, only the side to side motion from torque. Figures 53 and 54 show graphs of the motion that occurred during torsion tests in the vertical and horizontal directions, respectively.

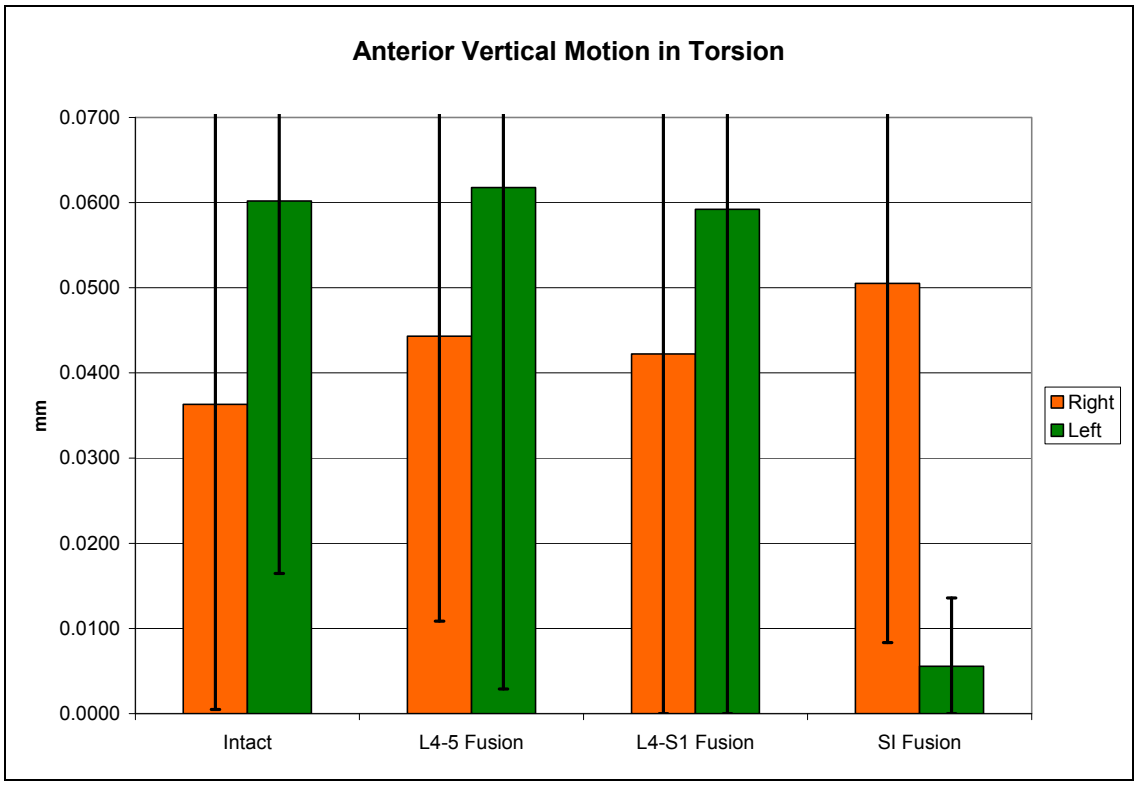

Figure 53: Anterior vertical motion in torsion.

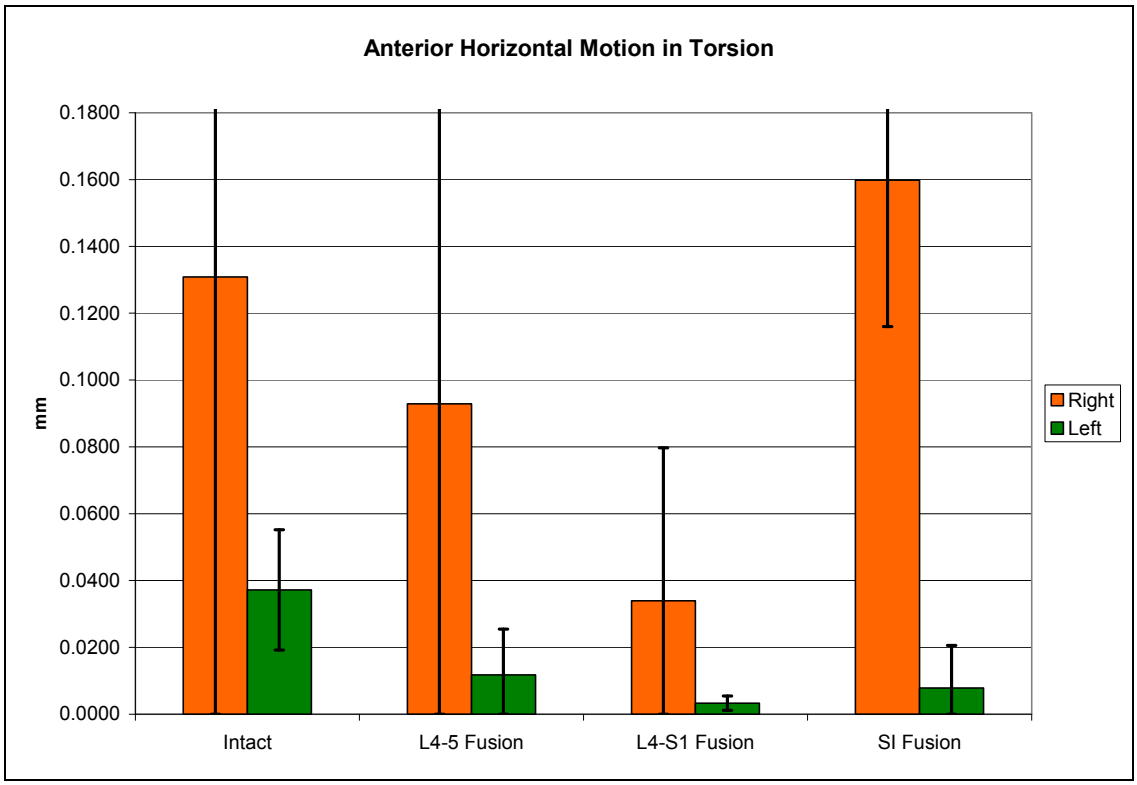

Figure 54: Anterior horizontal motion in torsion.

A few trends during the torsion tests were found; in the vertical direction the motion at the right SI joint increased 22.10% ($p = 0.344$) went L4-5 was fused compared to an intact specimen. An increase was again seen when comparing intact specimens to; lumbosacral fusion by 16.34% (0.414) and by 39.19% ($p = 0.226$) with unilateral fusions. Once more, it was noted that there was no statistical significance in these changes. Interestingly, the motions at the left SI joint followed the opposite trend from the right side and decreased as levels were fused. A 1.604% ($p = 0.479$) decrease in motion was found comparing an intact specimen to one with a L4-5 fusion, and a decrease of 4.139% ($p = 0.437$) occurred when L4-S1 was fused compared to an intact specimen. When intact specimens were compared to ones that underwent unilateral SI joint fusions, a decrease of 90.79% ($p = 0.012$) was found. This change was found to be statistically significant and understandably so, since the left SI joint was the one fused and nearly all the motion in this direction at this joint was eliminated compared to intact.

In the horizontal direction motion at both the right and left SI joints generally decreased as fusions occurred. On the right side, comparing intact specimens to; L4-5 fused ones, a decrease of 29.03% ($p = 0.245$) was found and a decrease of 74.11% ($p = 0.172$) for L4-S1 lumbosacral fusions. However, when comparing intact specimens to ones that had a unilateral fusion and increase in motion was seen at the right SI joint of 22.14% ($p = 0.435$). This may be due to the right SI joint compensating for the eliminated motion at the left SI joint because of the unilateral fusion. The left SI joint saw a decrease in motion across the board when compared to an intact specimen by 68.40% ($p = 0.302$) after a L4-5 fusion, by 91.14% ($p = 0.083$) after a L4-S1 fusion and by 78.94% ($p = 0.159$) after a unilateral SI joint fusion. Table 16 shows a summary of

the percent change in motion during torsion tests, while Table 17 shows the p-values from the Student's t-Test for these changes (statistical significance is highlighted in red).

Percent Change in Anterior Motion for Torsion				
	Intact vs. L4-5 Fusion	Intact vs. L4-S1 Fusion	L4-5 Fusion vs. L4-S1 Fusion	Intact vs. SIJ Fusion
Right Vertical	22.10%	16.34%	-4.725%	39.19%
Left Vertical	2.644%	-1.604%	-4.139%	-90.79%
Right Horizontal	-29.03%	-74.11%	-63.52%	22.14%
Left Horizontal	-68.40%	-91.14%	-71.95%	-78.94%

Table 16: Percent change in anterior motion for torsion tests.

p-values for Changes in Anterior Motion for Torsion				
	Intact vs. L4-5 Fusion	Intact vs. L4-S1 Fusion	L4-5 Fusion vs. L4-S1 Fusion	Intact vs. SIJ Fusion
Right Vertical	0.344	0.414	0.425	0.226
Left Vertical	0.431	0.479	0.437	0.012
Right Horizontal	0.245	0.172	0.168	0.435
Left Horizontal	0.302	0.083	0.105	0.159

Table 17: P-values for changes in anterior motion during torsion tests.

The next test parameter that showed even larger moments at the SI joints was the single leg compression test. In this test parameter the left femur was held in place with a vise while the right femur hung freely, a schematic diagram of this can be seen in Figure 10 in the *Development of the Experimental Model* section in the Methods subchapter (p.28). Figures 55 and 56 show graphs of the motions that occurred during the single leg compression tests in the vertical and horizontal directions, respectively.

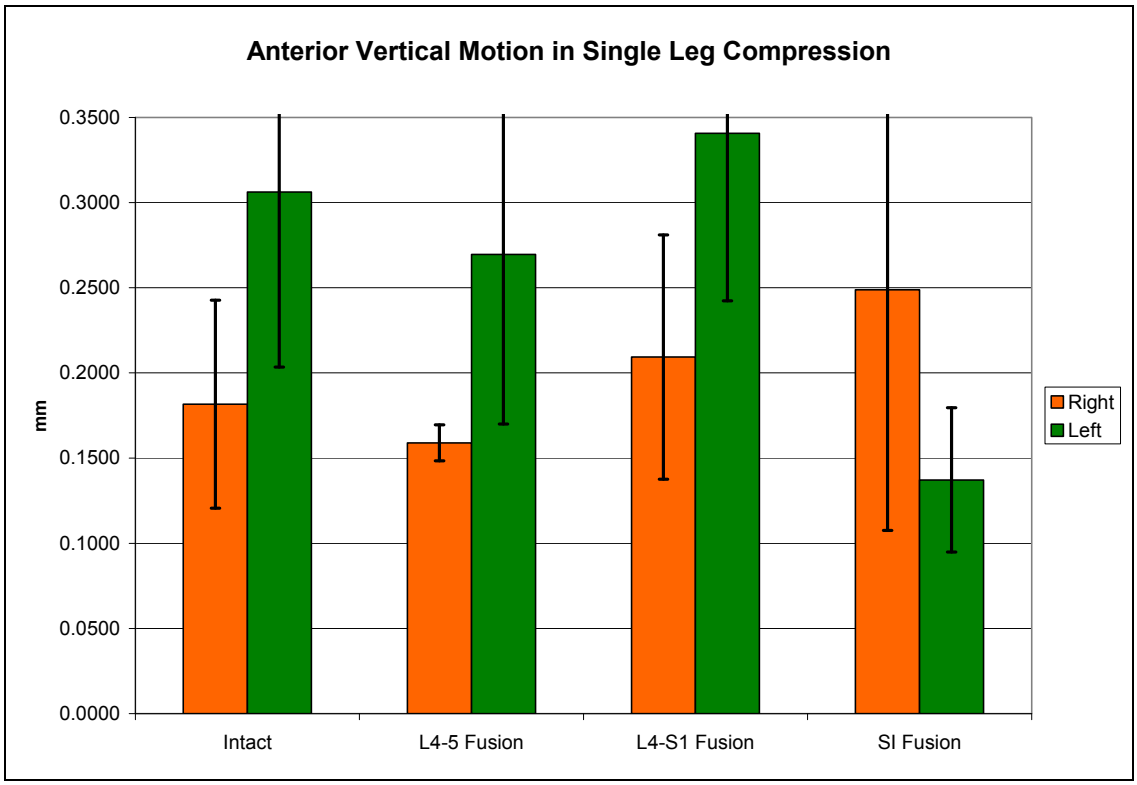

Figure 55: Anterior vertical motion in single leg compression.

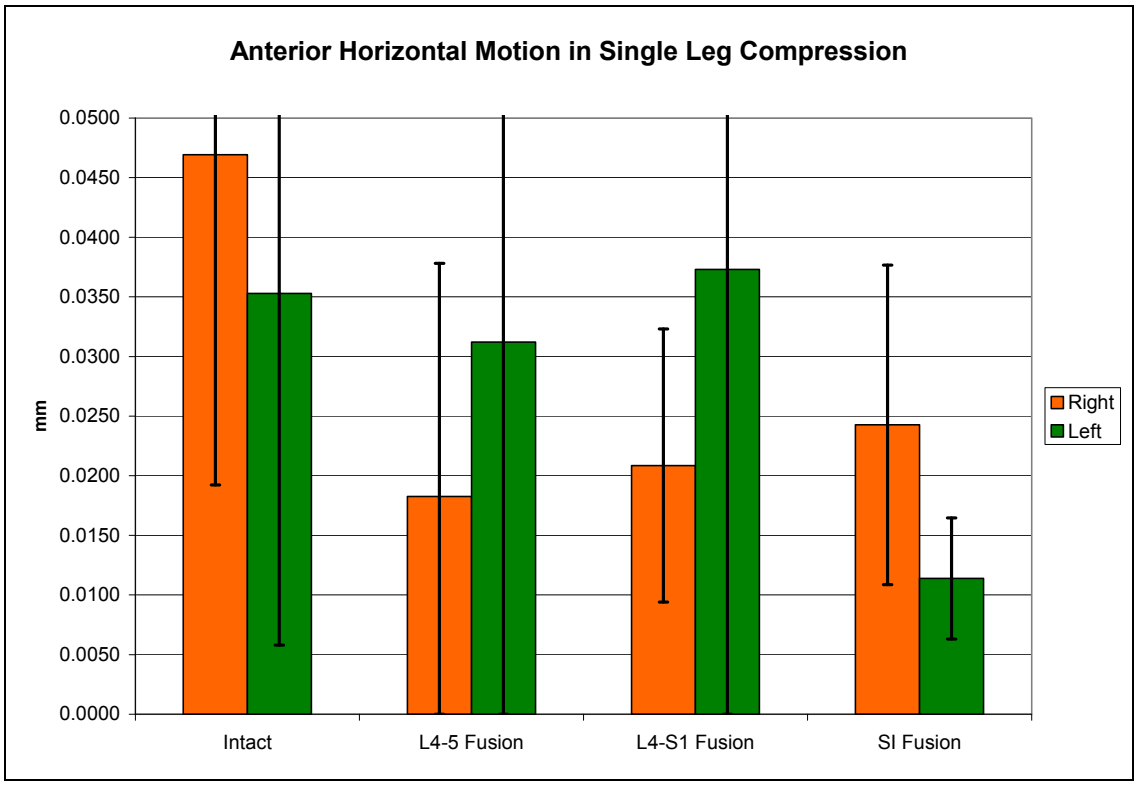

Figure 56: Anterior horizontal motion in single leg compression.

Trends were a little harder to find during this parameter of testing, however it was noticed that there was a decrease in motion, at both SI joints, comparing intact specimens to ones that had a L4-5 fusion in both the horizontal and vertical directions. The horizontal motion at right SI joint decreased by 61.08% ($p = 0.481$) while the motion at the left SI joint decreased by 11.53% ($p = 0.286$). The vertical motion at the right SI joint decreased 12.47% ($p = 0.399$) and a significant decrease of 11.96% ($p = 0.047$) occurred at the left SI joint. An increase in motion was seen when comparing intact specimens to ones with lumbosacral fusions in all directions except for the right SI joint in the horizontal direction, which actually decreased by 55.55% ($p = 0.325$). Nevertheless, both right and left SI joints had an increase in motion when comparing a L4-5 fusion to a L4-S1 lumbosacral fusion in both the horizontal and vertical directions. A decrease in motion was also observed comparing intact specimens to ones that had a unilateral SI joint fusion, in all directions except for the right SI joint in the vertical direction, which increased by 37.04% ($p = 0.126$). The decrease that occurred at the left SI joint, in the horizontal direction, of 67.72% ($p = 0.032$) was found to be statistically significant. A summary of all the percent changes in motion during the single leg compression test can be seen in Table 18, and the p-values from the Student's t-Test for these changes can be seen in Table 19 (statistical significance in red).

Percent Change in Anterior Motion for Single Leg Compression				
	Intact vs. L4-5 Fusion	Intact vs. L4-S1 Fusion	L4-5 Fusion vs. L4-S1 Fusion	Intact vs. SIJ Fusion
Right Vertical	-12.47%	15.25%	31.67%	37.04%
Left Vertical	-11.96%	11.28%	26.39%	-55.20%
Right Horizontal	-61.08%	-55.55%	14.21%	-48.28%
Left Horizontal	-11.53%	5.717%	19.49%	-67.72%

Table 18: Percent change in anterior motion for single leg compression tests.

p-values for Changes in Anterior Motion for Single Leg Compression				
	Intact vs. L4-5 Fusion	Intact vs. L4-S1 Fusion	L4-5 Fusion vs. L4-S1 Fusion	Intact vs. SIJ Fusion
Right Vertical	0.399	0.144	0.178	0.126
Left Vertical	0.047	0.282	0.145	0.114
Right Horizontal	0.481	0.325	0.225	0.324
Left Horizontal	0.286	0.435	0.344	0.032

Table 19: P-values for changes in anterior motion during single leg compression tests.

The last parameter tested was double leg compression, and the greatest amount of motion was detected during these tests. The double leg compression tests also produced the most statistically significant changes in motion, compared to all the other test parameters. Graphs showing the motions that occurred during the double leg compression tests can be seen in Figures 57 and 58 for the vertical and horizontal directions, respectively.

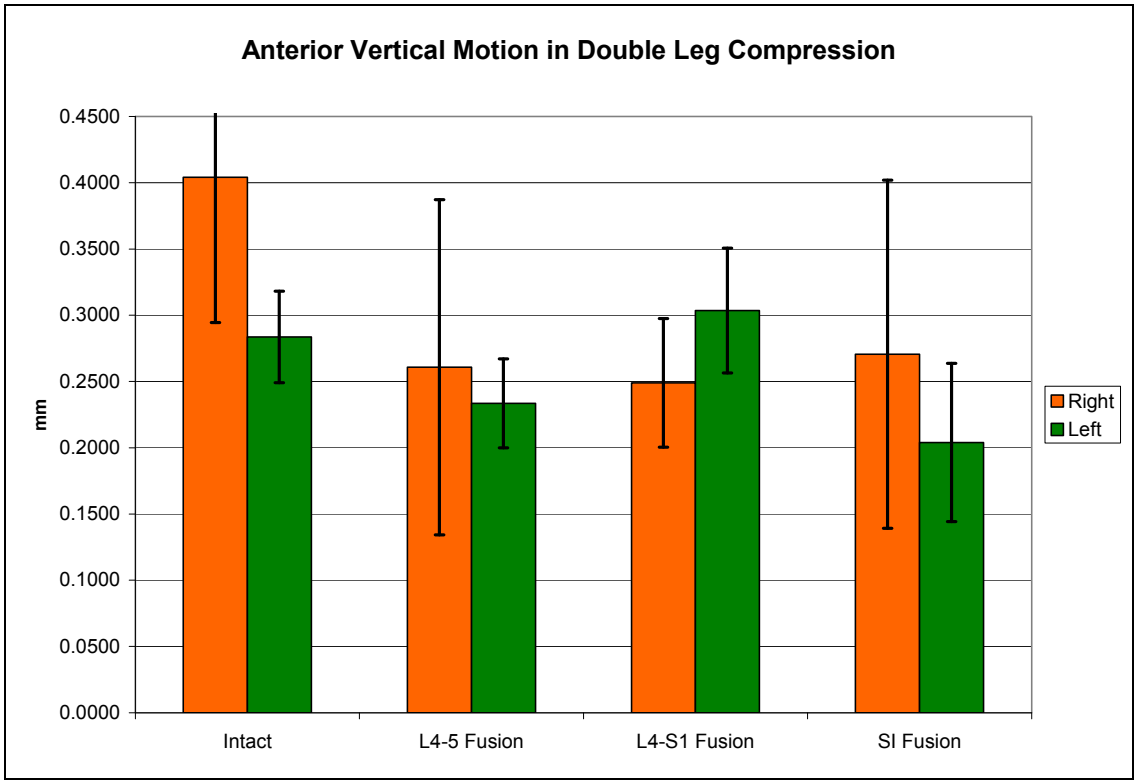

Figure 57: Anterior vertical motion in double leg compression.

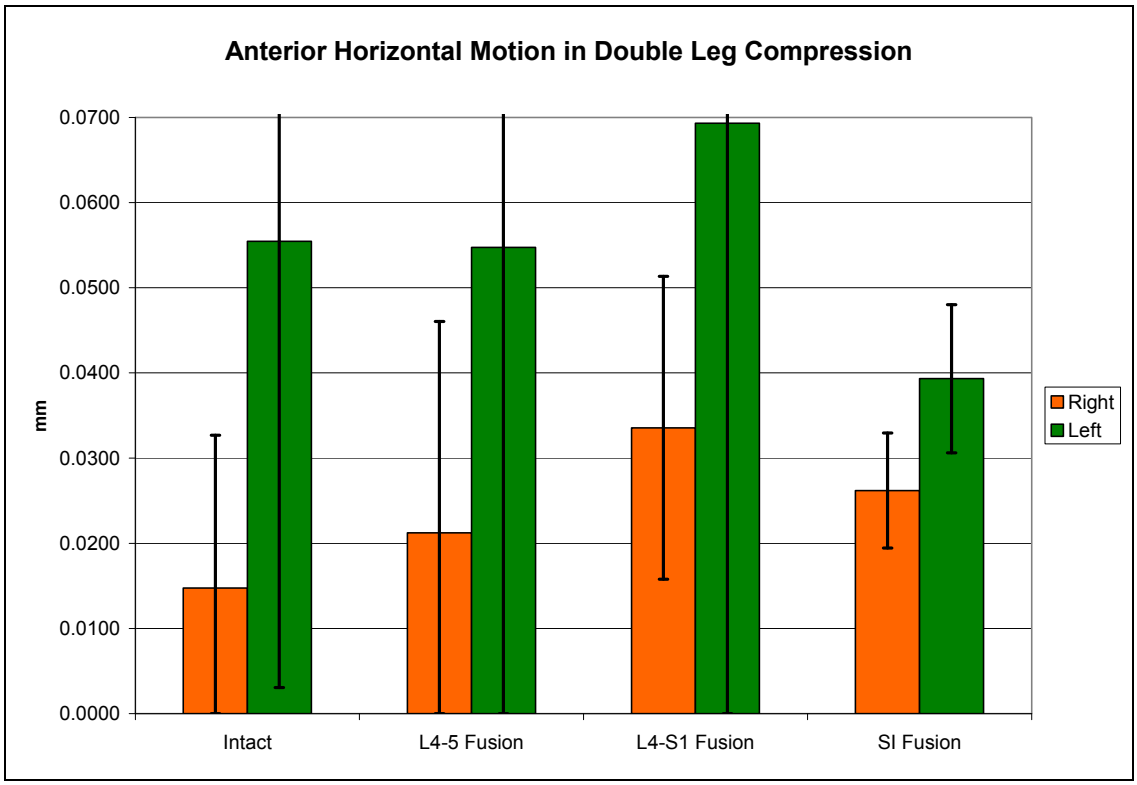

Figure 58: Anterior horizontal motion in double leg compression.

An interesting trend was observed at the right SI joint; as fusions occurred, the motion decreased in the vertical direction, but increased in the horizontal direction. When comparing intact specimens to L4-5 fused specimens, a decrease of 35.49% ($p = 0.021$) was seen in the vertical direction and a decrease of 38.41% ($p = 0.029$) was seen comparing intact to L4-S1 fused specimens. When comparing intact specimens to ones with a unilateral SI joint fusion, a decrease of 33.06% ($p = 0.044$) was seen in the vertical direction. All these decreases in vertical motion, as levels were fused, at the right SI joint were deemed to be statistically significant. In the horizontal direction, at the right SI joint, an increase of 43.96% ($p = 0.320$) was found when comparing intact to L4-5 fused specimens and an increase of 127.6% ($p = 0.424$) was seen comparing intact to L4-S1 fusions. Also, an increase of 77.73% ($p = 0.246$) was recorded when comparing intact

specimens to ones with unilateral SI joint fusions. All these increases, however, were not considered statistically significant. At the left SI joint a decrease in motion was observed, in both directions, when comparing intact specimens to L4-5 fused specimens and to ones with unilateral SI joint fusions; but there was an increase when comparing intact specimens to ones with L4-S1 fusions. A decrease in motion of 17.68% ($p = 0.036$) was seen in the vertical direction comparing intact specimens to L4-5 fused ones, while a decrease of 28.11% ($p = 0.004$) was observed comparing intact specimens to ones with unilateral SI joint fusions. Both these changes were found to be statistically significant, unlike the decreases seen in the horizontal direction of 1.293% ($p = 0.466$) comparing intact to L4-5 fused specimens and 29.08% ($p = 0.315$) between intact specimens and ones with SI joint fusions. Table 20 shows a summary of the percent change in motion during double leg compression tests, while Table 21 shows the p-values from the Student's t-Test for these changes (statistical significance highlighted in red).

Percent Change in Anterior Motion for Double Leg Compression				
	Intact vs. L4-5 Fusion	Intact vs. L4-S1 Fusion	L4-5 Fusion vs. L4-S1 Fusion	Intact vs. SIJ Fusion
Right Vertical	-35.49%	-38.41%	-4.519%	-33.06%
Left Vertical	-17.68%	7.024%	30.00%	-28.11%
Right Horizontal	43.96%	127.6%	58.11%	77.73%
Left Horizontal	-1.293%	25.04%	26.67%	-29.08%

Table 20: Percent change in anterior motion for double leg compression tests.

p-values for Changes in Anterior Motion for Double Leg Compression				
	Intact vs. L4-5 Fusion	Intact vs. L4-S1 Fusion	L4-5 Fusion vs. L4-S1 Fusion	Intact vs. SIJ Fusion
Right Vertical	0.021	0.029	0.326	0.044
Left Vertical	0.036	0.219	0.109	0.004
Right Horizontal	0.320	0.424	0.264	0.246
Left Horizontal	0.456	0.149	0.050	0.315

Table 21: P-values for changes in anterior motion during double leg compression tests.

An overall trend of increased motion at the SI joints was noticed when comparing intact specimens to specimens following a lumbosacral fusion during both, single and double leg compression tests and to a slightly lesser degree during the flexion/extension tests. These trends observed during this study may shed light on observations that have been made in the past by other clinical studies. In a study by Katz et al. it was stated that patients who previously had spine surgery were likely to complain of lower back pain, due to the SI joint, during follow-up visits and it was more common among patients with lumbosacral fusions.[33] Buchowski et al. stated that the SI joint is a cause of chronic lower back pain in 13%-30% of patients, however, that percentage may be quite a bit larger among patients with previous lumbosacral fusions.[7] The same trend was also seen in the clinical study conducted by Ha et al. which was discussed in the *Adjacent Segment Disease and the SI Joint* section of the SI Joint Pain subchapter (p.17). The increased motion detected at the SI joints in this study after lumbosacral fusion may be the cause of the higher rate of lower back pain, due to the SI joint, as mentioned in the clinical studies above.

Posterior SI Joint Motion

The motion observed at the SI joints on the posterior side of the pelvis, in general but not always, was of a greater magnitude than the anterior side. As mentioned above in the *Posterior SI Joint Motion* section in the Intact SI Joint Biomechanics subchapter (p.55) the data recorded during the single leg compression tests were thought to be faulty and did not accurately show movement at the SI joint. For this reason the single leg compression data will not be discussed in great detail, however, the data collected during

these tests is presented in Table 22 as a summary of the percent change in motion. The values for the left SI joint are thought to be more accurate then the right SI joint, but full confidence can not be placed on either. None of the changes in motion found during the single leg compression tests were considered statistically significant and a summary of the Student's t-Test p-values can be seen in Table 23.

Percent Change in Posterior Motion for Single Leg Compression				
	Intact vs. L4-5 Fusion	Intact vs. L4-S1 Fusion	L4-5 Fusion vs. L4-S1 Fusion	Intact vs. SIJ Fusion
Right X	-6.64%	-4.76%	2.02%	-17.7%
Left X	26.7%	1.81%	-19.6%	-1.58%
Right Y	9.27%	16.5%	6.65%	-2.57%
Left Y	-7.56%	-34.9%	-29.6%	-53.0%
Right Z	9.97%	22.1%	11.0%	5.93%
Left Z	5.80%	2.81%	-2.82%	-4.31%

Table 22: Percent change in posterior motion for single leg compression tests.

p-values for Changes in Posterior Motion for Single Leg Compression				
	Intact vs. L4-5 Fusion	Intact vs. L4-S1 Fusion	L4-5 Fusion vs. L4-S1 Fusion	Intact vs. SIJ Fusion
Right X	0.255	0.382	0.448	0.298
Left X	0.163	0.460	0.054	0.485
Right Y	0.364	0.329	0.449	0.475
Left Y	0.391	0.090	0.201	0.127
Right Z	0.114	0.101	0.128	0.371
Left Z	0.240	0.389	0.420	0.255

Table 23: P-values for changes in posterior motion during single leg compression tests.

Changes in motion were detected as levels were fused, during double leg compression tests, however, not too many trends were observed. The magnitude of motion observed at the SI joints on the posterior side was roughly the same, if not slightly higher in some instances, than the anterior side. Graphs showing the motions that

occurred during double leg compression tests can be seen in Figures 59 – 61 for the medial-lateral (x) direction, anterior-posterior (y) direction and vertical (z) direction, respectively.

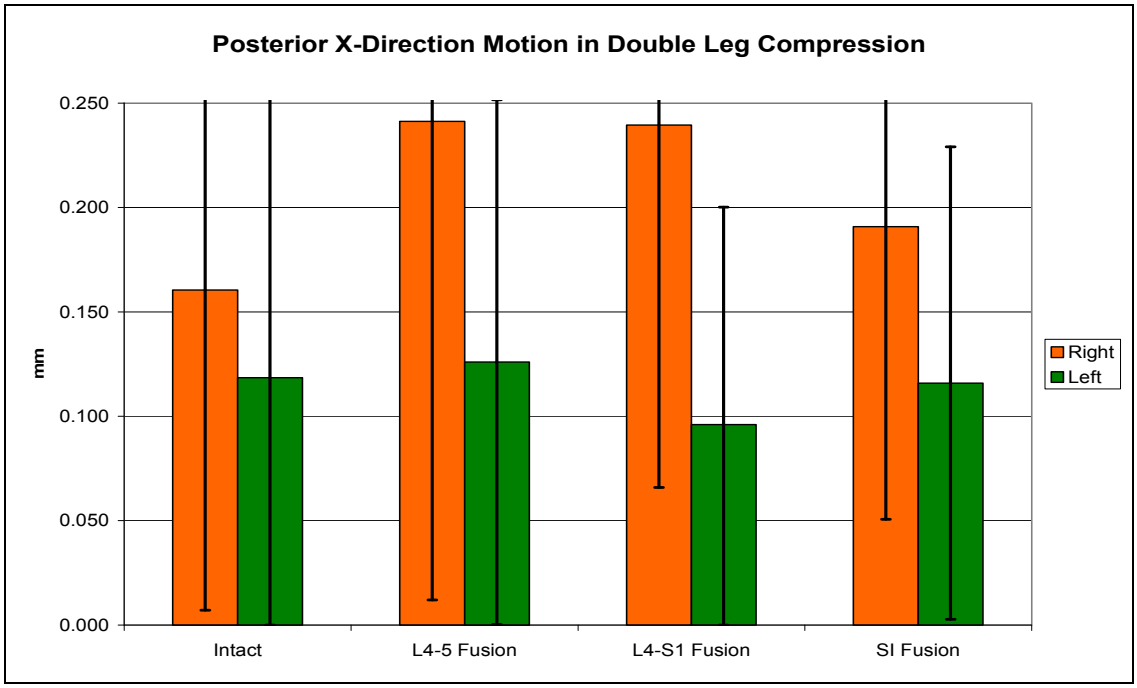

Figure 59: Posterior motion in the x-direction for double leg compression.

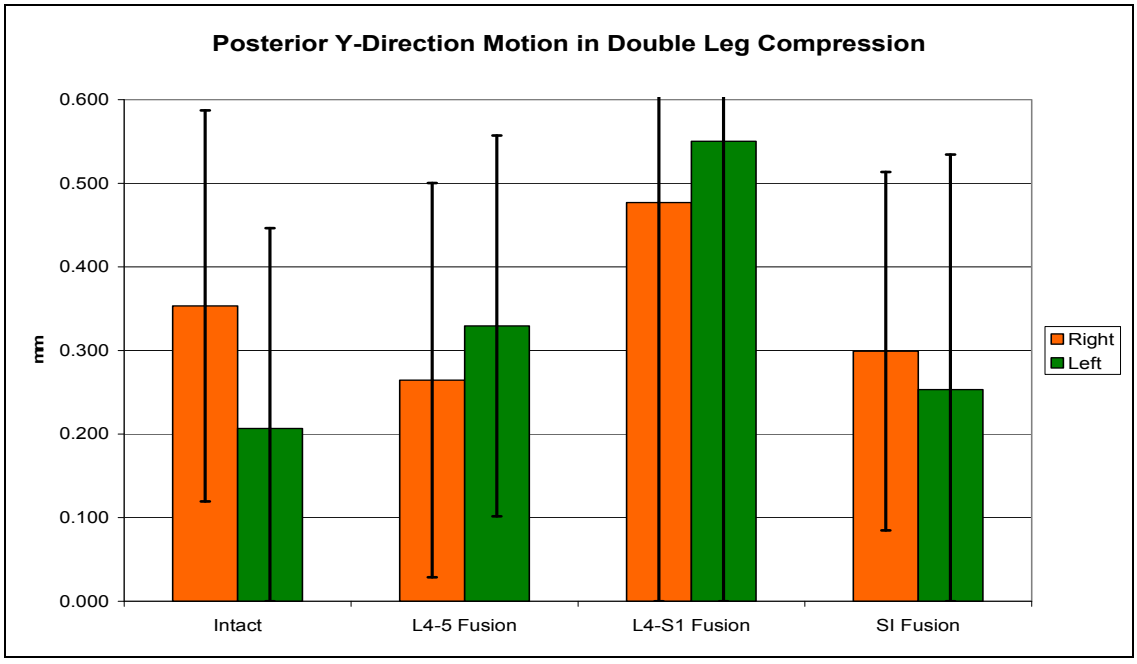

Figure 60: Posterior motion in the y-direction for double leg compression.

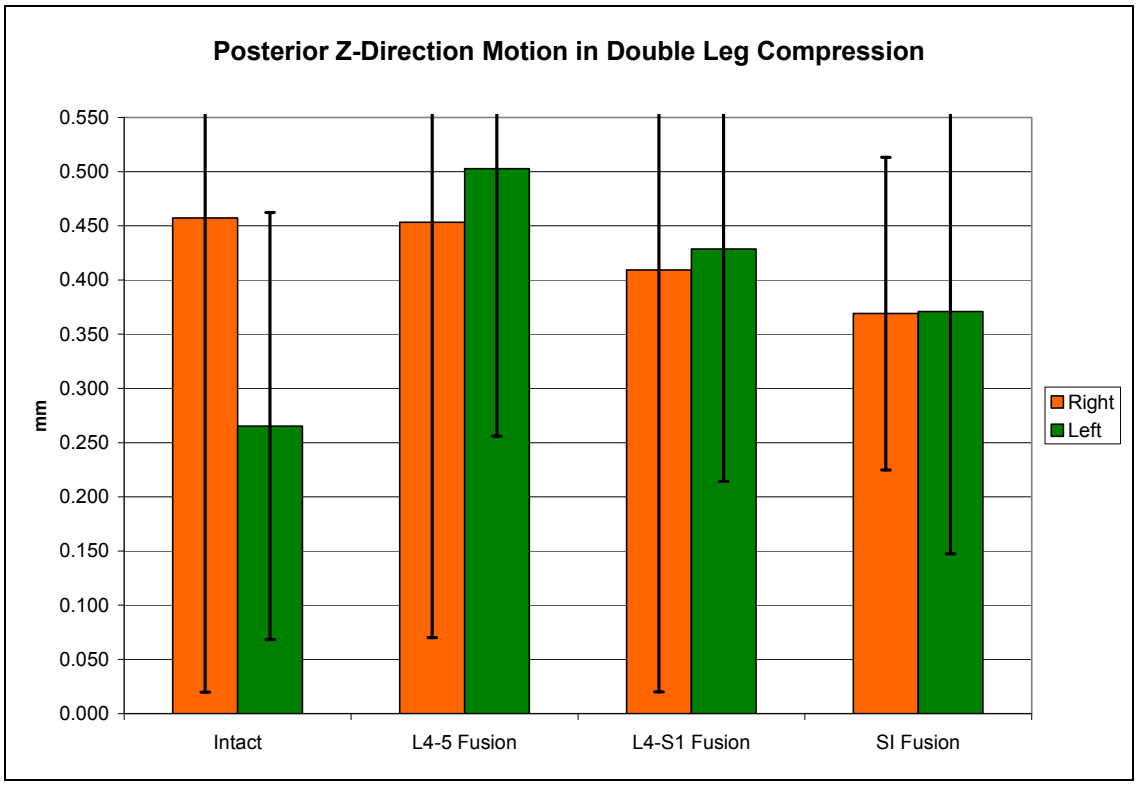

Figure 61: Posterior motion in the z-direction for double leg compression.

A decrease in motion was observed at the right SI joint in the vertical (z) direction when comparing intact specimens to; L4-5 fused ones by 0.869% ($p = 0.473$), by 10.5% ($p = 0.348$) to L4-S1 lumbosacral fused specimens and by 19.3% ($p = 0.314$) to specimens with unilateral SI joint fusions. On the other hand, an increase in motion was detected as levels were fused at the left SI joint in the y and z directions and at the right SI joint in the x direction. At the right SI joint in the medial-lateral (x) direction an increase of 50.3% ($p = 0.098$) was seen comparing an intact specimen to one with an L4-5 fusion, a 49.3% ($p = 0.173$) increase was observed when comparing intact to L4-S1 fused specimens and when comparing intact to unilateral SI joint fused specimen an increase of 18.9% ($p = 0.312$) was found. At the left SI joint in the anterior-posterior (y) direction an increase in motion of 59.4% ($p = 0.204$), 166% ($p = 0.219$) and 22.5%

(p = 0.398) were observed comparing intact specimens to L4-5 fusion, L4-S1 fusion and unilateral SI joint fusions, respectively. As for the vertical (z) direction of the left SI joint, increases in motion of 89.5% (p = 0.074), 61.6% (p = 0.125) and 39.8% (p = 0.207) were found while comparing the intact specimens to L4-5 fusion, L4-S1 fusion and unilateral SI joint fusions, respectively. None of the changes in motion during double leg compression showed statistical significance; except when comparing a L4-5 fusion to a L4-S1 lumbosacral fusion at the left SI joint in the vertical (z) direction, which decreased by 14.8% (p = 0.028), and was statistically significant. Tables 24 and 25 show a summary of the percent change in motion during double leg compression tests and the p-values from the Student's t-Test, respectively (statistical significance in red).

Percent Change in Posterior Motion for Double Leg Compression				
	Intact vs. L4-5 Fusion	Intact vs. L4-S1 Fusion	L4-5 Fusion vs. L4-S1 Fusion	Intact vs. SIJ Fusion
Right X	50.3%	49.3%	-0.721%	18.9%
Left X	6.31%	-18.9%	-23.7%	-2.21%
Right Y	-25.1%	35.0%	80.3%	-15.3%
Left Y	59.4%	166%	67.1%	22.5%
Right Z	-0.869%	-10.5%	-9.68%	-19.3%
Left Z	89.5%	61.6%	-14.8%	39.8%

Table 24: Percent change in posterior motion for double leg compression tests.

p-values for Changes in Posterior Motion for Double Leg Compression				
	Intact vs. L4-5 Fusion	Intact vs. L4-S1 Fusion	L4-5 Fusion vs. L4-S1 Fusion	Intact vs. SIJ Fusion
Right X	0.098	0.173	0.491	0.312
Left X	0.426	0.259	0.226	0.476
Right Y	0.274	0.316	0.227	0.366
Left Y	0.204	0.219	0.260	0.398
Right Z	0.473	0.348	0.267	0.314
Left Z	0.074	0.125	0.028	0.207

Table 25: P-values for changes in posterior motion during double leg compression tests.

Looking at the posterior motion data collected during torsion tests, trends were much easier to find than for double leg compression tests. In almost all the directions and at both SI joints, an increase in motion was observed as levels were fused. Figures 62 – 64 show graphs of the motions that occurred during torsion tests in the medial-lateral (x) direction, anterior-posterior (y) direction and vertical (z) direction, respectively.

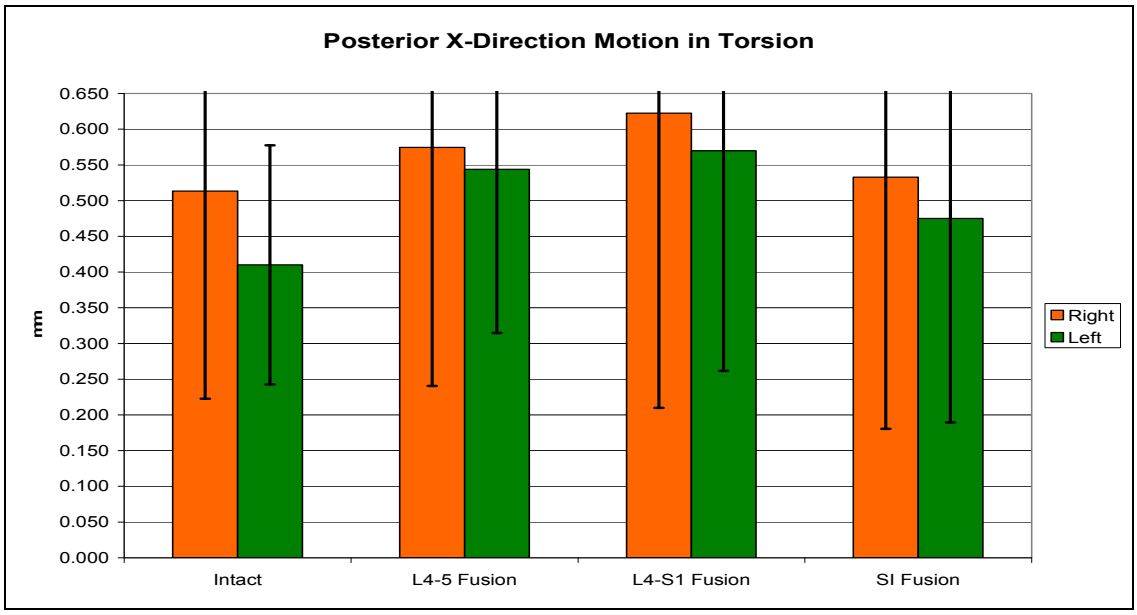

Figure 62: Posterior motion in the x-direction for torsion.

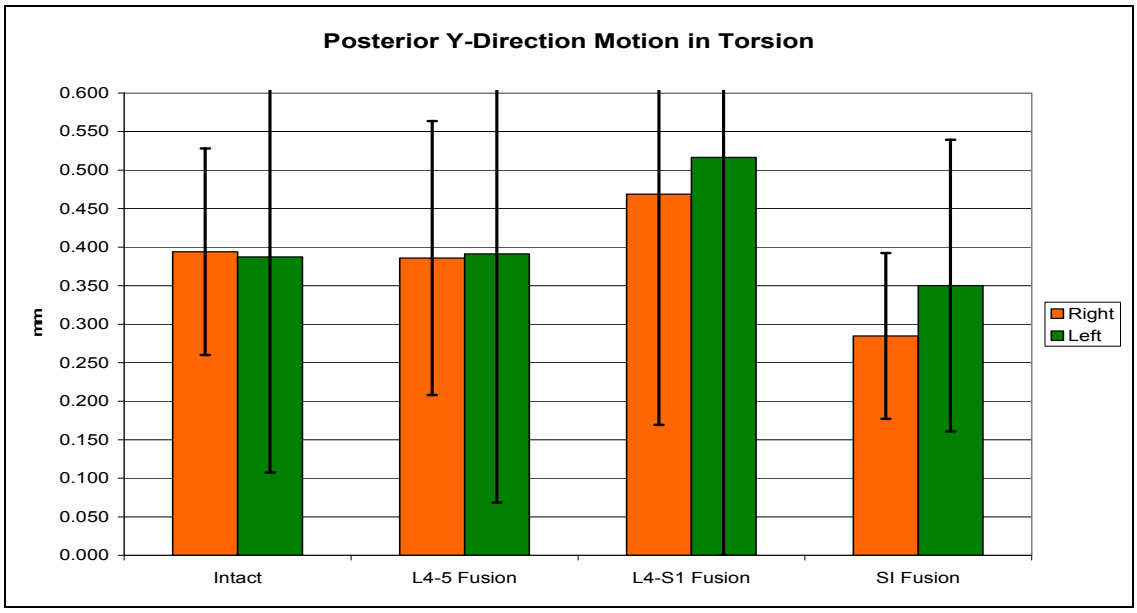

Figure 63: Posterior motion in the y-direction for torsion.

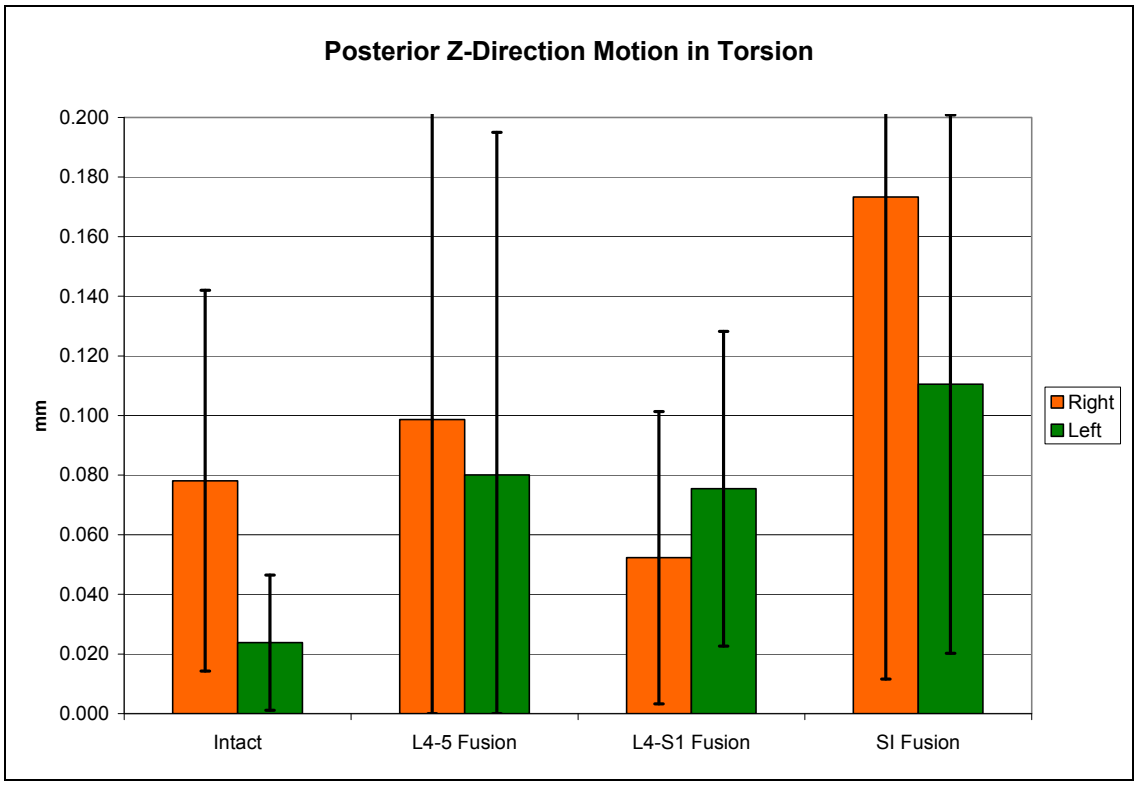

Figure 64: Posterior motion in the z-direction for torsion.

In the medial-lateral (x) direction increases in motion were seen for both right and left SI joints as levels were fused. For the right SI joint, comparing intact specimens to specimens after L4-5 fusion motion increased by 11.9% ($p = 0.379$) and increased by 21.2% ($p = 0.316$) when comparing intact to lumbosacral fusion. An increase of 3.78% ($p = 0.462$) was also seen at the right SI joint in the medial-lateral (x) direction when comparing intact specimens to ones after a unilateral SI joint fusion. Similarly, at the left SI joint in the medial-lateral (x) direction, when comparing intact specimens to L4-5 fused specimens an increase of 32.6% ($p = 0.154$) was found, when comparing intact to L4-S1 fusions an increase of 39.0% ($p = 0.164$) was found and finally, an increase of 15.8% ($p = 0.333$) was seen when comparing intact specimens to ones that had a unilateral SI joint fusion. The trend of motion increasing as levels were fused was also

seen in the vertical (z) direction at the left SI joint. When comparing intact specimens to L4-S1 lumbosacral fused specimens, an increase of 217% ($p = 0.047$) was seen, and an increase of 364% ($p = 0.034$) was seen comparing intact with unilateral SI joint fused specimens; both increase were considered statistically significant. An increase was also seen when comparing an intact specimen with one after a L4-5 fusion by 236% ($p = 0.157$), however, it was not considered statistically significant. Table 26 shows a summary of the percent change in motion during the torsion tests, while Table 27 shows the p-values from the Student's t-Test for these changes (statistical significance is highlighted in red).

Percent Change in Posterior Motion for Torsion				
	Intact vs. L4-5 Fusion	Intact vs. L4-S1 Fusion	L4-5 Fusion vs. L4-S1 Fusion	Intact vs. SIJ Fusion
Right X	11.9%	21.2%	8.36%	3.78%
Left X	32.6%	39.0%	4.79%	15.8%
Right Y	-2.07%	19.0%	21.5%	-27.7%
Left Y	1.01%	33.4%	32.0%	-9.60%
Right Z	26.3%	-33.1%	-47.0%	122%
Left Z	236%	217%	-5.79%	364%

Table 26: Percent change in posterior motion for torsion tests.

p-values for Changes in Posterior Motion for Torsion				
	Intact vs. L4-5 Fusion	Intact vs. L4-S1 Fusion	L4-5 Fusion vs. L4-S1 Fusion	Intact vs. SIJ Fusion
Right X	0.379	0.316	0.373	0.462
Left X	0.154	0.164	0.310	0.333
Right Y	0.435	0.219	0.133	0.106
Left Y	0.485	0.273	0.151	0.412
Right Z	0.364	0.137	0.211	0.125
Left Z	0.157	0.047	0.468	0.034

Table 27: P-values for changes in posterior motion during torsion tests.

Posterior motion detected during flexion/extension tests at the SI joints was much higher than what was observed on the anterior side. In fact, posterior motion in the vertical (z) direction was the highest during flexion/extension tests compared to the other parameters of torsion and double leg compression. However, the posterior motion in the medial-lateral (x) direction during the flexion/extension tests was the lowest of all the parameters, yet it was still higher than the anterior side. Figures 65 – 67 show graphs of the motion that occurred during flexion/extension tests in the medial-lateral (x) direction, anterior-posterior (y) direction and vertical (z) direction, respectively.

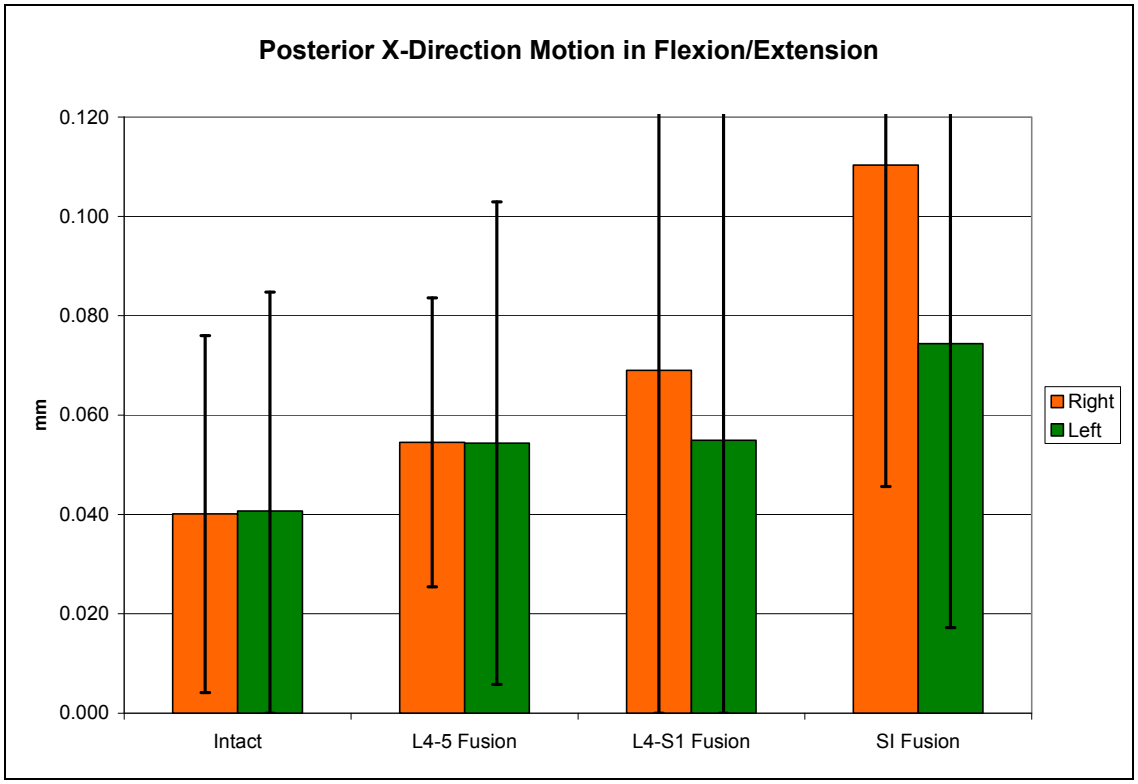

Figure 65: Posterior motion in the x-direction for flexion/extension.

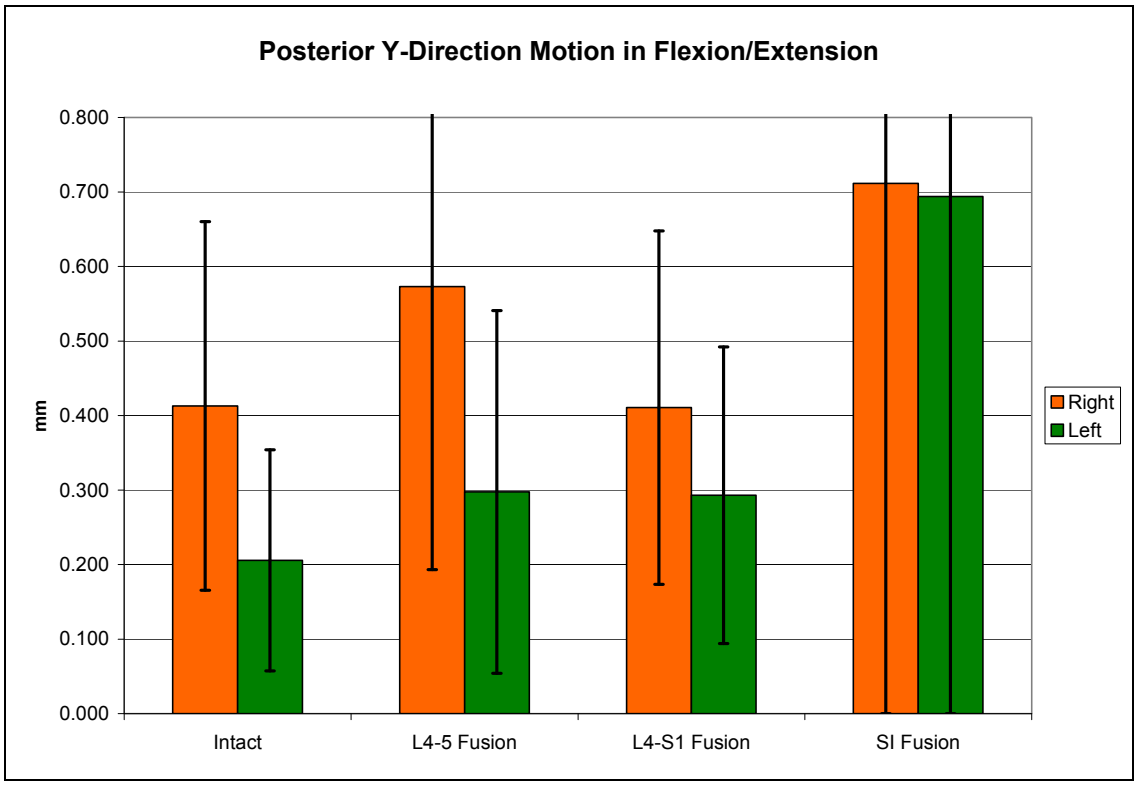

Figure 66: Posterior motion in the y-direction for flexion/extension.

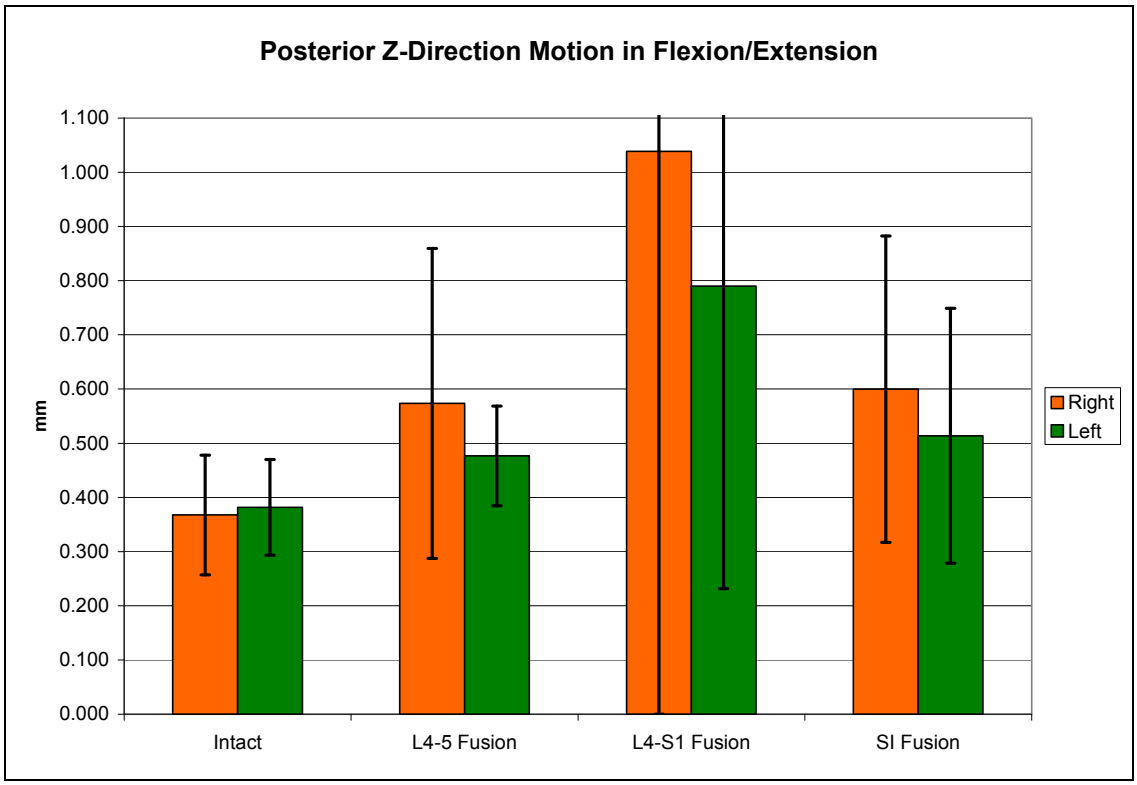

Figure 67: Posterior motion in the z-direction for flexion/extension.

The same trend that was seen with the torsion tests was also noticed during the flexion/extension tests, in that the changes in motion increased as levels were fused in almost all the directions and with both SI joints. In the vertical direction at the right SI joint, an increase of 56.0% ($p = 0.049$) was seen while comparing intact specimens to ones with an L4-5 fusion and an increase of 63.2% ($p = 0.043$) was noticed when comparing intact specimens to ones that underwent a unilateral SI joint fusion. Both these increases were considered statistically significant. The only exceptions, to the trend of increasing motion as levels are fused, were seen in the anterior-posterior (y) direction. At the right SI joint, there was a decrease in motion by 28.4% ($p = 0.215$) comparing a L4-5 fused specimen to one with a L4-S1 lumbosacral fusion and by 0.514% ($p = 0.495$) comparing an intact specimen to one with a L4-S1 fusion. The left SI joint also saw a decrease in motion when comparing a L4-5 fused specimen to a L4-S1 fused specimen by 1.48% ($p = 0.465$). Though, an increase in motion was seen when comparing intact specimens to ones with L4-S1 lumbosacral fusions, by 42.6% ($p = 0.245$). Table 28, below, shows a summary of the percent of change in motion during flexion/extension tests, while Table 29 shows the p-values from the Student's t-Test for these changes (statistical significance is highlighted in red).

Percent Change in Posterior Motion for Flexion/Extension				
	Intact vs. L4-5 Fusion	Intact vs. L4-S1 Fusion	L4-5 Fusion vs. L4-S1 Fusion	Intact vs. SIJ Fusion
Right X	36.0%	72.2%	26.6%	175%
Left X	33.5%	34.9%	1.03%	82.7%
Right Y	38.9%	-0.514%	-28.4%	72.4%
Left Y	44.7%	42.6%	-1.48%	238%
Right Z	56.0%	182%	81.1%	63.2%
Left Z	24.9%	107%	65.7%	34.7%

Table 28: Percent change in posterior motion for flexion/extension tests.

p-values for Changes in Posterior Motion for Flexion/Extension				
	Intact vs. L4-5 Fusion	Intact vs. L4-S1 Fusion	L4-5 Fusion vs. L4-S1 Fusion	Intact vs. SIJ Fusion
Right X	0.186	0.169	0.245	0.060
Left X	0.338	0.299	0.494	0.183
Right Y	0.241	0.495	0.215	0.256
Left Y	0.266	0.245	0.465	0.167
Right Z	0.049	0.099	0.186	0.043
Left Z	0.095	0.071	0.125	0.168

Table 29: P-values for changes in posterior motion during flexion/extension tests.

Overall, an increase in motion was noticed in all parameters tested, as more levels were fused and this is an important fact to keep in mind. As discussed in the *Adjacent Segment Disease* section in the Lower Back Pain subchapter (p. 12), a strong correlation has been found between increased motion and the risk of developing adjacent segment disease.[44] This correlation refers to motion at adjacent vertebral bodies, however, with the theory that the SI joints are the next adjacent joint to the lumbosacral segment, this correlation may apply in this case as well. It was also observed, in general, there is a higher percent of increase in motion after a L4-S1 lumbosacral fusion than after a L4-5 fusion. This again corroborates with the findings of clinical studies that state there is a greater chance for lower back pain, due to the SI joint, after lumboscaral fusions.[7, 28, 33]

CHAPTER 6 - CONCLUSIONS

A great deal was learned during the course of this study and a few conclusions have been reached. This study showed there certainly is motion at the SI joint, though it is quite variable between specimens and even in an individual pelvis between the right and left joints. Motion that occurred during flexion and extension consisted mostly of a rotation in the sagittal plane and could be described as a rocking, or nodding type of movement, as stated by Fick and Kapanji.[32, 67] However, during torsion and compression the motion at the SI joints was found to be translational, predominantly in the medial-lateral plane (x-direction) for torsion and predominantly in the vertical plane (z-direction), but also in the anterior-posterior plane (y-direction) during compression.

As fusions were performed (L4-5, L4-S1 and a unilateral SI joint fusion) altered biomechanics at the SI joints were noticed. Changes were seen in the amount of motion at the SI joints and also in the overall stiffness of the entire pelvic construct. On the anterior side of the pelvis an overall trend of increased motion was detected at the SI joints during axial compression, and to a lesser degree in flexion/extension, when comparing intact specimens to specimens following a L4-S1 lumbosacral fusion. The SI joints on the posterior side of the pelvis also, generally, saw an increase in motion as more levels were fused in all the parameters tested (flexion/extension, torsion and axial compression). Interestingly, it was noticed that that there was a higher percentage of increase in motion after L4-S1 lumbosacral fusions than following L4-5 fusions, similar to the results seen in the clinical study by Ha et al. The majority of the altered biomechanics that were observed due to fusions however, were not considered

statistically significant. This may be due, in part, to the small sample size and also the small scale of motion.

This study proves that changes in biomechanics do occur at the SI joints following lumbar and lumbosacral fusions. These changes could possibly have adverse effects on other adjacent spinal segments, including the SI joints, and lead to additional pain. The results of this study may help surgeons make more informed decisions on whether or not to perform lumbar or lumbosacral fusions to treat lower back pain. It is important to be aware and considering SI joint degeneration as a possible side effect of these fusion surgeries and take that into consideration when determining a treatment plan.

CHAPTER 7 - RECOMENDATIONS

A plethora of knowledge was gained and many goals were achieved during the course of this study. However, there is always room for improvement and a few recommendations for future SI joint/pelvic studies are listed below. A follow-up or continuation of this study with more specimens could possibly aid in developing more trends and significance. The addition of more female specimens would help balance out the study, since there was only one female specimen in this study. The addition of female test specimens could also add insight into potential differences at the SI joints of the different sexes. It has been said that during pregnancy, and sometimes premenstrually, hormonal changes cause greater movements and laxity in females. Additionally, altered posture, weight gain, increased lordosis and trauma caused during birth also play a possible role in changes at the SI joint of females. Therefore, it would be interesting to compare male versus female SI joint biomechanics, of both intact and fused specimens, to see whether they actually differ based on sex.

The experimental model that was derived for this study went through many phases and trials, as explained in the *Development of the Experimental Model* section in the Methods subchapter (p. 22). Though this model was found to be adequate for the study, it did have a few shortcomings, one major one being the fusion of the hip joints. Future work could be done to improve the current experimental model in an attempt to create a model that simulates natural physiologic conditions more accurately. A fine balance needs to be attained to achieve better physiologic accuracy as well as enough stability to withstand the stringent testing parameters.

One limitation that was noticed during this study was the lack of achieving a proper SI joint fusion. It was noticed, there was still some motion at the fused SI joint, and in some extreme cases, more motion than an intact specimen. A few ideas as to why the SI joint fusions weren't as effective as expected were contemplated. One idea was that there many be a need to use two screws instead of one in order to achieve proper fusion. This would secure the SI joint better and prevent rotation around the single screw. Another idea would be to pack bone graft into the single TSM screw that was used. This screw was specifically designed to have the capabilities to be used with or without bone graft. This would make an interesting future study to determine whether using bone graft with the TSM screw would create a significantly better fusion than without. Additionally, and perhaps the most prevalent reason for the unsatisfactory SI joint fusions was the lack of healing time. Under normal circumstances a patient would not be allowed to put any load, let alone such rigorous loads, on the joint after fusion surgery. It typically takes between 12 to 18 weeks to return to normal activities after a SI joint fusion; allowing for the bones and ligaments to heal and for the fusion to take. In this study the specimens were cadaver models and healing/bone growth was not an option. In this case, the cement injection may have been useful in order to improve the grip between the ilium and sacrum creating a more secure fusion. It should be considered that the effects of a unilateral SI joint fusion on the contralateral SI joint may be better suited as a clinical study. Overall, it is felt that this study has opened the door for future studies and put the idea of the SI joint in the forefront as an area that should be studied further.

REFERENCES

1. Anderson CE. Spondyloschisis Following Spine Fusion. Journal of Bone and Joint Surgery, America. 1956;38:1142-1146.

2. Aota Y, Kumano K, Hirabayashi S. Postfusion Instability at the Adjacent Segments After Rigid Pedicle Screw Fixation for Degenerative Lumbar Spinal Disorders. Journal of Spinal Disorders. 1995;8(6):464-473.

3. Baker WC, Thomas TG, Kirkaldy-Willis WH. Changes in Cartilage of Posterior Intervertebral Joints After Anterior Fusion. Journal of Bone and Joint Surgery, British volume. 1969;51B:736-746.

4. Bastian L, Lange U, Knop C, et al. Evaluation of the Mobility of Adjacent Segments After Posterior Thoracolumbar Fixation: A Biomechanical Study. European Spine Journal. 2001;10:295-300.

5. Bogduk N. The Sacroiliac Joint. Clinical Anatomy of the Lumbar Spine and Sacrum. 4th ed. New York: Elsevier, 2005:173-180.

6. Bogduk N. CT-Guided Intraarticular Injection of the Sacroiliac Joint. Journal of Spinal Disorders. 2000;13:365.

7. Buchowski JM, Kebaish KM, Sinkov V, et al. Functional and Radiographic Outcome of Sacroiliac Arthrodesis for the Disorders of the Sacroiliac Joint. Spine. 2005;5(5):520-528.

8. Buckwalter JA. Aging and Degeneration of the Human Intervertebral Disc. Spine. 1995;20:1307-1314.

9. Chen CS, Cheng CK, Liu CL, et al. Stress Analysis of the Disc Adjacent to Interbody Fusion in Lumbar Spine. Medical Engineering & Physics. 2001;23:483-491.

10. Chen WJ, Lai PL, Niu CC, et al. Surgical Treatment of Adjacent Instability After Lumbar Spine Fusion. Spine. 2001;26(22):E519-E524.

11. Chen WJ, Niu CC, Chen LH, et al. Survivorship Analysis of DKS Instrumentation in the Treatment of Spondylolisthesis. Clinical Orthopedics. 1997;339:113-120.

12. Chou R, Qaseem A, Snow V, et al. Diagnosis and Treatment of Low Back Pain: A Joint Clinical Practice Guideline from the American College of Physicians and the American Pain Society. Annals of Internal Medicine. 2007;147:478-491.

13. Chow DH, Luk KD, Evans JH, et al. Effects of Short Anterior Lumbar Interbody Fusion on Biomechanics of Neighboring Unfused Segments. Spine. 1996;21(5):549-555.

14. Cohen SP. Sacroiliac Joint Pain: A Comprehensive Review of Anatomy, Diagnosis, and Treatment. Anesthesia and Analgesia. 2005;101:1440-1453.

15. Comstock CP, van der Meulen MCH, Goodman SB. Biomechanical Comparison of Posterior Internal Fixation Techniques for Unstable Pelvic Fractures. Journal of Orthopedic Trauma. 1996;10(8):517-522.

16. Davis H. Increasing Rates of Cervical and Lumbar Spine Surgery in the United States, 1979-1990. Spine. 1994;19:1117-1124.

17. Dietrichs E. Anatomy of the Pelvic Joints: A Review. Scandinavian Journal of Rheumatology. 1991;88(Suppl):4-6.

18. Dreyfuss P, Dreyer S, Cole A, Mayo K. Sacroiliac Joint Pain. Journal of the American Academy of Orthopedic Surgeons. 2004;12:255-265.

19. Dujardin FH, Roussignol X, Hossenbaccus M, Thomine JM. Experimental Study of the Sacroiliac Joint Micromotion in Pelvic Disrution. Journal of Orthopedic Trauma. 2002;16(2):99-103.

20. Eck JC, Humpreys SC, Hodges SD. Adjacent-Segment Degeneration After Lumbar Fusion: A Review of Clinical, Biomechanical, and Radiologic Studies. American Journal of Orthopedics. 1999;28:336-340.

21. Esses SI, Doherty BJ, Crawford MJ, et al. Kinematic Evaluation of Lumbar Fusion Techniques. Spine. 1996;21(6):676-684.

22. Etebar S, Cahill DW. Risk Factors for Adjacent-Segment Failure Following Lumbar Fixation with Rigid Instrumentation for Degenerative Instability. Journal of Neurosurgery. 1999;90:163-169.

23. Foley BS, Buschbacher RM. Sacroiliac Joint Pain: Anatomy, Biomechanics, Diagnosis, and Treatment. American Journal of Physical Medicine & Rehabilitation. 2006;85(12):997-1006.

24. Frigerio NA, Stowe RR, Howe JW. Movement of the Sacroiliac Joint. Clinical Orthopedics. 1974;100:370-377.

25. Fronig EC, Frohman B. Motion of the Lumbosacral Spine after Laminectomy and Spine Fusion: Correlation of Motion with the Result. Journal of Bone and Joint Surgery, America. 1968;50:897-918.

26. Frymoyer JW, Hanley E, Howe J, et al. Disc Excision and Spine Fusion in the Management of Lumbar Disc Disease: A Minimum Ten-Year Follow-Up. Spine. 1978;3(1):1-6.

27. Frymoyer JW, Howe J, Kuhlmann D. The Long-Term Effects of Spinal Fusion on the Sacroiliac Joints and Ilium. Clinical Orthopedics. 1978;134:196-201.

28. Ha KY, Lee JS, Kim KW. Degeneration of Sacroiliac Joint After Instrumented Lumbar or Lumbosacral Fusion. Spine. 2008;33:1192-1198.

29. Ha KY, Schendel MJ, Lewis JL, Ogilvie JW. Effect of Immobilization and Configuration on Lumar Adjacent-Segment Biomechanics. Journal of Spinal Disorders. 1993;6(2):99-105.

30. Hambly MF, Wiltse LL, Raghavan N, et al. The Transition Zone Above A Lumbosacral Fusion. Spine. 1998;23(16):1785-1792.

31. Hsu K, Zucherman J, White A, et al. Deterioration of Motion Segments Adjacent to Lumbar Spine Fusions. Presented at North American Spine Society. Colorado Springs, CO. July 26, 1988. Ortho Transact. 12:605-606.

32. Kapandji IA. The Physiology of the Joints: Volume Three – The Trunk and the Vertebral Column. New York, New York: Churchill Livingstone, 1982:64.

33. Katz V, Schofferman J, Reynolds J. The Sacroiliac Joint: A Potential Cause of Pain After Lumbar Fusion to the Sacrum. Journal of Spinal Disorders. 2003;16:96-99.

34. Kumar MN, Baklanov A, Chopin D. Correlation Between Sagittal Plane Changes and Adjacent Segment Degeneration Following Lumbar Spine Fusion. European Spine Journal. 2001;10:314-319.

35. Lee CK, Langrana NA. Lumbosacral Spinal Fusion: A Biomechanical Study. Spine. 1984;9(6):574-581.

36. Lee CK. Accelerated Degeneration of the Segment Adjacent to a Lumbar Fusion. Spine. 1988;13:375-377.

37. Lehman TR, Spratt KF, Tozzi JE, et al. Long-Term Follow-Up of Lower Lumbar Fusion Patients. Spine. 1987;12(2):97-104.

38. MacAvoy MC, McClellan RT, Goodman SB, et al. Stability of Open-Book Pelvic Fractures Using a New Biomechanical Model of Single-Limb Stance. Journal of Orthopedic Trauma. 1997;11(8):590-593.

39. Maigne JY, Planchon CA. Sacroiliac Joint Pain After Lumbar Fusion. A study With Anesthetic Block. European Spine Journal. 2005;14:654-658.

40. Nagata H, Schendel MJ, Transfeldt EE, et al. The Effects of Immobilization of Long Segments of the Spine on the Adjacent and Distal Facet Force and Lumbosacral Motion. Spine. 1993;18(16):2471-2479.

41. Olson SA, Bay BK, Hamel A. Biomechanics of the Hip Joint and the Effects of Fracture of the Acetebulum. Clinical Orthopedics. 1997;339:92-104.

42. Olson SA, Kadrmas MW, Hernandez JD, et al. Augmentation of Posterior Wall Acetabular Fracture Fixation Using Calcium-Phosphate Cement: A Biomechanical Analysis. Journal of Orthopedic Trauma. 2007;21(9):608-616.

43. Onsel C, Collier BD, Kir KM, et al. Increased Sacroiliac Joint Uptake after Lumbar Fusion and/or Laminectomy. Clinical Nuclear Medicine. 1992;17:283-287.

44. Park P, Garton HJ, Gala VC, et al. Adjacent Segment Disease after Lumbar or Lumbosacral Fusion: Review of the Literature. Spine 2004;29(17):1938-1944.

45. Penta M, Sandhu A, Fraser RD. Magnetic Resonance Imaging Assessment of Disc Degeneration 10 Years After Anterior Lumbar Interbody Fusion. Spine. 1995;20(6):743-747.

46. Phillips FM, Carlson GD, Bohlman HH, et al. Results of Surgery for Spinal Stenosis Adjacent to Previous Lumbar Fusion. Journal of Spinal Disorders. 2000;13(5):432-437.

47. Pohlemann T, Angst M, Schneider E, et al. Fixation of Transforaminal Sacrum Fractures: A Biomechanical Study. Journal of Orthopedic Trauma. 1993;7(2):107-117.

48. Prather H, Hunt D. Conservative Management of Low Back Pain, Part I. Sacroiliac Joint Pain. Disease-A-Month. 2004; 50:670-683.

49. Rahm MD, Hall BB. Adjacent-Segment Degeneration After Lumbar Fusion With Instrumentation: A Retrospective Study. Journal of Spinal Disorders. 1996;9(5):392-400.

50. Regan, John. Spondylosis (Spinal Osteoarthritis). Spine Universe. February 2008. Available at: http://www.spineuniverse.com/displayarticle.php/article1440.html. Accessed on January 2009.

51. Ross J. Is the Sacroiliac Joint Mobile and How Should It Be Treated? British Journal of Sports Medicine. 2000;34(3):226.

52. Sacroiliac Joint Dysfunction. July 2003. Available at: http://www.coretherapy.com/health_news/articles_sacroiliac_joint_dysfunction.html. Accessed on January 2009.

53. Sagi HC, Ordway NR, DiPasquale T. Biomechanical Analysis of Fixation for Vertically Unstable Sacroiliac Dislocations With Iliosacral Screws and Symphyseal Plating. Journal of Orthopedic Trauma. 2004;18(3):138-143.

54. Schildhauer TA, Ledoux WR, Chapman JR, et al. Triangular Osteosynthesis and Iliosacral Screw Fixation for Unstable Sacral Fractures: A Cadaveric and Biomechanical Evaluation Under Cyclic Loads. Journal of Orthopedic Trauma. 2003;17(1):22-31.

55. Schlegel JD, Smith JA, Schleusener RL. Lumbar Motion Segment Pathology Adjacent to Thoracolumbar, Lumbar, and Lumbosacral Fusions. Spine. 1996;21(8):970-981.

56. Seitsalo S, Schlenzka D, Poussa M, et al. Disc Degeneration in Young Patients With Isthmic Spondylolisthesis Treated Operatively or Conservatively: A Long Term Follow-Up. European Spine Journal. 1997;6(6):393-397.

57. Shaw JA, Mino DE, Werner FW, Murray DG. Posterior Stabilization of Pelvic Fractures by Use of Threaded Compression Rods: Case Reports and Mechanical Testing. Clinical Orthopedics. 1985;192:240-254.

58. Simonian PT, Routt MLC, Harrington RM, Tencer AF. Anterior Versus Posterior Provisional Fixation in the Unstable Pelvis. Clinical Orthopedics. 1995;310:245-251.

59. Simonian PT, Routt MLC, Harrington RM, Tencer AF. Internal Fixation for the Transforaminal Sacral Fracture. Clinical Orthopedics. 1996;323:202-209.

60. Slipman CW, Shin CH, Patel RK, et al. Etiologies of Failed Back Surgery Syndrome. Pain Medicine. 2002;3(3):200-214.

61. Varga E, Hearn T, Powell J, Tile M. Effects of Method on Internal Fixation of Symphyseal Disruptions on Stability of the Pelvic Ring. Injury. 1995;26(2):75-80.

62. Vleeming A, Stoeckart R, Volkers AC, et al. Relation Between Form and Function in the Sacroiliac Joint. Part I: Clinical Anatomical Aspects. Spine. 1990;15:130-132.

63. Vleeming A, Volkers AC, Snijders CJ, et al. Relation Between Form and Function in the Sacroiliac Joint. Part II: Biomechanical Aspects. Spine. 1990;15:133-136.

64. Waguespack A, Schofferman J, Slosar P, Reynolds J. Etiologies of Long-term Failures of Lumbar Spine Surgery. Pain Medicine. 2002;3(1):18-22.

65. Walheim GG, Selvik G. Mobility of the Pubic Symphysis: In-vivo Measurements with an Electromechanic Method and a Roentgen Stereophotogrammetric Method. Clinical Orthopedics. 1984;191:129-135.

66. Weigel H. The movement of the sacroiliac joint. Acta Anatomica. 1955;23:80.

67. White A, Panjabi M. Clinical Biomechanics of the Spine. 2nd ed. Philadelphia, PA: J.B. Lippincott Company, 1990:112-114.

68. Whitecloud TS III, Davis JM, Olive PM. Operative Treatment of the Degenerated Segment Adjacent to a Lumbar Fusion. Spine. 1994;19(5):531-536.

69. Wimmer C, Gluch H, Krismer M, et al. AP-Translation in the Proximal Disc Adjacent to Lumbar Spine Fusion: A Retrospective Comparison of Mono-and Polysegmental Fusion in 120 Patients. Acta Orthopaedica. 1997;68:3:269-272.

70. Yang SW, Langrana NA, Lee CK. Biomechanics of Lumbosacral Spine Fusion in Combined Compression-Torsion Loads. Spine. 1986;11:937-941.

71. Yinger K, Scalise J, Olson SA, et al. Biomechanical Comparison of Posterior Pelvic Ring Fixation. Journal of Orthopedic Trauma. 2003;17(7):481-484.

APPENDIX A: Experimental Checklist

SIJP Checklist

□ 1. Thaw spine # _____ and separate the spine through the L3-L4 disc, making sure the lumbosacral spine (L4-S1) is intact and the iliolumbar ligaments, the pubic joint and SI joints and the sacrotuberous and sacrospinous ligaments are preserved as well.

□ 2. Mount the X-Y linear bearings on the MTS ram with a loading clevis compatible with the load lever arm.

□ 3. Calibrate the Selspot system for 2 cameras, #1 & #2.

□ 4. Apply DVRT fixture brackets on either side of both SI joints under fluoroscopy, making sure each bracket set is on either side of the joint.

□5. Cut sawbones femurs at distal diaphyseal (the proximal portion of the femurs shall be used for this study).

□ 6. Pot the distal ends of the sawbones femurs in PMMA and grip each in a vice while still soft to create a good gripping area.

□ 7. Screw sawbones femurs into the acetabulem, making sure that the pelvis is in the correct orientation with L4 level and there is no motion at the hip joint.

□ 8. Screw in three blunt-tipped half pins on one iliac wing to anchor turnbuckles for single leg stance.

□ 9. Mount the loading fixture block with PMMA to the superior surface of L4. Align load block so that it is in the center of L4 and horizontally level.

□ 10. Mount vice and roller plate & vice onto the MTS machine. Angle the set-up so a full sagittal view can be seen by the Selspot cameras and with a video camera.

□ 11. Apply one LED bracket with 3 LED's from the Selspot system to the sacrum and each of the pelvic rims as shown in Figure 1.

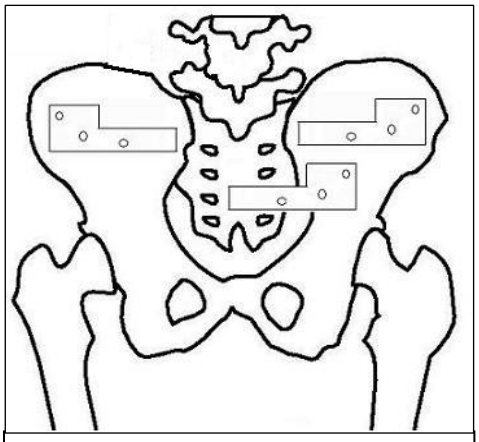

Figure 1: Location of LED brackets on posterior side of spine and pelvis.

□ 12. Set Selspot file to 9 LED's and 2 cameras. Check to see that each Selspot camera clearly views each LED and that the exposure levels are adequate for recording.

□ 13. Apply DVRT to fixture brackets, in x and y directions for both joints. Record location, orientation and channel of DVRT.

□ 14. Apply the load lever arm to the block on top of L4 and secure with the set screw.

□ 15. Photograph the spine from the sagittal view and a frontal view with a still camera. Also set up video recording device and tripod if necessary.

□ 16. ***Loading Step 1(Intact):*** Set MTS filename: ***SIJP__16***. Zero the MTS with flexion load on the table (60N).

□ 17. Fix the header: **Flexion-extension 17**. Note the rotational position of the ram for flexion. Set the MTS acquire time, axial force, axial displacement, torque and angle. Apply the preload of 60N to the flexion side of the load lever arm. Apply a cyclic extension load in load control from 16.8 N to 168 N (on the 10 cm loading lever to produce a peak of 16.8 N·m with a proportional axial compression load) at 0.25 Hz. After a few cycles of loading to reach a steady state, record measures for:

□DVRTs with filename: ***SIJP*** **__17**

□ Selspot LED's with filename: ***SIJP*** **__17**

□ 18. Fix the header: **Torsion 18**. Align load block with the axial rotation fixture, then take bearings out and lock entire setup on MTS table. Clamp the loading fixture on the top of the spine centered in the axial torque fixture and apply a cyclic axial torque in load control to peaks of ± 7.5 N·m at 0.25 Hz. After a few cycles of loading to reach a steady state in axial rotation, record measures for:

□DVRTs with filename: ***SIJP*** **__18**

□Selspot LED's with filename: ***SIJP*** **__18**

□ 19. Fix the header: **Double leg Compression 19**. Align load block with the axial rotation fixture. Apply a compression load, in stroke control from 150 N to 1500 N and cycle at 0.25 Hz. After a few cycles of loading to reach a steady state, record measures for:

□DVRTs with filename: ***SIJP*** **__19**

□Selspot LED's with filename: ***SIJP*** **__19**

□ 20. Remove one leg (R / L) from the roller vice and let it hang freely, creating a single-leg stance. Attach and tighten turnbuckles.

□ 21. Fix the header: **Single leg Compression 21**. Align load block with the axial rotation fixture. Apply a compression load, in stroke control from 60 N to 600 N and cycle at 0.25 Hz. After a few cycles of loading to reach a steady state, record measures for:

□DVRTs with filename: ***SIJP*** **__21**

☐Selspot LED's with filename: ***SIJP__21***

□ 22. Check the Selspot and DVRT data to make sure there were no large errors.

□ 23. Perform a single level 360ºfusion at L4-5 using ALIF cages and pedicle screws and rods.

□ 24. ***Loading Step 2(Single Level Fusion):*** Set MTS filename: ***SIJP__24***. Zero the MTS with flexion load on the table (60N).

□ 25. Photograph the spine from the sagittal view and a frontal view with a still camera. Also set up video recording device and tripod if necessary.

□ 26. Fix the header: **Single leg Compression 26**. Align load block with the axial rotation fixture. Apply a compression load, in stroke control from 60 N to 600 N and cycle at 0.25 Hz. After a few cycles of loading to reach a steady state, record measures for:

☐DVRTs with filename: ***SIJP__26***

☐Selspot LED's with filename: ***SIJP__26***

□ 27. Return to double leg stance, with both femurs in their vices and loosening turnbuckles.

□ 28. Fix the header: **Double leg Compression 28**. Align load block with the axial rotation fixture. Apply a compression load, in stroke control from 150 N to 1500 N and cycle at 0.25 Hz. After a few cycles of loading to reach a steady state, record measures for:

☐DVRTs with filename: ***SIJP__28***

☐Selspot LED's with filename: ***SIJP__28***

□ 29. Fix the header: **Torsion 29**. Align load block with the axial rotation fixture, then take bearings out and lock entire setup on MTS table. Clamp the loading fixture on the top of the spine centered in the axial torque fixture and apply a cyclic axial torque in load control to peaks of ± 7.5 N·m at 0.25 Hz. After a few cycles of loading to reach a steady state in axial rotation, record measures for:

☐DVRTs with filename: ***SIJP__29***

☐Selspot LED's with filename: ***SIJP__29***

□ 30. Fix the header: **Flexion-extension 30**. Note the rotational position of the ram for flexion. Set the MTS acquire time, axial force, axial displacement, torque and angle. Apply the preload of 60N to the flexion side of the load lever arm. Apply a cyclic extension load in load control from 16.8 N to 168 N (on the 10 cm loading lever to

produce a peak of 16.8 N·m with a proportional axial compression load) at 0.25 Hz. After a few cycles of loading to reach a steady state, record measures for:

☐DVRTs with filename: ***SIJP __30***

☐ Selspot LED's with filename: ***SIJP __30***

☐ 31. Check the Selspot and DVRT data to make sure there were no large errors.

☐ 32. Perform a double level 360ºfusion L4-S1, using ALIF cages and pedicle screws and rods.

☐ 33. ***Loading Step 3(Double Level Fusion):*** Set MTS filename: ***SIJP__33***. Zero the MTS with flexion load on the table (60N).

☐ 34. Photograph the spine from the sagittal view and a frontal view with a still camera. Also set up video recording device and tripod if necessary.

☐ 35. Fix the header: **Flexion-extension 35**. Note the rotational position of the ram for flexion. Set the MTS acquire time, axial force, axial displacement, torque and angle. Apply the preload of 60N to the flexion side of the load lever arm. Apply a cyclic extension load in load control from 16.8 N to 168 N (on the 10 cm loading lever to produce a peak of 16.8 N·m with a proportional axial compression load) at 0.25 Hz. After a few cycles of loading to reach a steady state, record measures for:

☐DVRTs with filename: ***SIJP __35***

☐ Selspot LED's with filename: ***SIJP __35***

☐ 36. Fix the header: **Torsion 36**. Align load block with the axial rotation fixture, then take bearings out and lock entire setup on MTS table. Clamp the loading fixture on the top of the spine centered in the axial torque fixture and apply a cyclic axial torque in load control to peaks of ± 7.5 N·m at 0.25 Hz. After a few cycles of loading to reach a steady state in axial rotation, record measures for:

☐DVRTs with filename: ***SIJP __36***

☐Selspot LED's with filename: ***SIJP __36***

☐ 37. Fix the header: **Double leg Compression 37**. Align load block with the axial rotation fixture. Apply a compression load, in stroke control from 150 N to 1500 N and cycle at 0.25 Hz. After a few cycles of loading to reach a steady state, record measures for:

☐DVRTs with filename: ***SIJP __37***

☐Selspot LED's with filename: ***SIJP __37***

☐ 38. Remove one leg (R / L) from vice and let it hang freely, creating a single-leg stance.

□ 39. Fix the header: **Single leg Compression 39**. Align load block with the axial rotation fixture. Apply a compression load, in stroke control from 60 N to 600 N and cycle at 0.25 Hz. After a few cycles of loading to reach a steady state, record measures for:

□DVRTs with filename: ***SIJP*** **__39**

□Selspot LED's with filename: ***SIJP*** **__39**

□ 40. Check the Selspot and DVRT data to make sure there were no large errors.
□ 41. Perform a fusion at the (R / L) SI joint using SI joint screws.

□ 42. ***Loading Step 4(Unilateral SIJ Fusion):*** Set MTS filename: ***SIJP__42***. Zero the MTS with flexion load on the table (60N).

□ 43. Photograph the spine from the sagittal view and a frontal view with a still camera. Also set up video recording device and tripod if necessary.

□ 44. Fix the header: **Single leg Compression 44**. Align load block with the axial rotation fixture. Apply a compression load, in stroke control from 60 N to 600 N and cycle at 0.25 Hz. After a few cycles of loading to reach a steady state, record measures for:

□DVRTs with filename: ***SIJP*** **__44**

□Selspot LED's with filename: ***SIJP*** **__44**

□ 45. Return to double leg stance, with both femurs in their vices and loosening turnbuckles.

□ 46. Fix the header: **Double leg Compression 46**. Align load block with the axial rotation fixture. Apply a compression load, in stroke control from 150 N to 1500 N and cycle at 0.25 Hz. After a few cycles of loading to reach a steady state, record measures for:

□DVRTs with filename: ***SIJP*** **__46**

□Selspot LED's with filename: ***SIJP*** **__46**

□ 47. Fix the header: **Torsion 47**. Align load block with the axial rotation fixture, then take bearings out and lock entire setup on MTS table. Clamp the loading fixture on the top of the spine centered in the axial torque fixture and apply a cyclic axial torque in load control to peaks of ± 7.5 N·m at 0.25 Hz. After a few cycles of loading to reach a steady state in axial rotation, record measures for:

□DVRTs with filename: ***SIJP*** **__47**

□Selspot LED's with filename: ***SIJP*** **__47**

□ 48. Fix the header: **Flexion-extension 48**. Note the rotational position of the ram for flexion. Set the MTS acquire time, axial force, axial displacement, torque and angle. Apply the preload of 60N to the flexion side of the load lever arm. Apply a cyclic extension load in load control from 16.8 N to 168 N (on the 10 cm loading lever to produce a peak of 16.8 N·m with a proportional axial compression load) at 0.25 Hz. After a few cycles of loading to reach a steady state, record measures for:

□DVRTs with filename: ***SIJP*** **__48**

□ Selspot LED's with filename: ***SIJP*** **__48**

□ 49. Check the Selspot and DVRT data to make sure there were no large errors.

□ 50. Remove all hardware from the specimen and place in red bag for proper disposal.

APPENDIX B: Load/Displacement Curves

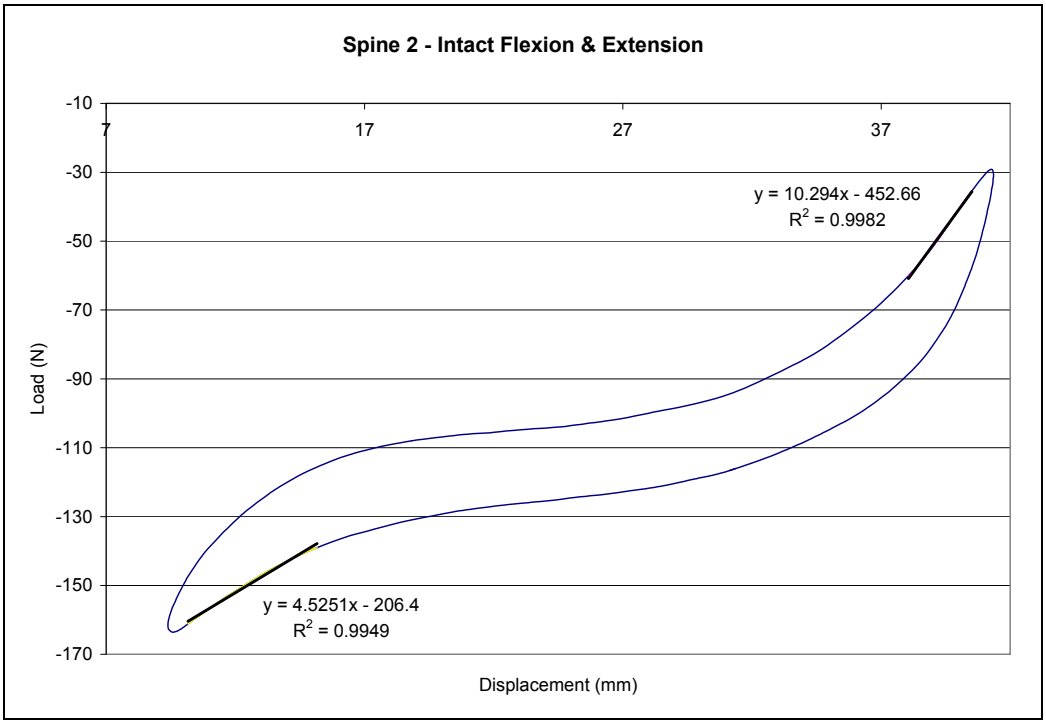

Figure 68: Spine 2 load/displacement curve intact flexion/extension.

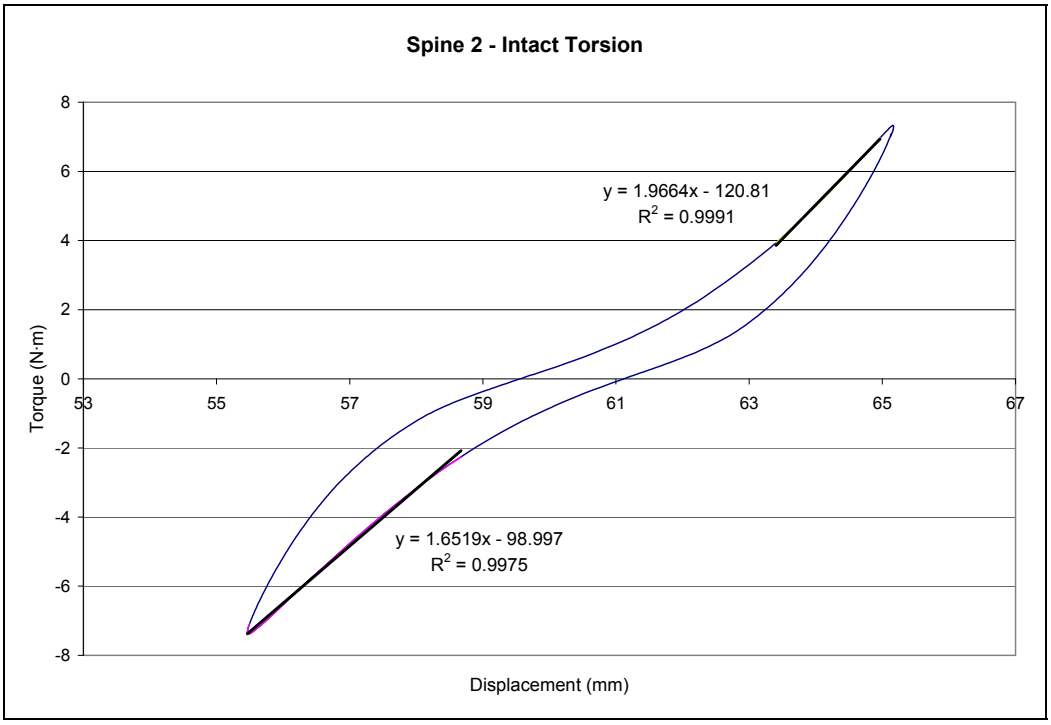

Figure 69: Spine 2 load/displacement curve intact torsion.

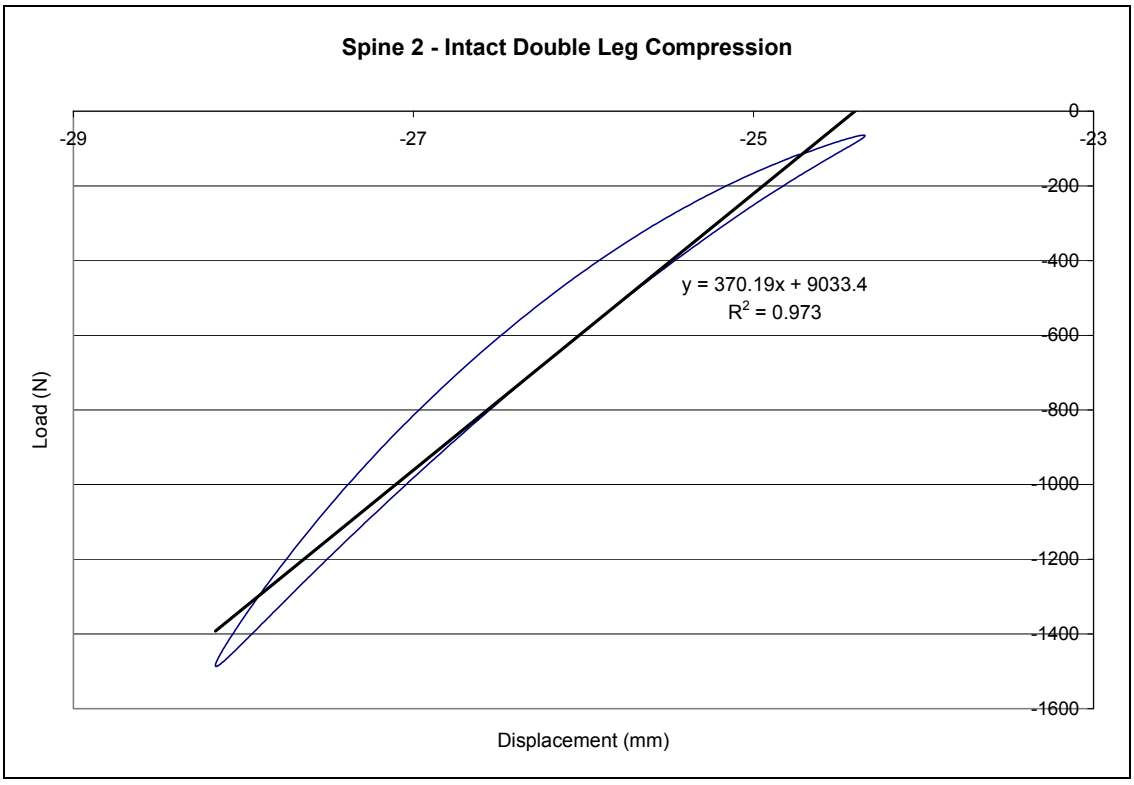

Figure 70: Spine 2 load/displacement curve intact double leg compression.

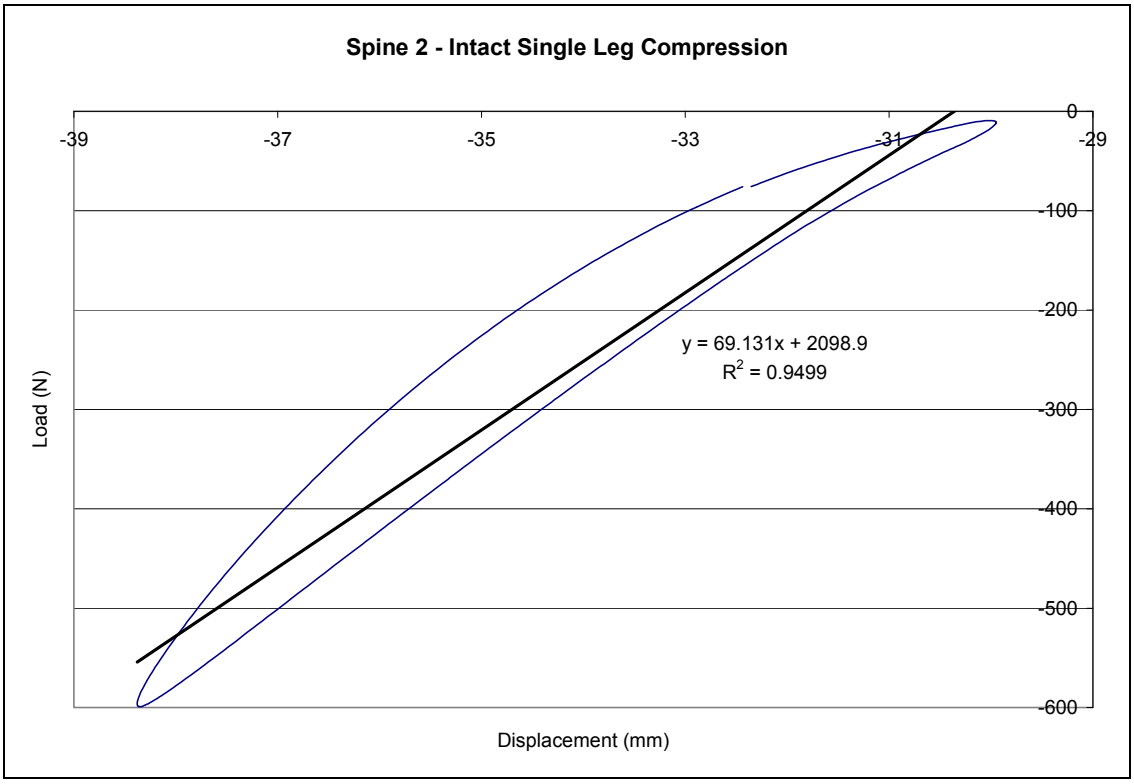

Figure 71: Spine 2 load/displacement curve intact single leg compression.

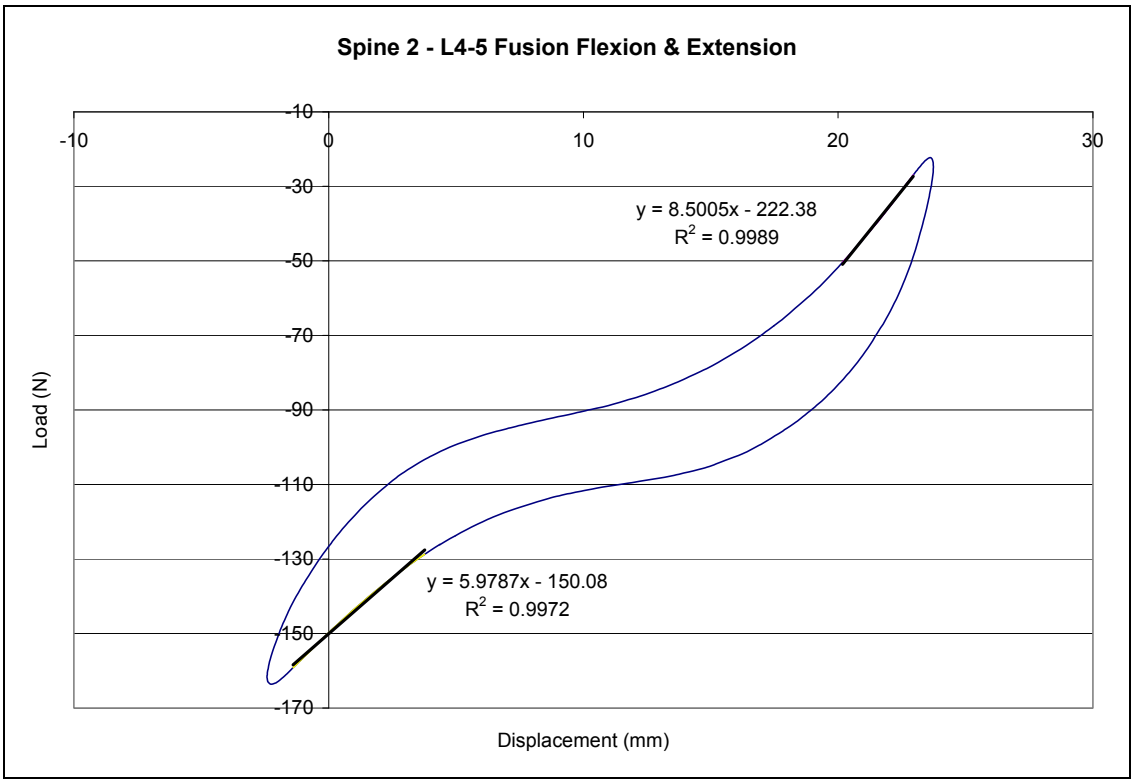

Figure 72: Spine 2 load/displacement curve flexion/extension L4-5 fusion.

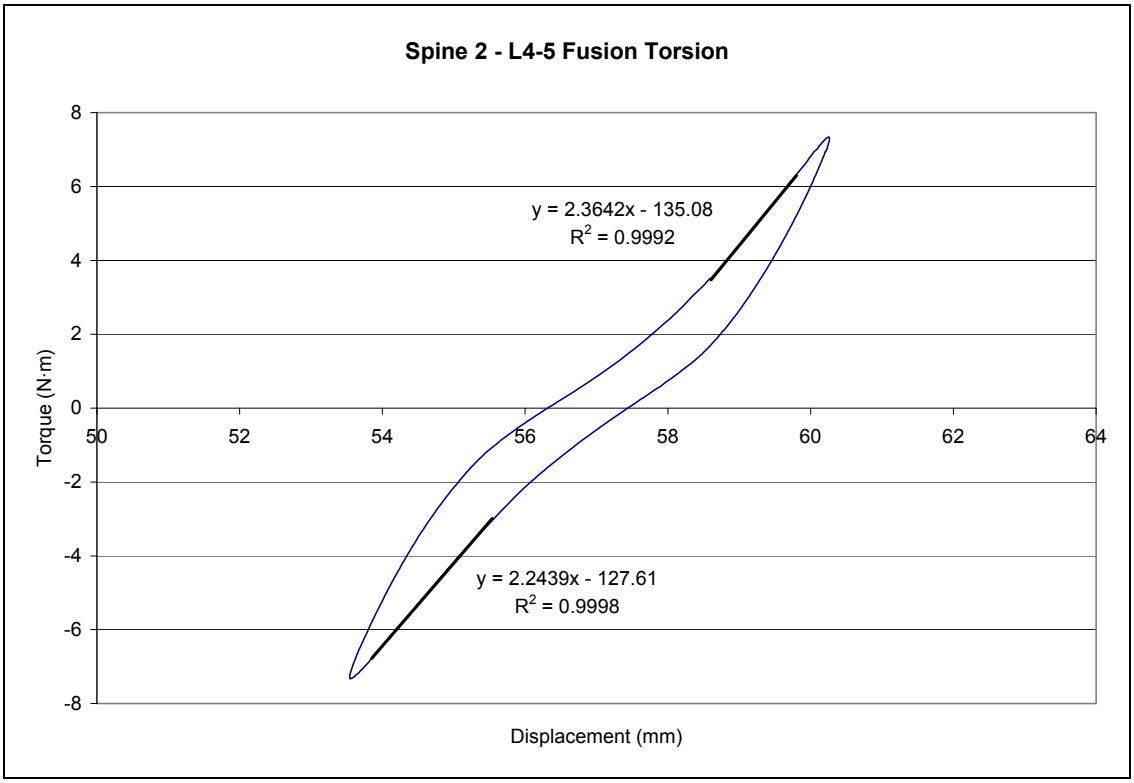

Figure 73: Spine 2 load/displacement curve torsion L4-5 fusion.

Figure 74: Spine 2 load/displacement curve double leg compression L4-5 fusion.

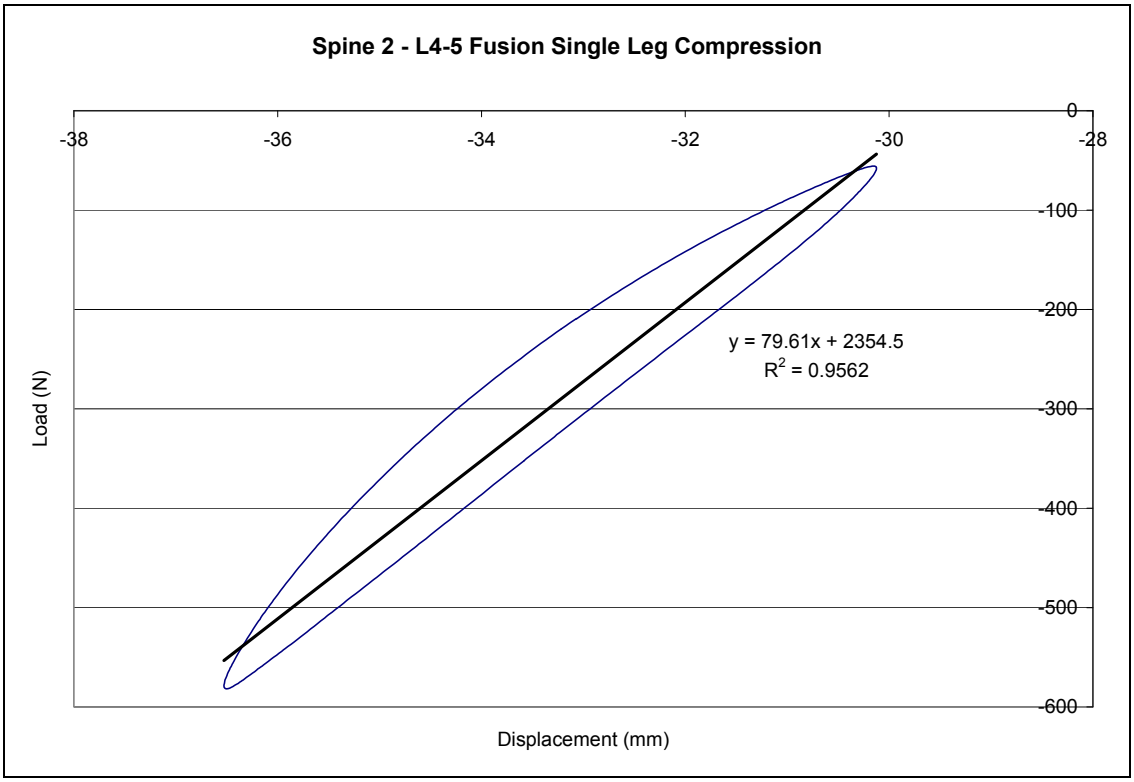

Figure 75: Spine 2 load/displacement curve single leg compression L4-5 fusion.

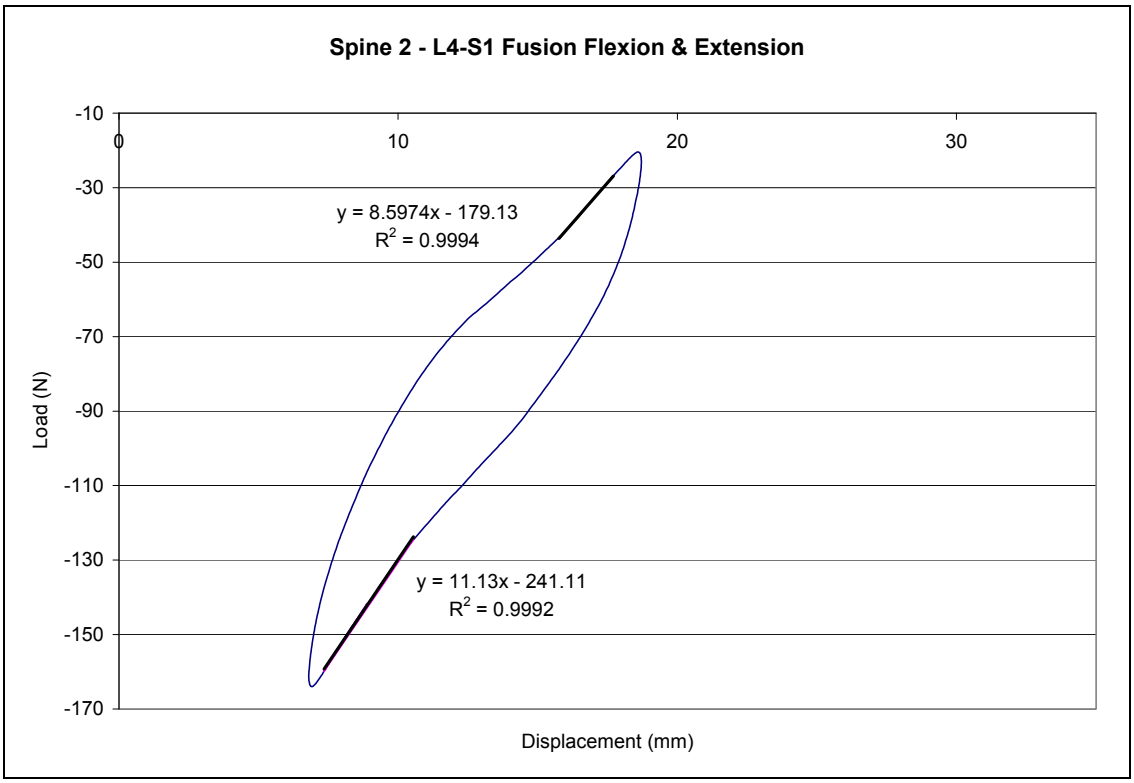

Figure 76: Spine 2 load/displacement curve flexion/extension L4-S1 fusion.

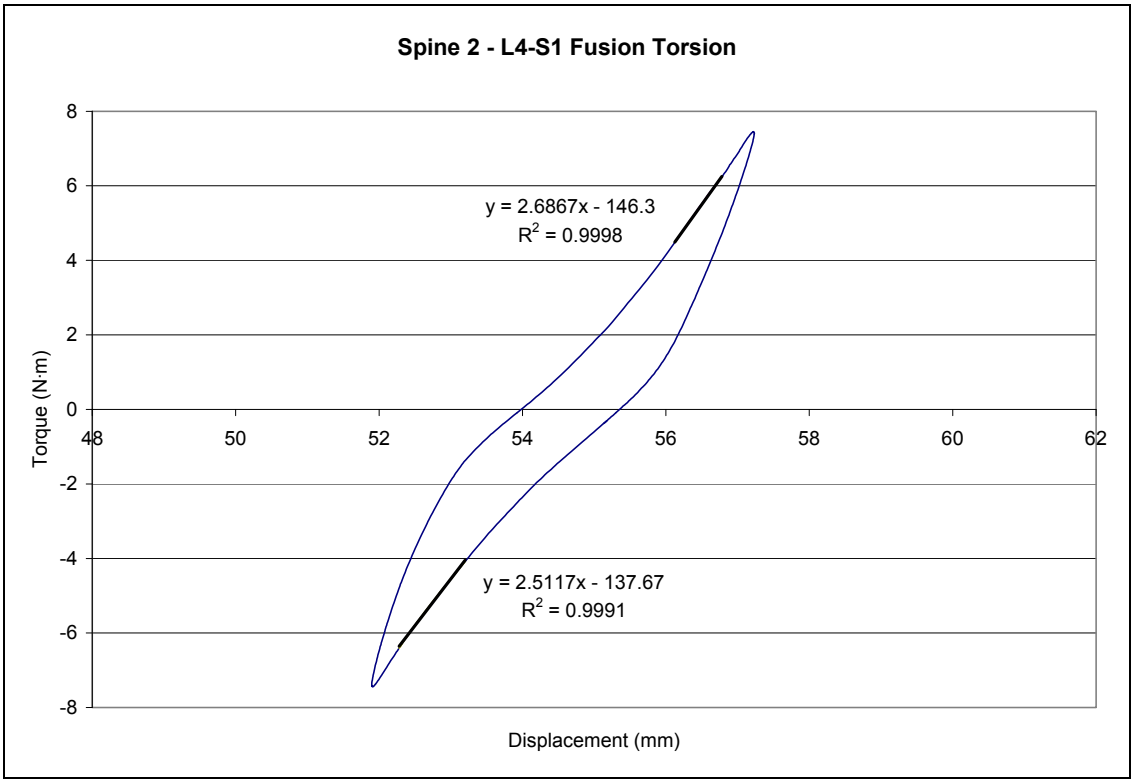

Figure 77: Spine 2 load/displacement curve torsion L4-S1 fusion.

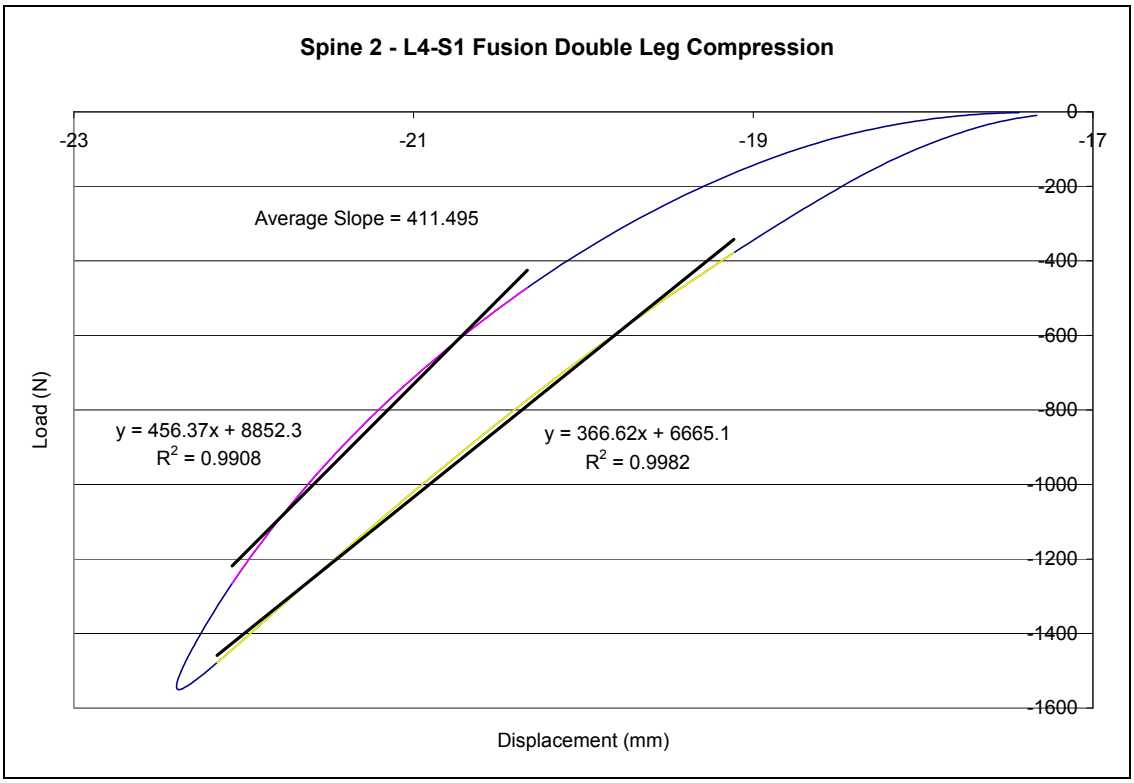

Figure 78: Spine 2 load/displacement curve double leg compression L4-S1 fusion.

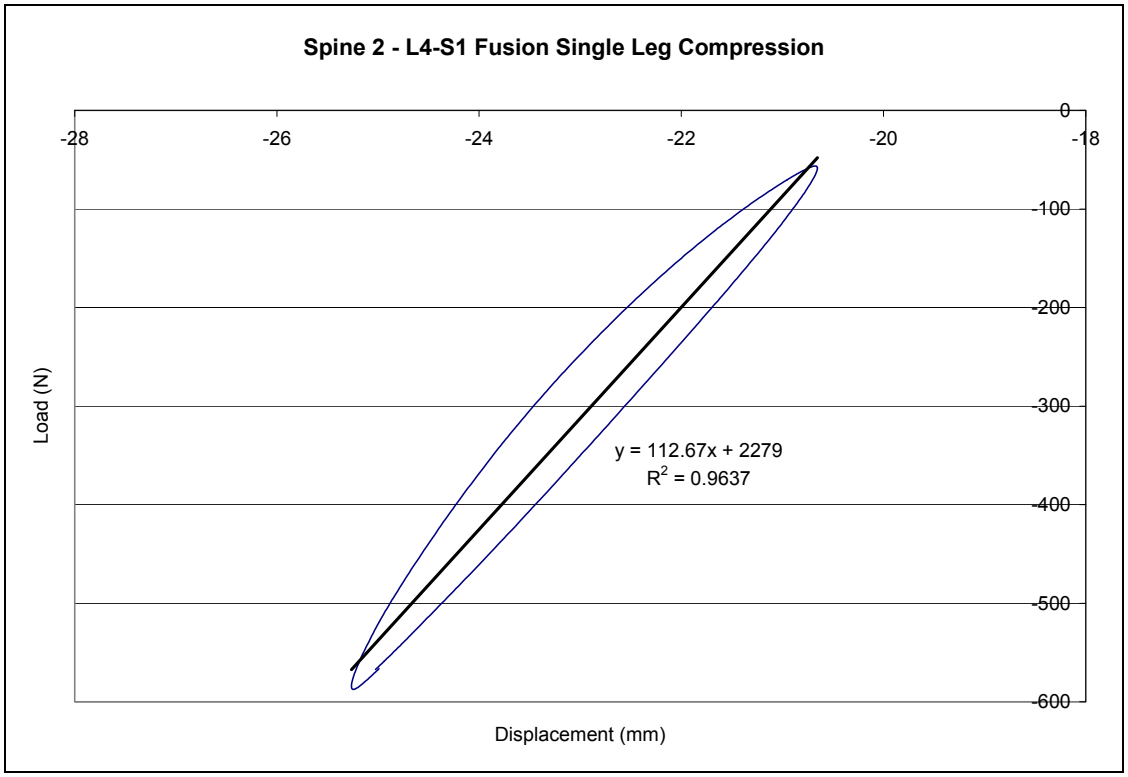

Figure 79: Spine 2 load/displacement curve single leg compression L4-S1 fusion.

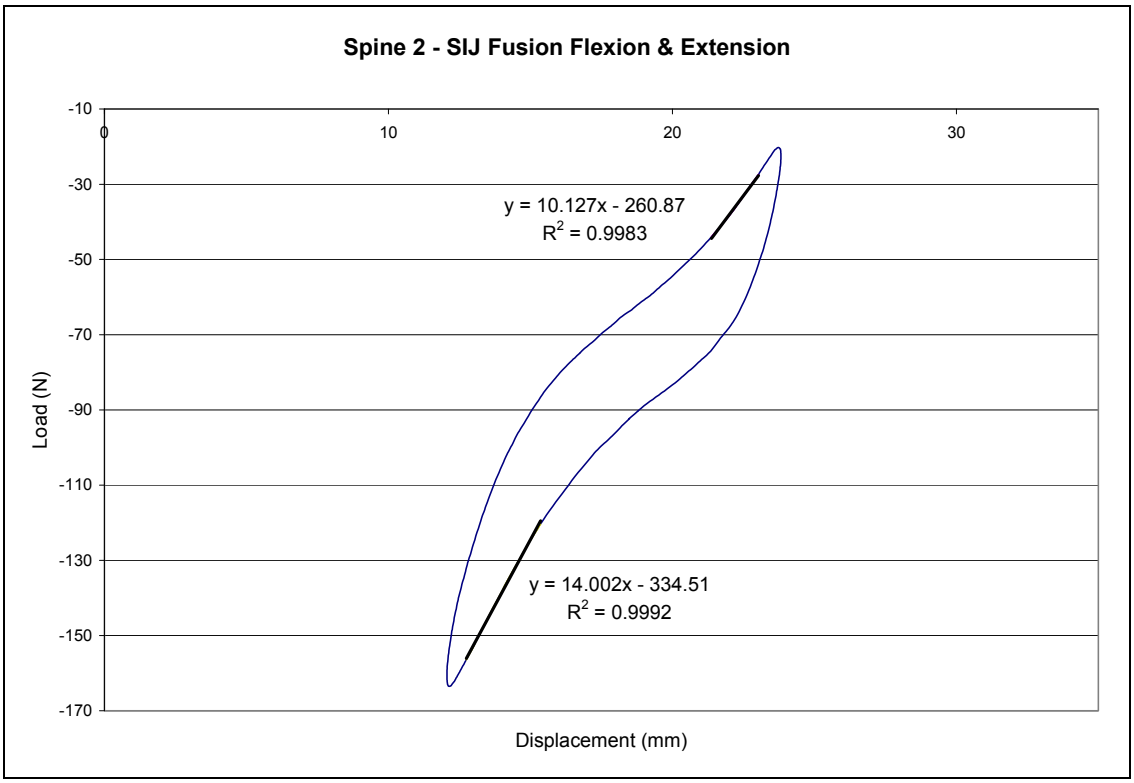

Figure 80: Spine 2 load/displacement curve flexion/extension SIJ fusion.

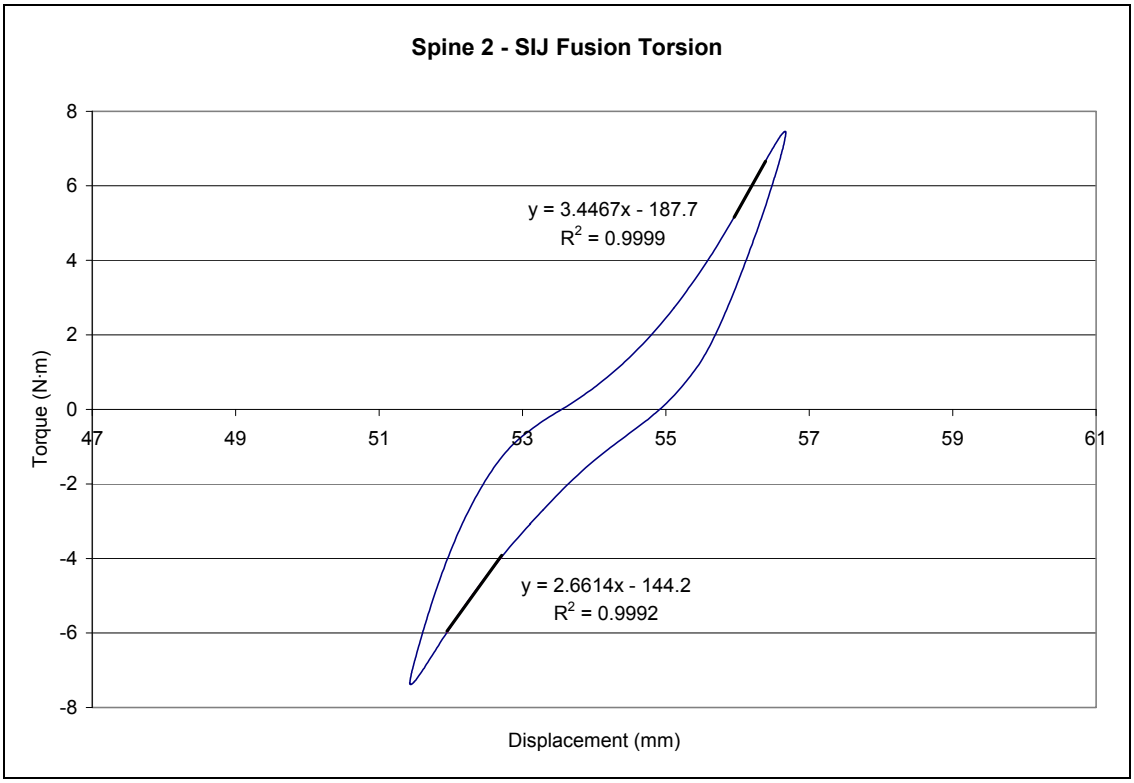

Figure 81: Spine 2 load/displacement curve torsion SIJ fusion.

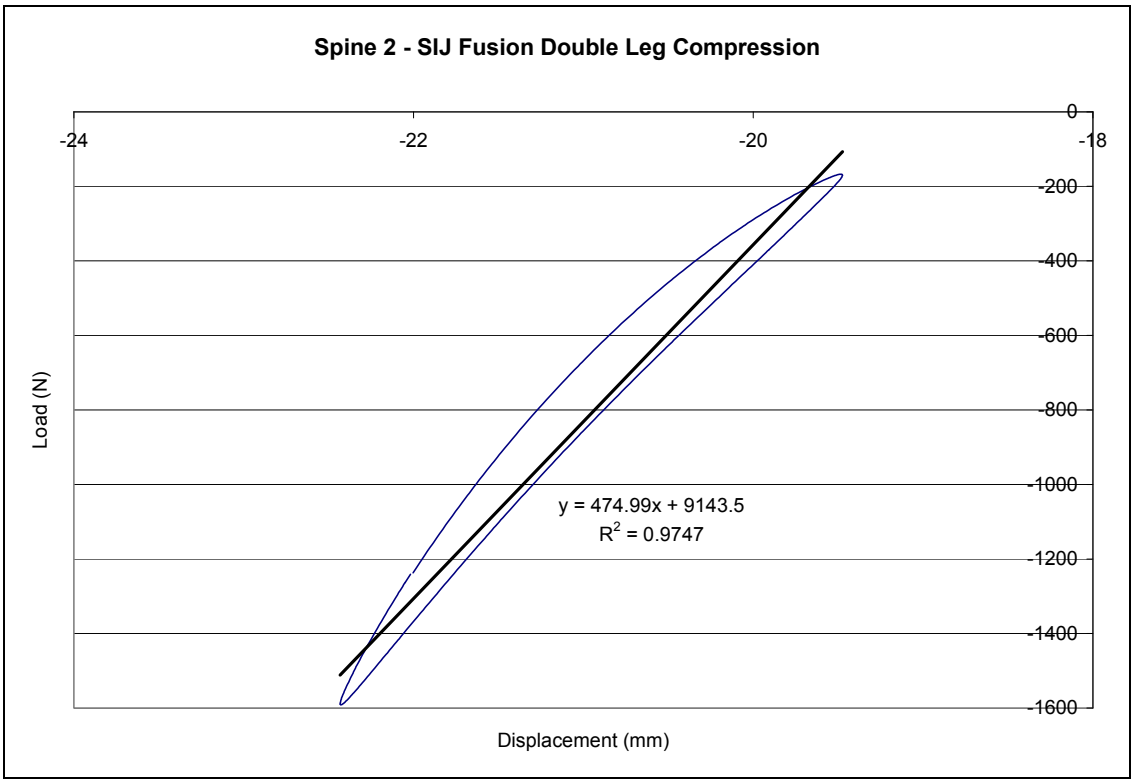

Figure 82: Spine 2 load/displacement curve double leg compression SIJ fusion.

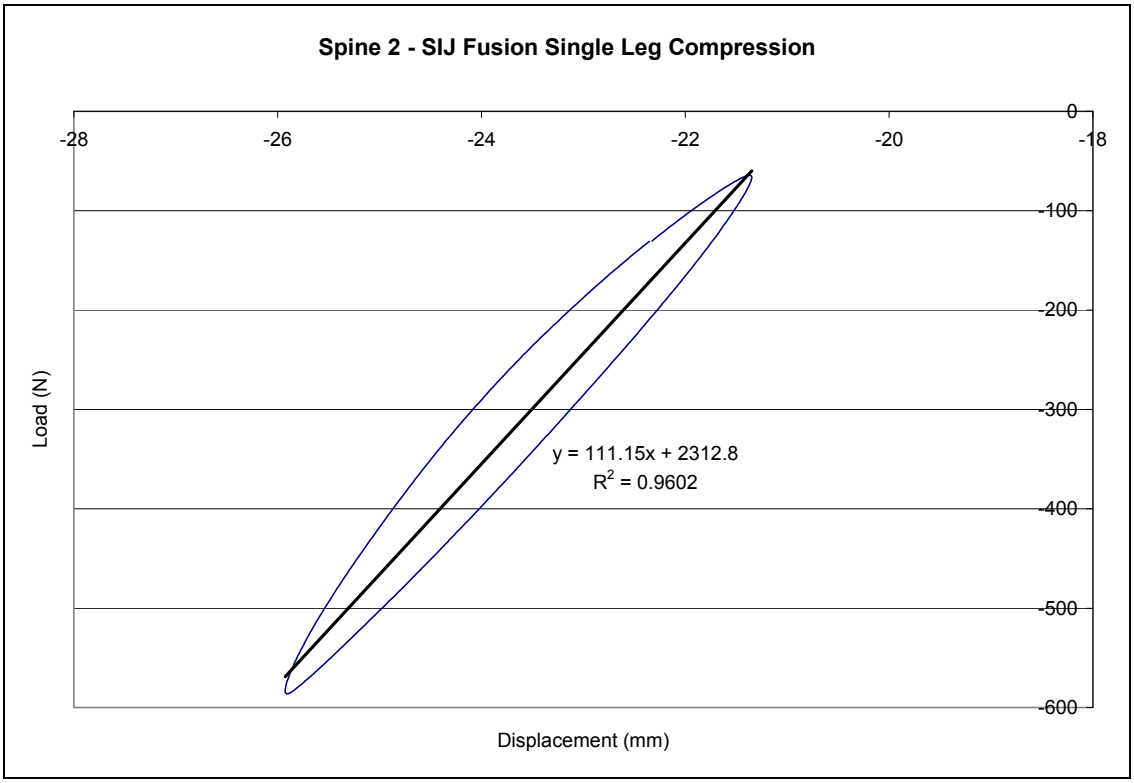

Figure 83: Spine 2 load/displacement curve single leg compression SIJ fusion.

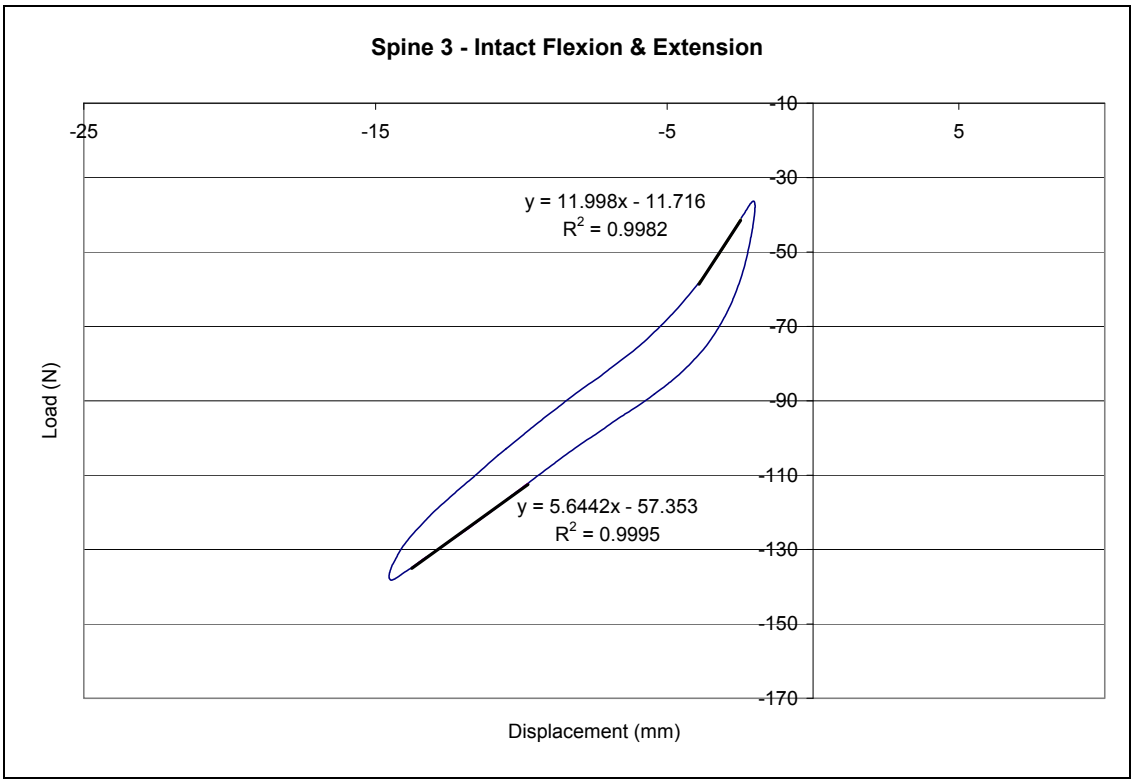

Figure 84: Spine 3 load/displacement curve intact flexion/extension.

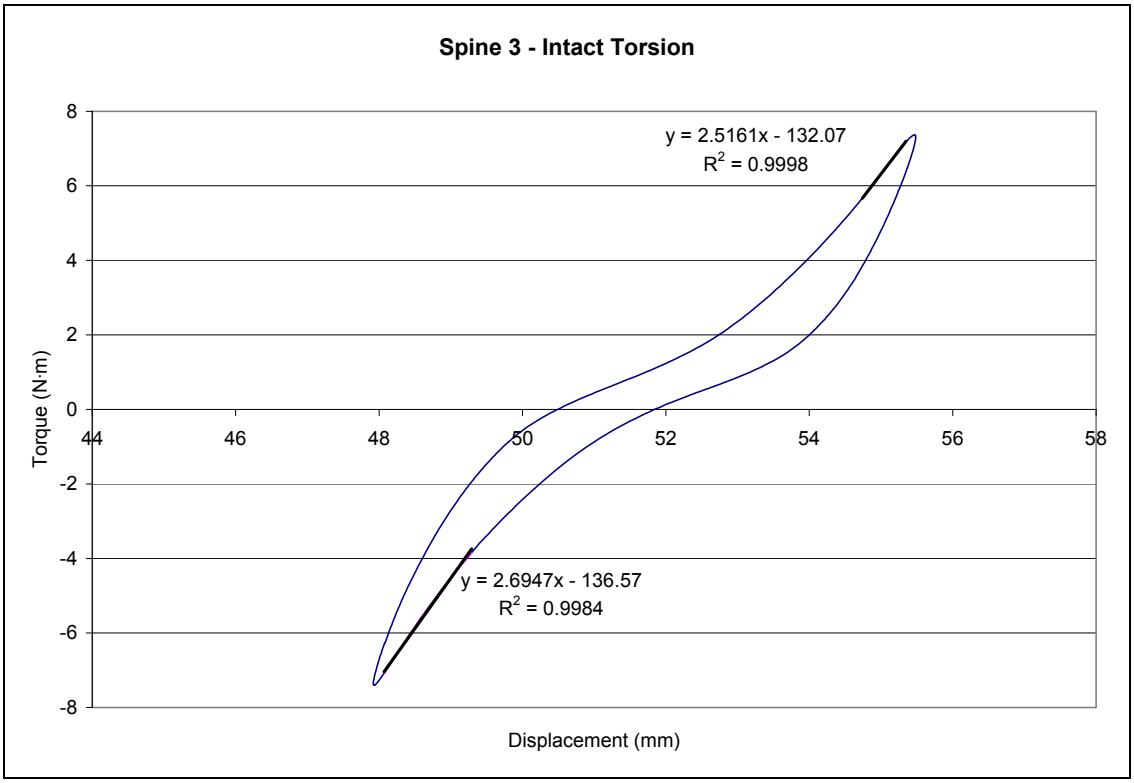

Figure 85: Spine 3 load/displacement curve intact torsion.

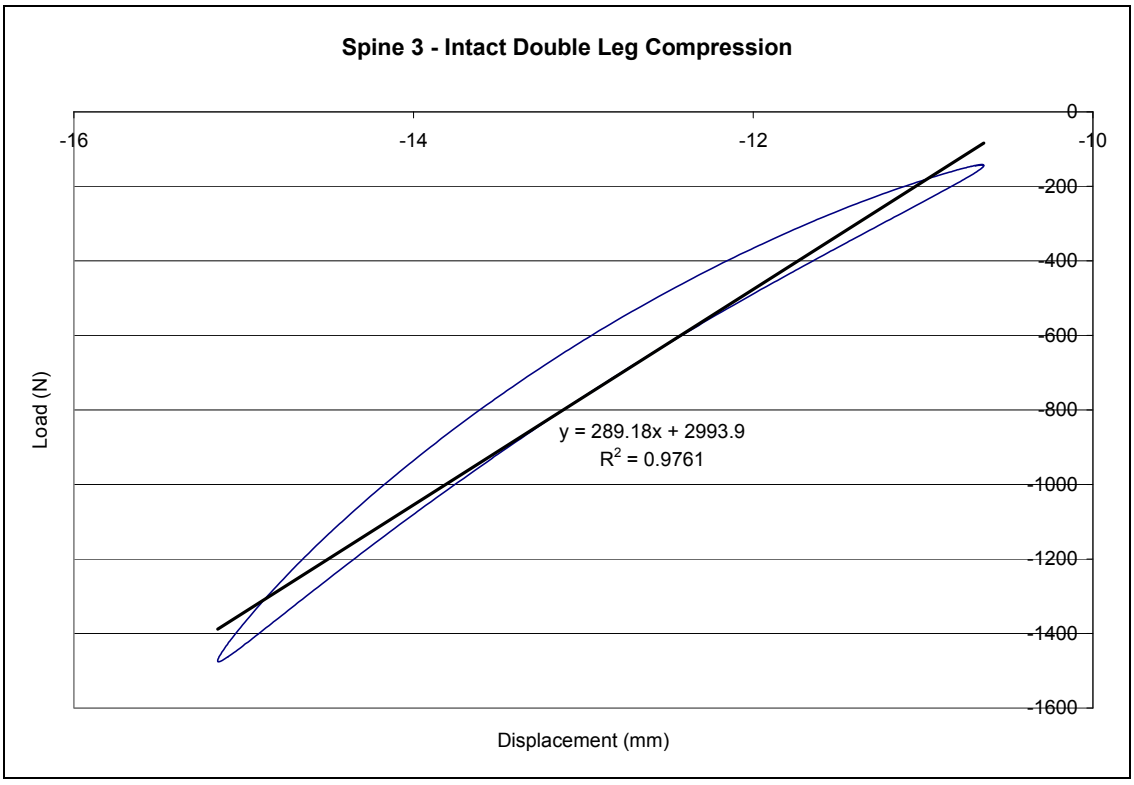

Figure 86: Spine 3 load/displacement curve intact double leg compression.

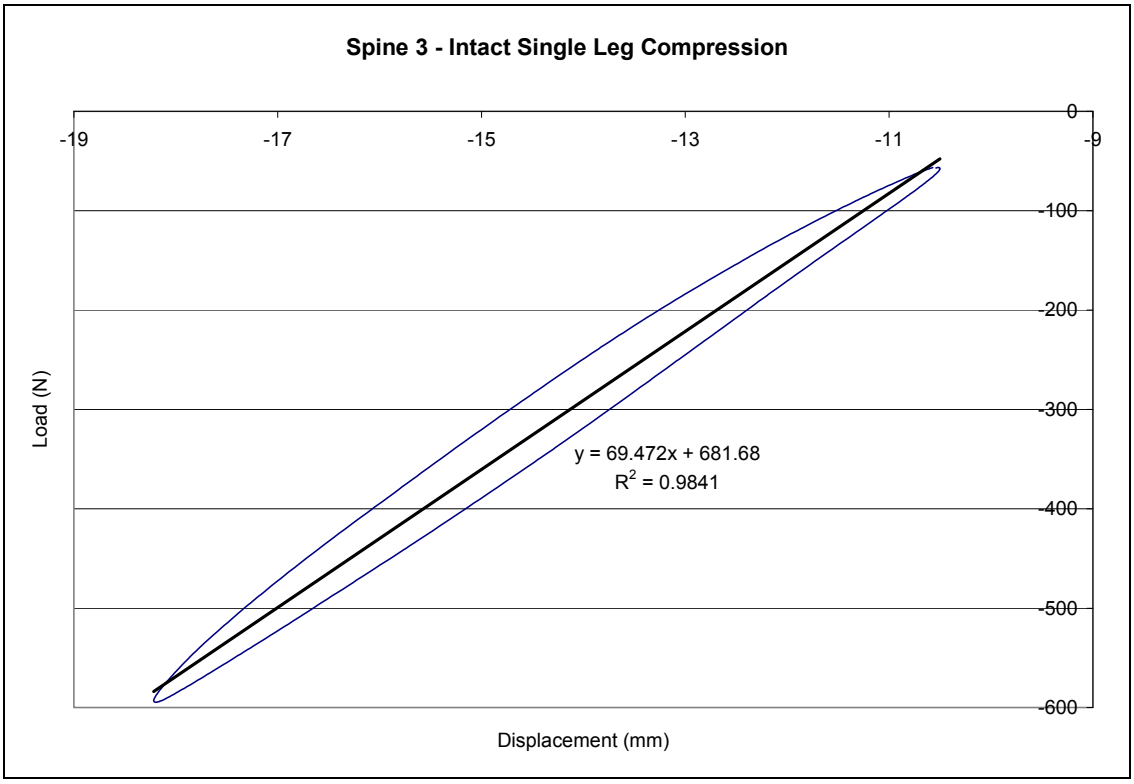

Figure 87: Spine 3 load/displacement curve intact single leg compression.

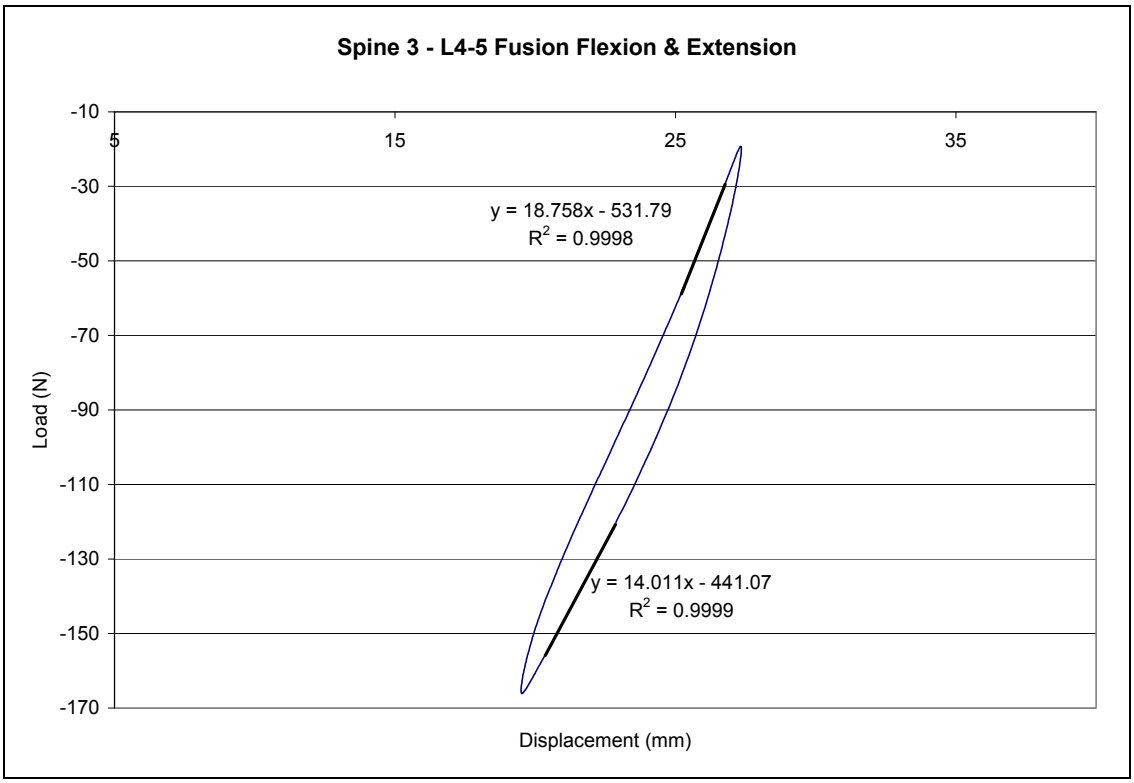

Figure 88: Spine 3 load/displacement curve flexion/extension L4-5 fusion.

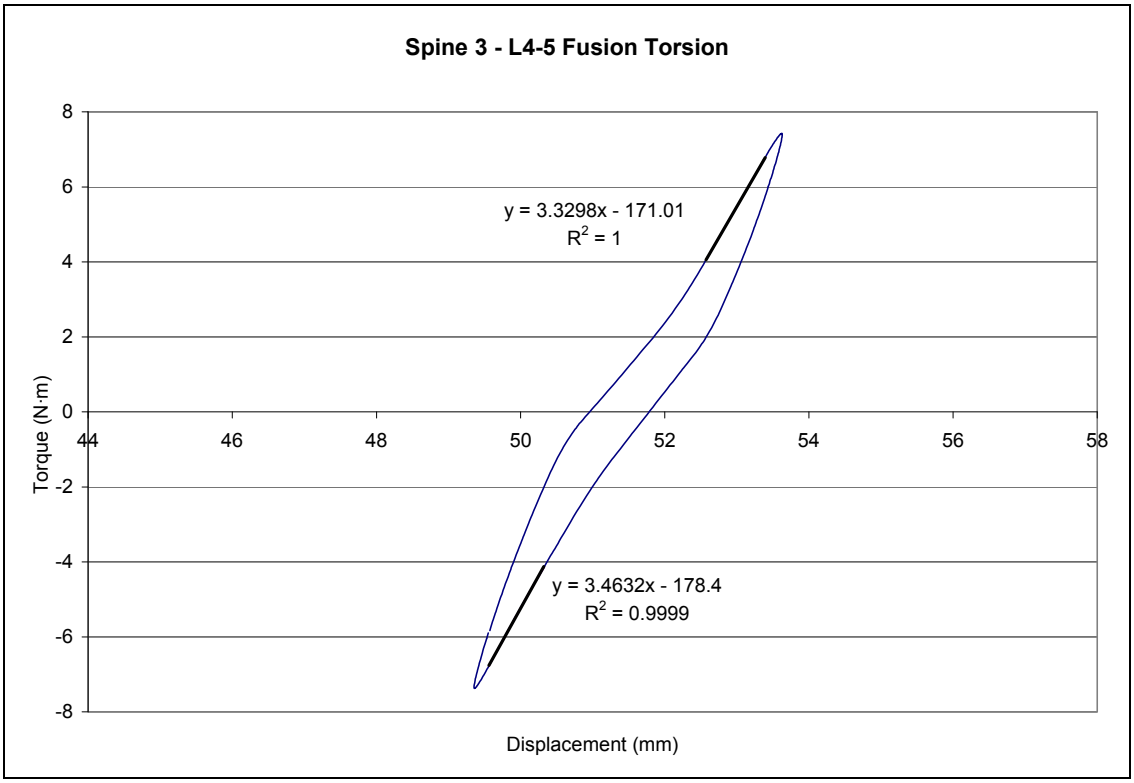

Figure 89: Spine 3 load/displacement curve torsion L4-5 fusion.

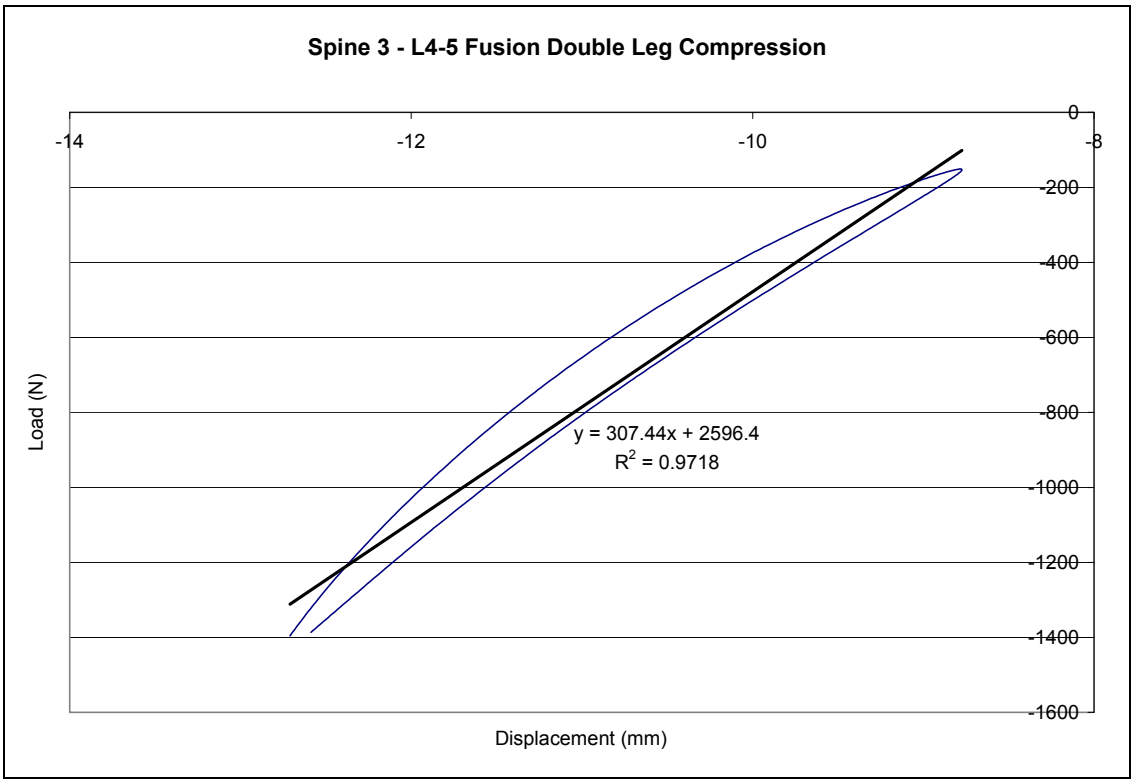

Figure 90: Spine 3 load/displacement curve double leg compression L4-5 fusion.

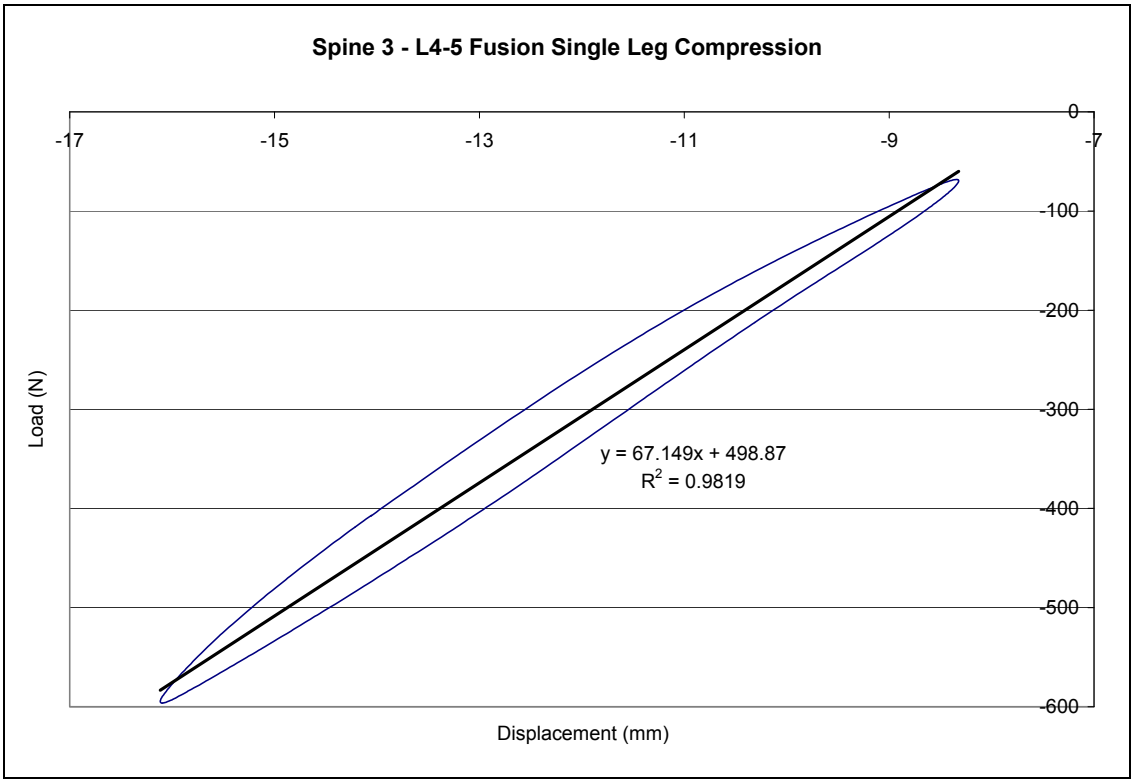

Figure 91: Spine 3 load/displacement curve single leg compression L4-5 fusion.

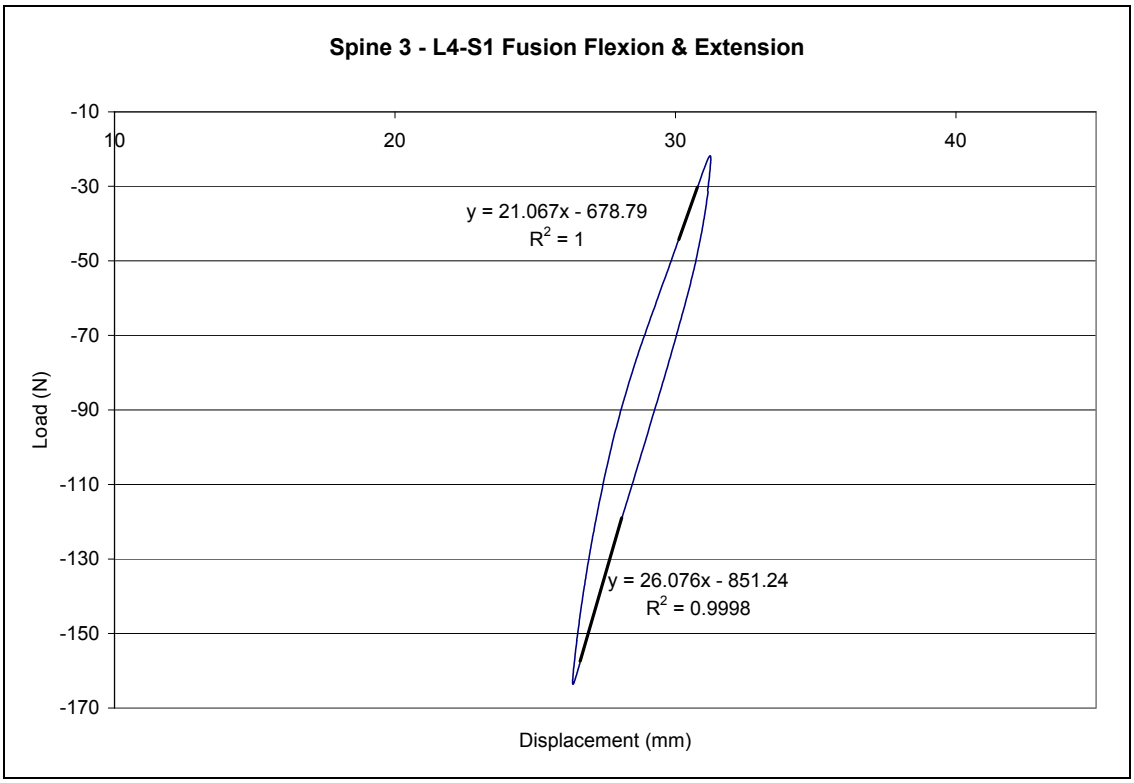

Figure 92: Spine 3 load/displacement curve flexion/extension L4-S1 fusion.

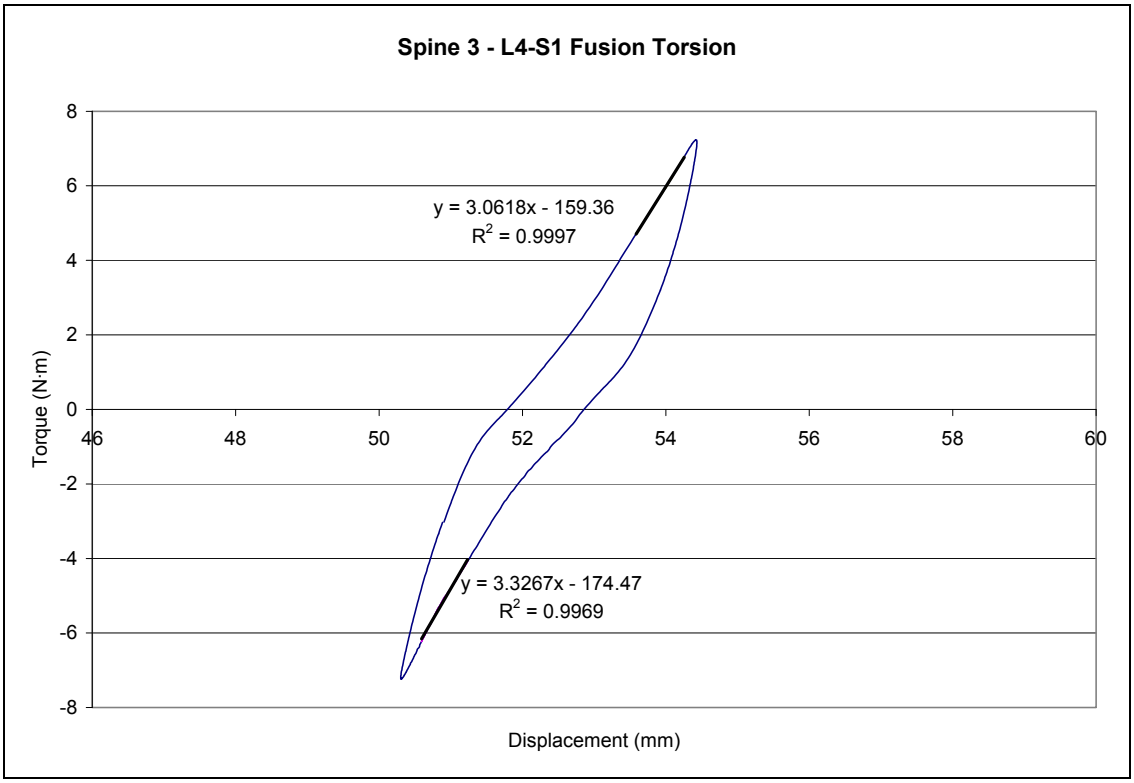

Figure 93: Spine 3 load/displacement curve torsion L4-S1 fusion.

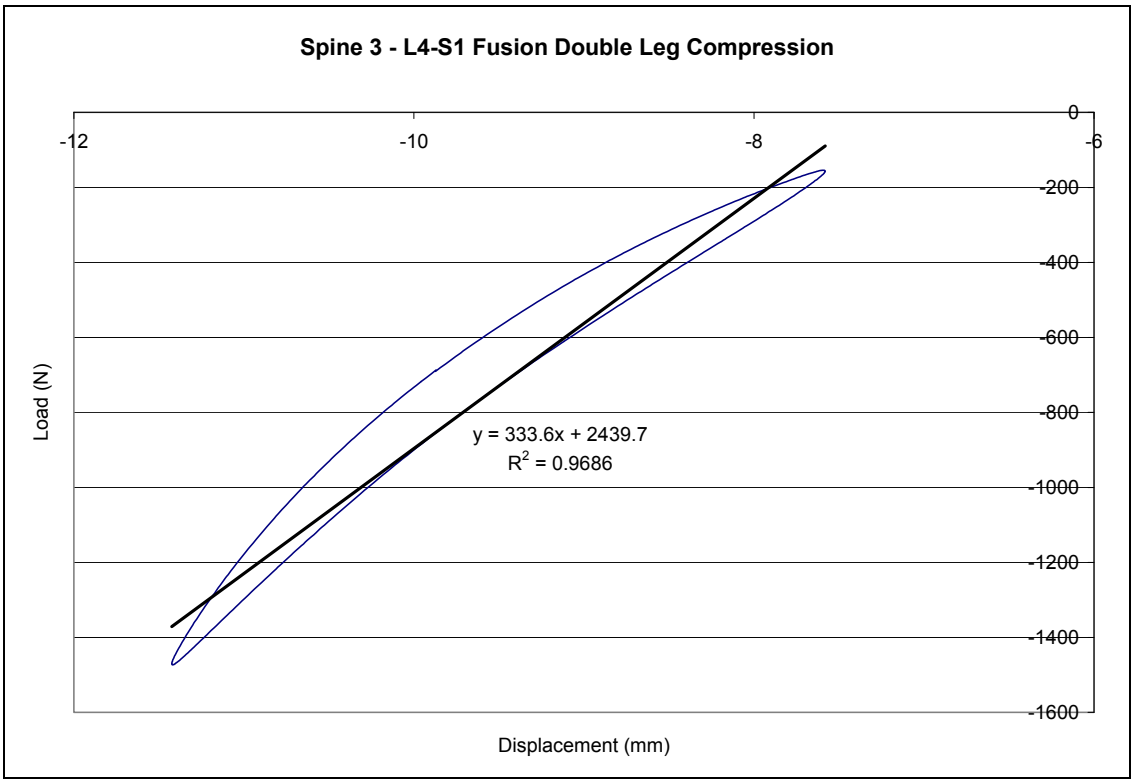

Figure 94: Spine 3 load/displacement curve double leg compression L4-S1 fusion.

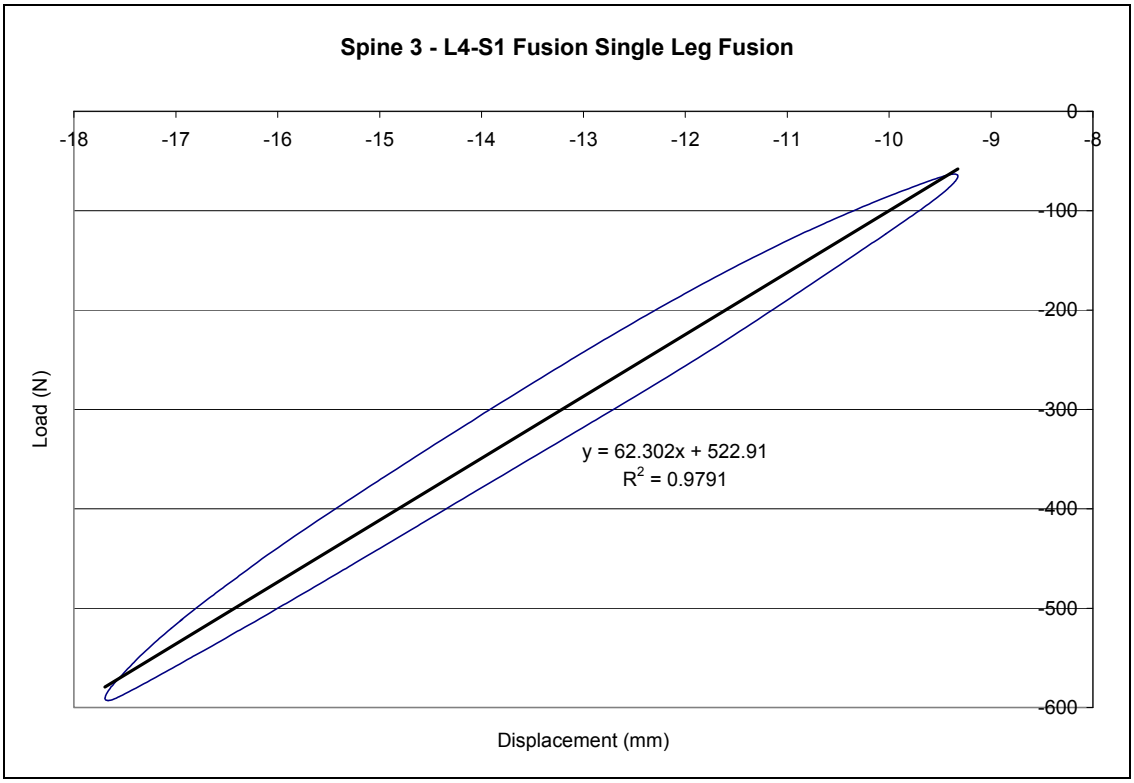

Figure 95: Spine 3 load/displacement curve single leg compression L4-S1 fusion.

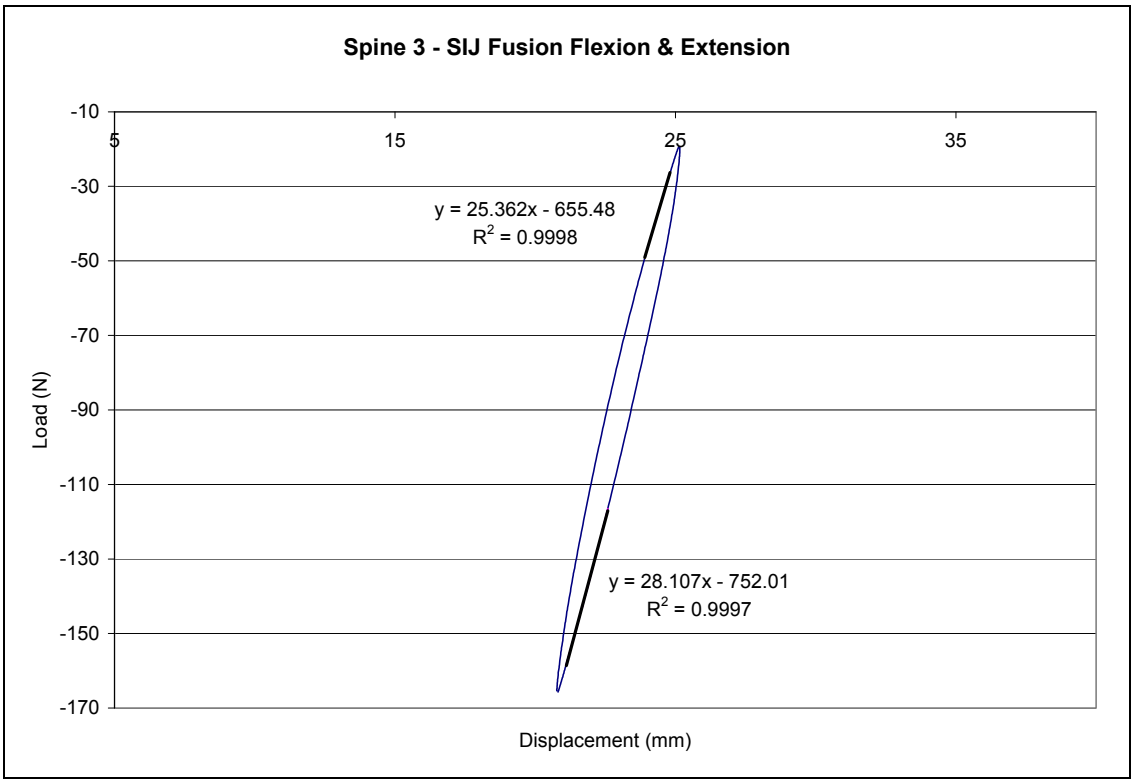

Figure 96: Spine 3 load/displacement curve flexion/extension SIJ fusion.

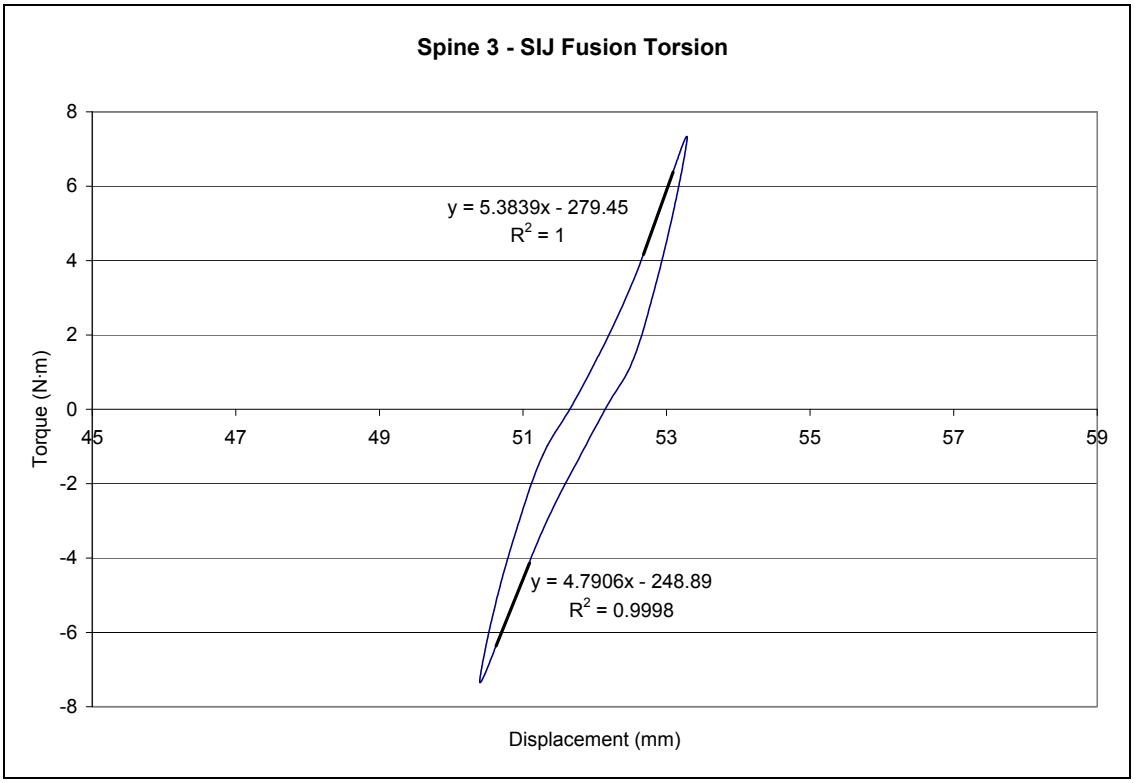

Figure 97: Spine 3 load/displacement curve torsion SIJ fusion.

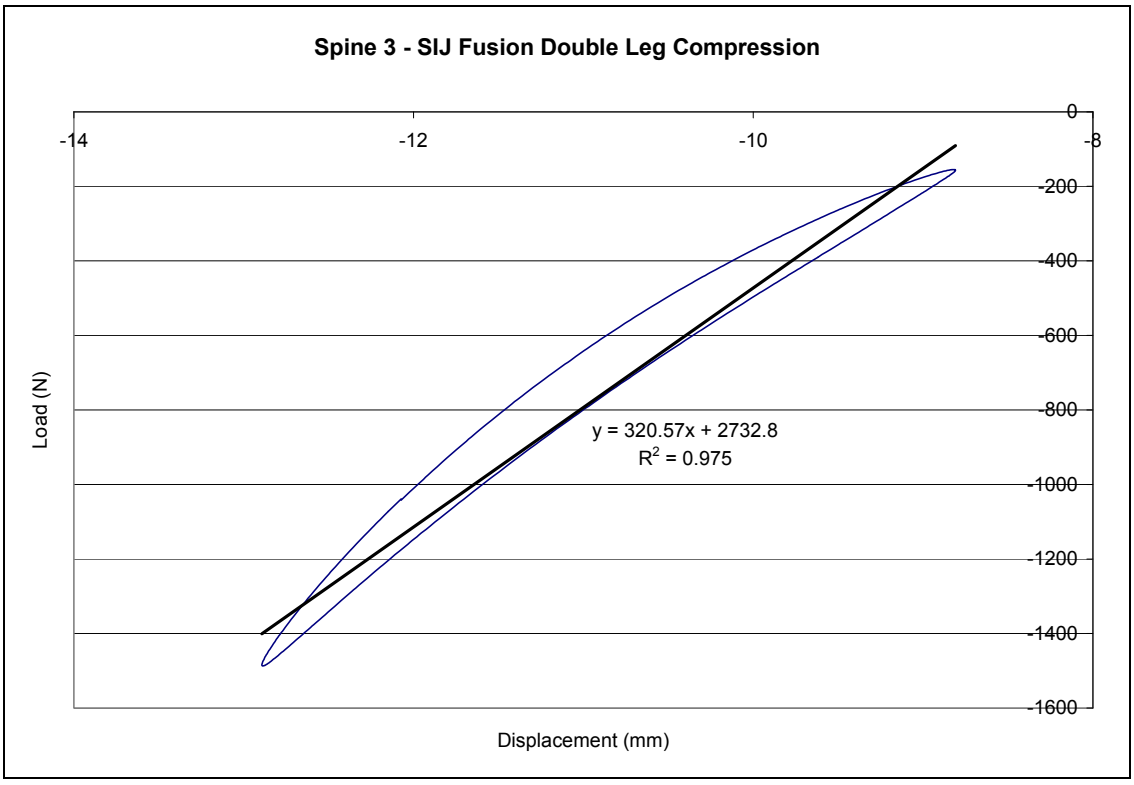

Figure 98: Spine load/displacement curve double leg compression SIJ fusion.

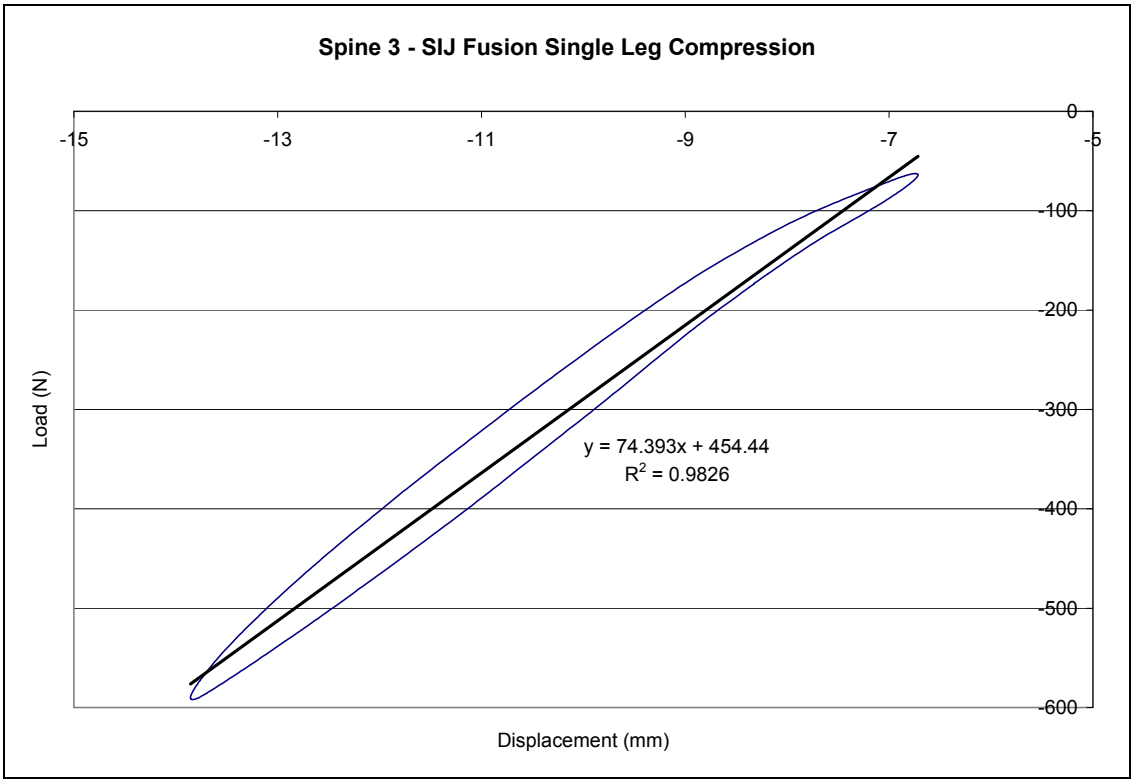

Figure 99: Spine 3 load/displacement curve single leg compression SIJ fusion.

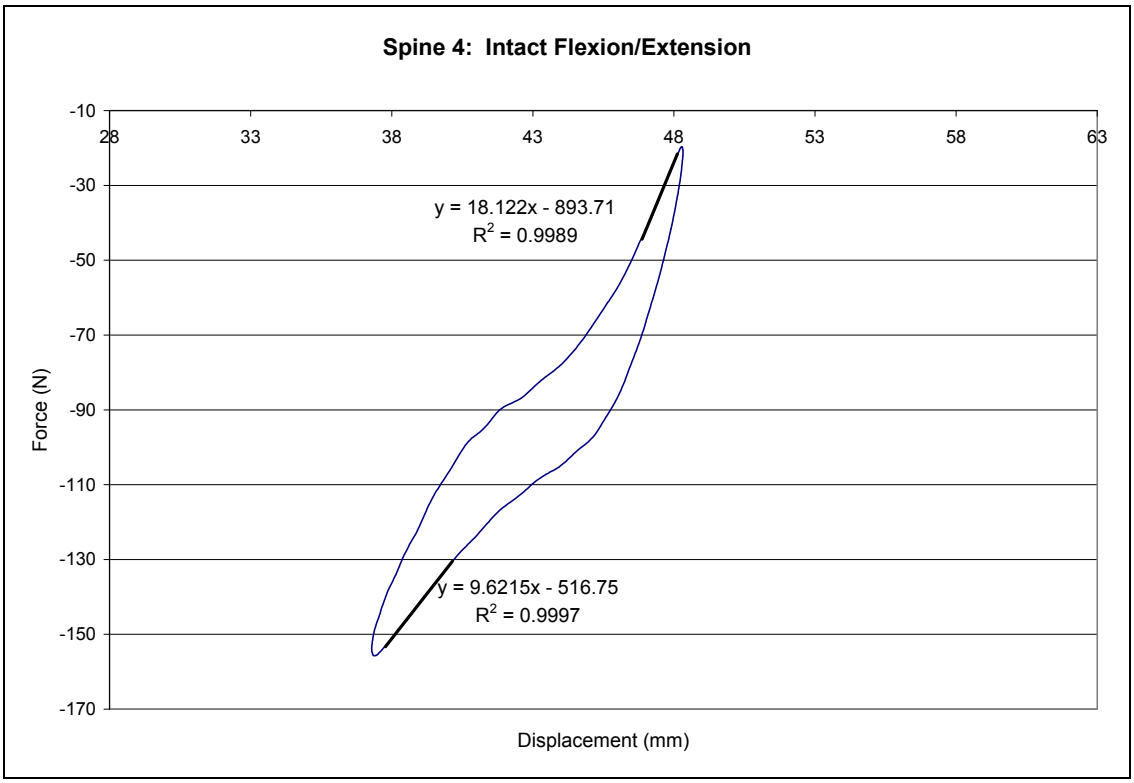

Figure 100: Spine 4 load/displacement curve intact flexion/extension.

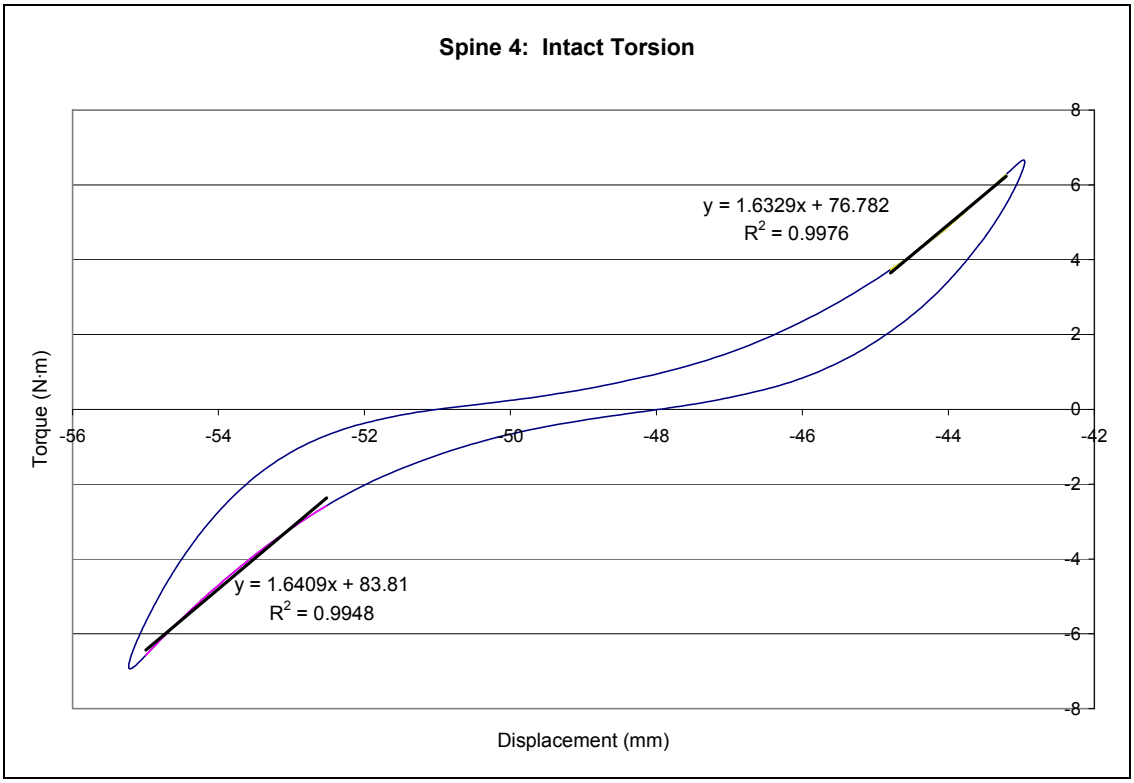

Figure 101: Spine 4 load/displacement curve intact torsion.

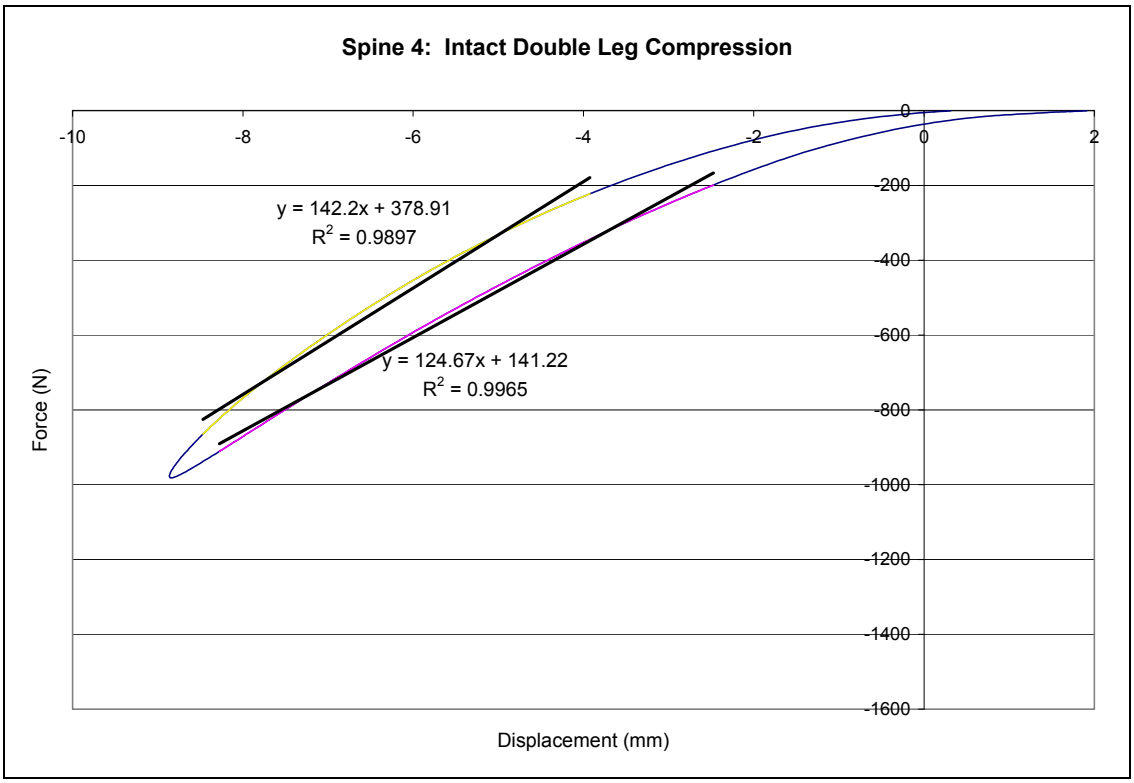

Figure 102: Spine 4 load/displacement curve intact double leg compression.

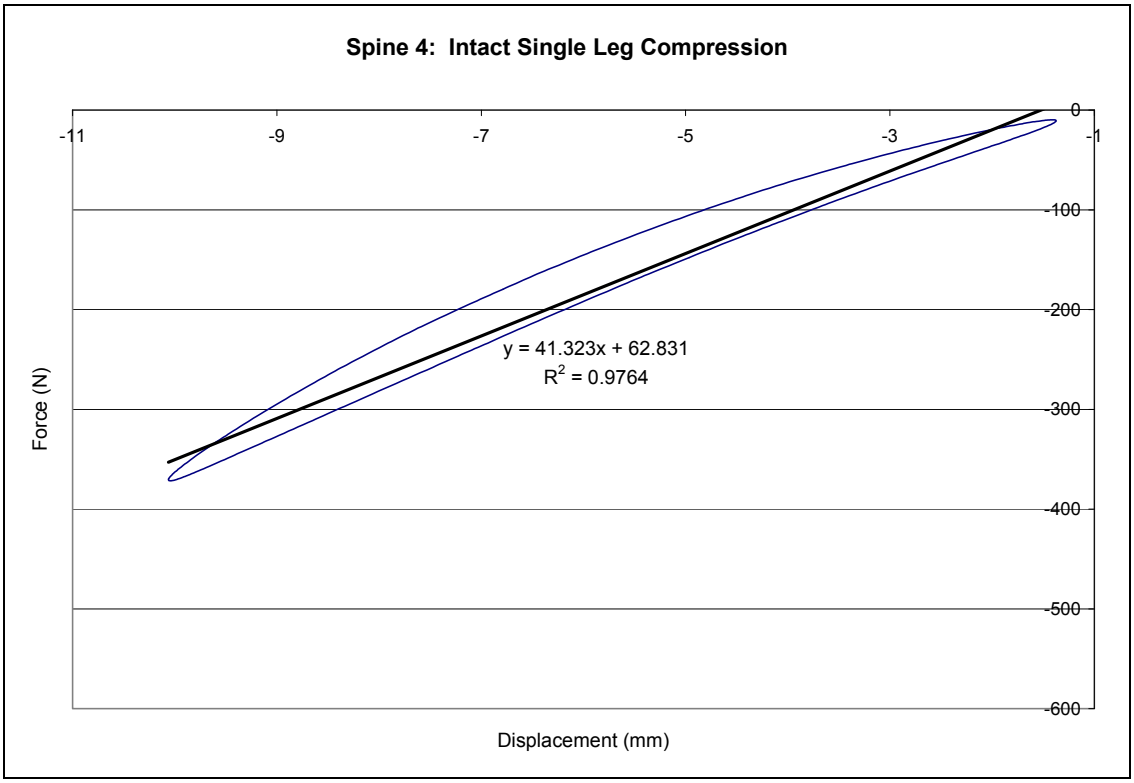

Figure 103: Spine 4 load/displacement curve intact single leg compression.

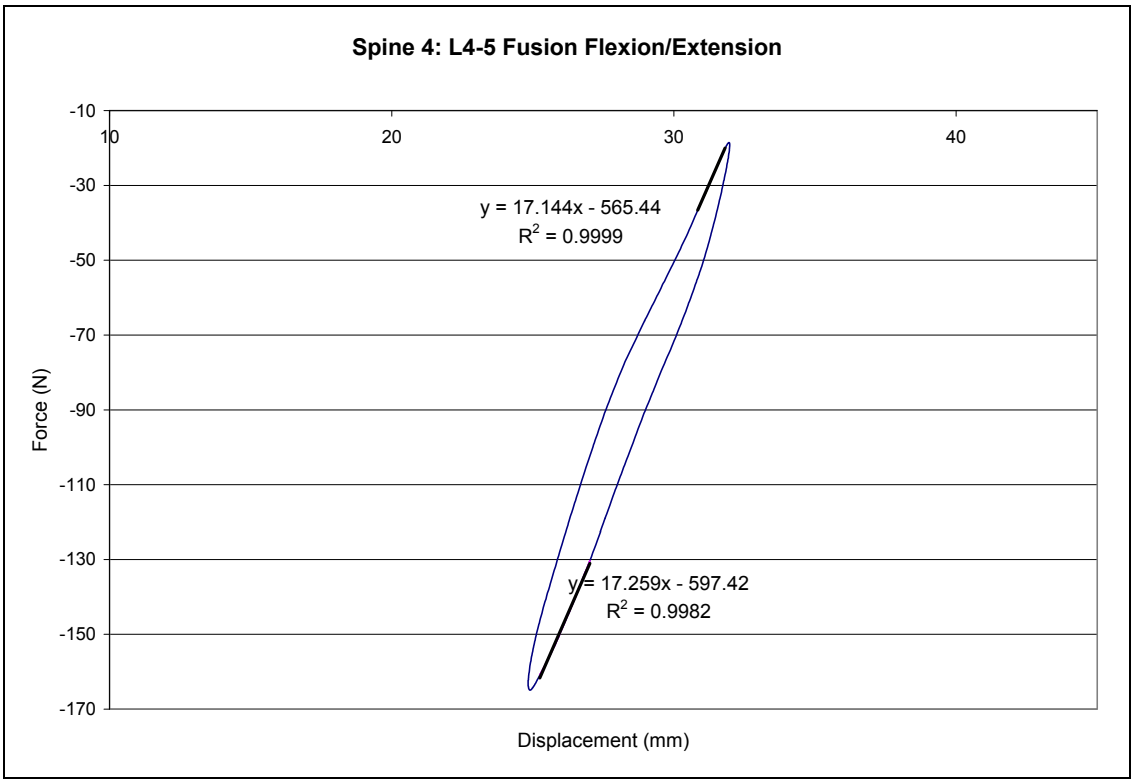

Figure 104: Spine 4 load/displacement curve flexion/extension L4-5 fusion.

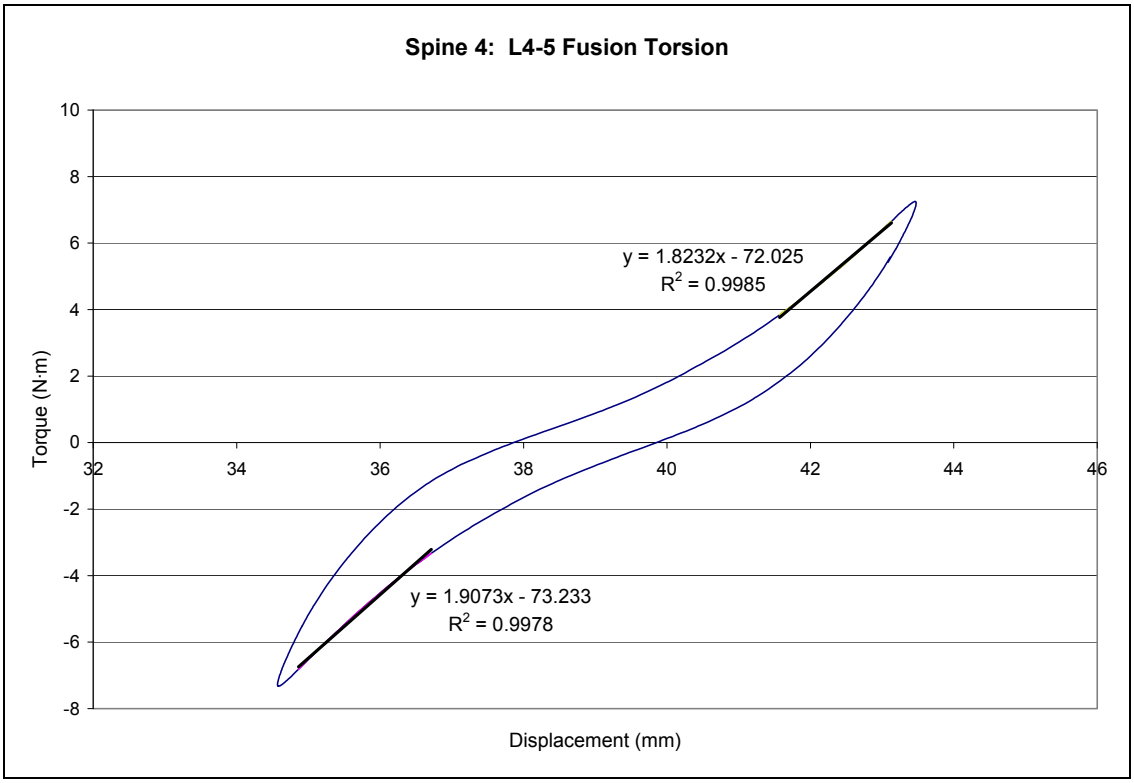

Figure 105: Spine 4 load/displacement curve torsion L4-5 fusion.

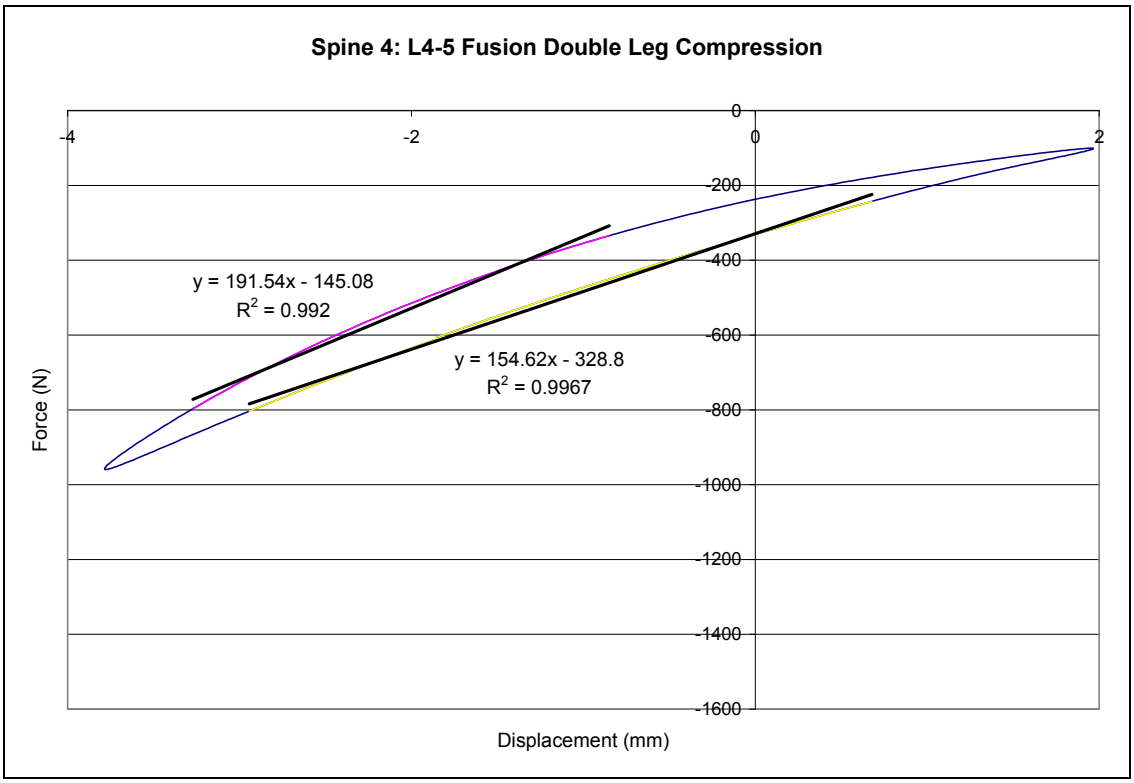

Figure 106: Spine 4 load/displacement curve double leg compression L4-5 fusion.

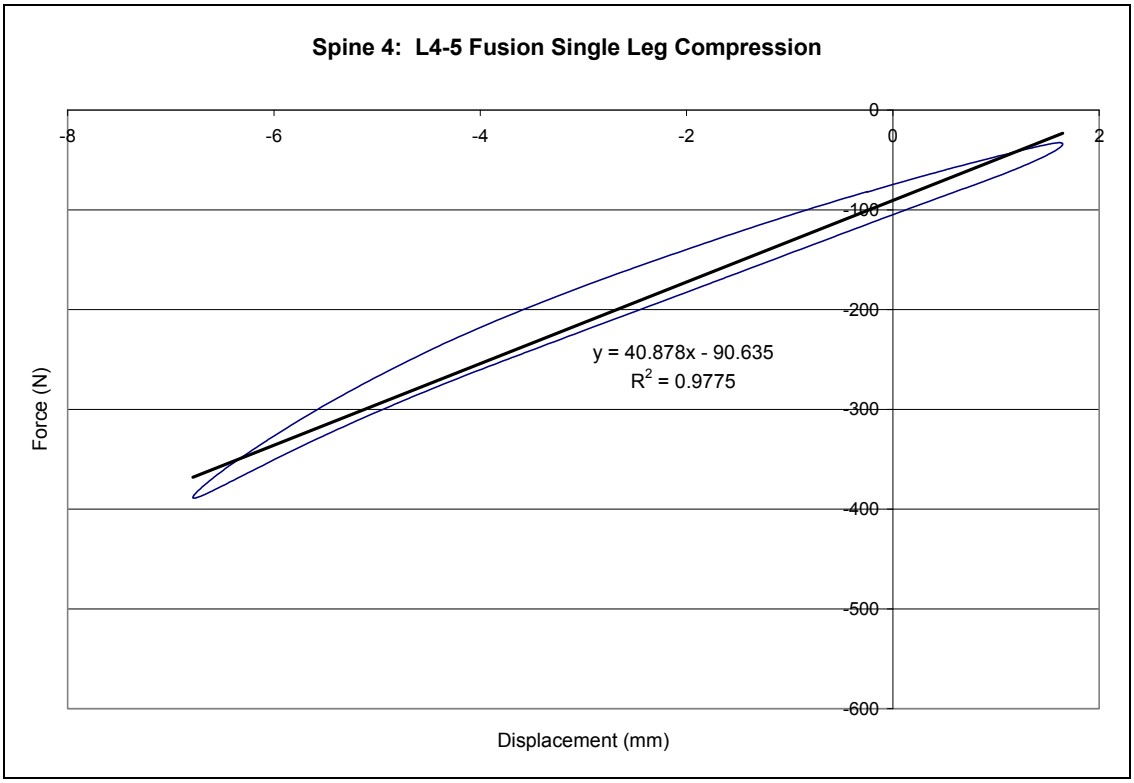

Figure 107: Spine 4 load/displacement curve single leg compression L4-5 fusion.

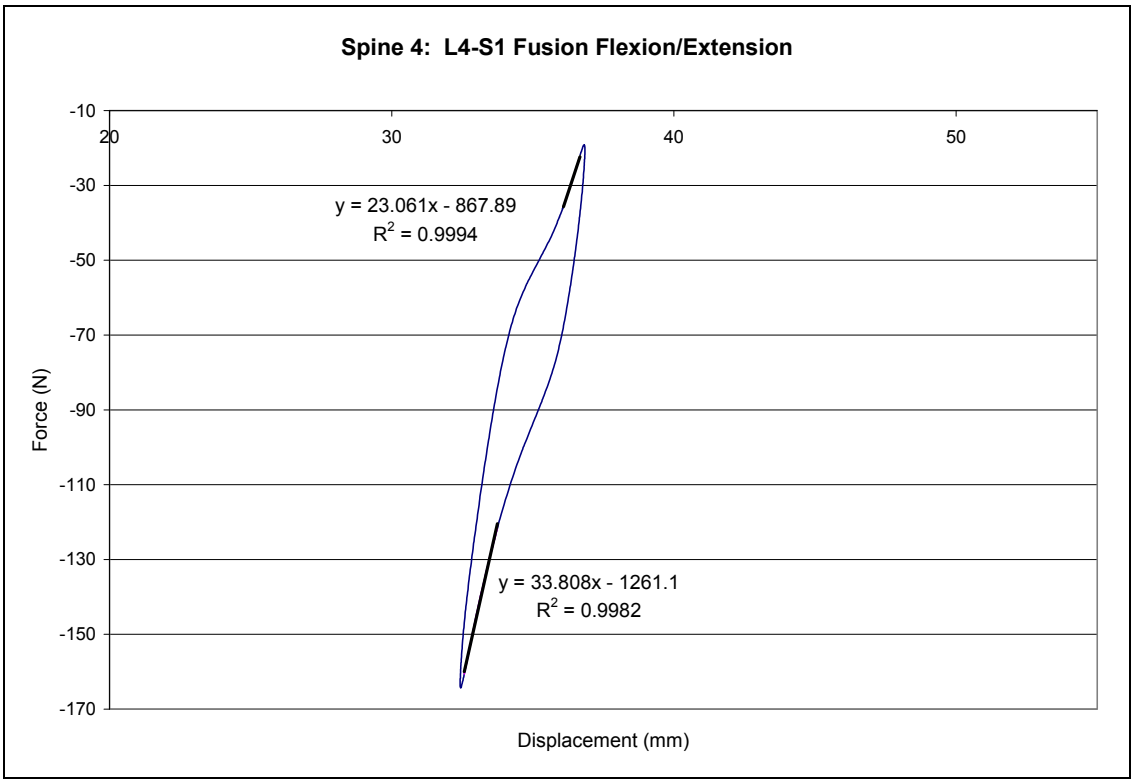

Figure 108: Spine 4 load/displacement curve flexion/extension L4-S1 fusion.

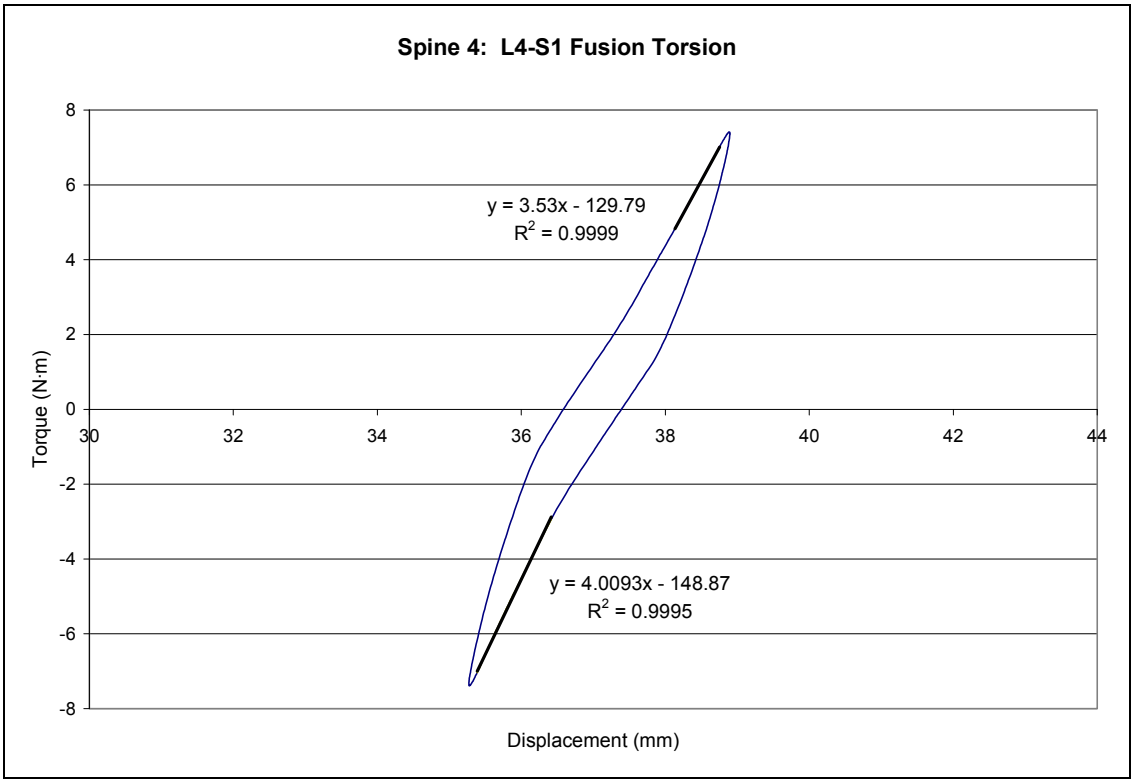

Figure 109: Spine 4 load/displacement curve torsion L4-S1 fusion.

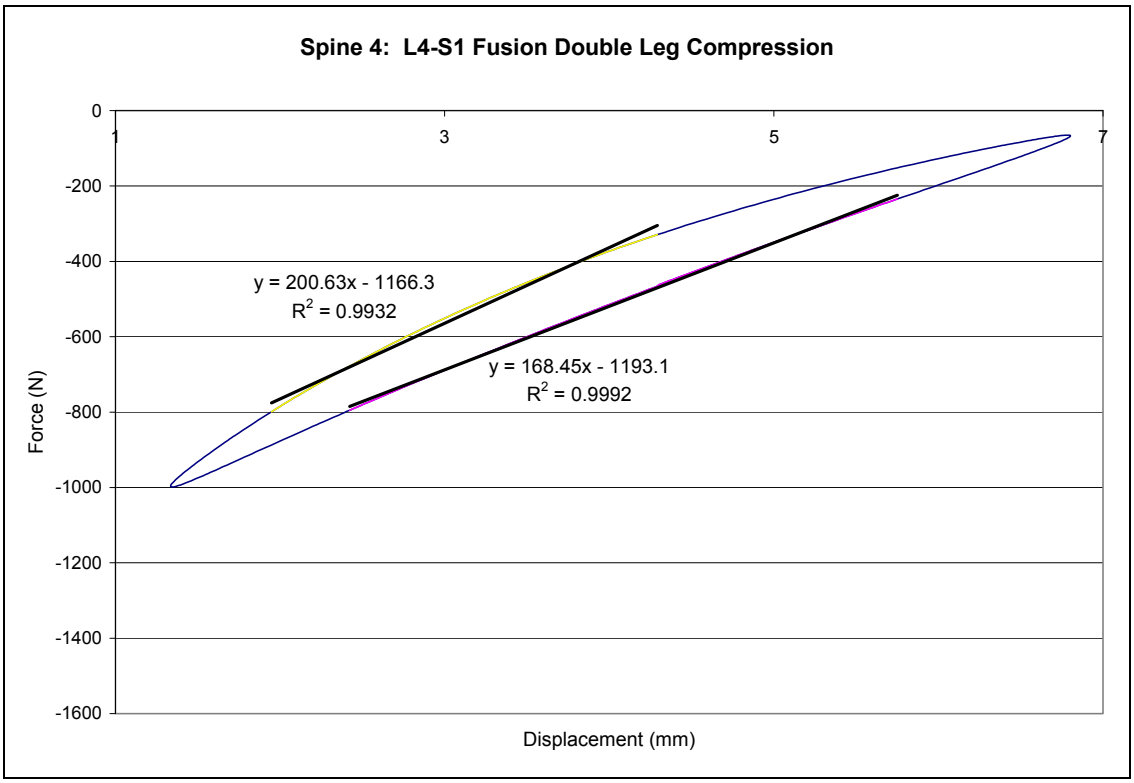

Figure 110: Spine 4 load/displacement curve double leg compression L4-S1 fusion.

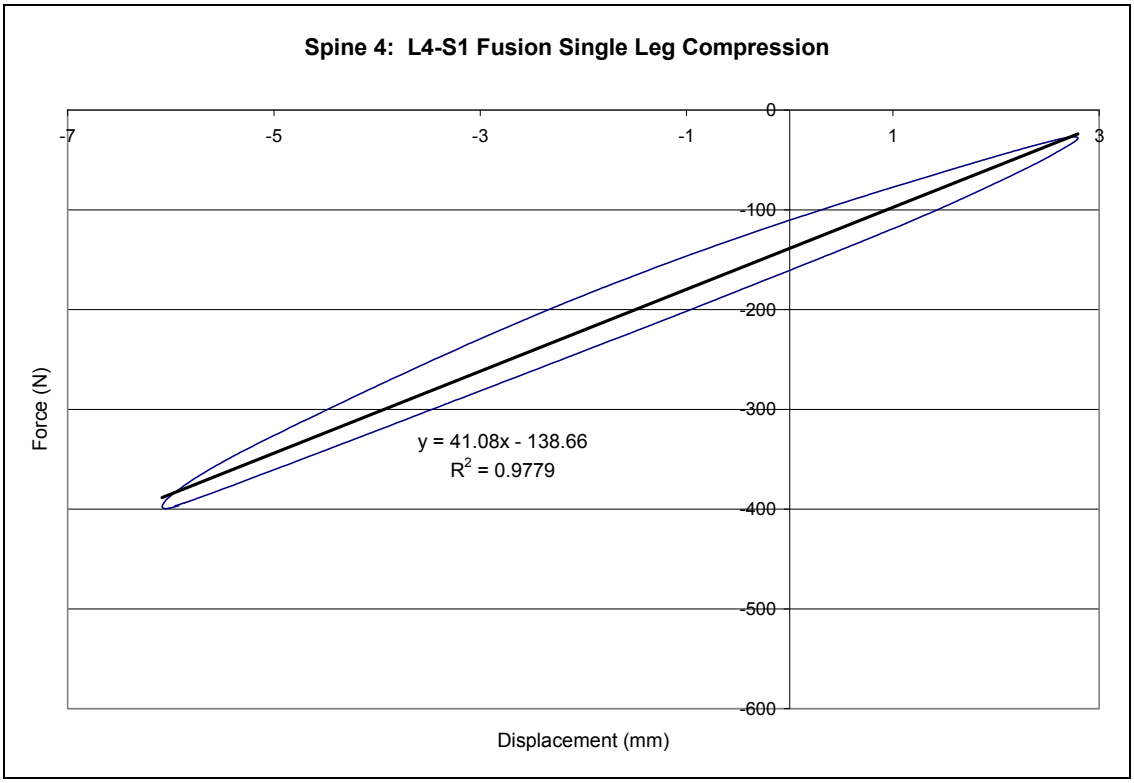

Figure 111: Spine 4 load/displacement curve single leg compression L4-S1 fusion.

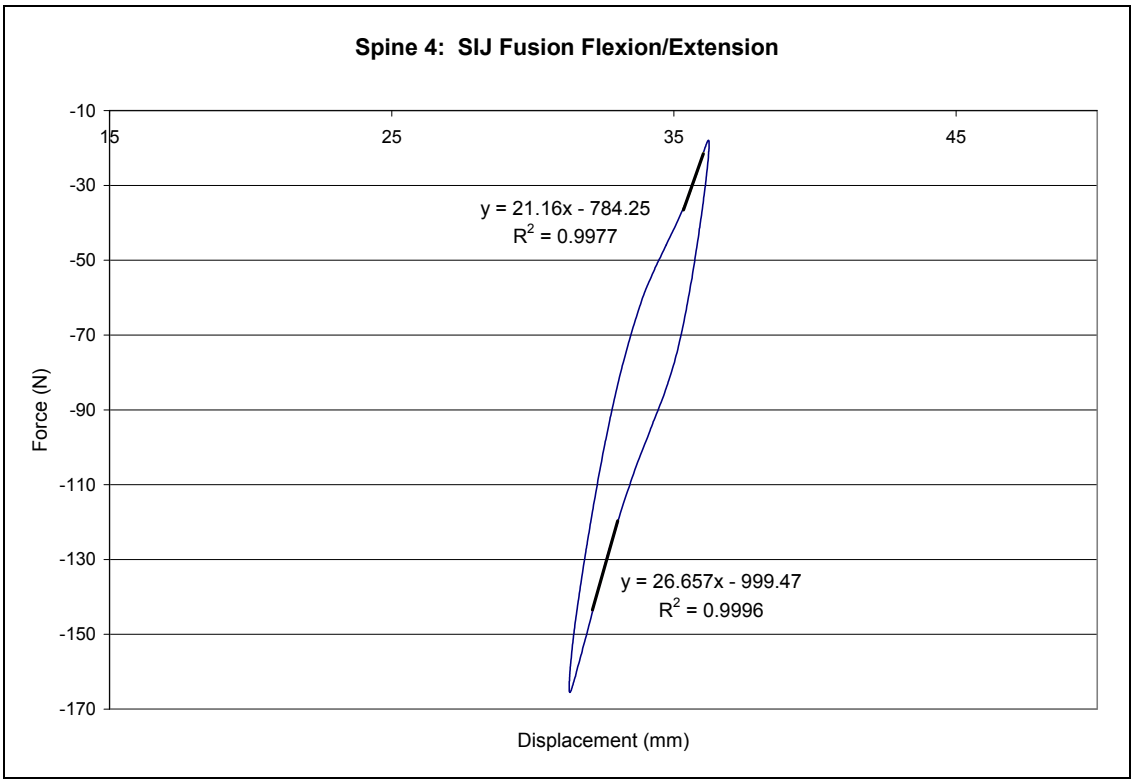

Figure 112: Spine 4 load/displacement curve flexion/extension SIJ fusion.

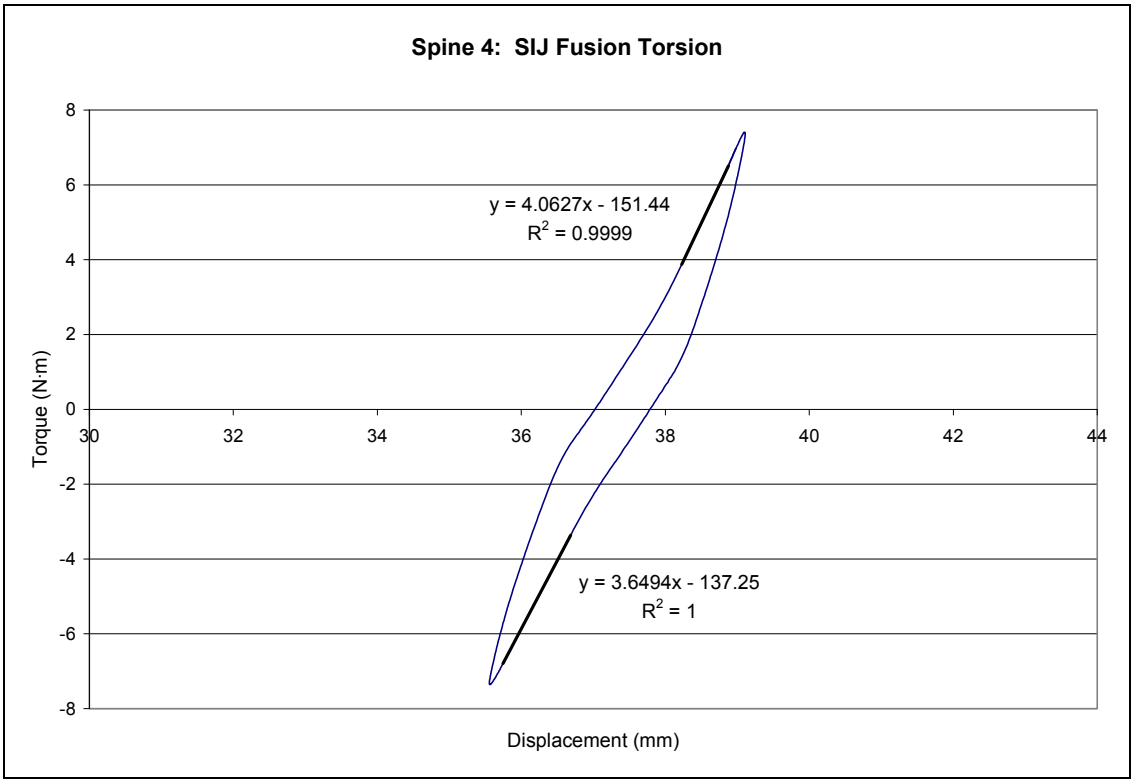

Figure 113: Spine 4 load/displacement curve torsion SIJ fusion.

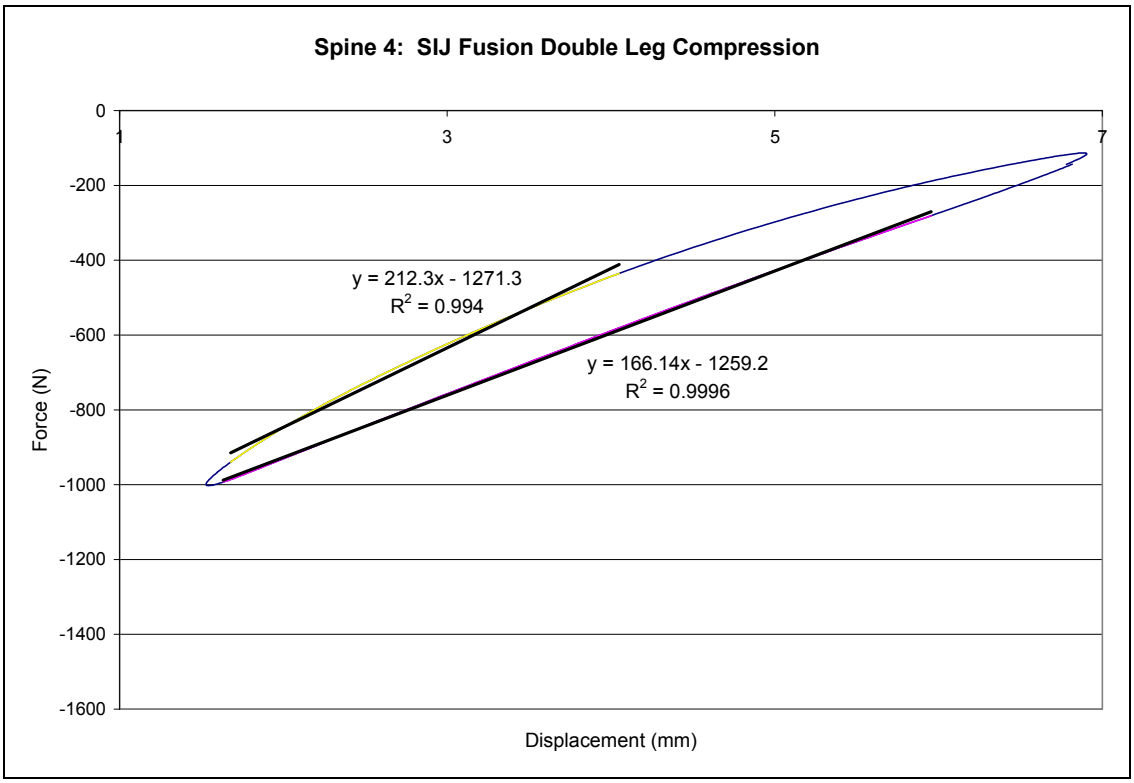

Figure 114: Spine 4 load/displacement curve double leg compression SIJ fusion.

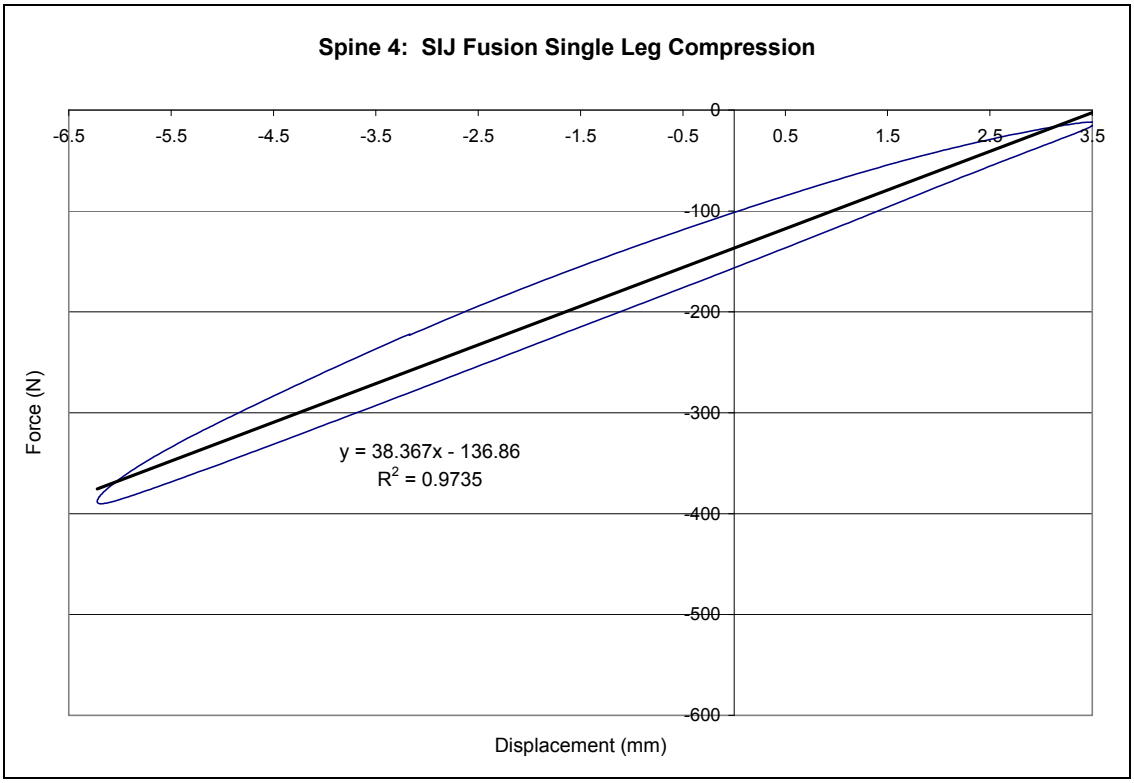

Figure 115: Spine 4 load/displacement curve single leg compression SIJ fusion.

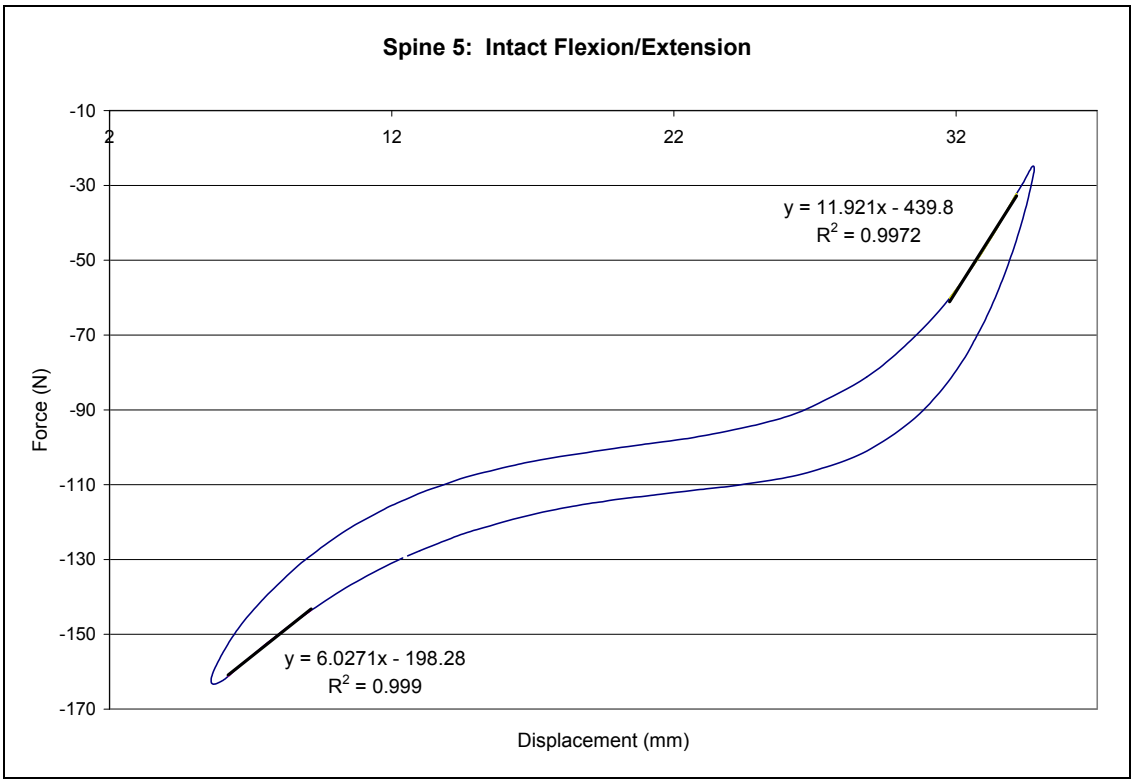

Figure 116: Spine 5 load/displacement curve intact flexion/extension.

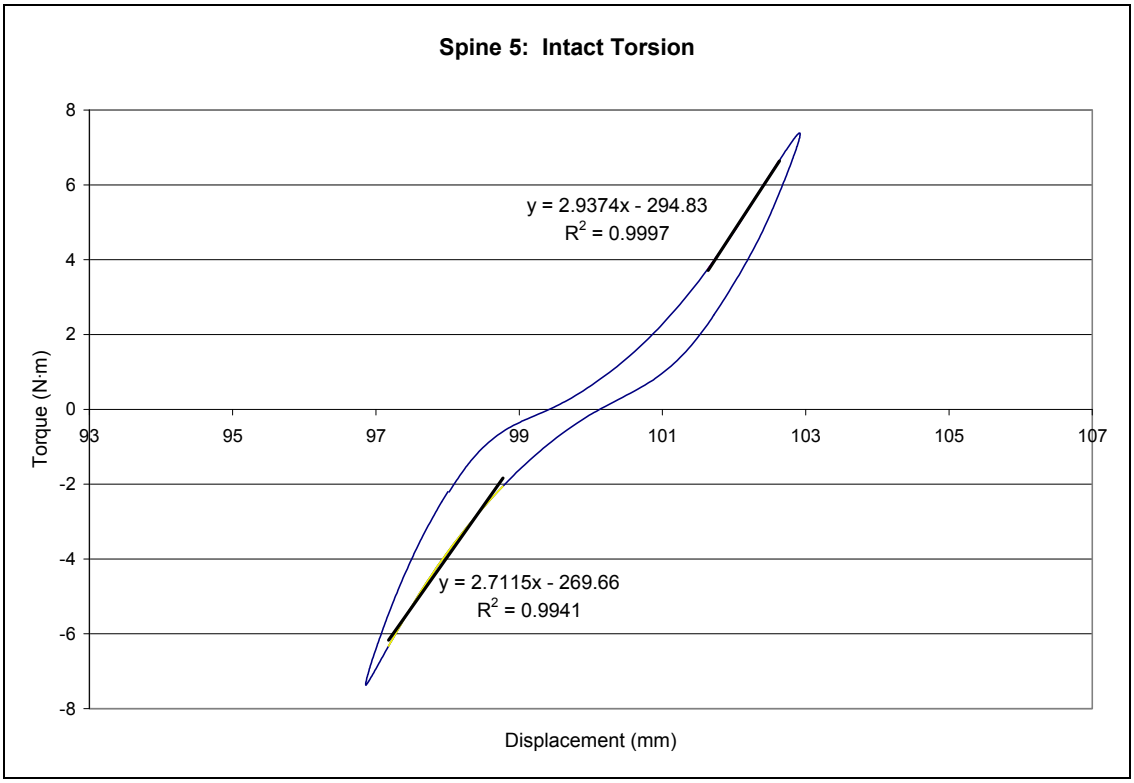

Figure 117: Spine 5 load/displacement curve intact torsion.

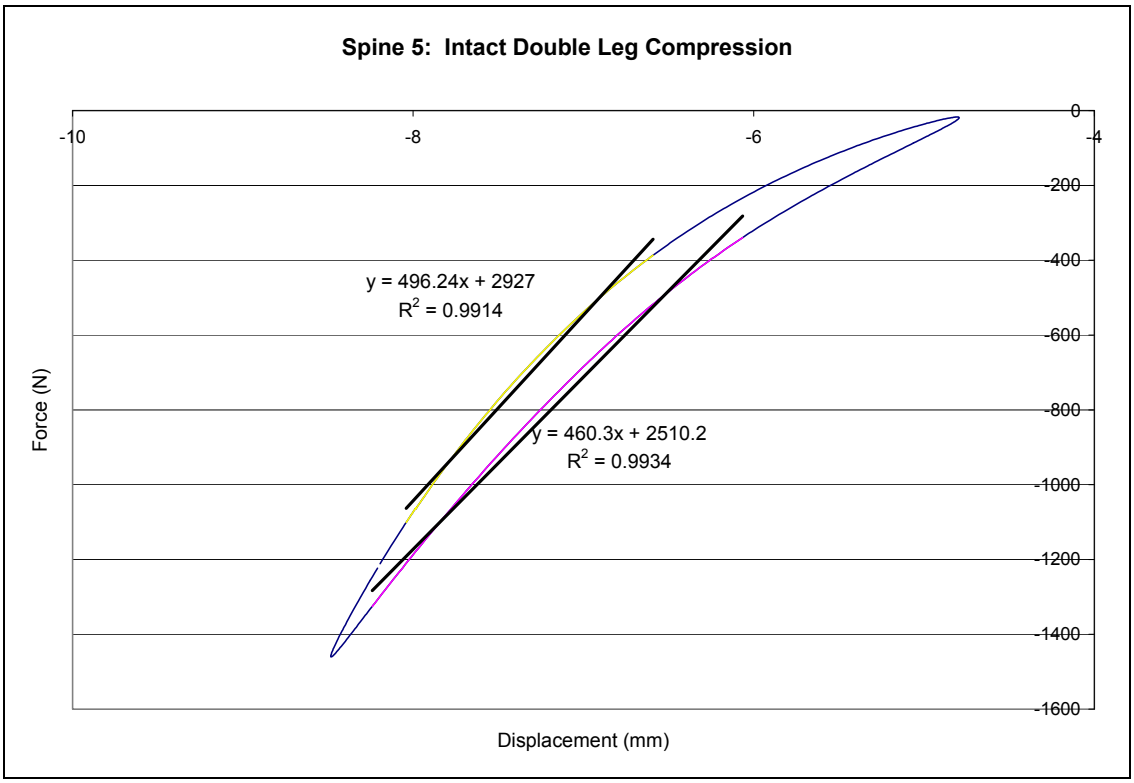

Figure 118: Spine 5 load/displacement curve intact double leg compression.

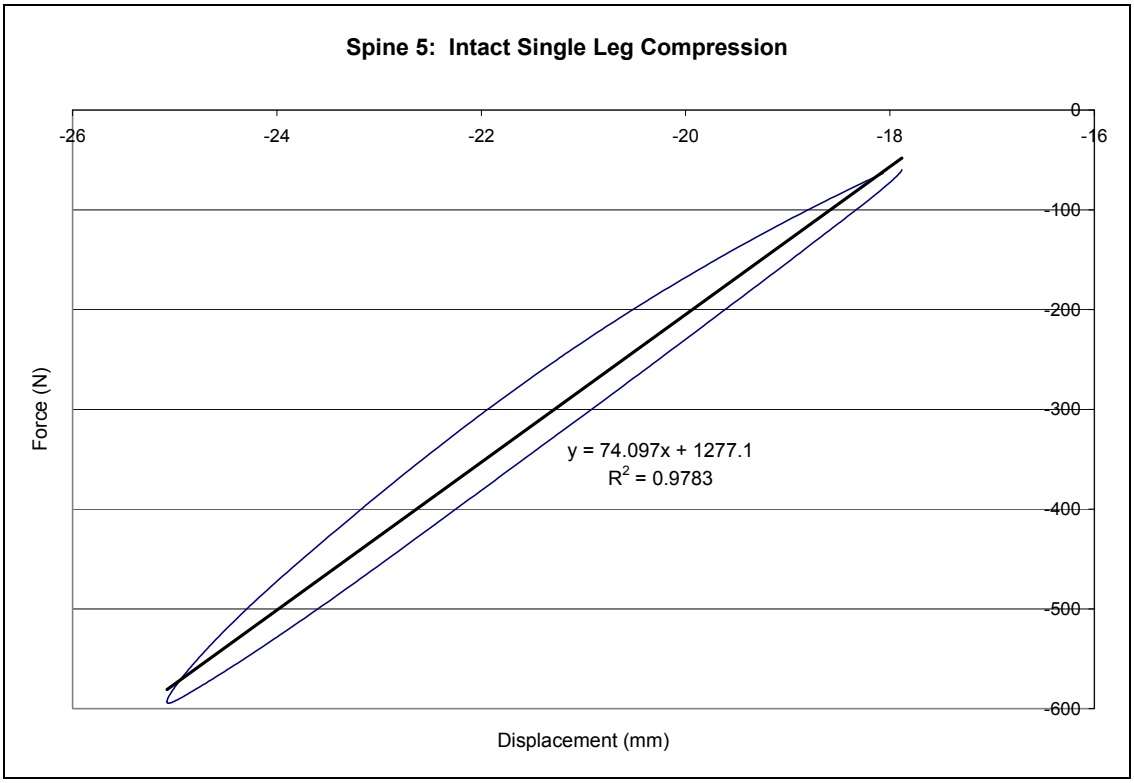

Figure 119: Spine 5 load/displacement curve intact single leg compression.

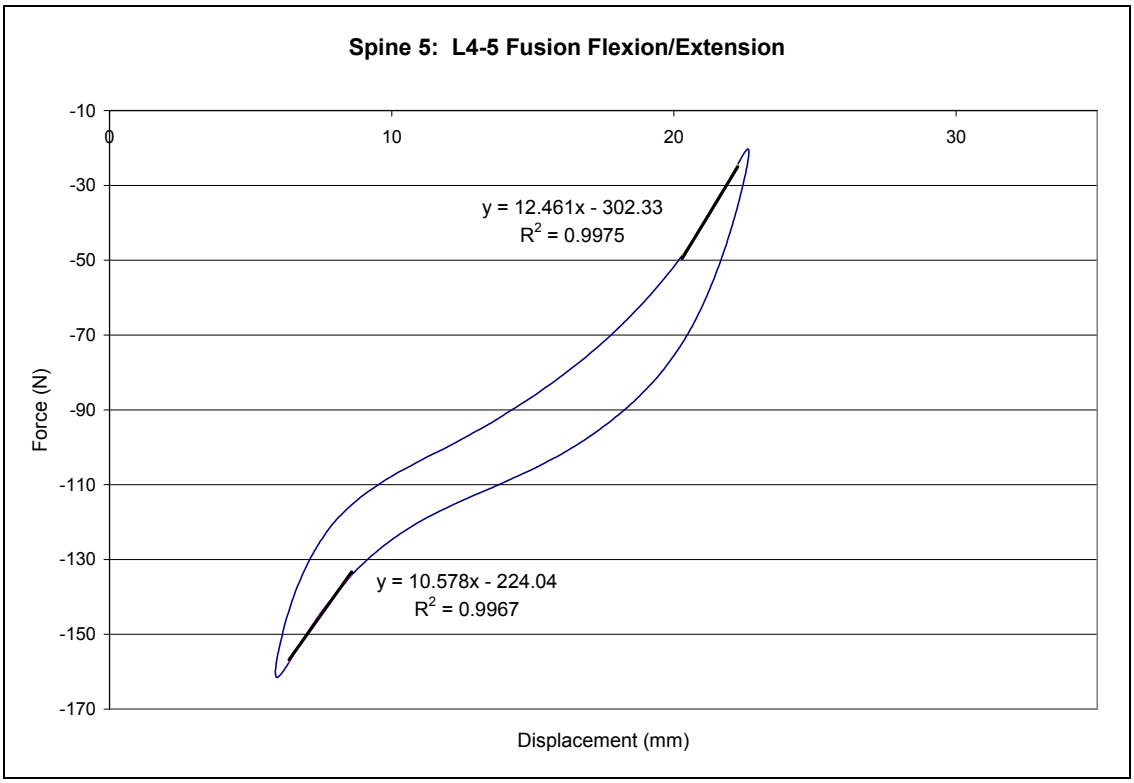

Figure 120: Spine 5 load/displacement curve flexion/extension L4-5 fusion.

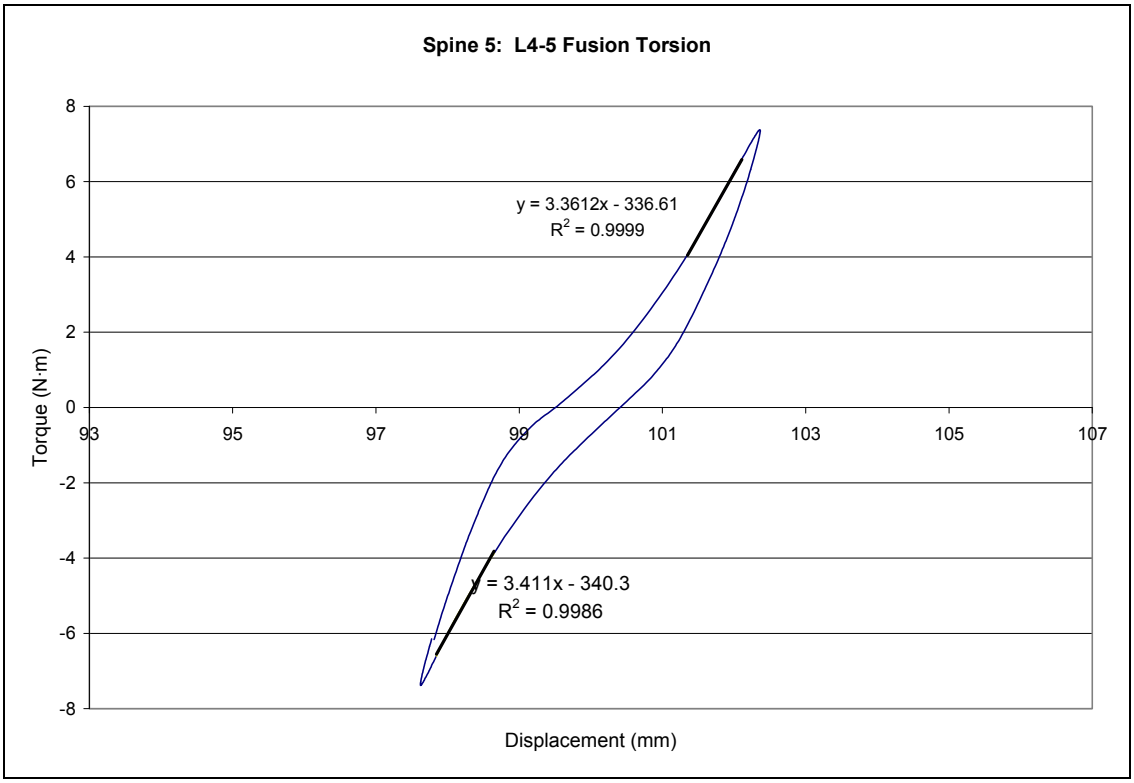

Figure 121: Spine 5 load/displacement curve torsion L4-5 fusion.

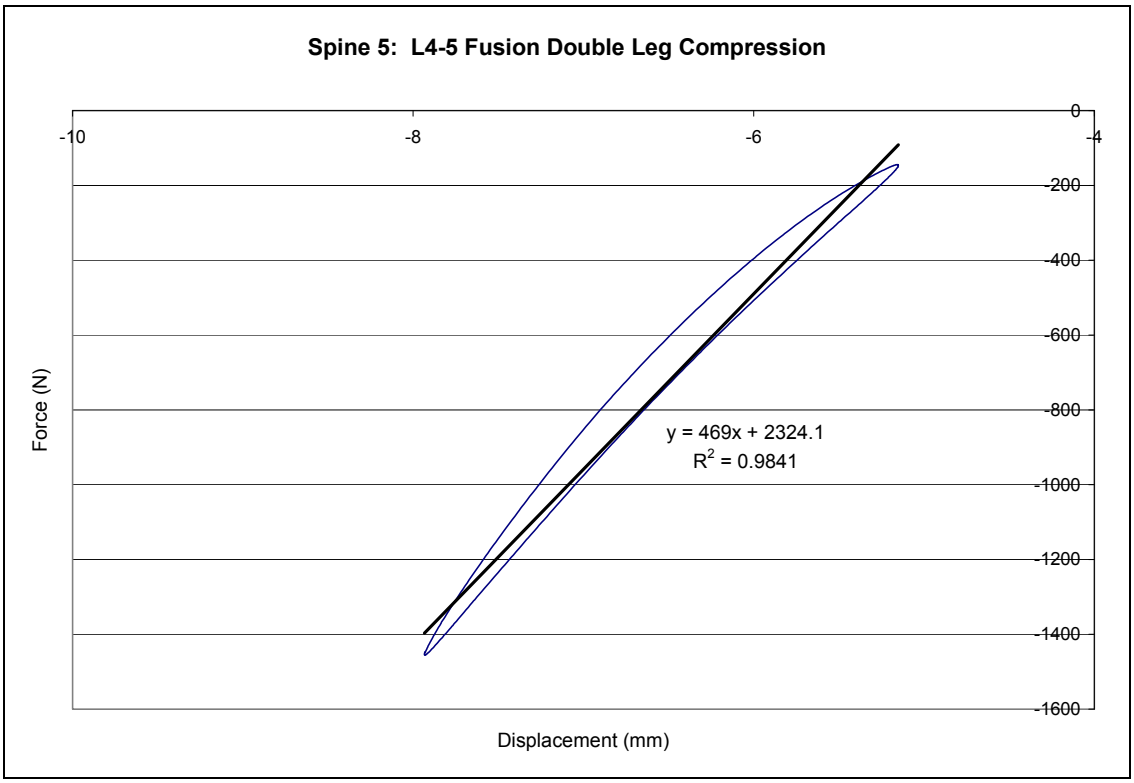

Figure 122: Spine 5 load/displacement curve double leg compression L4-5 fusion.

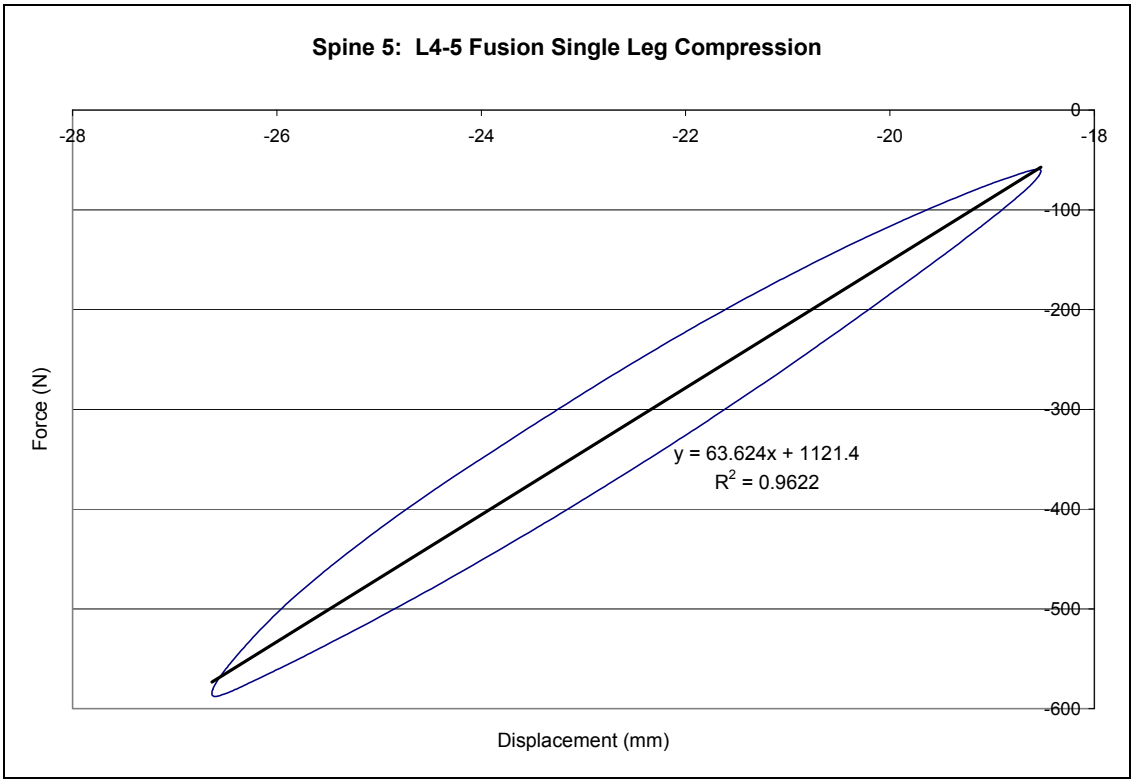

Figure 123: Spine 5 load/displacement curve single leg compression L4-5 fusion.

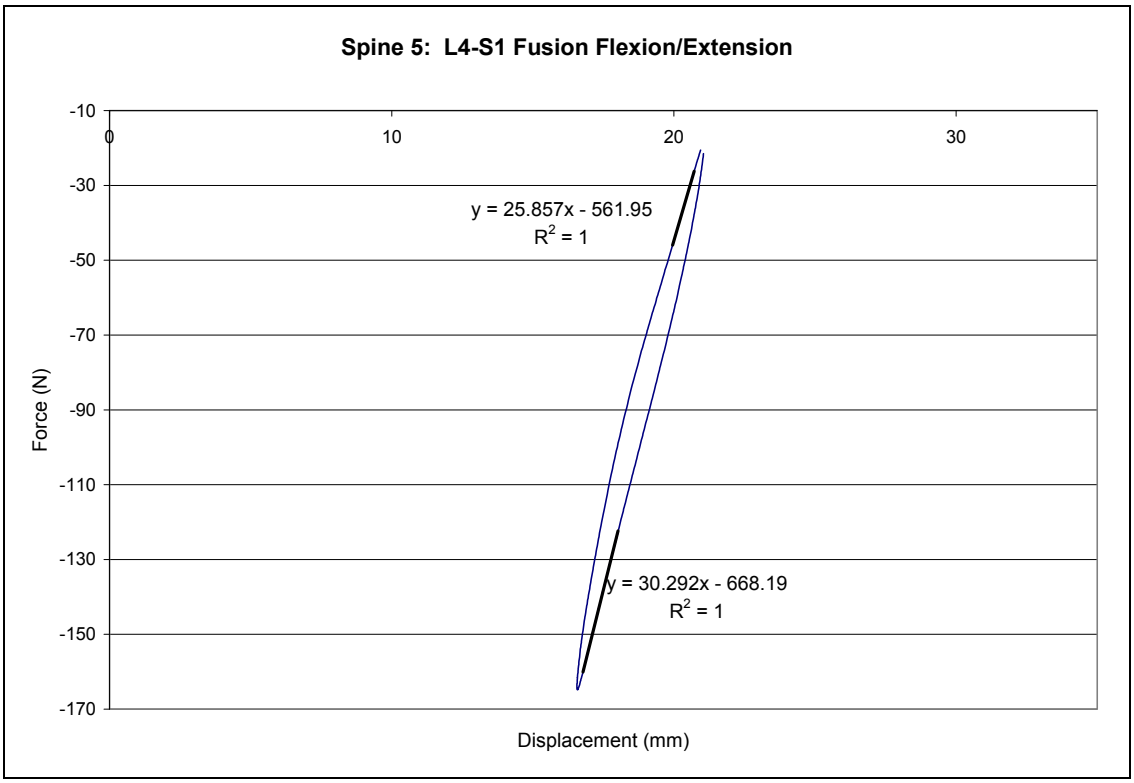

Figure 124: Spine 5 load/displacement curve flexion/wxtension L4-S1 fusion.

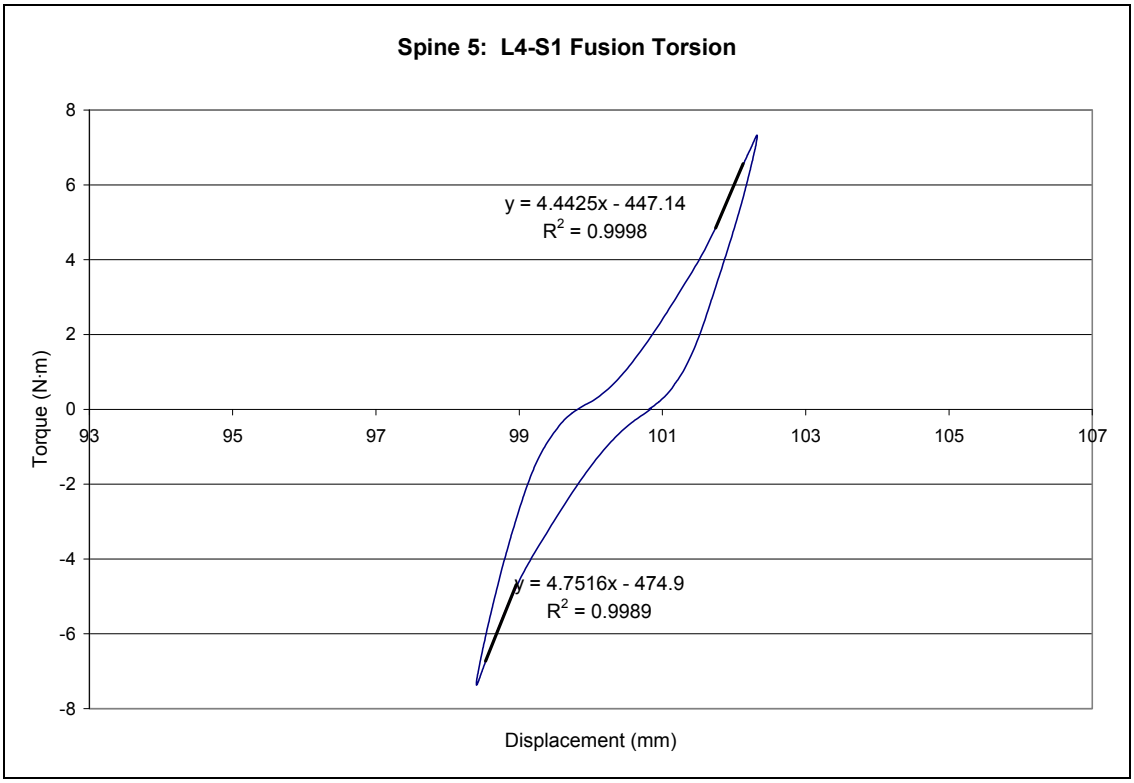

Figure 125: Spine 5 load/displacement curve torsion L4-S1 fusion.

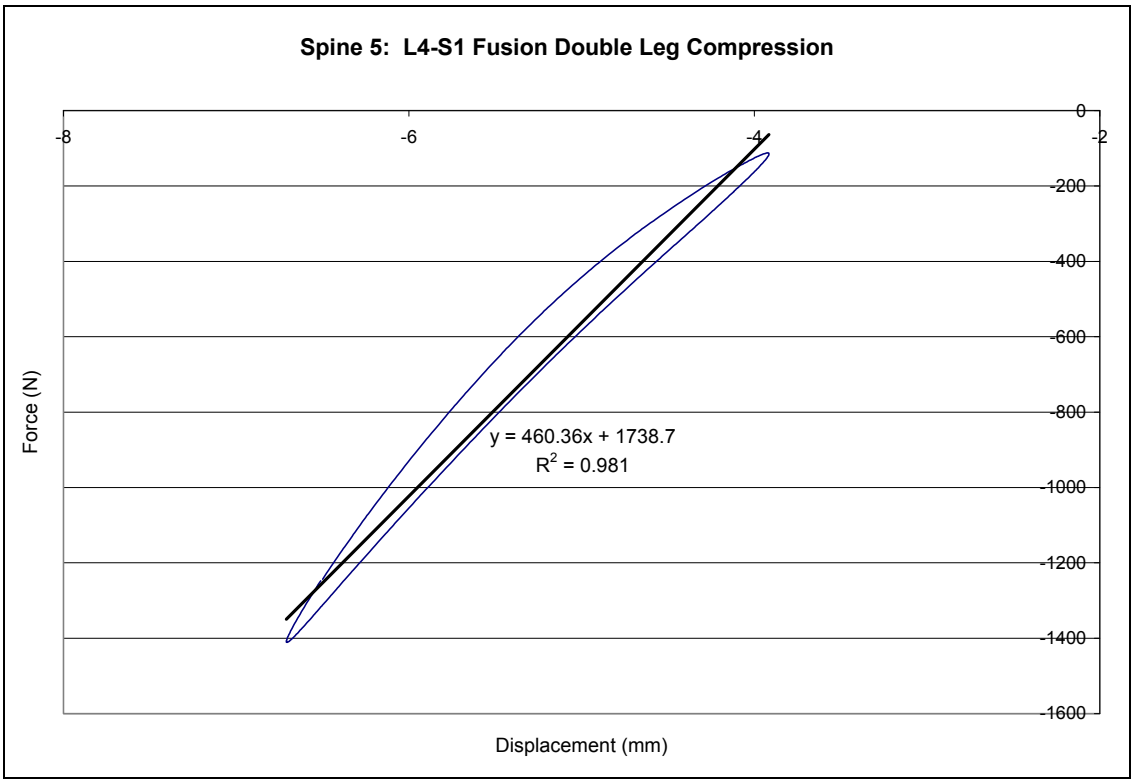

Figure 126: Spine 5 load/displacement curve double leg compression L4-S1 fusion.

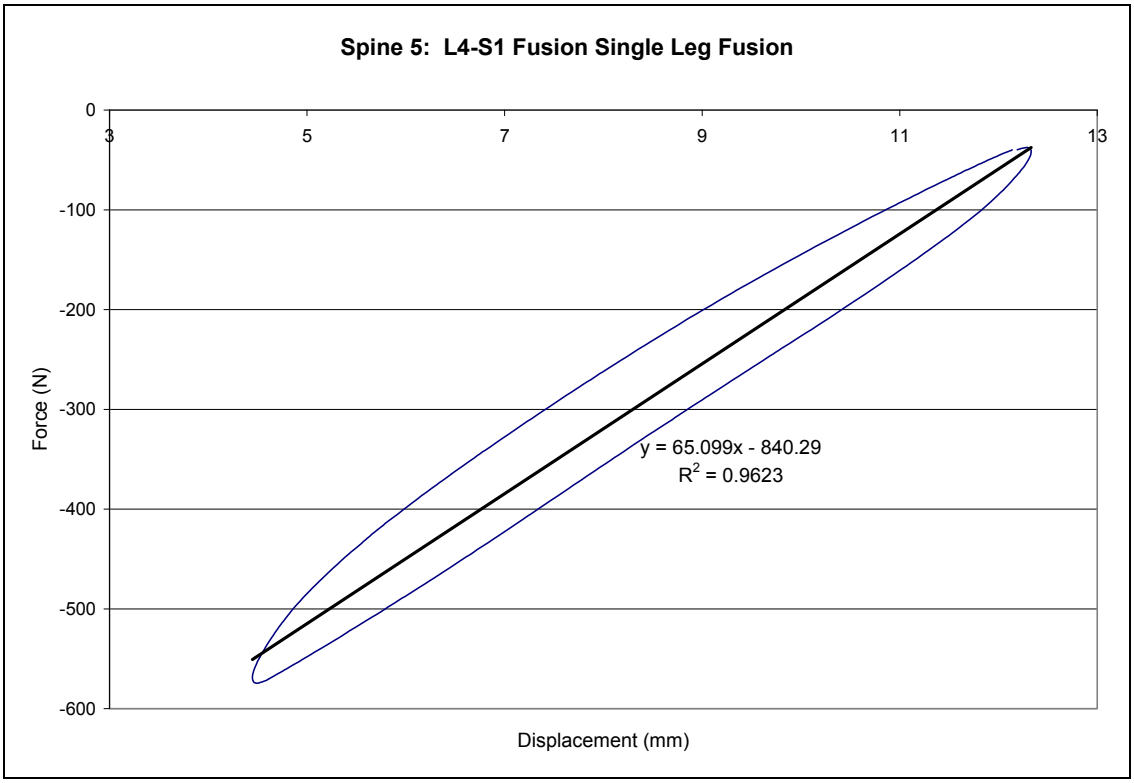

Figure 127: Spine 5 load/displacement curve single leg compression L4-S1 fusion.

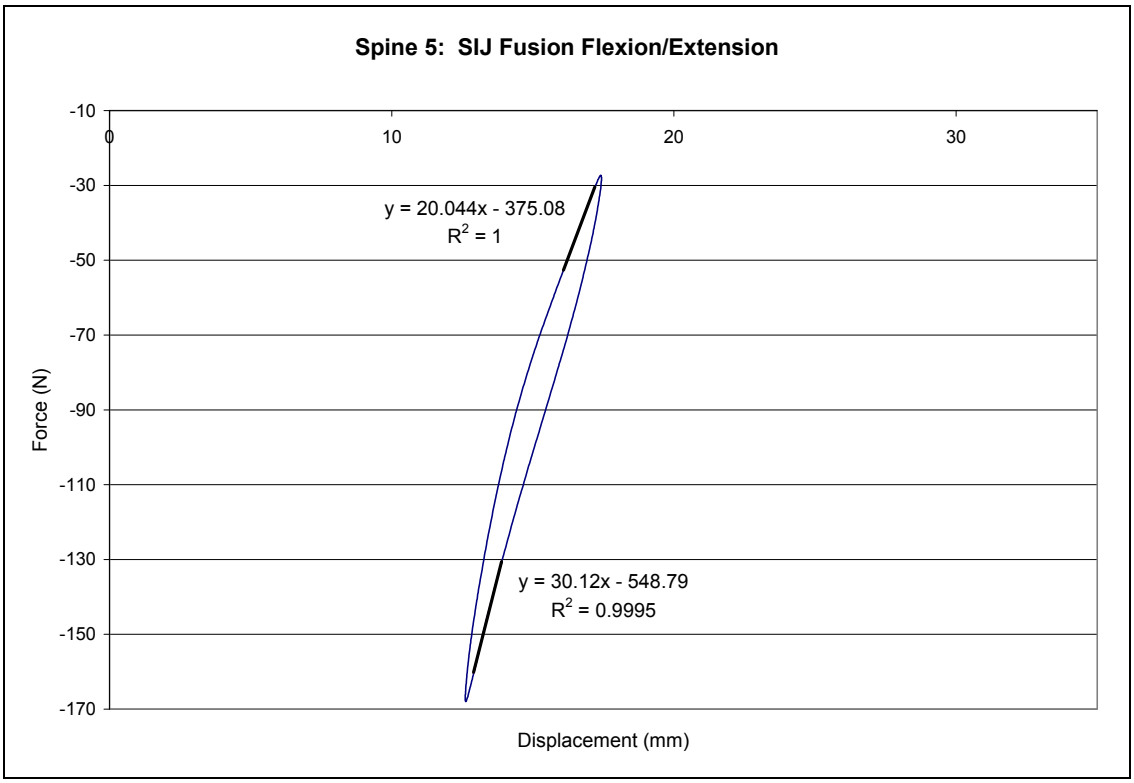

Figure 128: Spine 5 load/displacement curve flexion/extension SIJ fusion.

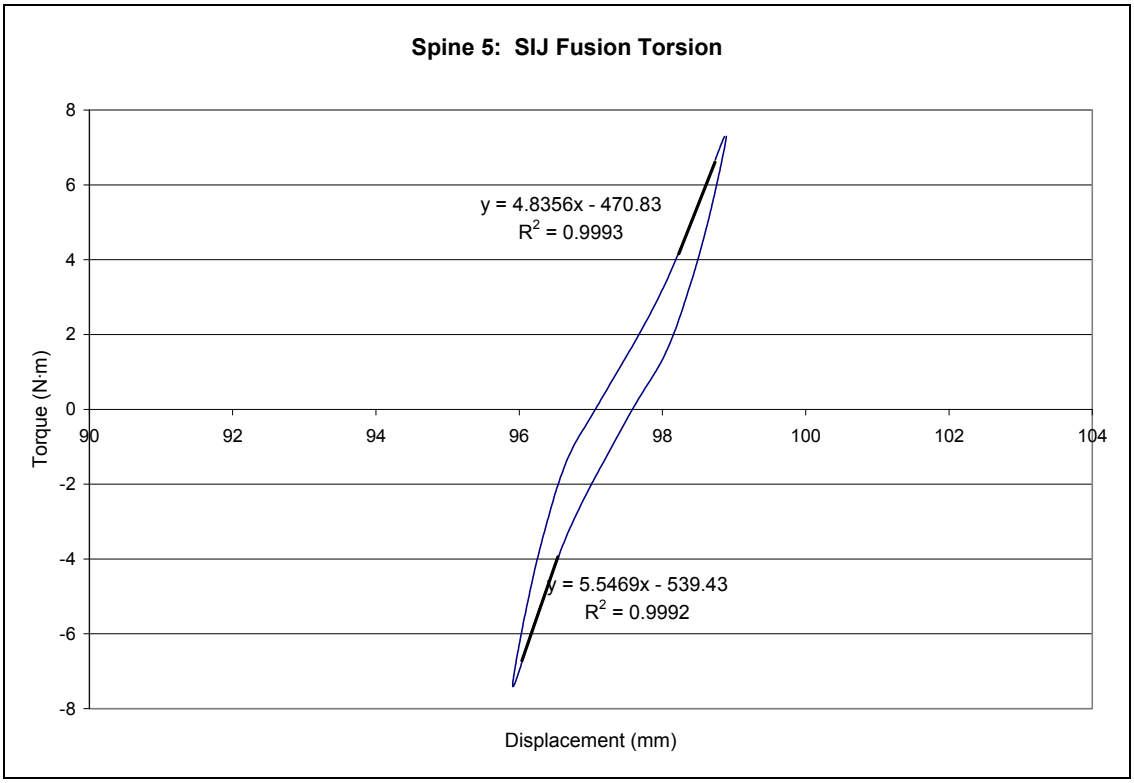

Figure 129: Spine 5 load/displacement curve torsion SIJ fusion.

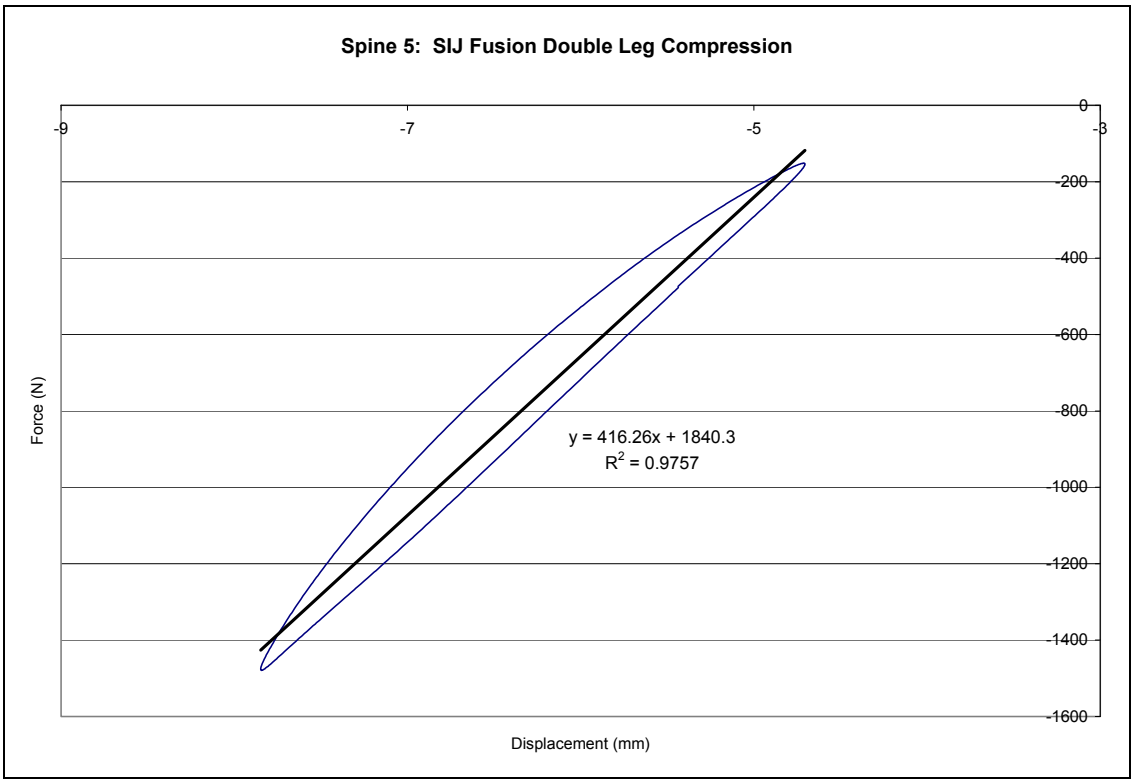

Figure 130: Spine 5 load/displacement curve double leg compression SIJ fusion.

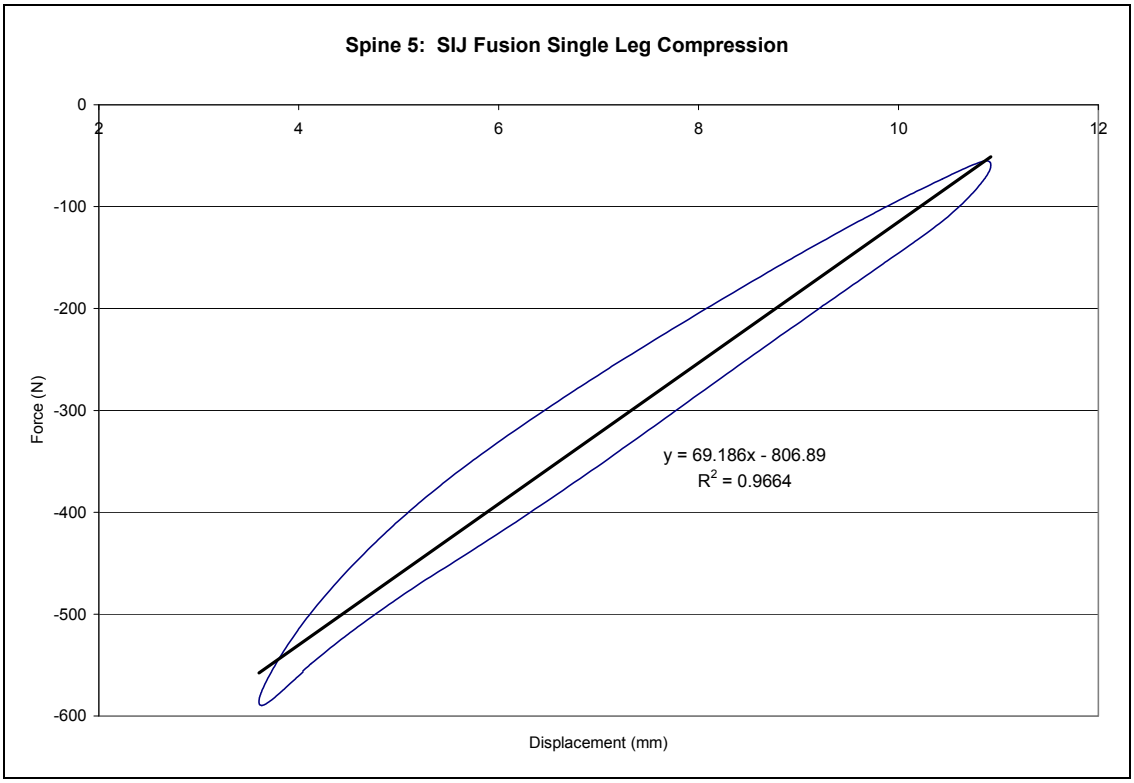

Figure 131: Spine 5 load/displacement curve single leg compression SIJ fusion.

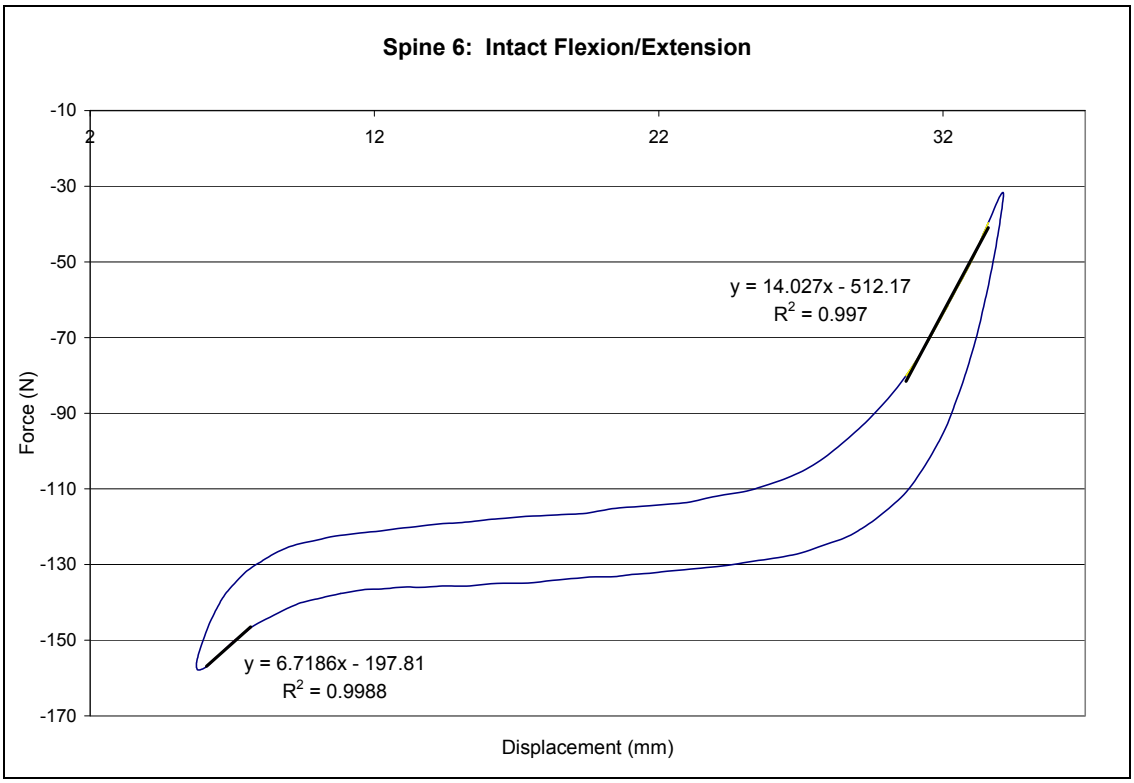

Figure 132: Spine 6 load/displacement curve intact flexion/extension.

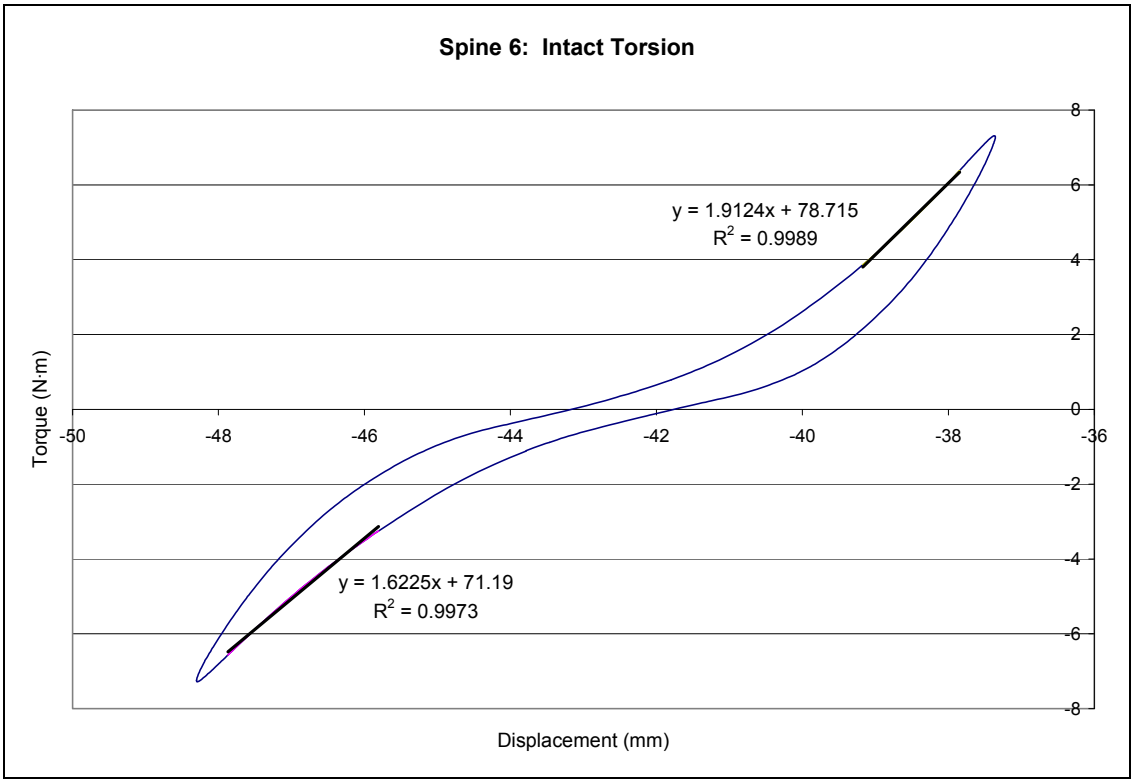

Figure 133: Spine 6 load/displacement curve intact torsion.

Figure 134: Spine 6 load/displacement curve intact double leg compression.

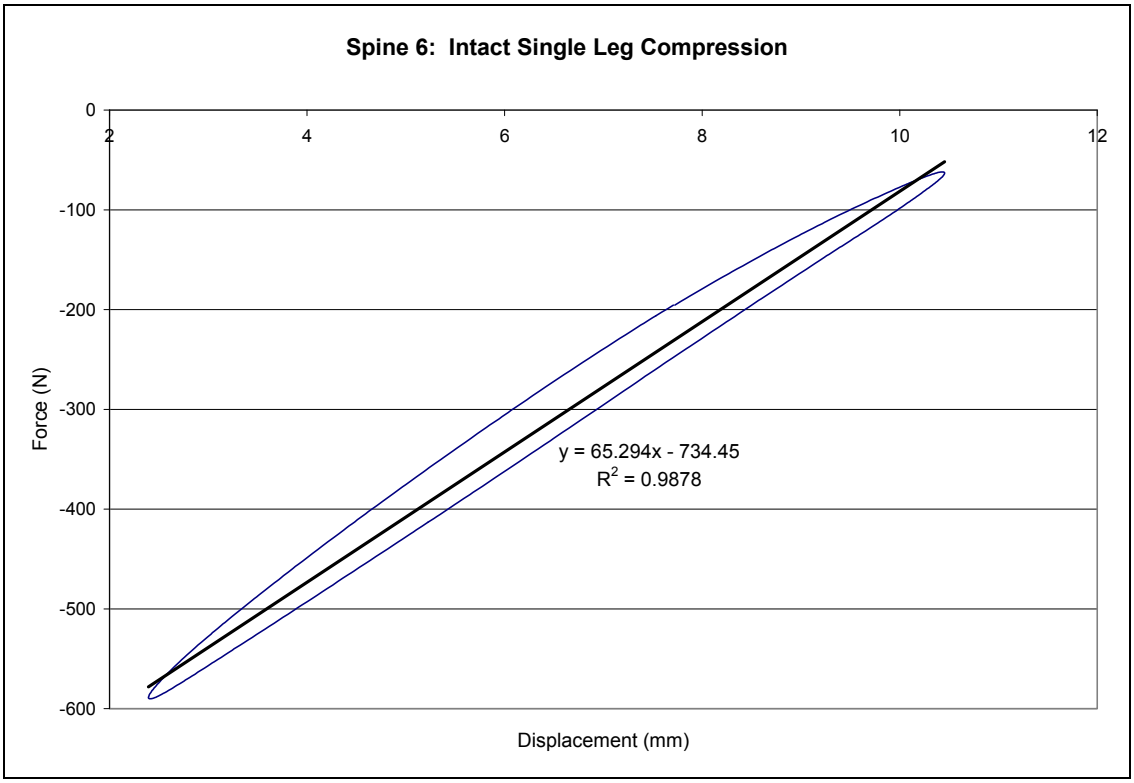

Figure 135: Spine 6 load/displacement curve intact single leg compression.

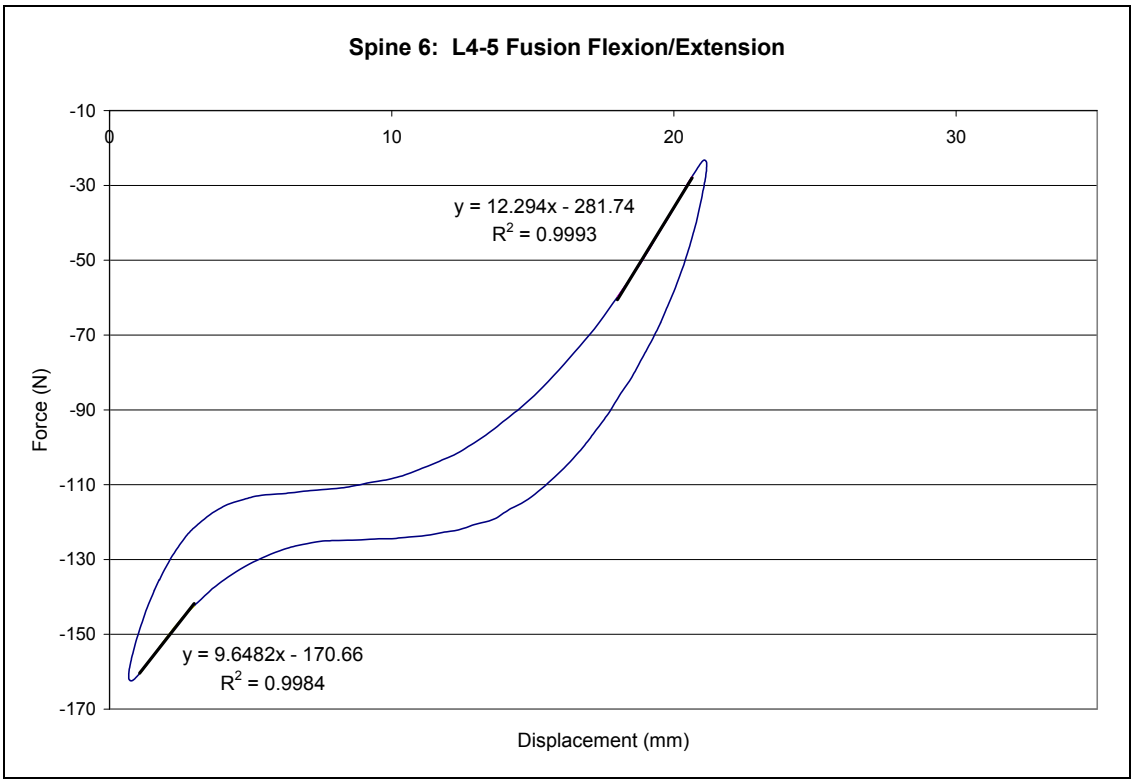

Figure 136: Spine 6 load/displacement curve flexion/extension L4-5 fusion.

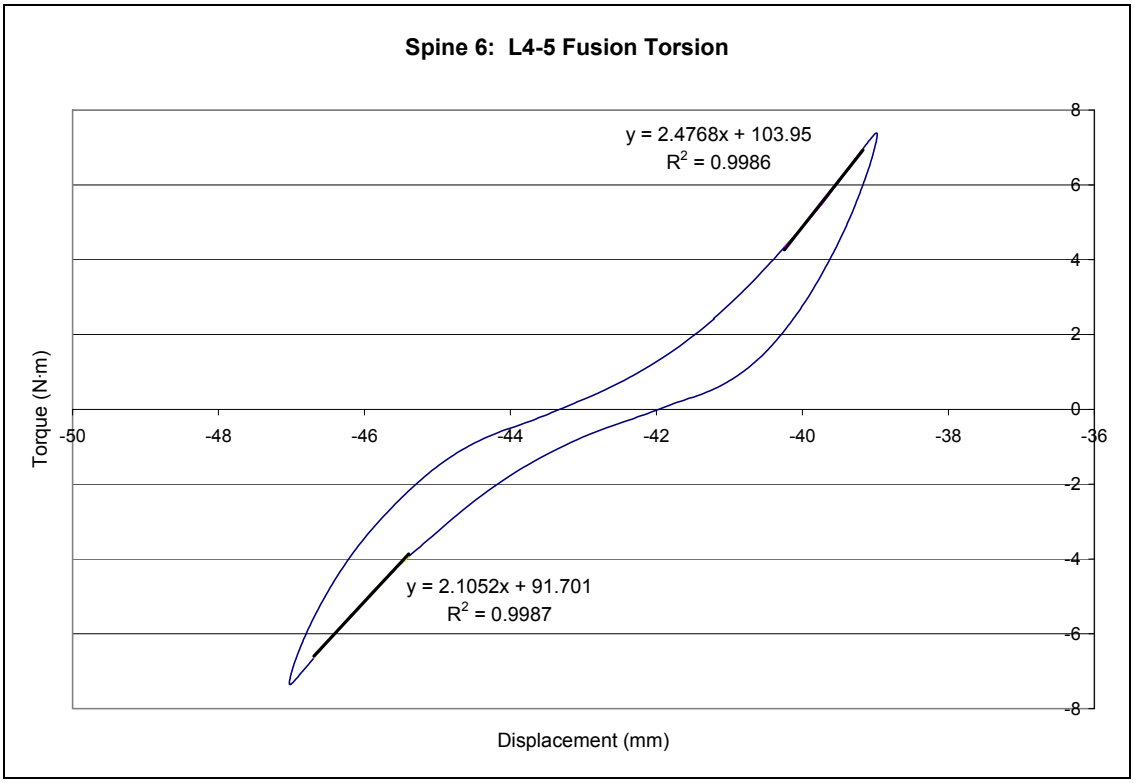

Figure 137: Spine 6 load/displacement curve torsion L4-5 fusion.

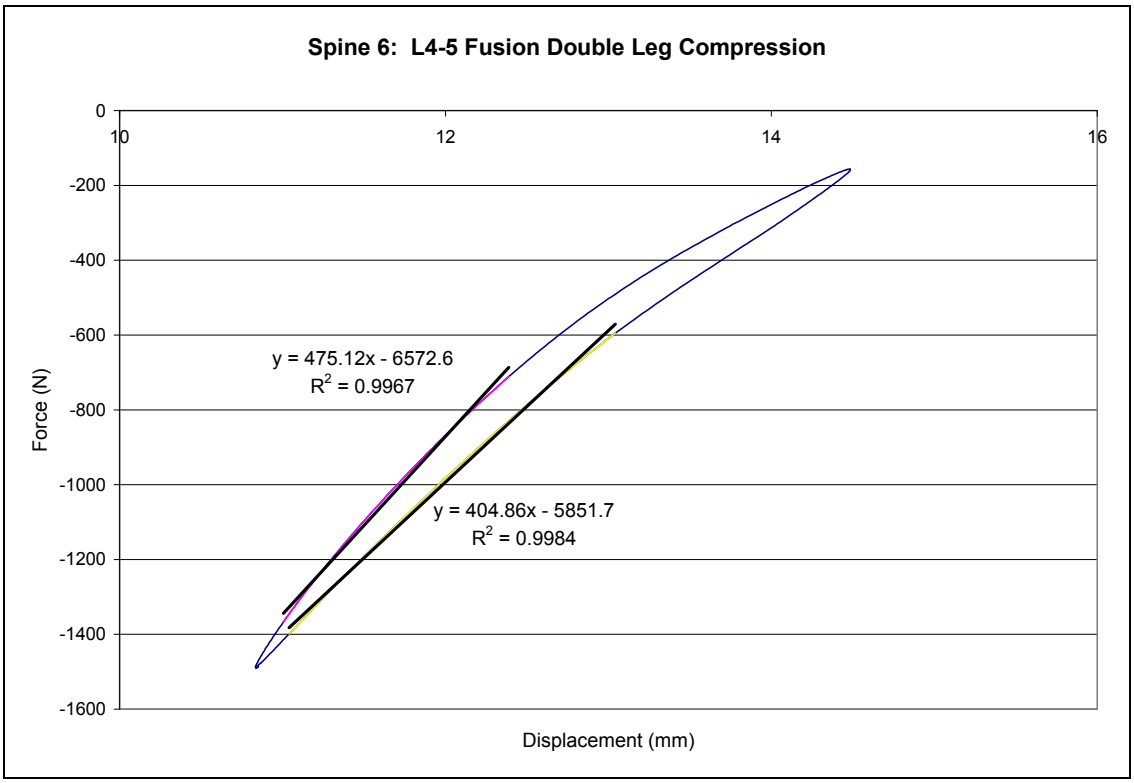

Figure 138: Spine 6 load/displacement curve double leg compression L4-5 fusion.

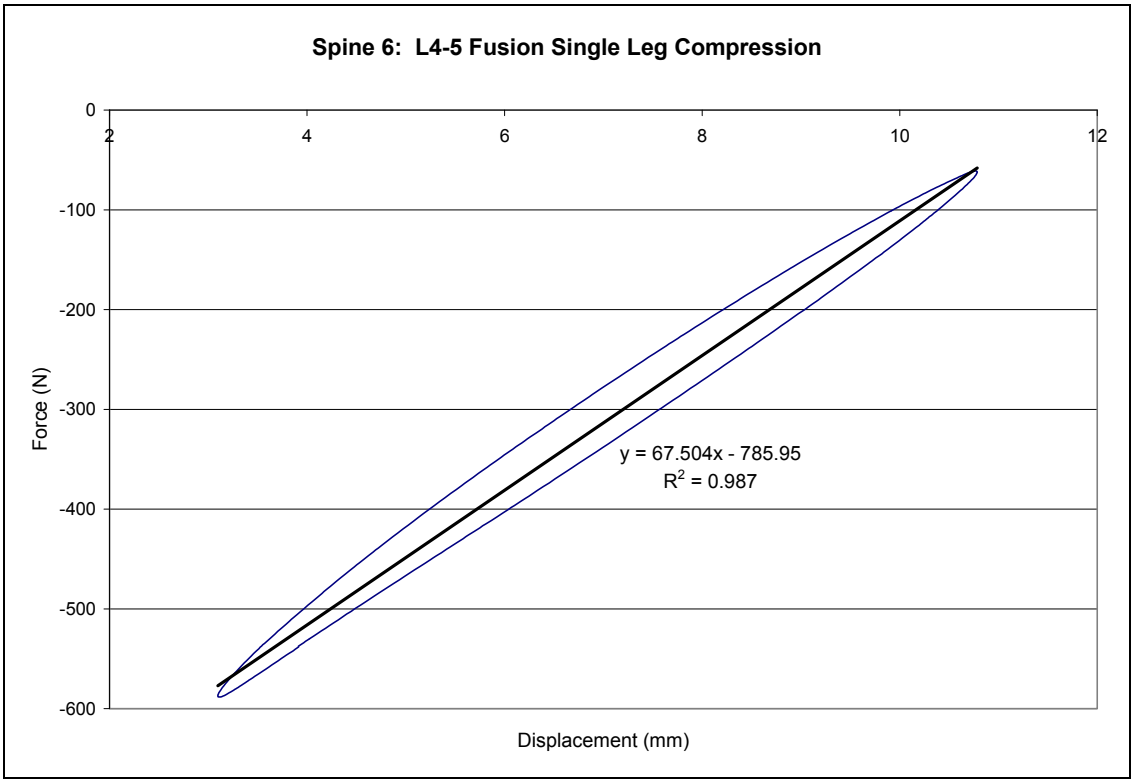

Figure 139: Spine 6 load/displacement curve single leg compression L4-5 fusion.

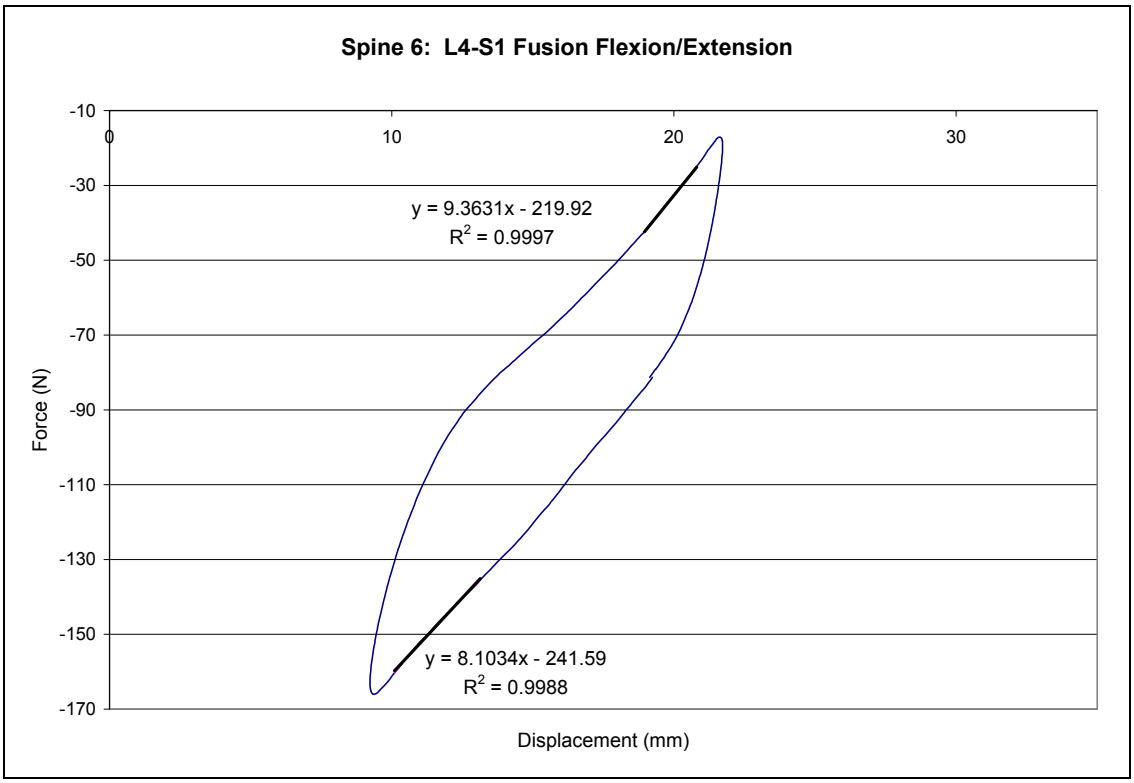

Figure 140: Spine 6 load/displacement curve flexion/extension L4-S1 fusion.

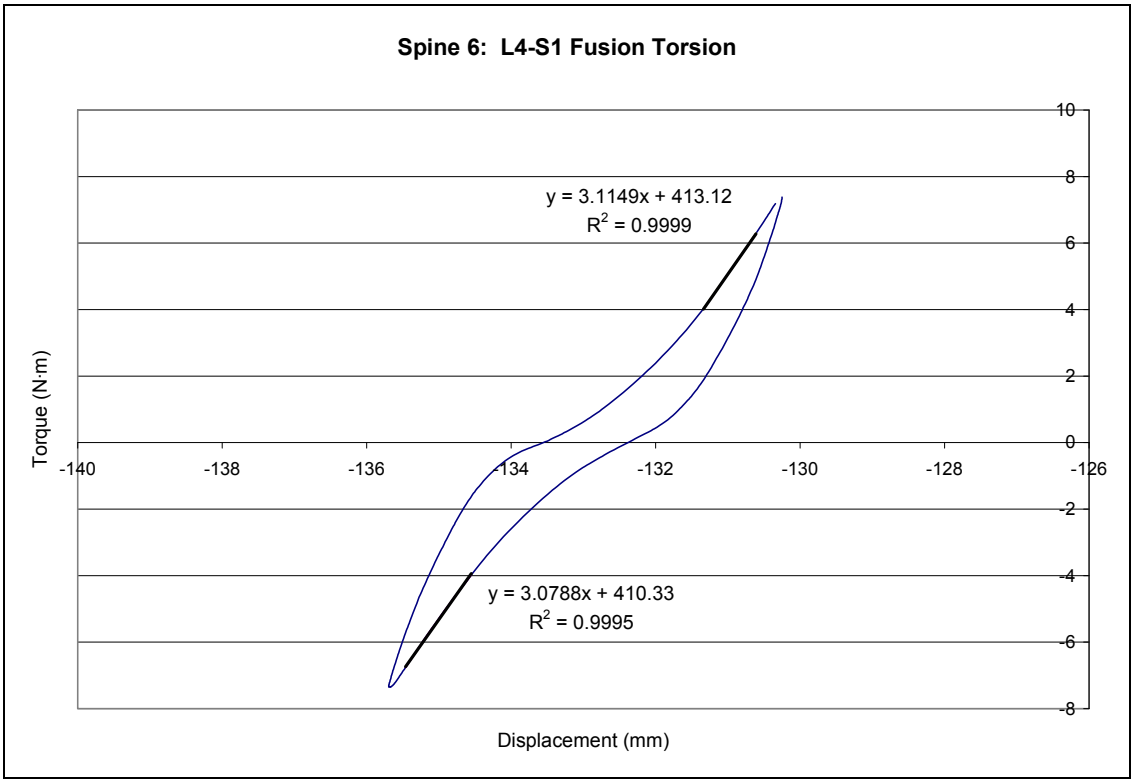

Figure 141: Spine 6 load/displacement curve torsion L4-S1 fusion.

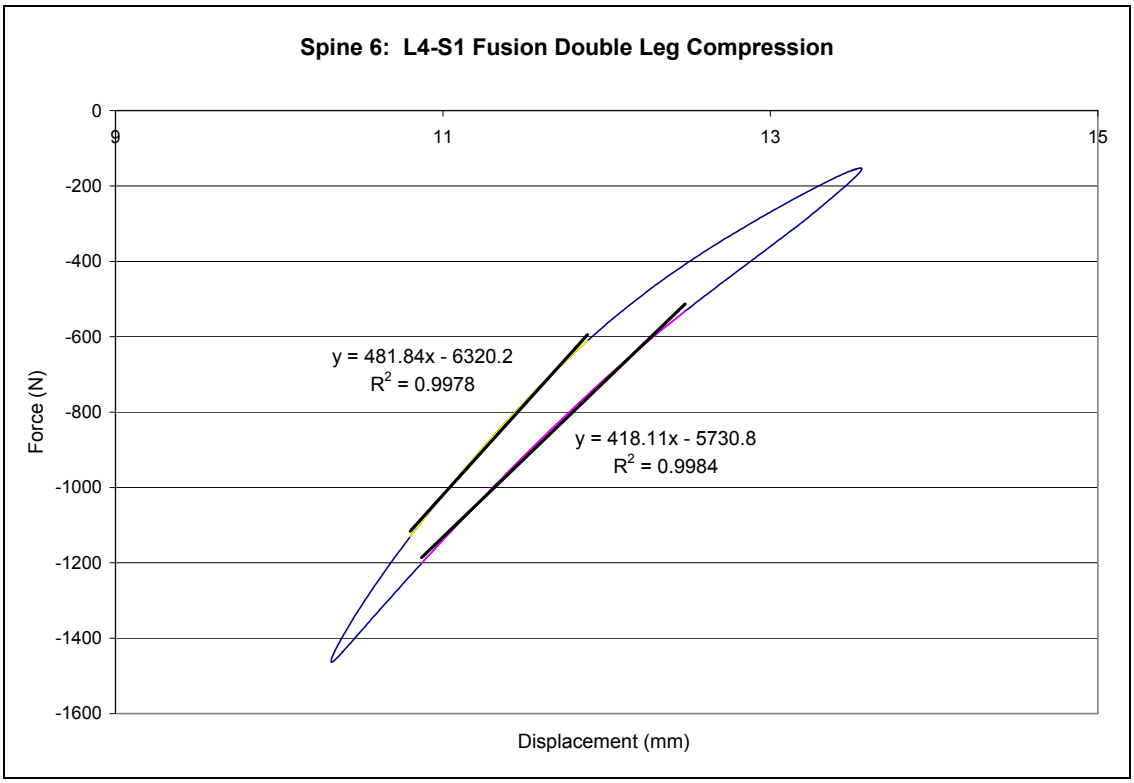

Figure 142: Spine 6 load/displacement curve double leg compression L4-S1 fusion.

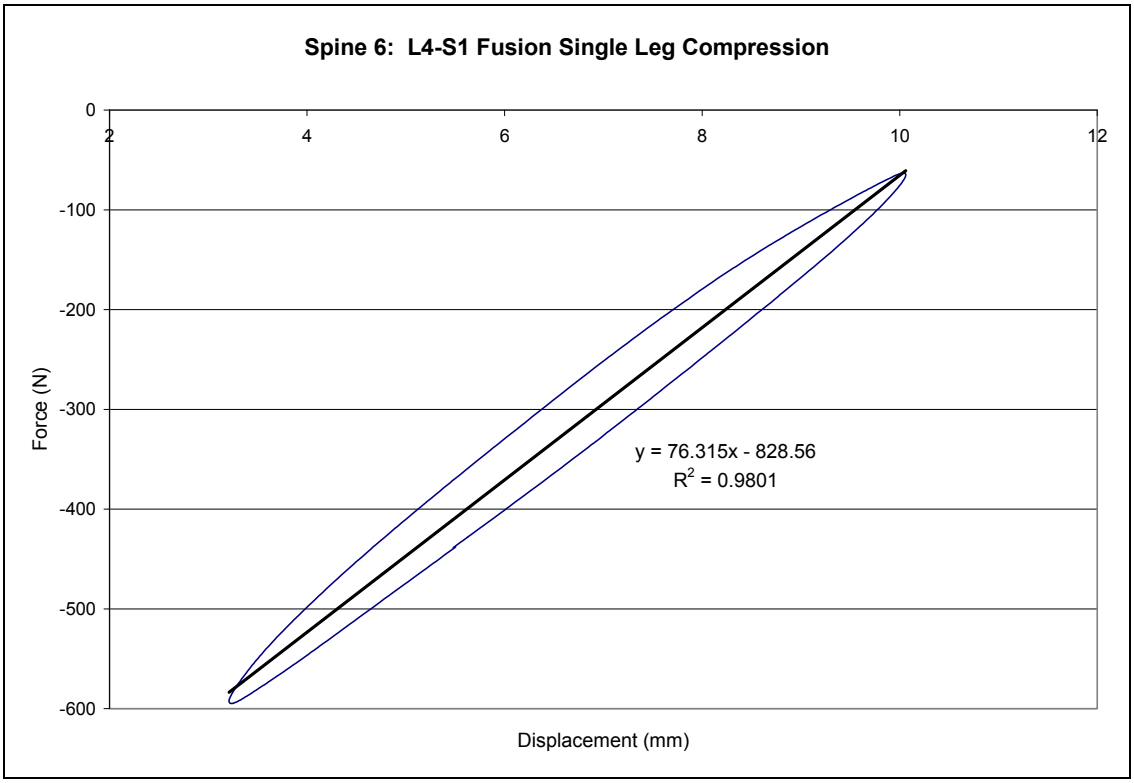

Figure 143: Spine 6 load/displacement curve single leg compression L4-S1 fusion.

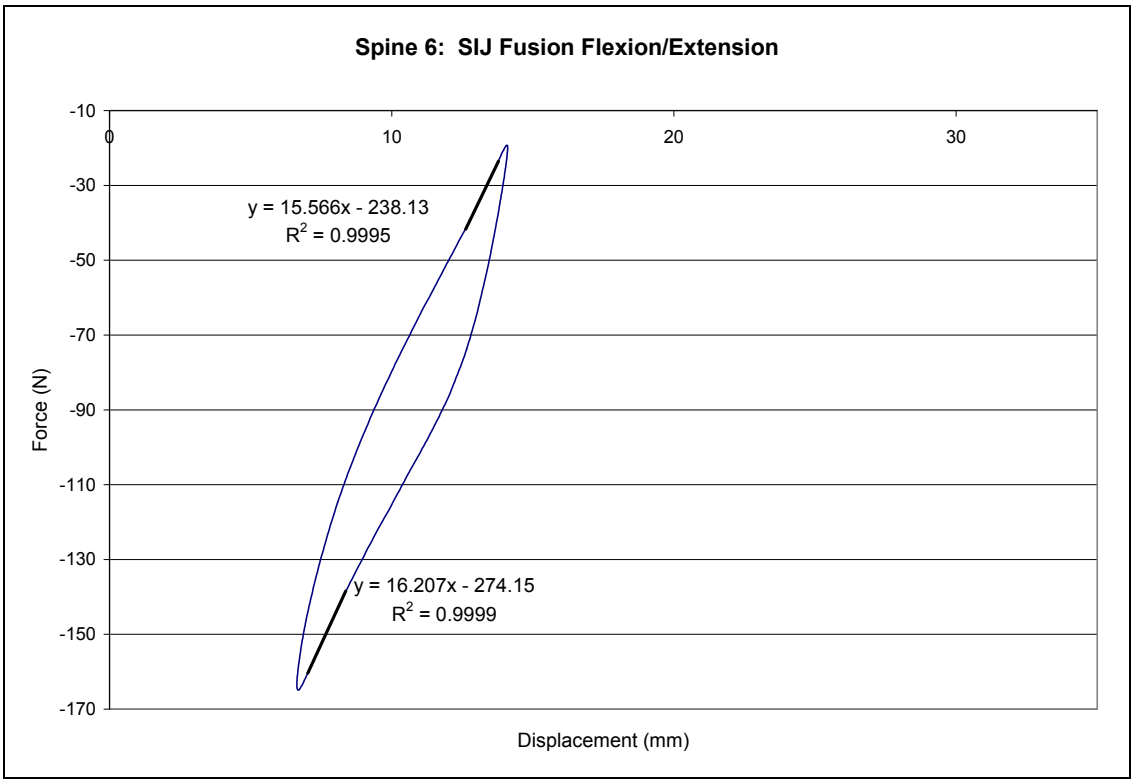

Figure 144: Spine 6 load/displacement curve flexion/extension SIJ fusion.

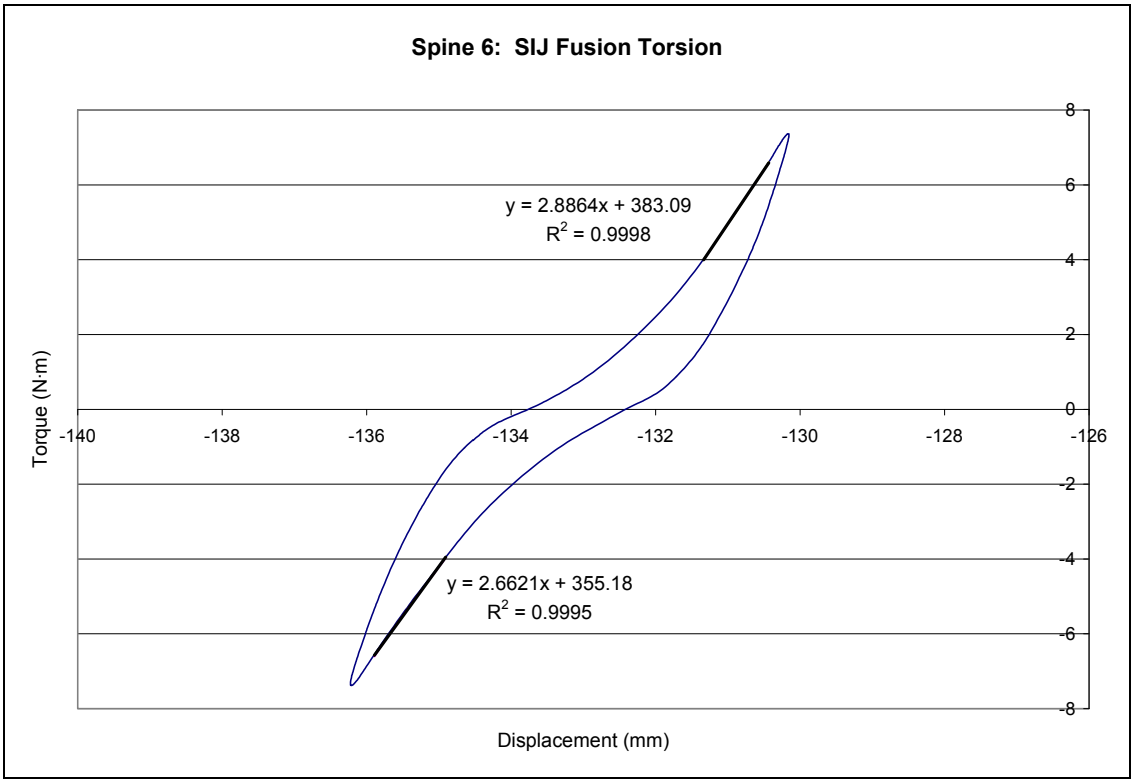

Figure 145: Spine 6 load/displacement curve torsion SIJ fusion.

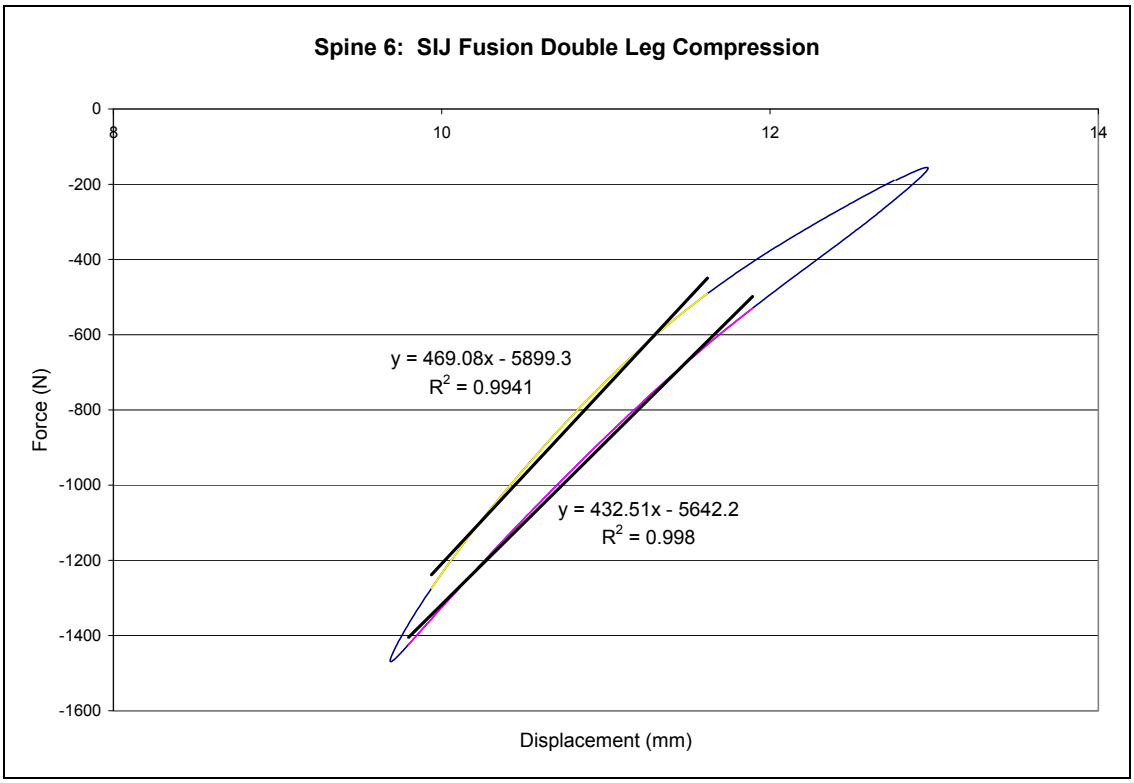

Figure 146: Spine 6 load/displacement curve double leg compression SIJ fusion.

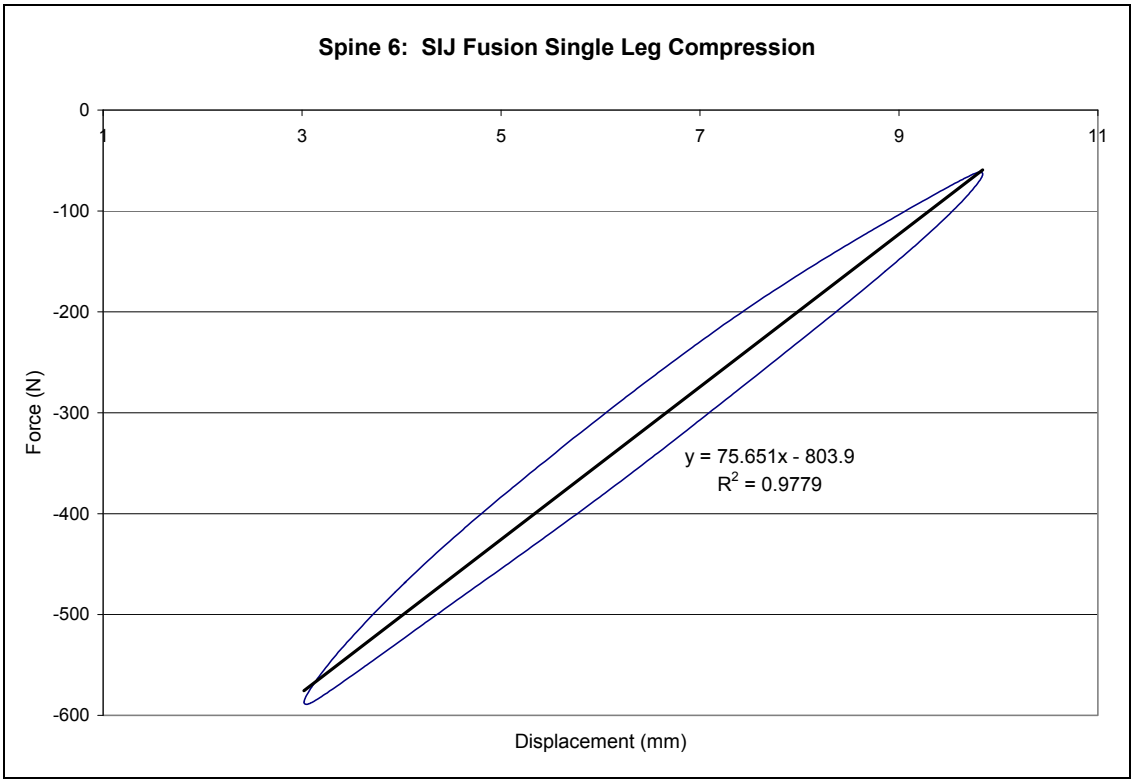

Figure 147: Spine 6 load/displacement curve single leg compression SIJ fusion.

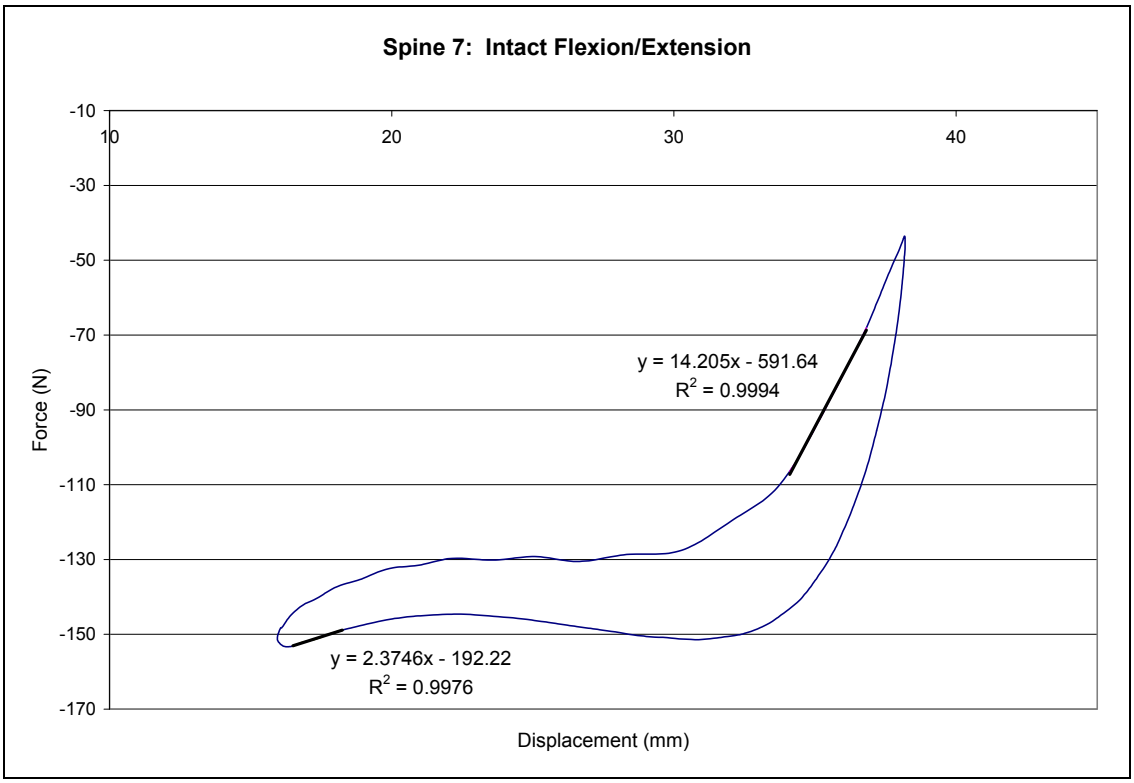

Figure 148: Spine 7 load/displacement curve intact flexion/extension.

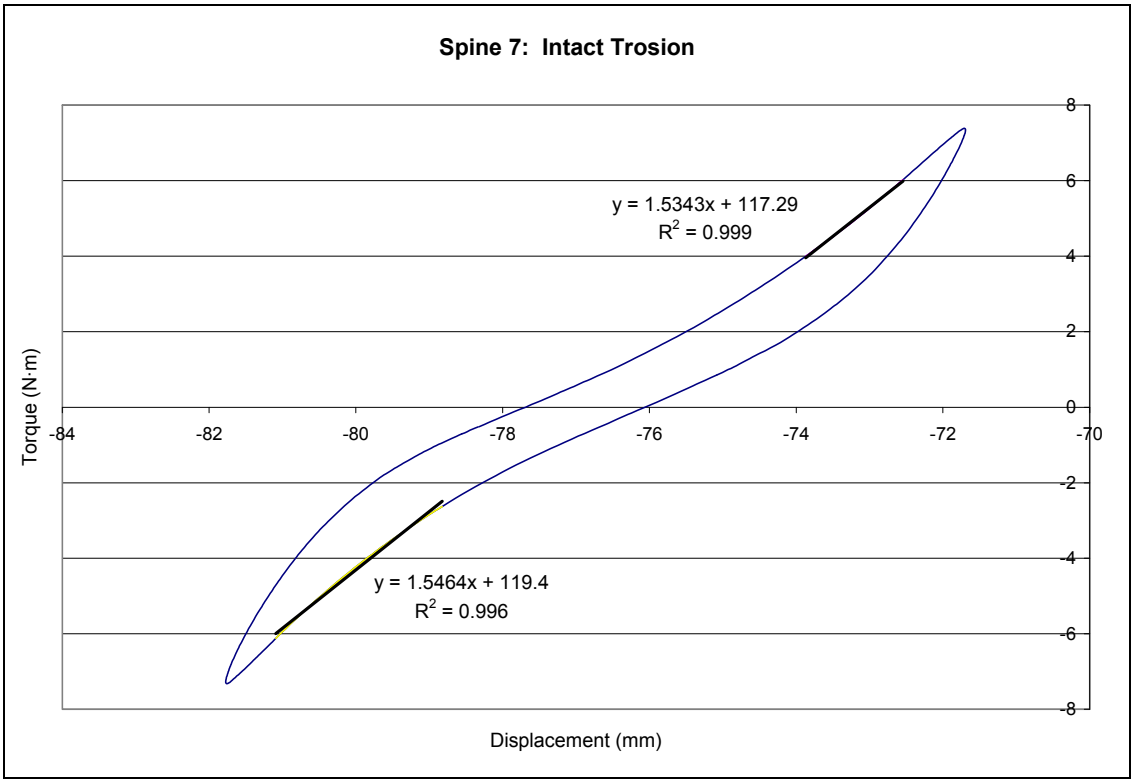

Figure 149: Spine 7 load/displacement curve intact torsion.

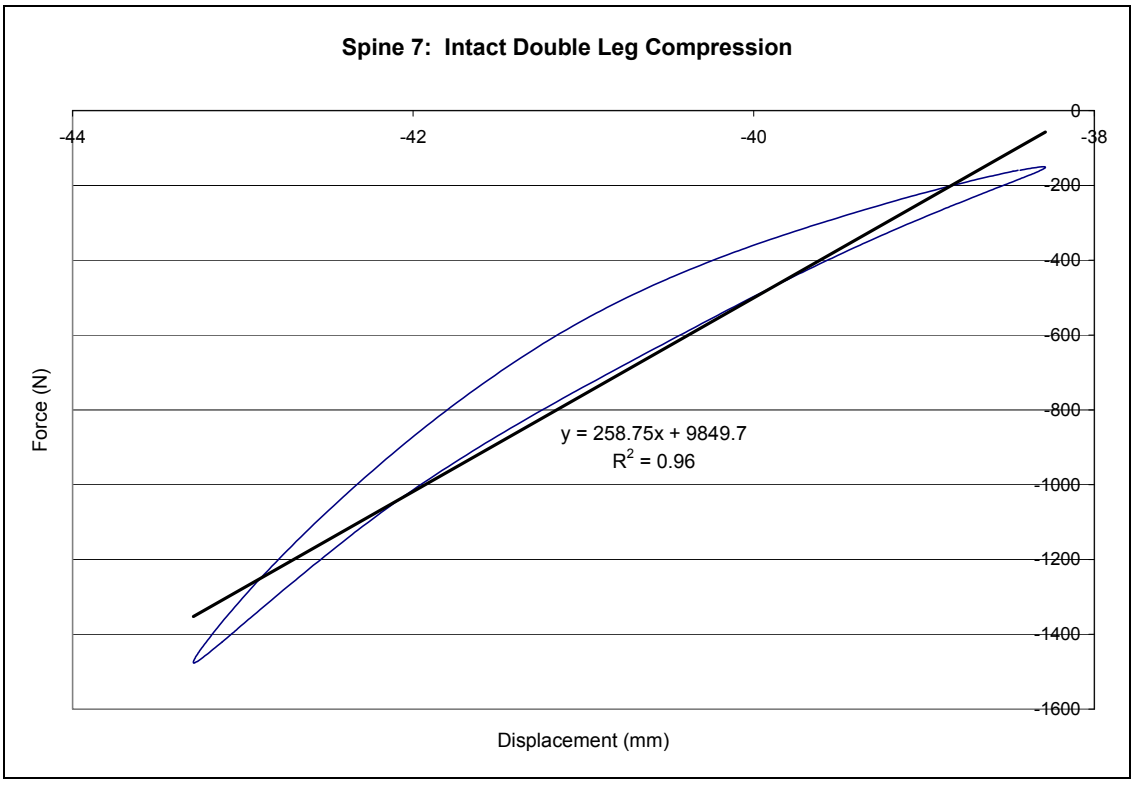

Figure 150: Spine 7 load/displacement curve intact double leg compression.

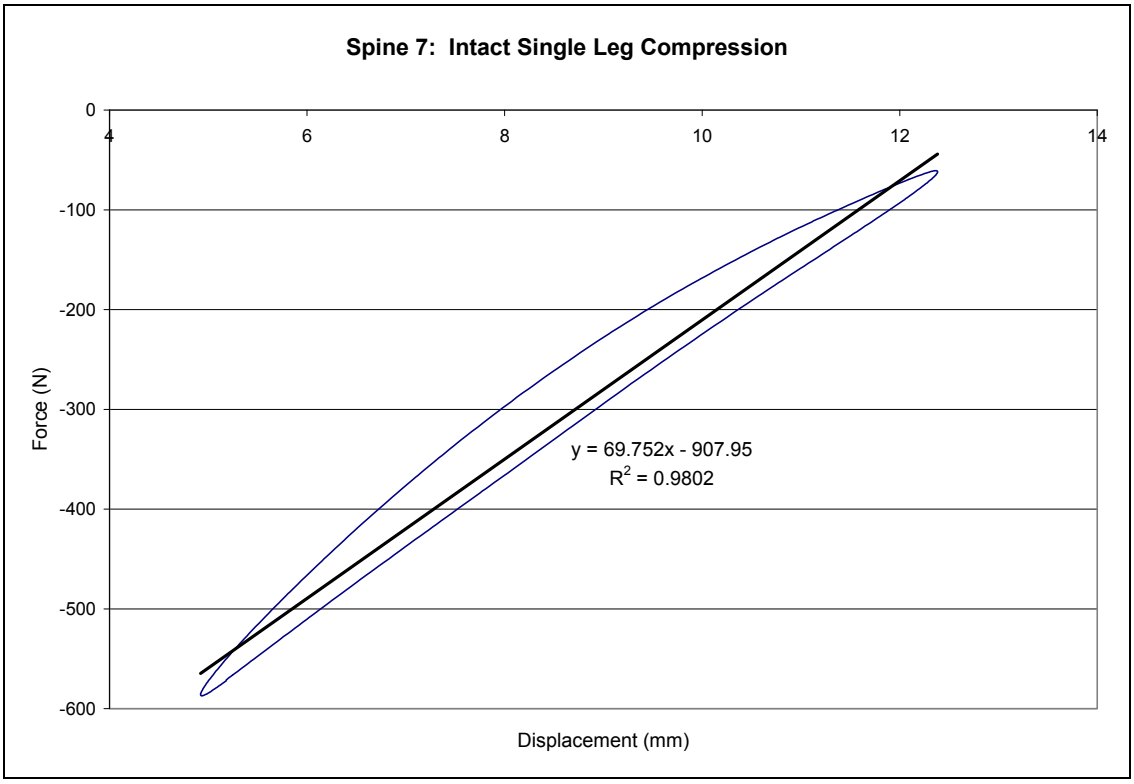

Figure 151: Spine 7 load/displacement curve intact single leg compression.

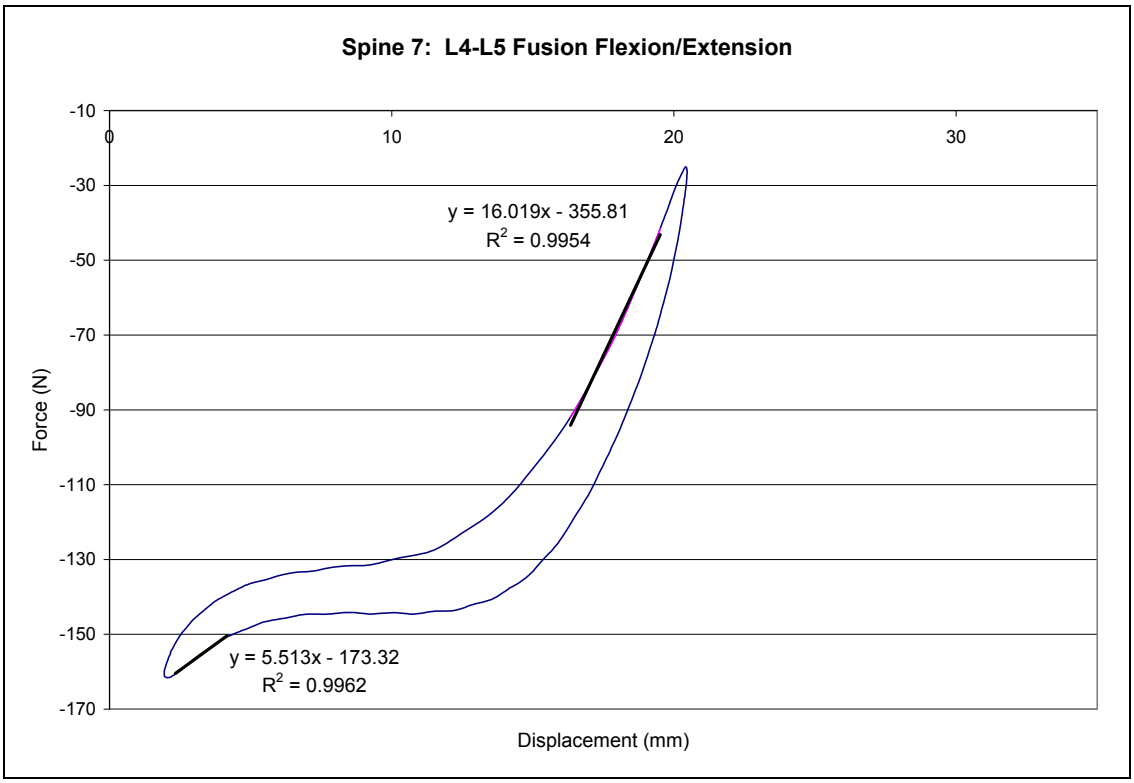

Figure 152: Spine 7 load/displacement curve flexion/extension L4-5 fusion.

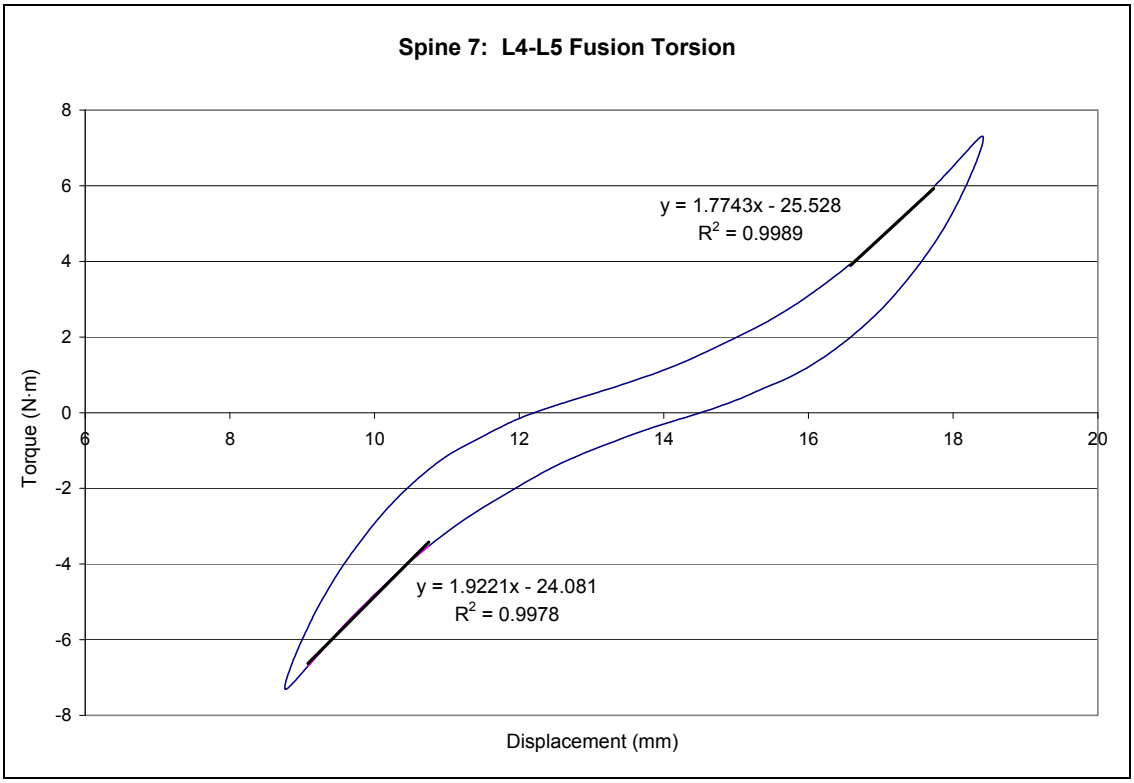

Figure 153: Spine 7 load/displacement curve torsion L4-5 fusion.

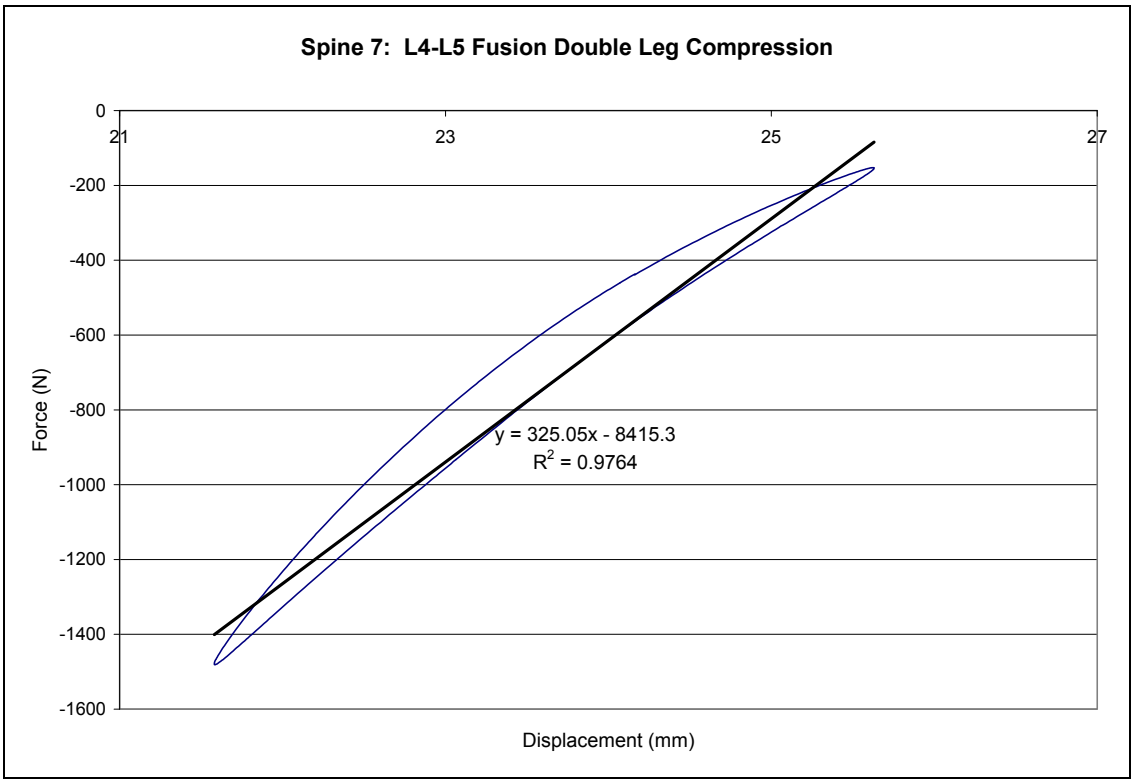

Figure 154: Spine 7 load/displacement curve double leg compression L4-5 fusion.

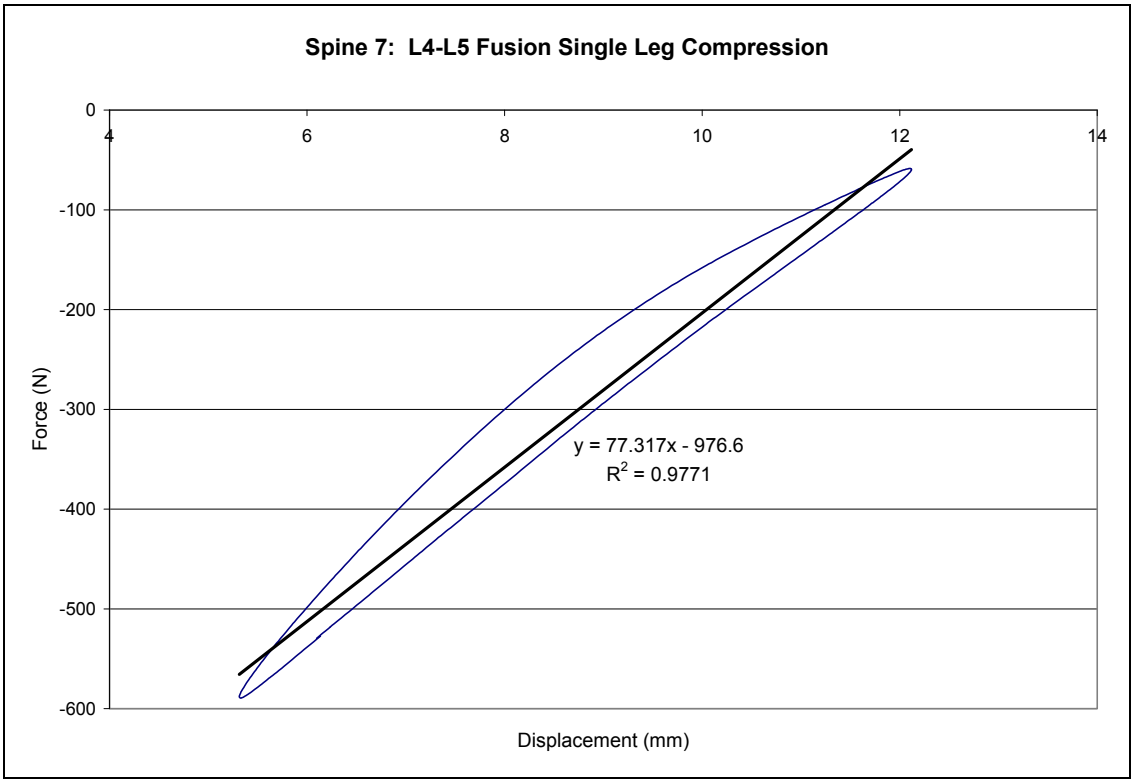

Figure 155: Spine 7 load/displacement curve single leg compression L4-5 fusion.

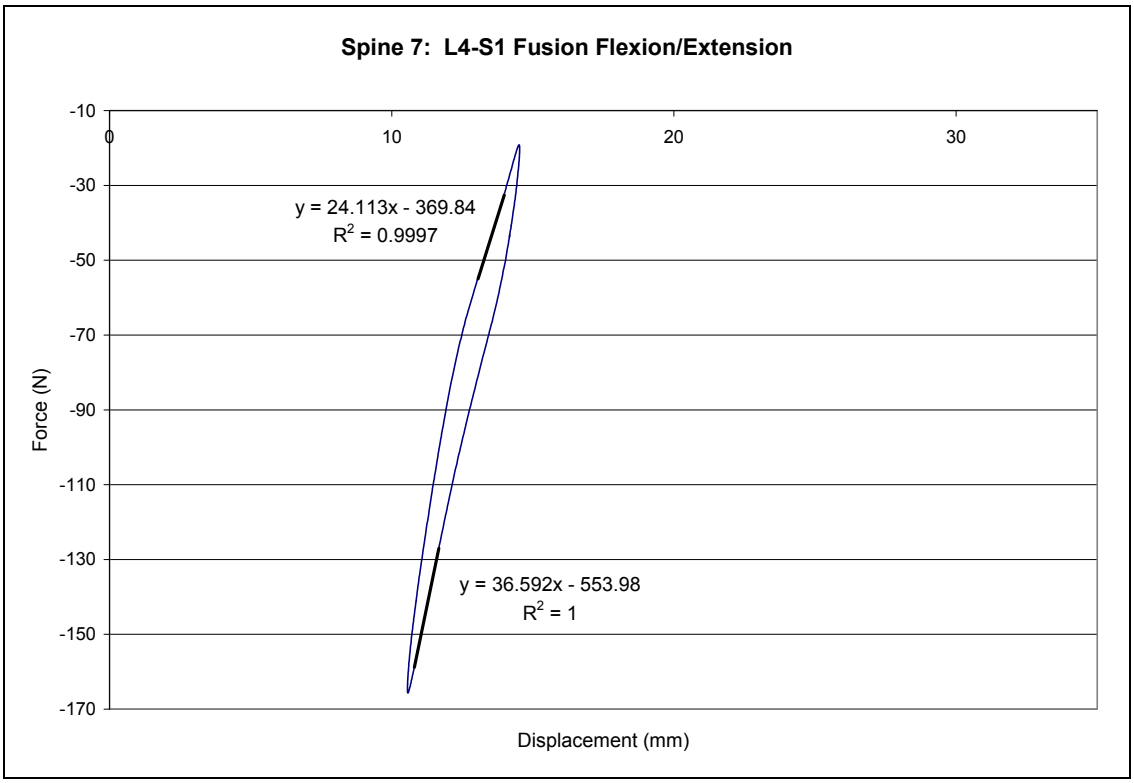

Figure 156: Spine 7 load/displacement curve flexion/extension L4-S1 fusion.

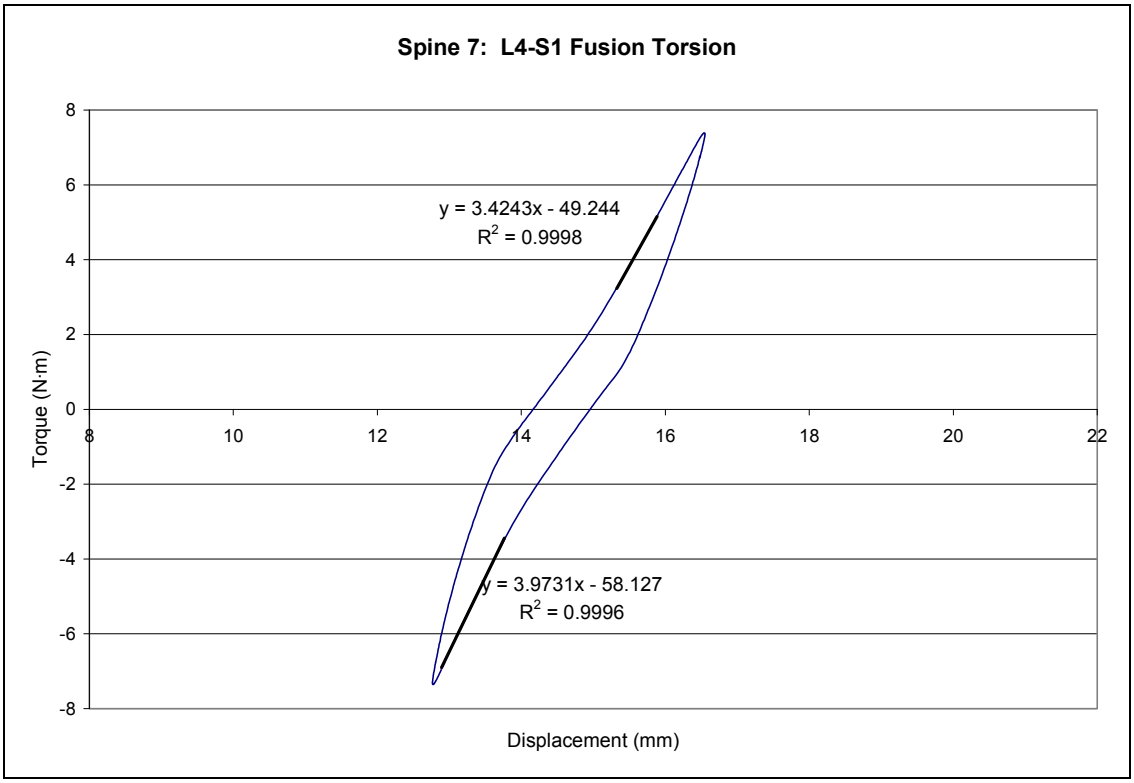

Figure 157: Spine 7 load/displacement curve torsion L4-S1 fusion.

Figure 158: Spine 7 load/displacement curve double leg compression L4-S1 fusion.

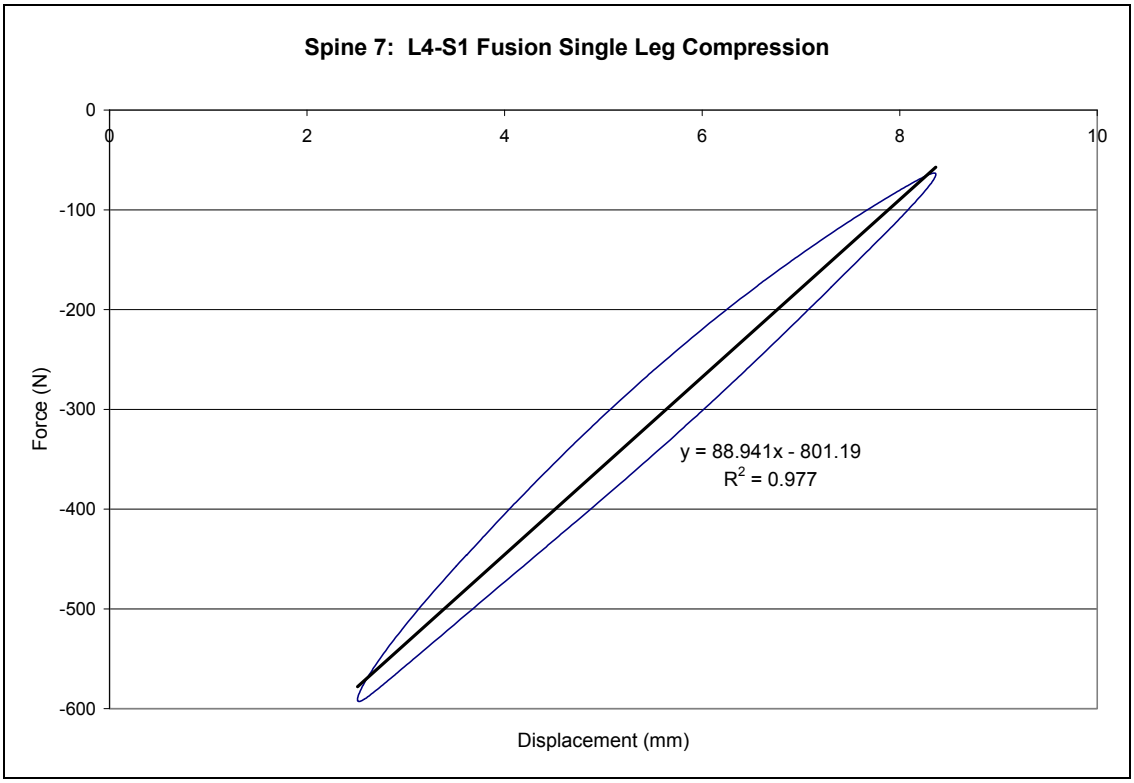

Figure 159: Spine 7 load/displacement curve single leg compression L4-S1 fusion.

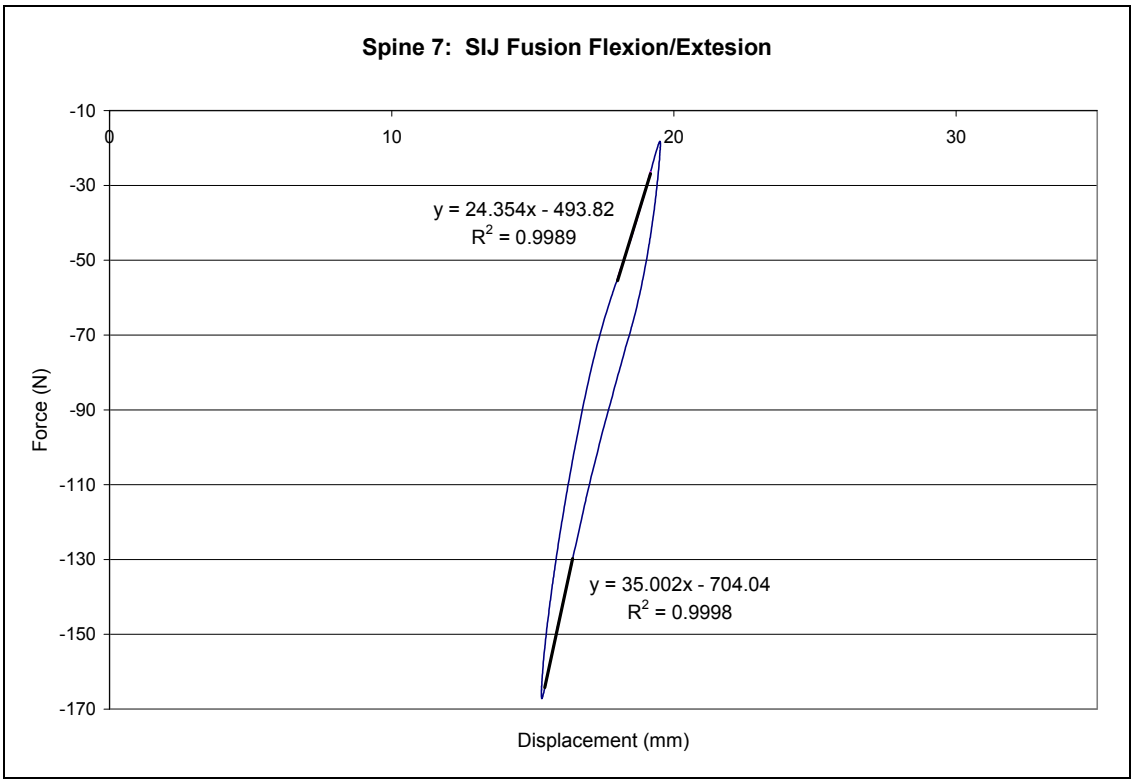

Figure 160: Spine 7 load/displacement curve flexion/extension SIJ fusion.

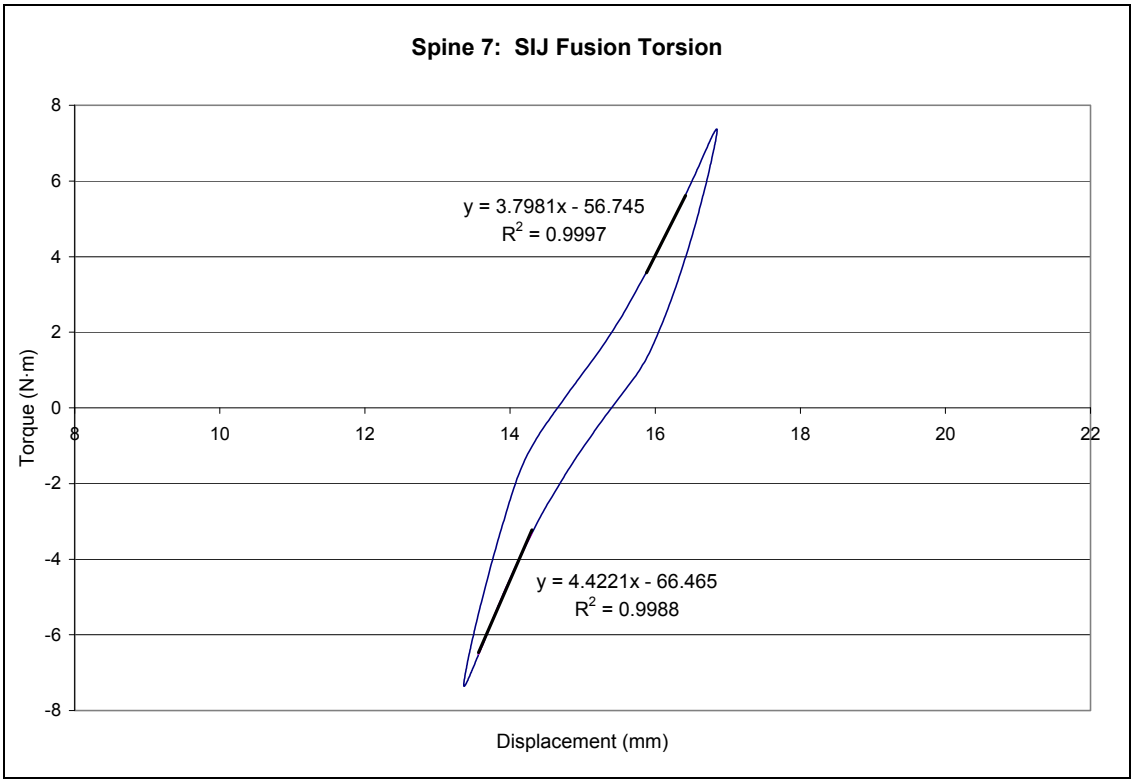

Figure 161: Spine 7 load/displacement curve torsion SIJ fusion.

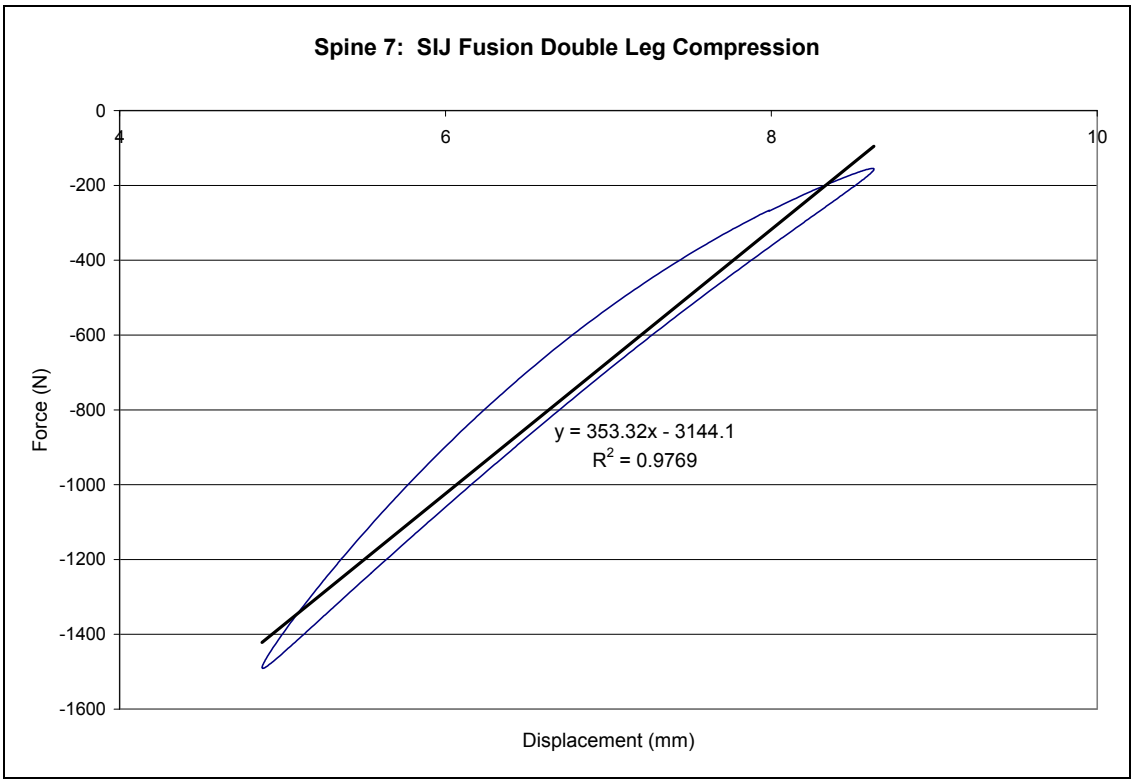

Figure 162: Spine 7 load/displacement curve double leg compression SIJ fusion.

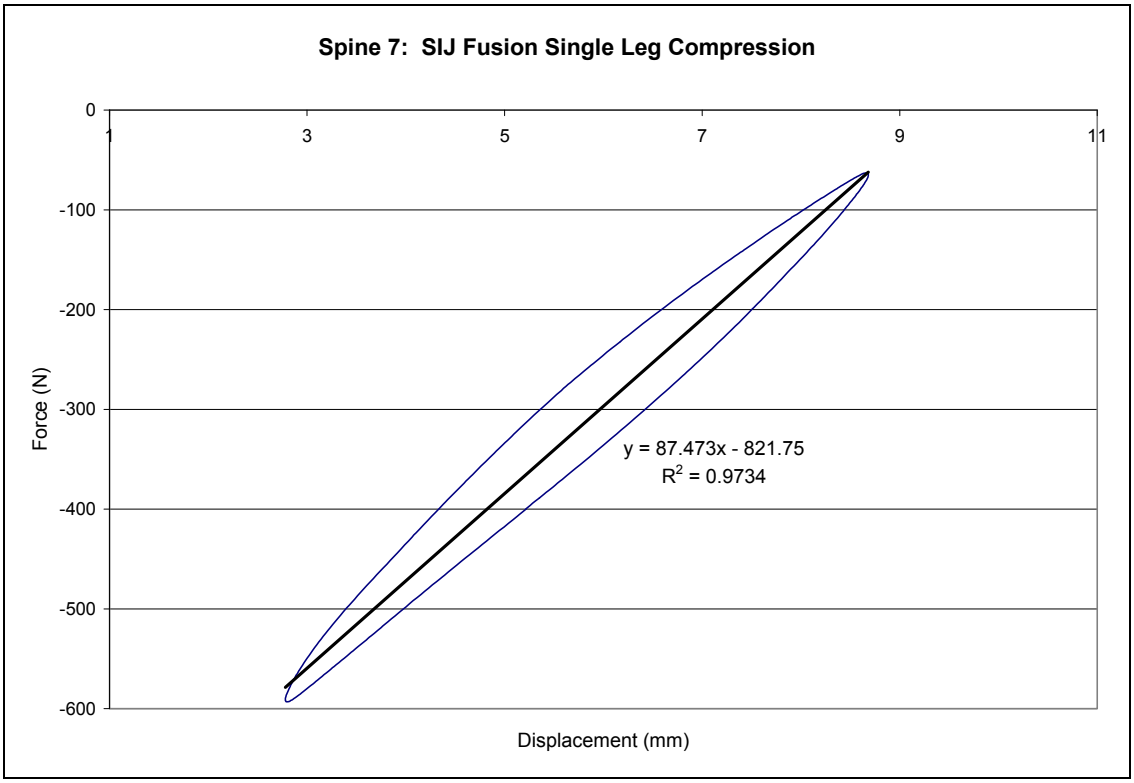

Figure 163: Spine 7 load/displacement curve single leg compression SIJ fusion.

APPENDIX C: DVRT Conversion Factors and Graphs

Yellow Transducer

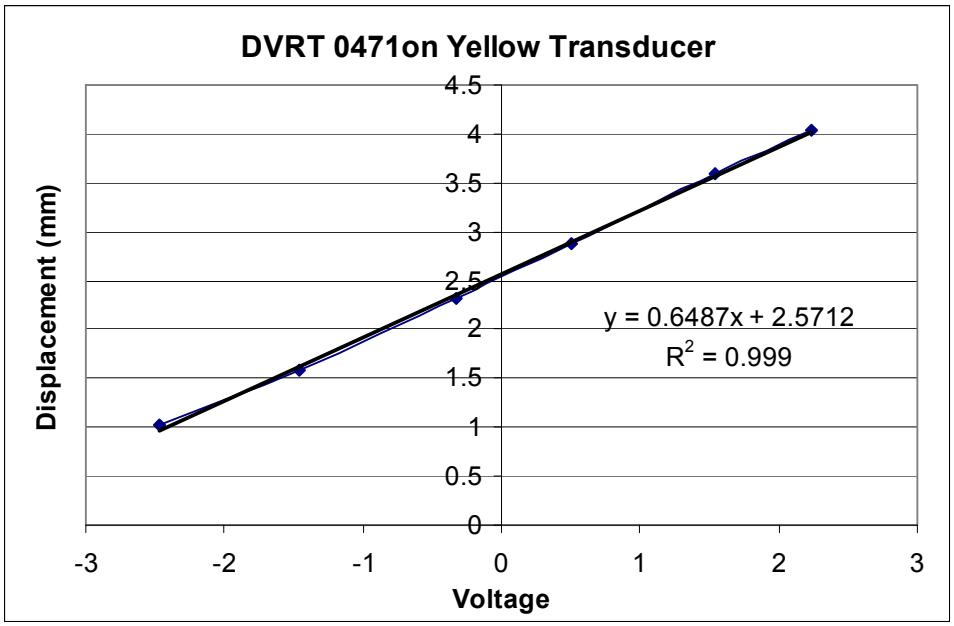

Figure 164: DVRT 0471 calibration with yellow transducer.

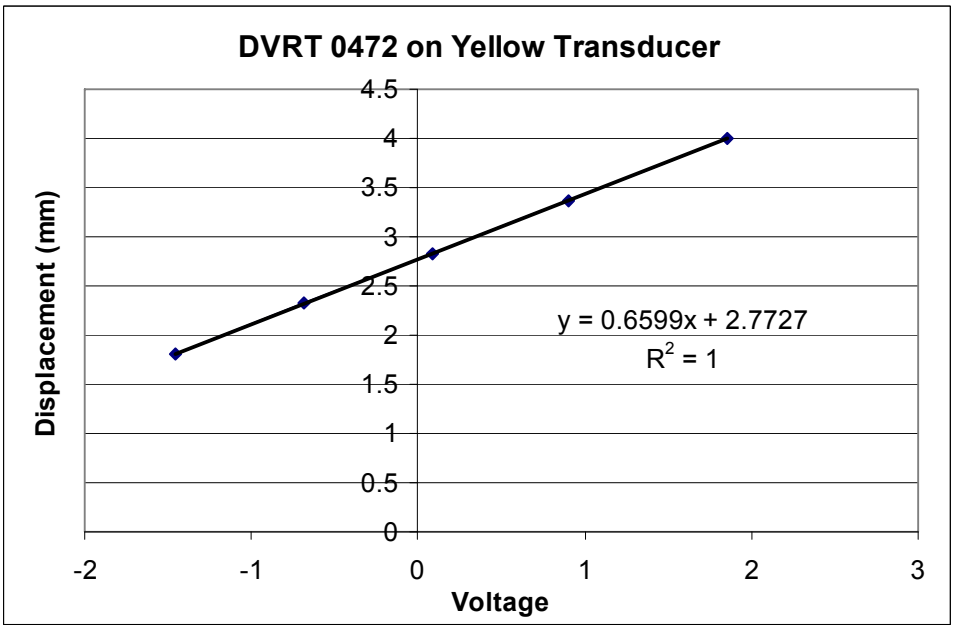

Figure 165: DVRT 0472 calibration with yellow transducer.

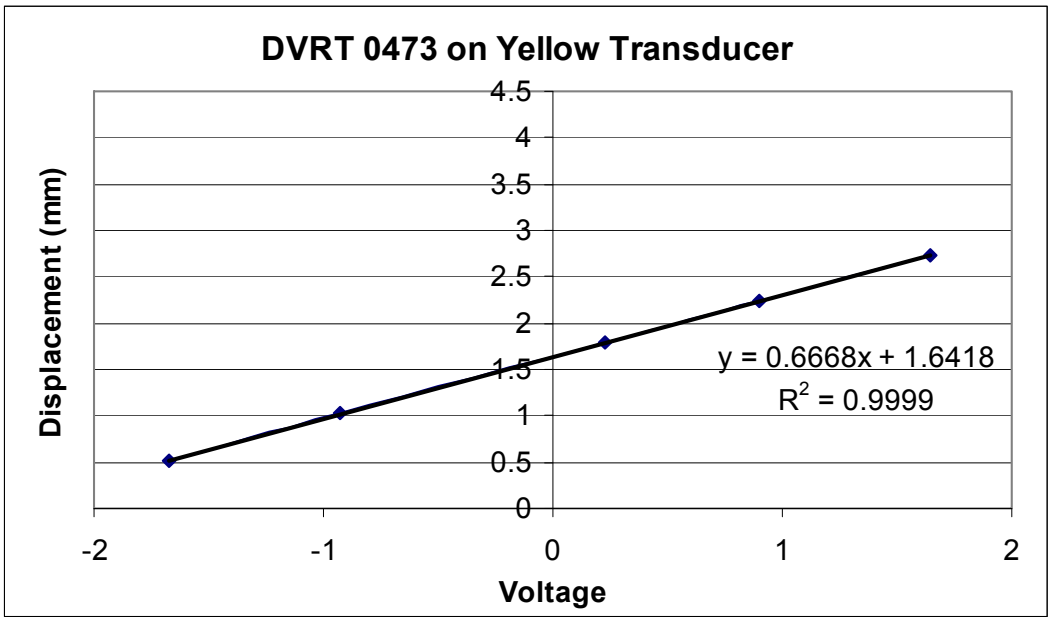

Figure 166: DVRT 0473 calibration with yellow transducer.

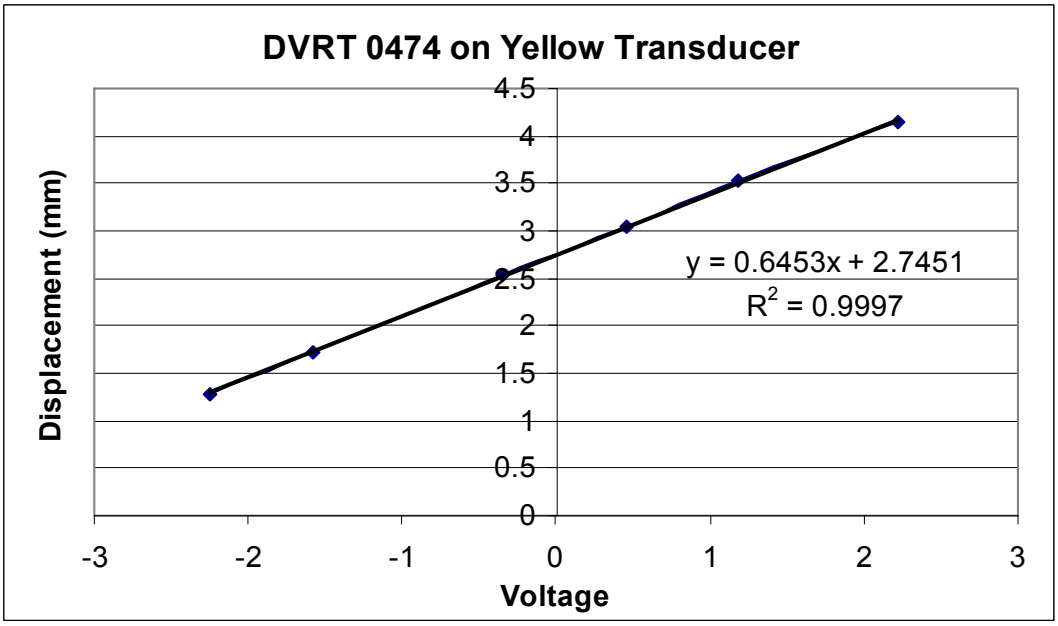

Figure 167: DVRT 0474 calibration with yellow transducer.

The calibration equation used for the yellow transducer was:

Displacement (mm) = 0.6552 * Voltage

Blue Transducer

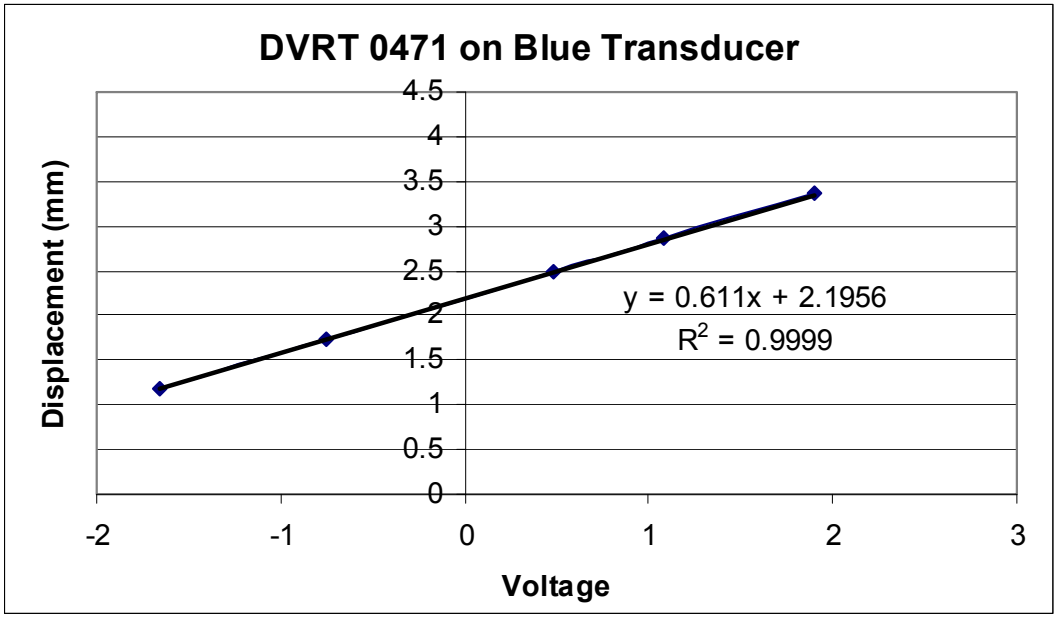

Figure 168: DVRT 0471 calibration with blue transducer.

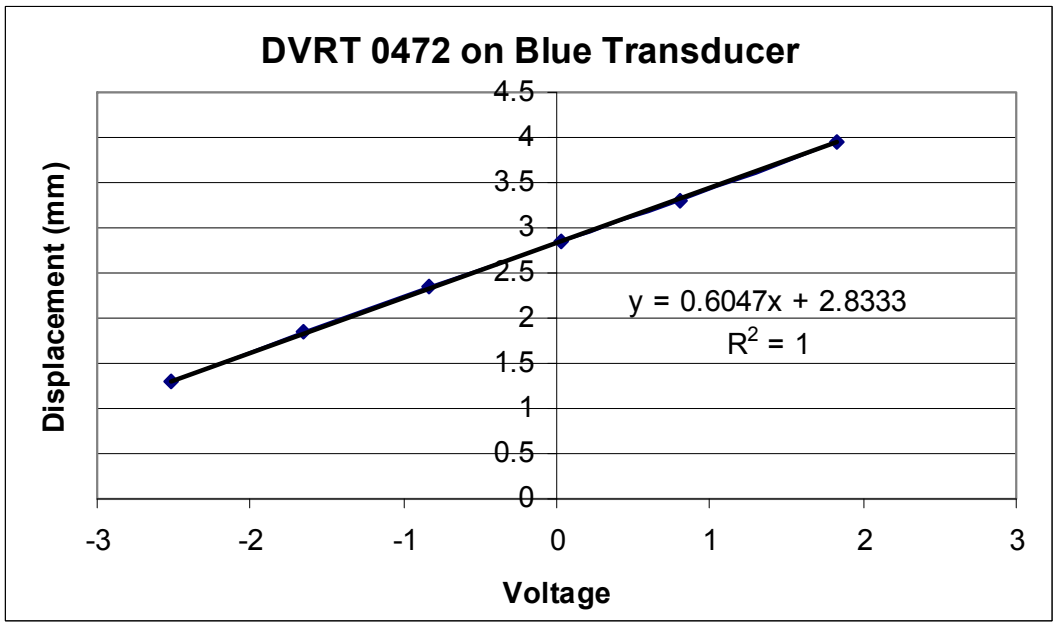

Figure 169: DVRT 0472 calibration with blue transducer.

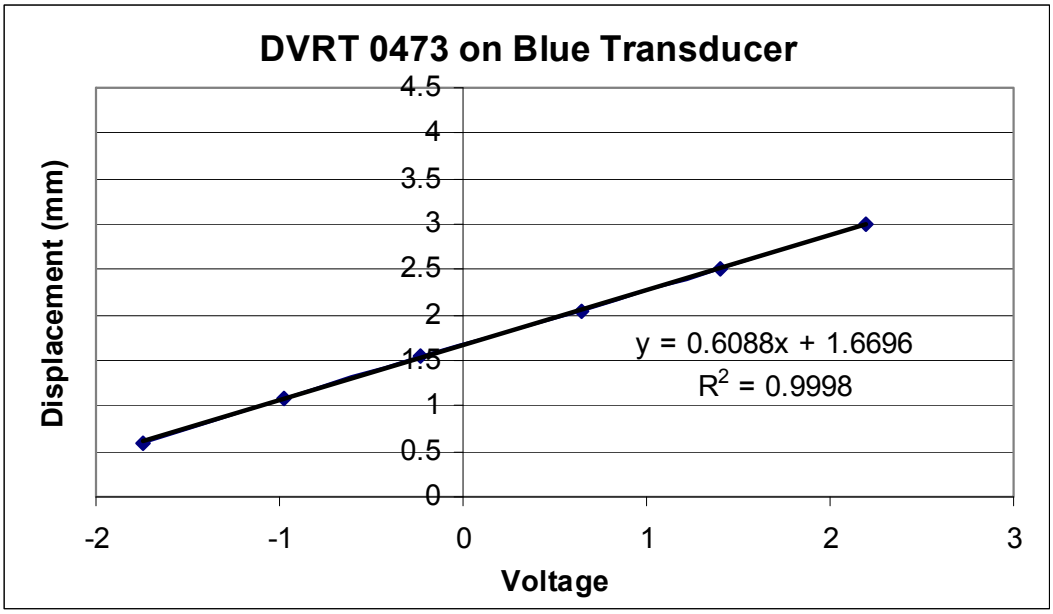

Figure 170: DVRT 0473 calibration with blue transducer.

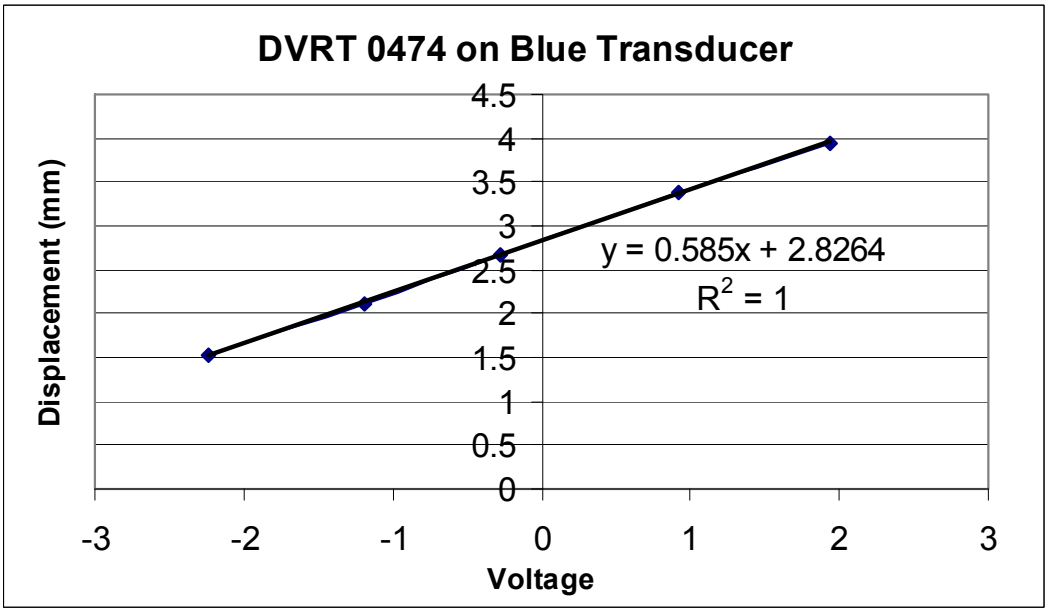

Figure 171: DVRT 0474 calibration with blue transducer.

The calibration equation used for the blue transducer was:

Displacement (mm) = 0.6024 * Voltage

Red Transducer

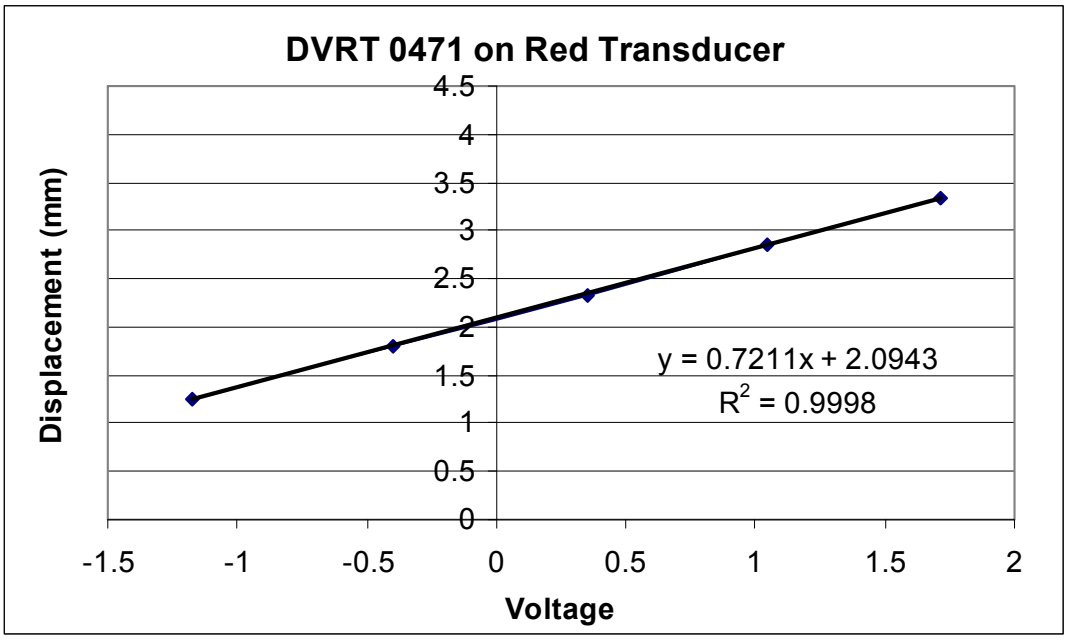

Figure 172: DVRT 0471 calibration with red transducer.

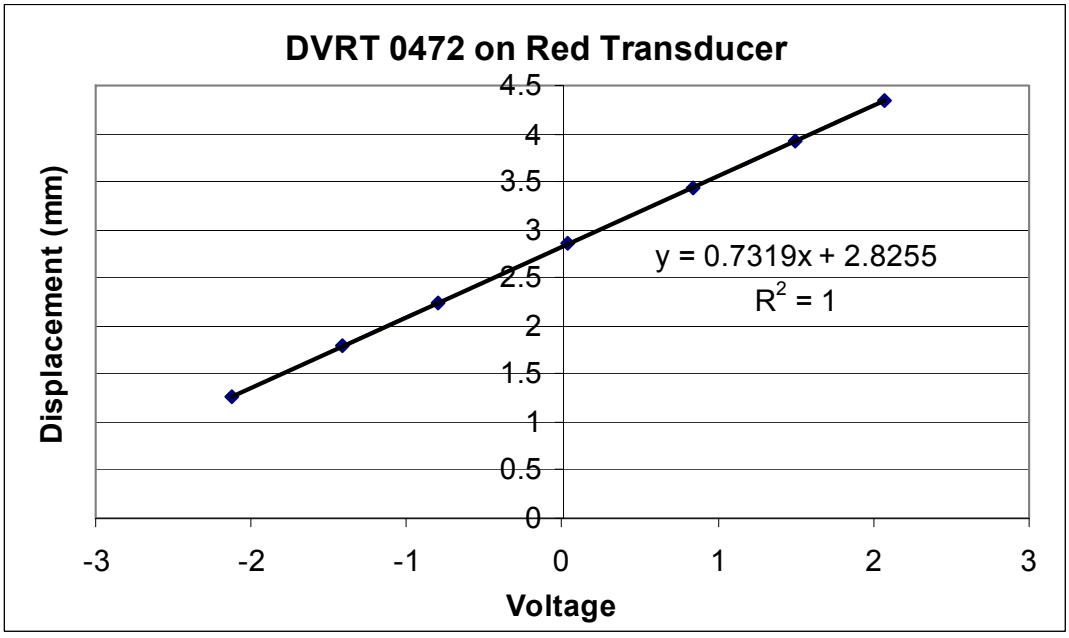

Figure 173: DVRT 0472 calibration with red transducer.

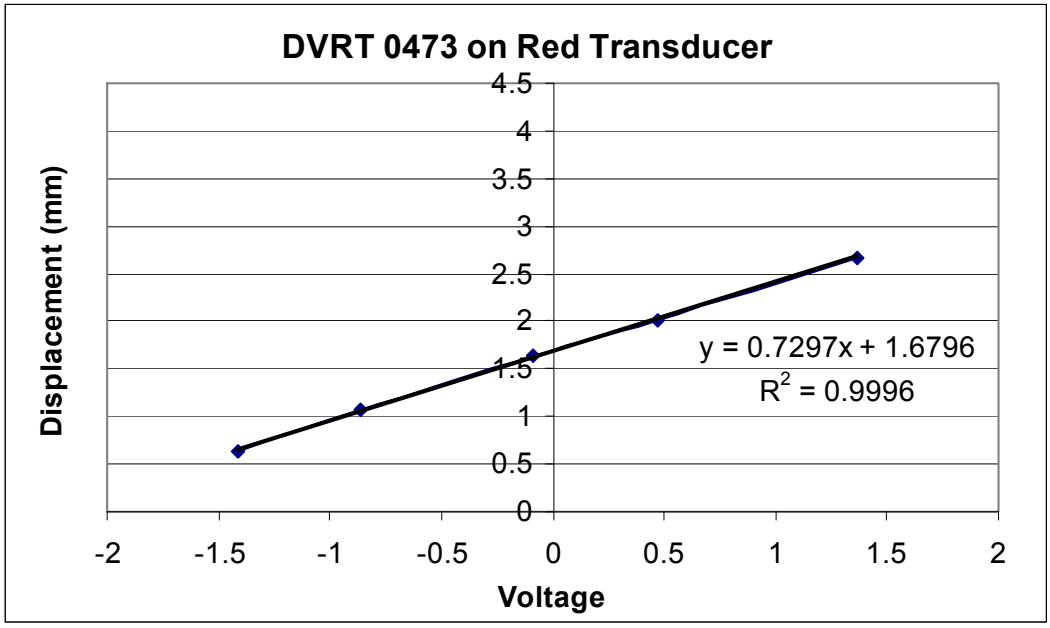

Figure 174: DVRT 0473 calibration with red transducer.

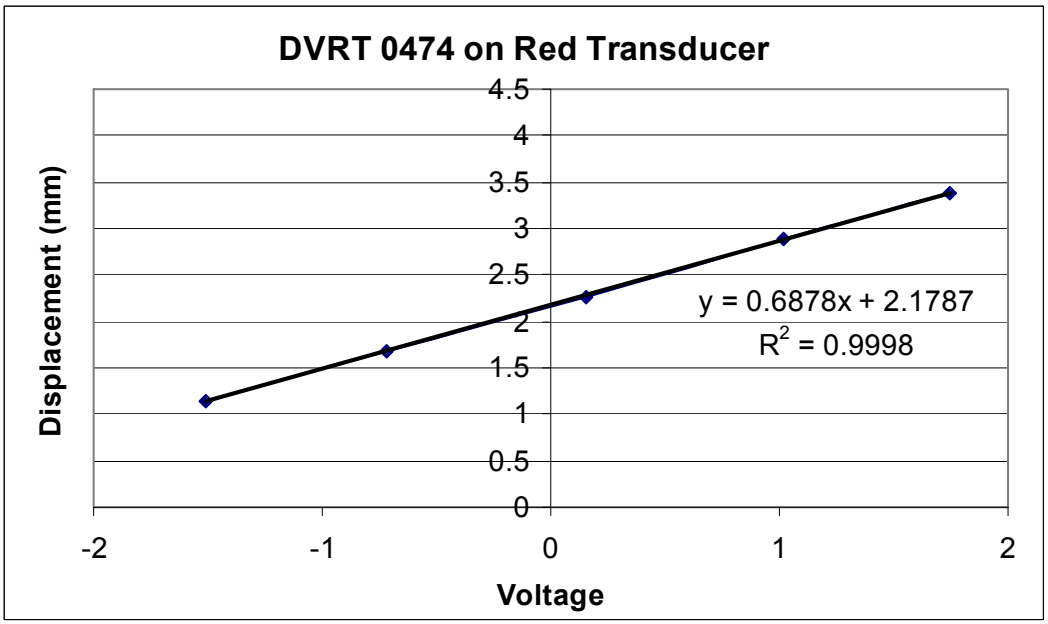

Figure 175: DVRT 0474 calibration with red transducer.

The calibration equation used for the red transducer was:

Displacement (mm) = 0.7176 * Voltage

Black Transducer

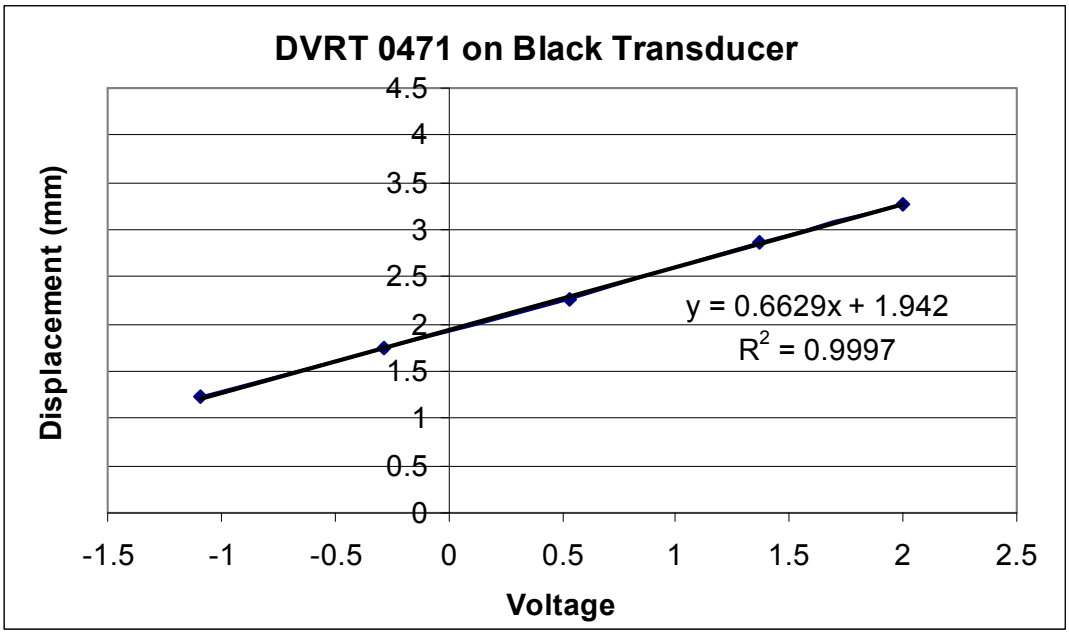

Figure 176: DVRT 0471 calibration with black transducer.

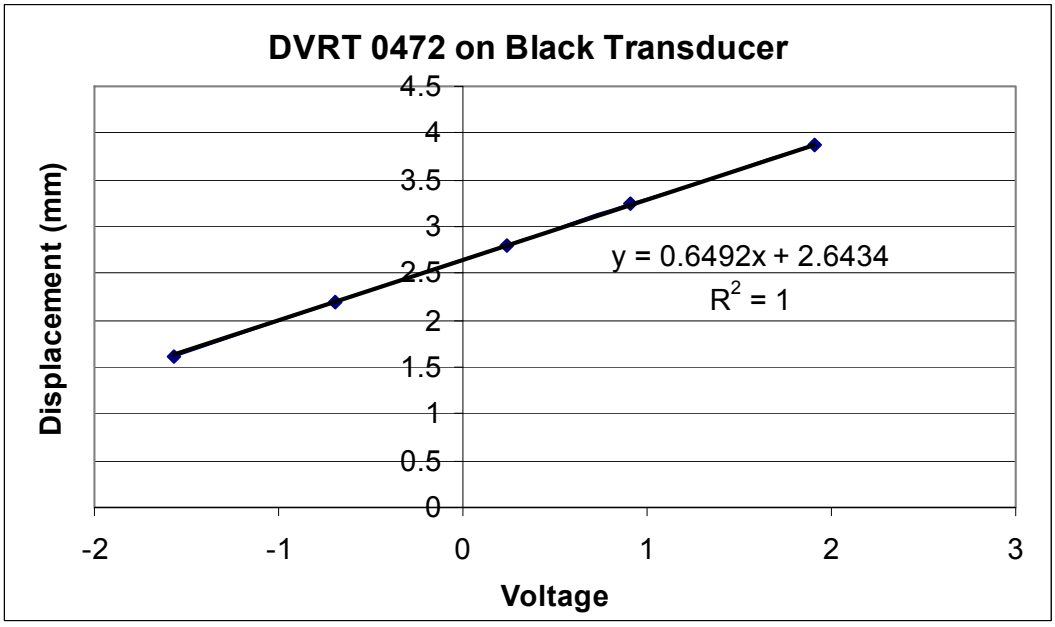

Figure 177: DVRT 0472 calibration with black transducer.

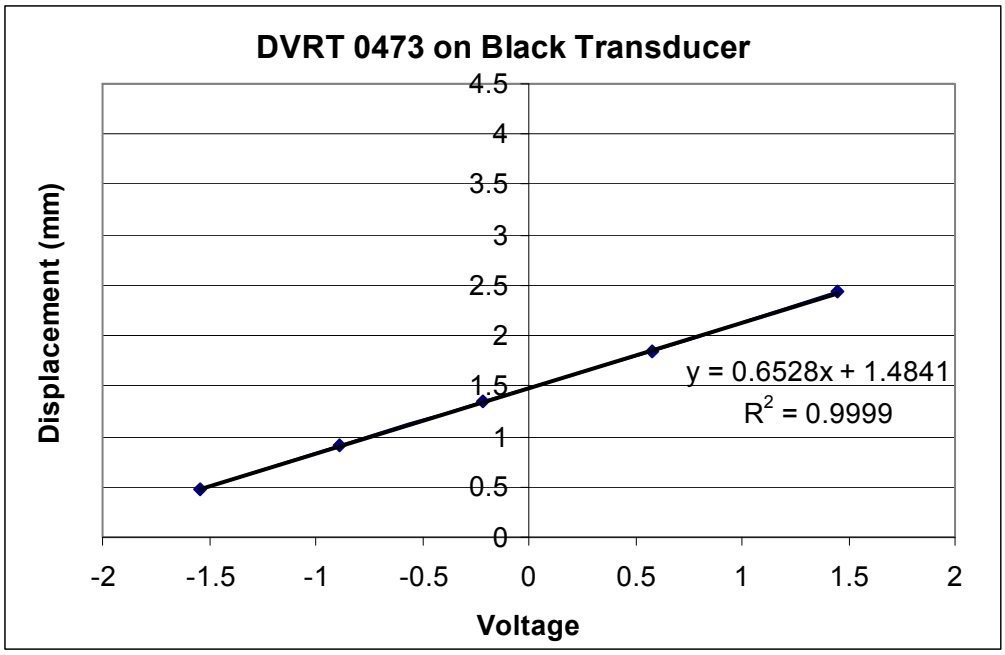

Figure 178: DVRT 0473 calibration with black transducer.

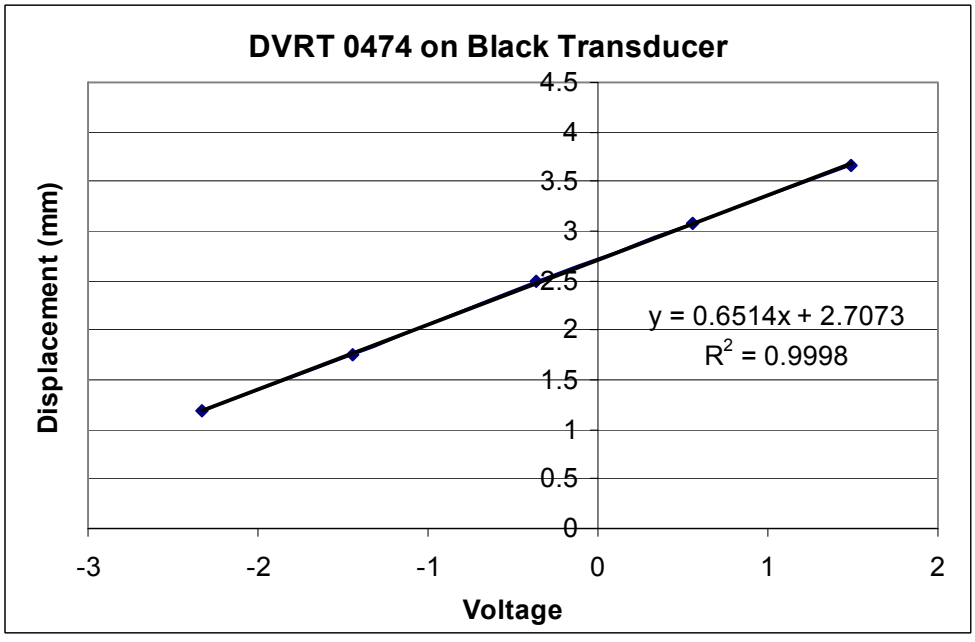

Figure 179: DVRT 0474 calibration with black transducer.

The calibration equation used for the black transducer was:

Displacement (mm) = 0.6541 * Voltage